IMPERIAL COLLEGE OF SCIENCE, TECHNOLOGY & MEDICINE

University of London

VALIDATION OF LARGE STRUCTURAL DYNAMICS MODELS USING MODAL TEST DATA

by

Nedzad Imamovic

A thesis submitted to the University of London
for the degree of Doctor of Philosophy

Department of Mechanical Engineering
Imperial College of Science, Technology & Medicine
London
February 1998

Abstract

This thesis presents research ideas and findings about structural dynamics model validation when applied to real engineering problems. Since most practical engineering problems involve modelling of complicated structures, the theoretical models used are generally quite large and so this thesis focuses on application of model validation to these large models.

Model validation consists of: data requirements, test planning, experimental testing, correlation, error location and updating. The goal of data requirements is to define the required amount of experimental data for successful validation of a model. This requirement for the optimum experimental data is coupled with test planning to design an optimum modal test in terms of specifying the best suspension, excitation and response locations.

Test planning analysis uses the initial theoretical model (the model which is being validated) and all new test planning methods are designed in such way that they minimise the influence of any errors of the initial model to the results of test planning.

Correlation is presented as a refined tool for automatic selection of correlated mode pairs during updating, but correlation is also used for determination of completeness of experimental data and determination of main discrepancies between the two models.

Error location is studied extensively together with new practical limitations for model updating parameters. No new updating method is introduced, but instead the existing sensitivity-based method is examined for its applicability to large industrial test cases. Particular attention is paid to automatic selection of updating parameters during updating in order to keep the sensitivity matrix well-conditioned and to obtain an accurate solution for updating parameters.

Every test case presented in this thesis uses real experimental data rather than simulated data and this gives a particular value of this work, as it is presented on several industrial applications throughout the text.

Acknowledgements

I would like to express my gratitude to my supervisor Prof. D J Ewins and to Dr. M Imregun for their valuable advice, interest and encouragement throughout this project.

I would like to thank all my colleagues from Imperial College Dynamics Section for valuable scientific discussions about the subject described in this thesis.

I am also grateful to Rolls-Royce plc. (particularly the Whole Engine Modelling Group) for providing the financial and technical support for this project.

Special thanks are due to my parents, Resad and Alma and my brother Adem for all their love and support they provided during the course of this work, especially during the last few months. Without them this thesis would not have been completed.

Nomenclature

Basic Terms, Dimensions and Subscripts

x, y, z	translational degrees-of-freedom
N	number of degrees-of-freedom of the complete theoretical model
n	number of (measured) degrees-of-freedom of experimental model
s	number of slave / secondary / unmeasured degrees-of-freedom
m	number of modes of experimental model / number of master degrees-of-freedom
ω, f	frequency of vibration (in $^{rad}/_{s}$; Hz respectively)
ε	tolerance value
i, j, k, r	integer indices
i	$\sqrt{-1}$
A, B, a, b	real constants

Matrices, Vectors and Scalars

$[\ ]$	two dimensional matrix
$\{\ \}$	column vector
$[\ddots]$	diagonal matrix
$[\ ]^T$	transpose of a matrix
$\{\ \}^T$	transpose of a vector
$[I]$	identity matrix
$[\ ]^{-1}$	inverse of a matrix
$[\ ]^+$	generalised / pseudo inverse of a matrix
$[\ ]^*$	complex conjugate of a matrix
$[U], [V]$	matrices of left and right singular vectors
$[\Sigma]$	rectangular matrix of singular values

$[S]$ sensitivity matrix

$[T]$ transformation matrix

$\|\|$ norm of a matrix / vector

$|\,|$ absolute value of a complex number

Spatial and Modelling Properties

$[M]$ mass matrix

$[K]$ stiffness matrix

$[D]$ structural damping matrix

$[C]$ viscous damping matrix

Modal and Frequency Response Properties

ω_r natural frequency of r-th mode

η_r structural damping loss factor of r-th mode

m_r generalised mass of r-th mode

k_r generalised stiffness of r-th mode

$[\lambda]$ eigenvalue matrix

$[\psi]$ unit-normalised mode shape / eigenvector matrix

$[\phi]$ mass-normalised mode shape / eigenvector matrix

$\{\psi\}_r ; \{\phi\}_r$ r-th mode shape / eigenvector

$[\alpha(\omega)]$ receptance matrix

$[Z(\omega)]$ dynamic stiffness matrix

$\alpha_{jk}(\omega) = \frac{x_j}{f_k}$ individual element of receptance matrix between coordinates j and k (response at DOF j due to excitation at DOF k)

${}_r A_{jk} = \phi_{jr}\phi_{kr}$ modal constant

$[R]$ residual matrix

Standard Abbreviations

DOF(s)	degree(s)-of-freedom
EMM	error matrix method
FE	finite element
FRF	frequency response function
MAC	modal assurance criterion
NCO	normalised cross-orthogonality
SCO	SEREP cross-orthogonality
COMAC	coordinate modal assurance criterion
RFM	response function method
SVD	singular value decomposition
CMP(s)	correlated mode pair(s)
ADPR	Average Driving Point Residue
ADDOFD	Average Driving DOF Displacement
ADDOFV	Average Driving DOF Velocity
ADDOFA	Average Driving DOF Acceleration
ODP	Optimum Driving Point
NODP	Non-Optimum Driving Point
EI	Effective Independence

Structure of Thesis

Each chapter consists of several sections. Every section is numbered separately using the chapter number to which the section belong followed by a separate number for section, such as 1.1, 3.4, etc. Some sections have further subsections which have separate identification using section number followed by subsection number such as 5.6.1, 7.2.5, etc.

All mathematical expressions (equations) in the text are numbered. Each expression number consists of chapter, section and/or subsection number followed by the expression number, such as 3-1, 4.2-3, 5.3.7-1, etc.

All figures given in the text also have a unique identification which is equivalent to the numbering system for the equations. Majority of Figures are given within the text, but some of them are given at the end of the relevant chapter.

For instance, if expression 4.3.2-6 is referenced somewhere in the text, then the advantage of this numbering system is that the reader can instantly identify the position of the equation in the text, in this case it is chapter 4, section 3 and subsection 2. In most cases, the reader is given an opportunity to identify the mentioned method by simply looking into the contents, or if it is necessary to find a particular section then this numbering system gives an advantage.

Contents

3.0 Planning of Modal Tests

4.0 Model Correlation

5.0 Error Location Theory

6.0 Model Updating

1. Introduction

This chapter provides a general introduction to structural dynamic model validation technology. Fundamental concept of model validation and its application in the overall design process are outlined and some basic definitions for model validation topics are introduced. In addition, a classification and comparison of existing validation techniques from different branches of mechanical engineering are presented in this chapter. Finally, in the light of the application of model validation technology, the scope of this thesis is given at the end of the chapter.

1.1. Need for Model Validation in Practice

A traditional form of the "design-to-production-line" cycle of a product is shown in Figure 1.1. After the initial outline design of a product has been made, preliminary analysis including dynamic effects is performed and the first prototype is built. Various tests are carried out on the prototype, and if the prescribed properties of the design of the product are met, then full production can begin. However, it is very unlikely that the initial design of a product will have all the previously-prescribed design properties and so some changes to the initial design become necessary. After these changes are made, i.e. after the product has been re-designed, the whole validation process has to begin again, from analysis to building a new prototype and testing. It can be seen that this route to final production might be very expensive and time-consuming, because in the case of any changes being made to the initial design of the product, the whole process of building a new prototype to testing has to be repeated.

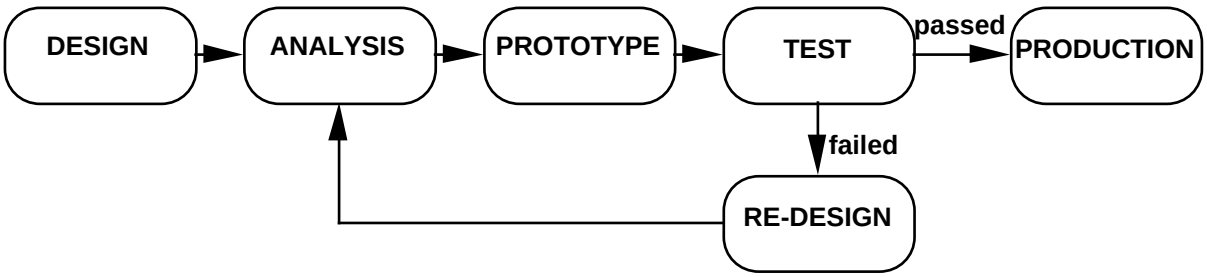

Figure 1.1. Simplified "Design-to-Production-Line" Cycle

A more modern form of the "design-to-production-line" cycle is shown in Figure 1.2. Here, after the initial design of the product, a preliminary analysis is performed and a prototype is built. Some "simple" non-destructive experiments, such as modal tests, may be performed on the prototype and the measured results compared with analysis. This comparison between two data sets is known as the **correlation** process. If the analytical predictions correlate (i.e. agree) well with the experimental results, then further analysis (aeroelasticity, transient dynamic, etc.) can be performed using the same model. However, it is very unlikely that the initial model of the structure will represent the measured behaviour accurately, and therefore it becomes necessary to refine the initial model so that the predictions using the refined model are in acceptable agreement with the experimental results. Once a refined model which possesses the measured characteristics is found, it is possible to **simulate** important verification tests that may be destructive and may require complete or partial destruction of the prototype. This simulation of verification tests provides a possibility of verifying the design without destruction of the prototype, and consequently the whole design and production process would have a lower cost for the manufacturer. If any of these simulated verification tests are not passed, the structure undergoes a re-design process and the whole cycle is repeated from the previous analysis step. Once the design specifications are met by a re-designed model, production can begin. It is clear that this route to the final product is cheaper than the traditional way of design and verification since it does not require a new prototype after changes to the initial design.

To illustrate the above discussion, we shall compare these two design-and-verification approaches in the production of aircraft engines. When the first aircraft engine prototype is constructed, many design and working engine requirements have to be verified. Some of these constraints are the containment, blade-off and bird-strike requirements at specific running conditions. These requirements are crucial from the point of view of safety and every type of aircraft engine must be tested in order to verify compliance with these requirements. These tests are destructive and are consequently very expensive. However, if an accurate model of the structure is available, then it would be possible to simulate these tests for different conditions, to predict engine behaviour during the events in question and to verify the design without destroying the whole engine every time one of these tests is carried out. At this stage of development of model validation technology the research is concentrated on development of validation techniques which would

enable engineers to carry out only one destructive test and to simulate other tests with different operating conditions, and therefore destroy only one engine instead of several.

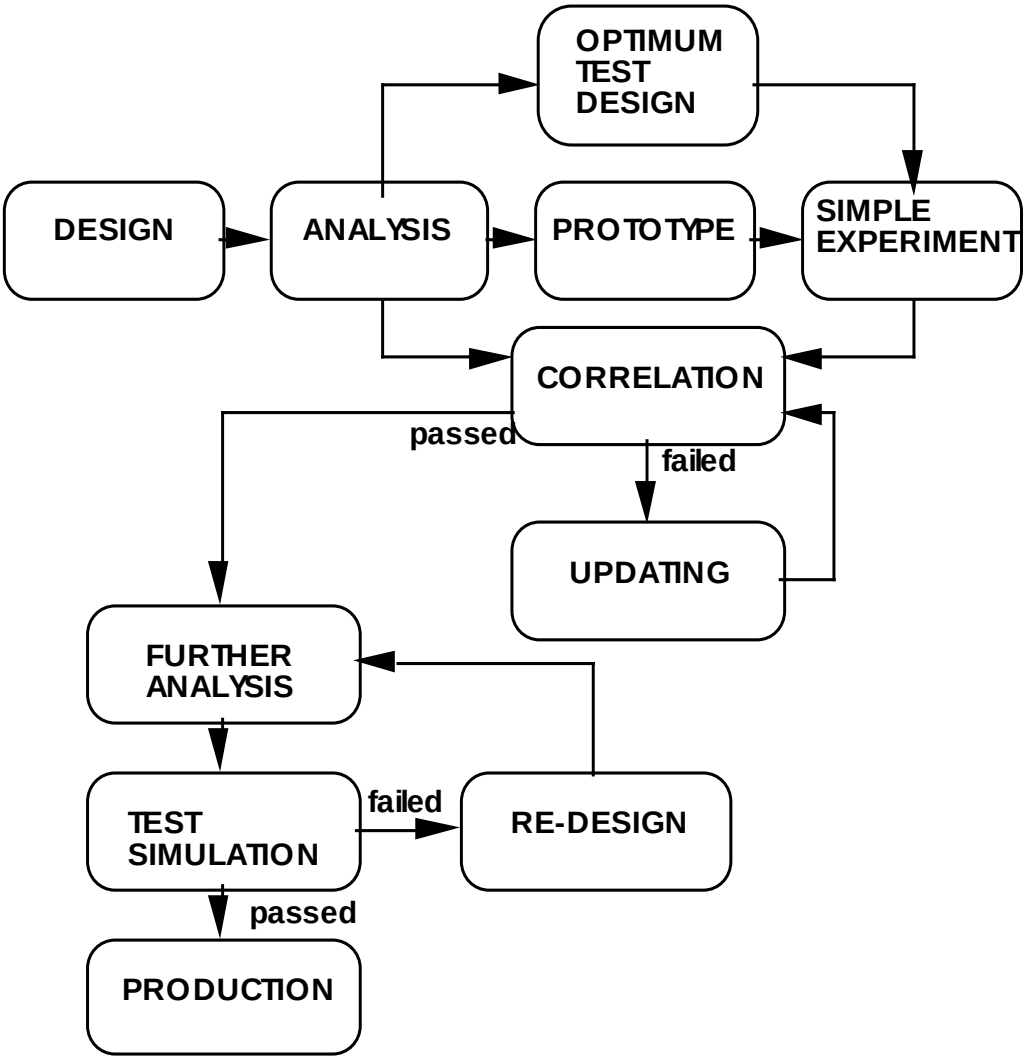

Figure 1.2. Simplified Modern “Design-to-Production-Line” Cycle.

Another example of the application of this technology is to aeroelasticity analysis, where the behaviour of coupled fluid-structure models is simulated in the computer. Although the predictions in fluid dynamic analysis are generally less accurate than those in structural dynamics, it is evident that having a verified structural model would increase the accuracy of aeroelasticity predictions.

1.2. Model Validation Definitions

The development of fast digital computers, numerical simulation techniques and measurement technology has led to an increase in the use of theoretical model validation techniques in practice. Validation techniques combine the theoretical simulation of a phenomenon with experimental testing of an actual structure, leading to comparison and refinement of the theoretical model on the basis of experimental results. There are several scientific fields in which validation techniques are used extensively, e.g. static-, stress-, fatigue-, fracture- and dynamic analysis, but the fastest growing usage of validation techniques is in structural dynamics. The reason for this rapid and extensive growth lies in the applicability of vibration theory, well-established modal testing technology and well-developed methods for numerical simulation of vibration phenomena whose theoretical models can be used for other analysis. These reasons have contributed to a demand for the development of a new area in structural dynamics analysis known as **validation of structural dynamic models** or, more commonly, **model correlation and updating**.

Another important part of model validation process is **test planning** which has emerged in the last few years as a precondition for successful correlation. **Test planning** is a process of determining the optimum test parameters such as suspension, excitation and measurement locations on the basis of preliminary theoretical predictions before commencement of the actual test. Clearly, the result of test planning is dependent on the very model which is being validated and, as such, carries some uncertainties which have to be resolved during the validation process. This makes the test planning an extremely difficult problem since it relies on a model which may have any degree of error and uncertainty.

Correlation is a process of comparison of the dynamic properties between two data sets. Although correlation is described as a comparison process, essentially it is more than a simple comparison and in reality is also a process of assessment of the result of test planning and the global completeness of experimental data set.

There are many ways of defining **model updating** but the simplest and most common definition is "adjustment of the theoretical model on the basis of modal test results in order to minimise the discrepancies between theoretical and experimental behaviour of a structure" [1]. The advantages of an efficient model updating method for the simulation of structural behaviour are obvious, i.e. by performing only one series of modal tests on a structure, the initial model can be updated to match the experimental results and this updated model can then be used for a wide range of further dynamic analyses. Any results which come from further analysis need not be validated since the model which was used to calculate those results was already shown to be 'correct'. In practice, this means that once a successful updating of the model of a structure is completed, there would be no need to perform and repeat expensive experiments because the behaviour can be simulated theoretically using the updated model. Model validation can also be used to learn how to model various structures, structural joints and other uncertainties in the modelling.

1.3. Literature Survey

This section gives a concise introduction to existing methods for model validation and it provides a list of the most important references. More details about some methods described in this section can be found in relevant chapters and therefore only discussion about some existing methods is given here.

1.3.1. Test Planning

Test planning consists of determining the optimum suspension, optimum excitation and optimum response locations. Although each of these three requirements is equally important for a successful test, selection of optimum suspension is generally viewed as being less significant than the other two requirements. Consequently, it appears that very little systematic research has been reported about selection of optimum suspension positions. Usually, the suspension for a modal test is selected as such that there is least interference between the structure and the ground, and the decision about suspension locations and orientation is based on the experience of the experimentalists. Some good tips about selection of suspension are described by Ewins, [2].

Selection of excitation location(s) is of paramount importance for a successful modal test. There are two types of modal test as far as excitation strategy is concerned. One is the type where one reference point is used in the test to measure all modes within certain frequency range, and in this case the reference point must be selected in a region of structure where all modes are clearly recorded on the reference point FRF. An interesting study of this type of excitation was done by Lim, [3]. Another type of modal test is where multi-source of excitation is used for isolation of certain modes, usually when heavy damping is present in a structure. Some reference to this particular case of mode isolation can be found in [4].

Selection of measurement locations is critical for a successful modal test. There are numerous instances where, after the test has been completed, it was concluded that either an insufficient number of measurement locations was selected or too many points were measured and valuable time and resources were spent unnecessarily. One standard procedure for selection of measurement locations is to perform a Guyan reduction on the theoretical model and to select the same locations for measurement as described in [5]. Another very efficient method was introduced by Kammer which is based on estimation of the contribution of each observation to the least-squares problem. The method is called Effective Independence and a full description can be found in [6]. This method will be used (in this thesis) as a basis for developing a new method for selecting optimum measurement locations.

1.3.2. Correlation

Correlation is probably the most mature area of model validation process. The most fundamental form of correlation is a comparison between mode shapes using Modal Assurance Criterion (MAC) introduced by Allemang and Brown in [7]. A more advanced form of correlation based on the MAC formulation but using the mass or stiffness orthogonality property was introduced by Lieven in [8]. Modal Scale Factor was introduced by Ewins, [2] and represents a measure of the slope between two mode shapes. The final result from this correlation is to produce a list of correlated mode pairs (CMPs). It is important that each mode shape in a given data set is linearly independent of any other mode shape from the same data set. Clearly, this requirement is highly dependent on the choice of measurement locations and it is necessary to evaluate the suitability of measurement locations. In most practical cases, the MAC coefficient is used for this evaluation, but some other procedures

can be successfully used, such as singular value decomposition (SVD), [9], or a measure of the kinetic energy per mode, [10].

There are other forms of correlation, and another useful one is cross-orthogonality for every DOFs for selected number of modes. This procedure is known as Co-ordinate Modal Assurance Criterion and was introduced by Lieven and Ewins in [11].

1.3.3. Model Updating

Model updating is the most difficult part of the model validation process and as such is the most challenging. Model updating is described as an area where most effort was concentrated within structural dynamics community. Although recently solving model updating problem in general is portrayed to have a similar fate as general solution of model identification problem, still model updating as a primary part of model validation process has its established role.

One of the major problems in model updating is incompleteness of experimental model in terms of the number of measured DOFs. This problem has been overcome in some situations either by reducing the theoretical (usually the larger data set) model or by expanding the experimental model, although the author came across a few practical cases in which experimental data set had larger number of DOF thanks to laser scanning techniques applied in modal testing. Several reduction and expansion techniques can be found in [12],[13],[14],[5] and [15].

Model updating methods can be classified in two groups as far as the data used for updating is concerned. One group includes methods which use direct frequency response data for updating, and the other group contains methods which use modal data. Methods which use modal data for updating can be further divided into two groups; (i) direct methods and (ii) iterative methods.

One of the most simple direct updating approaches is Error Matrix Method (EMM) proposed by Sidhu and Ewins [16]. The method proposed earlier by Baruch[17] assumes that the mass matrix is correct and updated the stiffness matrix using Lagrange multipliers. The problem with these methods is that they correct either mass or stiffness matrix globally, usually ruining the sparseness of the system matrices which is unacceptable for large models.

Methods based on force balance assume that mass matrix is accurate and they correct the stiffness matrix using the force balance equation as describes by Berger, Chaquin and Ohayon [18]. Link [19],[20] used this approach to develop a new method for model updating by minimising the force residue using a weighted least-squares approach. Also, methods based on orthogonality were proposed by Niedbal [21] to solve the updating problem, usually as a least-squares approach. Many different variations of the force balance and orthogonality methods have been proposed, but their major weakness is that they require full experimental mode shape vectors and as such they are not directly applicable for updating of large models because their use would require either reduction of larger model or expansion of smaller model.

The sensitivity method [22],[23] is a prime representative of the updating approach which allows selection of updating parameters but does not require full experimental mode shapes and as such this method seems to be suitable for updating of large models. Also, it is worth noting that model updating methods based on control methods, such as eigenstructure assignment method proposed by Minas and Inman [24],[25] are quite promising since they can be defined in such a way that they do not require full experimental mode shape matrix.

Lin and Ewins [26] proposed a method which uses frequency response data for updating of structural models instead of modal data. There is another family of methods which use frequency response data directly, such as method of minimisation of response equation errors proposed by Natke [1]. Again, there are several variations of this updating approach, and most of them allow selection of updating parameters and can cope with incompleteness of experimental data quite well. A major shortcoming of these methods is that they usually do not lead to a proper least-squares approach due to the presence of noise in the experimental data, as will be explained in more detail in chapter 6.

There is a new family of updating approaches based on stochastic optimisation methods such as the genetic algorithm (GE) method. Genetic algorithms are mainly used for solving complicated optimisation problems and they have the advantage over deterministic optimisation approaches, such as simulated annealing (SA), that they provide faster convergence to near global minimum value. These two methods (GA and SA) seem to be very promising, but at this stage their contribution to model updating is more of an academic character and they are still not ready for application to large models.

1.4. Scope of the Thesis

Model validation has reached a critical stage when it is rapidly becoming an essential tool in the design process. There is no doubt that the aerospace industry is becoming a major user of model validation technology. At this stage, many different updating methods were developed, and many researchers rushed to produce yet another different method for model updating, which works well on simulated case studies but often fails to produce good results when used with real experimental data.

In order to apply model validation technology to real engineering problems, it is necessary to close the gaps between the test planning, correlation and updating processes. These three processes have to be integrated with the requirements described for the final updated model so that a model validation strategy can be defined which can offer solutions for real engineering problems.

In order to reach these goals the following needs to be done and forms the basis of research in this thesis:

(i) It is necessary to define the minimum data requirements for correlation and updating using the information about the final application of the models to be validated;

(ii) development of methods which will enable the user to plan a modal test using any available preliminary knowledge about the model. Test planning has to be used to ensure that the minimum effort is spent obtaining the most valuable information about the structure’s dynamic behaviour;

(iii) a comprehensive study of error location theory is required;

(iv) experience suggests that currently the most promising numerical updating approach is the sensitivity method and therefore this method has to be adapted for application to large theoretical models;

(v) an additional constraint for this study is that any new method has to be tested and verified using practical experimental data. There seems to be too many academically valuable algorithms which work successfully only when simulated experimental data is used.

These tasks constitute the work reported in this thesis which is structured as follow: Chapter 2 provides theoretical background information about vibration theory and finite element modelling technology. Chapter 3 gives details about test planning. Chapter 4 describes the correlation process and defines a new automatic correlation procedure to be used in updating. Chapter 5 provides a comprehensive study about error location in finite element models. Chapter 6 gives detailed analysis about limitations of the sensitivity least-squares updating approach. Chapter 7 gives details about two practical model validation test cases. Chapter 8 presents some overall conclusions and provides a list of specific contributions made in this project and suggestions for further research.

1.5. Closing Remarks

It is the author's belief that recognising and identifying the role of model validation in the overall design process is an important process that should be well understood before attempting a systematic study of model validation such as this. Positions and roles of model validation technology within the design process are clearly identified and highlighted in this chapter.

2.0 Theoretical Modelling

2.1. Introduction

This chapter provides an introduction to the basis of theoretical modelling used in model validation technology.

2.1.1. Analytical and Numerical Methods

Theoretical prediction techniques used in structural dynamics can be divided into two main families: one based on classical analytical methods and the other on numerical methods.

Classical analytical methods are restricted to simple types of structure (one- and two-dimensional structures of simple geometric form) because they do not discretise the structural domain but the solution is found continuously for the whole domain.

Numerical methods approximate and divide the solution domain and find a solution for a certain number of discrete points throughout the domain. Numerical methods are applicable to structures of arbitrary geometry and these methods will be used to predict and validate the dynamic behaviour of structures in this work.

2.1.2. Discrete Models and Concepts of Mass, Stiffness and Damping

A discrete model of a structure consists of elements that are defined by several nodes. Adjacent elements are connected through common nodes to form an assembled discrete model of the structure. Each element is defined by its nodes, material and physical properties, and these data are used for defining mass, stiffness and damping matrices of the element. Each node has six degrees-of-freedom, three translations and three rotations.

The mass matrix of an element is a basic representation of its inertia properties concentrated at degrees-of-freedom at nodes which define the element.

The stiffness matrix of an element provides information about stiffness properties at degrees-of-freedom at nodes which define the element.

The damping matrix of an element defines damping properties at degrees-of-freedom at nodes which define the element.

Thus, using simple concepts of mass, stiffness and damping formulations, any structure can be represented at a number of nodes. The sum of all degrees-of-freedom at all defined nodes of a model is called the total number of degrees-of-freedom and this number is an important characteristic of the model. The total number of degrees-of-freedom can vary for different models, but experience shows that for accurate predictions of the dynamic properties of practical structures this number can be quite large. It is quite common to come across models which have several hundred thousand degrees-of-freedom and these models can be somewhat difficult to analyse because of their size. This work is particularly focused on the application of model validation techniques for these large models. The term 'large model' is explained in section 2.5.

2.2. Numerical Modelling Analyses

Numerical prediction methods can be implemented in either the **time** or the **frequency** domains.

2.2.1. Time-domain Analysis

Time-domain predictions (transient analysis) are the most general and can deal with any type of excitation pattern or structural non-linearity (geometrical, material, etc.), but the calculations are expensive and CPU time-consuming. The disadvantage of time-domain analysis is the difficulty in performing the equivalent experiment, and the repeatability, impracticality and cost of transient experiments. Furthermore, transient analysis can be performed as either **direct** or **segregated**. A **direct transient** analysis generates and assembles the full structural matrices and solves all unknowns at every time step (e.g. the Finite Element Method), while the **segregated transient analysis** partitions the solution equations into several sets of unknowns instead and solves each unknown set separately, using the last values of the unknowns when solving for a new unknown set until all unknowns converge to stable solution values (e.g. the Finite Volume and Boundary Element Methods).

Also, a transient analysis requires the modelling of the damping and the solution tends to be very dependent on the damping model used, which is generally unknown and difficult to specify.

A general limitation of the transient type of analysis is the incremental time step used, $\Delta t_{\min}$. Usually, in order to obtain convergence in a transient analysis, the time step is determined by consideration of wave propagation and the size of the mesh. It is common practice to set the time step to a value small enough such that the waves can be 'caught' between the two nearest nodes several times before the change transfers from one node to the other. If the distance between any two adjacent nodes in the mesh is $\Delta X_{\min}$, and the maximum wave velocity in the material domain is c_{wave}, then the maximum allowed transient analysis time step $\Delta t_{\max}$ is defined by the following expression:

$$\Delta t_{\max} = \frac{\Delta X_{\min}}{c_{wave}} \qquad (2.2.1\text{-}1)$$

The actual transient analysis time step must be smaller than this maximum allowed value but too small a value would require a huge CPU effort and would be impractical, i.e.:

$$A_{THRESHOLD} \ll \Delta t_{min} \leq \Delta t_{max} \qquad (2.2.1\text{-}2)$$

where $A_{THRESHOLD}$ is the computer threshold value. The time step used must be significantly larger than the threshold value, which is dependent on the number of digits that the computer can store for one number. The threshold value is defined as the minimum value of variable ε for which the expression below holds:

$$A_{THRESHOLD} = min(\varepsilon) \text{ such that } a + \varepsilon > a, \quad a \in R. \qquad (2.2.1\text{-}3)$$

For double-precision representation of real numbers (each real number is represented by 16 digits only), the threshold value obtained by applying the above algorithm is

$$A_{THRESHOLD(16-digits)} = 2.2204460492503130 \text{ x } 10^{-16} \qquad (2.2.1\text{-}4)$$

while for single-precision real number the threshold value is

$$A_{THRESHOLD(8-digits)} = 1.1920929 \times 10^{-7} \qquad (2.2.1\text{-}5)$$

The threshold coefficient value is an important parameter that will be used throughout this text and constitutes a general limitation of the application of numerical methods.

2.2.2. Frequency-domain Analysis

The **frequency-domain** method of analysis has a major advantage in the practicality of vibration theory, namely: repeatable and cheap numerical analysis. The main disadvantage of numerical analysis in the frequency domain is the difficulty of modelling material and geometrical non-linearities and of other types of non-linearity. From the computational point of view, this type of analysis is not particularly CPU-time expensive but does require a large amount of active (RAM) memory. Frequency-domain analysis does not necessarily require modelling of damping in the model, which further simplifies the analysis and makes the computational effort more realistic and affordable. The main limitation of frequency domain analysis is the maximum frequency value, $f_{\max}$, above which the natural frequencies and mode shapes cannot be extracted from the spatial model. Generally, it is not possible to calculate all the natural frequencies and mode shapes from an FE model and only a limited number of them would be accurate, even if convergence is obtained, as the higher mode shapes would resemble noise. Another limitation, as far as the upper value of the frequency range of interest is concerned, is the time-sampling of the measured signal in order to measure the higher frequency responses.

2.2.3. Relationship between Time- and Frequency-domain Analyses

After obtaining a solution in the time domain, it is possible to convert the results into the frequency domain. This transformation is based on Fourier Analysis and will be described in more detail in section 3.2. It is, however, appropriate to give here the relationship between the limits of the transient, $\Delta t_{\min}$, and the frequency, $f_{\max}$, analyses. If the structural model has been validated in a frequency range

whose upper limit is $f_{\max}$, then the minimum transient analysis time step which should be used is defined by the following expression:

$$\Delta t_{\min} = \frac{C}{f_{\max}}. \qquad (2.2.3\text{-}1)$$

The constant C takes a value typically in the range 5-10 in order to ensure that only those modes which belong to the validated frequency range contribute to the transient analysis. It will be shown later that the contribution of each mode to the total response is inversely proportional to the square of the natural frequency of that mode. Since the higher modes have larger natural frequencies, their contribution to the total response decreases with increasing mode number.

Numerical example of corresponding limits in the time and frequency domain:

$$f_2 = 500\ Hz$$
$$C = 5$$
$$\Delta t_{\min} = 0.01\,\text{sec}$$

The above example shows that if the structural model has been validated up to the limiting frequency, $f_{\max}$, then any transient analysis with a time step value greater than $\Delta t_{\min}$ should give a time history result that is accurate up to a level which is determined by the maximum contribution of the first omitted mode inside the validated frequency range.

2.3. Finite Element Method

The most commonly-used modelling technique for prediction of the dynamic properties of structures (natural frequencies and mode shapes) and of their response characteristics is that of **Finite Element Analysis** [27],[28],[29],[30],[31]. The Finite Element Method is based on discretisation of the structural geometry domain into separate elements which are used to create global mass, stiffness and damping matrices.

2.3.1. Finite Element Mass and Stiffness Matrices Formulation

The Finite Element Method is based on discretisation of the structural domain into separate elements for which shape functions are defined and each element is

constructed from several nodes. The stiffness matrix of a finite element is defined using the principle of minimum potential energy. If a finite element consists of r nodes, then the co-ordinates, x, and the displacements, u, of interior points can be expressed in terms of the co-ordinates, x_i, and the displacements, u_i, at those nodes, as follows:

$$x = \sum_{i=1}^{r} N_i x_i \tag{2.3.1-1}$$

$$u = \sum_{i=1}^{r} N_i u_i \tag{2.3.1-2}$$

The general formulation of the structural mass and stiffness matrices, when the shape functions are defined in the local co-ordinate system, is as follows:

$$[M_e] = \int_{-1}^{1}\int_{-1}^{1}\int_{-1}^{1} [N]^T \rho [N] \det(J) d\xi_1 d\xi_2 d\xi_3 \tag{2.3.1-3}$$

$$[K_e] = \int_{-1}^{1}\int_{-1}^{1}\int_{-1}^{1} [B]^T [D][B] \det(J) d\xi_1 d\xi_2 d\xi_3 \tag{2.3.1-4}$$

where $[N]$ is the shape function matrix,

$[B]$ is the derivative of the shape function matrix,

$[D]$ is the matrix of material constants ,

$[J]$ is the Jacobian matrix between the global and a local element co-ordinate system.

As can be seen from expressions (2.3.1-3) and (2.3.1-4), the terms in the structural mass and stiffness matrices are not explicit functions of the finite element design parameters such as node positions, material properties, area, second moment of area and physical dimensions of the structure. In order to obtain the values of the mass and stiffness matrix terms, integration is required over the domain of the single element. Unfortunately, it is not possible to solve the integrals in the expressions (2.3.1-3) and (2.3.1-4) analytically; only a numerical solution can be found, which further complicates the function between mass and stiffness matrix elements and the finite element design parameters.

The overall mass and stiffness matrices are obtained by assembling mass and stiffness matrices of the individual elements at the common nodes and are defined by the following expressions:

$$[M_A] = \sum_{i=1}^{N_{elem}} [M_e] \tag{2.3.2-5}$$

$$[K_A] = \sum_{i=1}^{N_{elem}} [K_e] \tag{2.3.2-6}$$

The mass matrix formulation using expression (2.3.1-3) gives a so-called 'consistent' mass matrix and predictions using this formulation are usually more accurate than predictions using a lumped mass matrix formulation. The lumped mass matrix formulation is a simple concentration of the mass at the translational degrees-of-freedom; this leads to a diagonal form of mass matrix.

Unfortunately, it is not possible to derive an expression that would define a damping matrix for a general structural element, such as the mass or stiffness matrix expressions given in (2.3.1-3) and (2.3.1-4). In practice, a global damping matrix is assembled from damping values between several pairs of degrees-of-freedom, and these damping values are simply specified by the analyst. A damping coefficient between two degrees-of-freedom cannot be derived from the physical properties of elements and these parameters are extremely complex to model accurately.

2.4. Governing Equation and Solution

The equation of motion for a structural system which has N degrees-of-freedom, and considering general viscous damping, is of the following form:

$$[M_A]\{\ddot{x}\} + [C_A]\{\dot{x}\} + [K_A]\{x\} = \{f\} \tag{2.4-1}$$

Since it is very difficult to model damping accurately, different forms of damping (e.g. proportional damping) can be assumed in order to simplify the analysis, but in most cases damping can be excluded when natural frequencies and mode shapes are calculated so that the following equation is obtained:

$$[M_A]\{\ddot{x}\} + [K_A]\{x\} = \{f\} \tag{2.4-2}$$

Considering the homogeneous part of the expression (2.4-2) and assuming a harmonic response of the following form:

$$\{x(t)\} = \{\phi\}e^{i\omega t} \tag{2.4-3}$$

the generalised form of the eigenproblem can be written in the form

$$([K_A] - \omega^2[M_A])\{\phi\} = \{0\} \tag{2.4-4}$$

where natural frequencies are defined by solution of the following expression

$$\det([K_A] - \omega^2[M_A]) = 0 \tag{2.4-5}$$

The solution of the equation (2.4-5) leads to N values of the natural frequency, $\omega_1, .. \omega_r ., \omega_N$, which can be substituted back into equation (2.4-4) to yield the mode shapes $\{\phi_1\}, ..., \{\phi_N\}$ (also called normal modes), which describe the deformation shapes of the structure when it vibrates at each of the corresponding natural frequencies.

By performing a simple algebraic manipulation, it can be shown that the mass-normalised mode shapes satisfy the orthogonality conditions with respect to mass and stiffness matrices as defined in the following expressions:

$$[\phi]^T[M][\phi] = [I] \tag{2.4-6}$$

$$[\phi]^T[K][\phi] = [\omega_r^2] \tag{2.4-7}$$

Later, it will be seen that the orthogonality conditions are important features of mode shapes for both correlation and updating.

The basic equation (2.4-2) may need reduction prior to solution in the case of null column appearance in a mass matrix. These massless degrees-of-freedom can be effectively removed using static (i.e. Guyan) reduction without altering the final solution. In the case of having too large a model there are other reductions which

can be applied in order to make the solution of expression (2.4-5) possible, but any reduction of the full set (apart from the massless degrees-of-freedom) would alter the calculated dynamic properties of the system. The most common reduction techniques are: (i) Static (Guyan) reduction, (ii) Generalised Dynamic reduction, and (iii) SEREP reduction. These reduction techniques are described in detail in the following sections.

2.4.1. Guyan (or Static) Reduction

The Guyan [5] or Static reduction technique is a simple approach which has the particular feature of removing massless degrees-of-freedom without altering the final solution of the eigenproblem described in expression (2.4-4). The mass and stiffness matrices of the full model are partitioned into master and slave degrees-of-freedom, as indicated in the following expression:

$$\begin{bmatrix} M_{mm} & M_{ms} \\ M_{sm} & M_{ss} \end{bmatrix} \begin{Bmatrix} \ddot{x}_m \\ \ddot{x}_s \end{Bmatrix} + \begin{bmatrix} K_{mm} & K_{ms} \\ K_{sm} & K_{ss} \end{bmatrix} \begin{Bmatrix} x_m \\ x_s \end{Bmatrix} = \begin{Bmatrix} 0 \\ 0 \end{Bmatrix} \tag{2.4.1-1}$$

Neglecting the inertia terms for the second set of equations, and after expressing the x_s set of co-ordinates as functions of stiffness terms, the following transformation matrix is obtained:

$$\begin{Bmatrix} x_m \\ x_s \end{Bmatrix} = \begin{bmatrix} I \\ -K_{ss}^{-1} K_{sm} \end{bmatrix} \{x_m\} = [T_s]\{x_m\} \tag{2.4.1-2}$$

The Guyan-reduced mass and stiffness matrices are then defined as

$$[M_R] = [T_s]^T [M][T_s] \quad \text{and} \tag{2.4.1-3}$$

$$[K_R] = [T_s]^T [K][T_s], \quad \text{respectively.} \tag{2.4.1-4}$$

In the case of removing non-massless degrees-of-freedom, this reduction technique will produce an exact response only at zero frequency.

2.4.2. Generalised Dynamic Reduction

The previous section describes how to reduce system matrices by neglecting the inertia terms from expression (2.4.1-1). If, however, the inertia terms are not neglected when expressing slave co-ordinates as a function of master co-ordinates, then the following transformation matrix can be obtained:

$$\begin{Bmatrix} x_m \\ x_s \end{Bmatrix} = \begin{bmatrix} I \\ -\left(K_{ss} - \omega^2 M_{ss}\right)^{-1}\left(K_{sm} - \omega^2 M_{sm}\right) \end{bmatrix} \{x_m\} = [T_D]\{x_m\} \qquad (2.4.2\text{-}1)$$

This method is an extension of the Guyan reduction process in that the response properties are equivalent to those of the full matrices only for the frequency that was specified in the reduction process [14]. The transformation matrix is used in the same way as specified in expressions (2.4.1-3) and (2.4.1-4) to obtain reduced system matrices.

2.4.3. SEREP Reduction

Most reduction processes reduce the size of the model but do not generally retain the properties of the initial model, expect in the SEREP reduction process, [14]. This process reduces the size of the original model while retaining the exact modal properties and is not dependent on the choice of master co-ordinates [56].

The SEREP transformation can be written as follows

$$\{X\}_N = [\phi]_{Nxm}\{P\}_m \qquad (2.4.3\text{-}1)$$

We can rewrite equation (2.4.3-1) with respect to the master and slave degrees of freedom, X_n and X_s, respectively as:

$$\begin{Bmatrix} X_n \\ X_s \end{Bmatrix} = \begin{bmatrix} \phi_n \\ \phi_s \end{bmatrix}_{Nxm} \{P\}_m \qquad (2.4.3\text{-}2)$$

where n is the number of measured co-ordinates and m is the number of measured modes.

From equation (2.4.3-2), the vector of displacements in the master co-ordinates is

$$\{X\}_n = [\phi]_{nxm}\{P\}_m \tag{2.4.3-3}$$

Using equation (2.4.3-3), it is possible to determine the displacement vector in modal co-ordinates as follows:

$$\{P\}_m = [\phi]^+_{mxn}\{X\}_n \tag{2.4.3-4}$$

where $[\phi]^+_{mxn}$ denotes the pseudo-inverse of $[\phi]_{nxm}$. In order to have a **unique** solution of the least-squares problem in equation (2.4.3-4), the following condition must be satisfied [9]:

$$rank([\phi]_{nxm}) = m \tag{2.4.3-5}$$

and this means that a **required** condition is that $n \geq m$, i.e. the number of measurement co-ordinates must be greater than or equal to the number of measured modes. However, the condition $n \geq m$ is not **sufficient**, even if there are more co-ordinates than modes, as the rank may or may not be equal to the number of modes. The rank of the measured mode shape matrix depends on the **choice** of the measured co-ordinates as well as their number. For example, if five modes have been extracted by measuring ten degrees-of-freedom all near the tip of a cantilever beam, the $[\phi]_{nxm}$ matrix will almost certainly be rank-deficient. This requirement will be used later in order to determine the minimum data requirements for correlation.

In order to satisfy condition (2.4.3-5), the relation between the full set of co-ordinates and the master co-ordinates is:

$$\{X\}_N = [T]_{Nxn}\{X\}_n \tag{2.4.3-6}$$

where the transformation matrix, $[T]$, is given by:

$$[T]_{Nxn} = [\phi]_{Nxm}[\phi]^+_{mxn} \tag{2.4.3-7}$$

Reduced mass and stiffness system matrices are given by:

$$[M_R]_{nxn} = [T]^T_{nxN}[M]_{NxN}[T]_{Nxn} \tag{2.4.3-8}$$

$$[K_R]_{nxn} = [T]^T_{nxN}[K]_{NxN}[T]_{Nxn} \tag{2.4.3-9}$$

After substituting equation (2.4.3-7) into equations (2.4.3-8) and (2.4.3-9), the reduced mass and stiffness matrices become

$$[M_R]_{nxn} = [\phi]^{+T}_{nxm}[\phi]^{+}_{mxn} \tag{2.4.3-10}$$

$$[K_R]_{nxn} = [\phi]^{+T}_{nxm}[\omega^2]_{mxm}[\phi]^{+}_{mxn} \tag{2.4.3-11}$$

For more details of the properties of these matrices, see reference [56].

2.5. Eigensolution of Large Models

Most engineering structures are quite complicated and consequently their finite element models are also complicated and large. The description ‘large’ applied to a finite element model is a relative one and cannot be precisely defined. Usually, ‘large’ is defined by the size of the RAM and ROM memory of the computer used. Model validation technology application almost certainly requires several iterations to be performed, but there is no guarantee that an accurate model will be found after analysis and therefore nobody will invest an excessive amount of money for application of this technology. Also, there are some methods in model validation technology that require a large amount of memory, such as the calculation of eigenvector sensitivities, and there are physical limitations imposed by the available facilities on the size of the largest finite element model. In addition, model validation methods involve complex calculations of matrices whose sizes are determined from the total number of degrees-of-freedom of the finite element model, and special care has to be taken to ensure that some practically-impossible criteria are not generated by use of improper numerical methods.

What, then, does the term ‘large finite element model’ mean here?
A simple answer to this question is that the word ‘large’ is not associated with a particular number. The use of the term ‘large’ finite element model means that these methods obviate the need for some conditions or calculations which may be impossible in practical terms. One good example of these practically unattainable conditions is one which requires calculation of all mode shapes of a finite element model of a structure in order to eliminate the residual effects on the Frequency Response Functions. Even though this task could be performed for some models provided that available facilities do not impose limits, in most practical situations there is no method that would offer an accurate solution for the calculation of the higher mode shapes.

2.6. Conclusions

Numerical modelling techniques, and the Finite Element Method in particular, are ultimately tools for prediction of the dynamic behaviour of structures. The time-domain method of analysis is the most general but is computationally very expensive, while the frequency-domain analysis is not as generally applicable for simulation but is computationally less expensive and as such it has a place as a primary validation type of analysis. Most simulation techniques are based on time-domain analysis methods, but the equivalent experiments are very expensive and inappropriate for model validation. The relationship between the limitations of the time- and frequency-domain analyses gives a clear starting point for defining general data requirements for validation of structural dynamic models. After defining further analysis of a structural dynamic model, the analyst can define the minimum transient analysis time step for the further analysis, and this information can be used for determination of the frequency range in which the structural model has to be validated. This frequency range is a base for determination of the minimum data requirements for model validation, as will be pointed out in the following chapters.

3.0 Planning of Modal Tests

3.1. Introduction

Modal testing is one of the fastest-growing experimental techniques of the last two decades. There are a number of different industrial sectors which use modal testing as a standard link in the production chain. Modal testing is a method of constructing a mathematical model of the structure's dynamic behaviour based on vibration test data rather than on a theoretical analysis of the structure.

Although the mathematical basis of modal testing is well developed, experience shows that the quality of results obtained by applying modal testing can be sensitive to the set-up of experiments. There are some elements of these experiments that are not easy to incorporate in modal testing but, fundamentally, they are an important part of it. These elements are normally assumed to be perfect in the theory of modal testing, and are: (i) suspension of the test piece, (ii) choice of driving positions and (iii) choice of measurement positions. This chapter provides a theoretical basis that can be applied to determine the optimum suspension, driving and measurement positions or, more precisely, to plan optimum modal tests.

3.1.1. Pre-Test Planning

Each time a modal test is undertaken on a structure, one of the first things which has to be decided is how many and which responses should be measured, how the structure should be suspended and which positions are most suitable as excitation locations. Usually, experience and intuition are used to answer these questions, but in many cases, after the test is finished and when reviewing the experimental results, it is realised that not all the best measurement points were always selected or maybe that some of them need not have been measured at all, and the same applies to suspension and excitation position.

One of the approaches used to select measurement points is to show visually a preliminary estimate of the theoretical mode shapes and the corresponding natural frequencies of the structure and, on the basis of these data, to select the optimum suspension, excitation and measurement positions. This is not a strongly-recommended approach since any prior knowledge of the values for modal parameters of a theoretical model can influence measurements and, in extreme

cases, the experimentalist can end up tuning the experimental set-up in order to measure values of modal parameters which are close to the theoretically-predicted ones.

One major goal of planning a modal test is determination of the data requirements for a particular test. Depending on the final purpose of the experimental results, such as: (i) measuring the structure's natural frequencies only; (ii) correlation with theoretical predictions, or (iii) updating of a theoretical model of a structure, the number and position of the measurement points will be decided, but in any case it is desirable that an optimum set of points is selected. This means that before any actual selection of the measurement points is made, an evaluation of all degrees-of-freedom has to be made in order to select the minimum number and the best choice for suspension, excitation and measurement points.

There are limited numbers of measurement positions and modes that can be measured during a modal test and, in general, test data tend to be incomplete by comparison with theoretical data. There are two main sources of incompleteness in the experimental data obtained from modal tests; the extent of the measured frequency range (or number of measured modes) and the number of measurement degrees-of-freedom. The number of the measured degrees-of-freedom mainly depends on the final application of the experimental results and/or the number of measured modes, although most correlation and updating methods require that the number of measured degrees-of-freedom is greater than the number of meaured modes.

3.2. Signal Processing and Modal Analysis Mathematical Basics

Signal processing [32] is based on the principle that any signal which is periodic in time can be represented as a series of harmonics with different amplitudes and frequencies as indicated by the following expression

$$x(t) = \frac{a_0}{2} + \sum_{n=1}^{\infty}\left(a_n \cos\left(\frac{2\pi nt}{T}\right) + b_n \sin\left(\frac{2\pi nt}{T}\right)\right) \qquad (3.2\text{-}1)$$

where T is the period of the time signal.

In fact, expression (3.2-1) provides the transformation between the time and frequency domains for a periodic time signal, $x(t)$, where the coefficients a_n and b_n can be found as functions of a known $x(t)$ via the following expressions:

$$a_n = \left(\frac{2}{T}\right)\int_0^T x(t)\cos\left(\frac{2\pi nt}{T}\right)dt \qquad (3.2\text{-}2a)$$

$$b_n = \left(\frac{2}{T}\right)\int_0^T x(t)\sin\left(\frac{2\pi nt}{T}\right)dt \qquad (3.2\text{-}2b)$$

In the case that $x(t)$ is discretised and defined only at a set of N time points, $t_k, (k = 1, N)$, the Discrete Fourier Transformation (DFT) has to be employed which is defined as

$$x_k\left(= x(t_k)\right) = \frac{a_0}{2} + \sum_{n=1}^{N/2}\left(a_n\cos\left(\frac{2\pi nt_k}{T}\right) + b_n\sin\left(\frac{2\pi nt_k}{T}\right)\right) \quad k = 1,\ldots N\ (N\,even) \qquad (3.2\text{-}3)$$

The coefficients a_n and b_n are called Fourier or Spectral coefficients for the function, $x(t)$. The measurement signals (accelerometer and force transducer outputs) are in the time domain and the corresponding spectral properties are in the frequency domain.

During measurement, the accelerometer and force time signals are digitised and recorded for a set of N evenly-spaced time values in the period, T. Assuming that the measured signal is periodic in time T, there is a simple relationship between the frequency range $(0 - \omega_{\max})$ and the resolution of the analyser with the number of discrete values (N) and sample length (T), described by the following expressions:

$$\omega_{\max} = \frac{1}{2}\left(\frac{2\pi N}{T}\right) \qquad (3.2\text{-}4)$$

$$\Delta\omega = \frac{2\pi}{T} \qquad (3.2\text{-}5)$$

The above equations show the limitation when measurement of the higher frequency responses is attempted.

The basic equation for solution of the Fourier or Spectral coefficients is of the following form:

$$\begin{Bmatrix} x_1 \\ . \\ . \\ x_N \end{Bmatrix} = \begin{bmatrix} 0.5\cos(2\pi/T)... \\ ... \\ ... \\ 0.5\cos(2N\pi/T) \end{bmatrix} \begin{Bmatrix} a_0 \\ a_1 \\ b_1 \\ . \end{Bmatrix} \tag{3.2-6}$$

Discrete Fourier Transform analysis can lose on accuracy when applied to experimental data and this loss of accuracy can magnify during the analysis if transient signals are not properly treated. These effects are known as (a) aliasing and (b) leakage. The treatment methods for the above features are windowing, zooming, averaging and filtering. For more details about these properties of the Discrete Fourier Transformation can be found in reference [2],[32].

The Frequency Response Function (FRF) is defined as the ratio of the Fourier Transforms of the response and the excitation signal, or, mathematically stated:

$$H_{ij}(\omega) = \frac{X_i(\omega)}{F_j(\omega)}, \quad F_k(\omega) = 0, k = 1,...N, k \neq j \tag{3.2-7}$$

Once the measured FRFs are obtained by experiment, they need to be further analysed in order to extract the modal parameters, which consists of the natural frequencies, damping factors and mode shapes. There are several methods for extraction of the modal parameters from these response data and selection of a method for the analysis depends on the influence of damping on the FRFs, the presence of close modes etc.. It is important to be aware that some modal parameter extraction methods do not consider the influence of the out-of-range modes while others compensate for the residual terms and this indicates that the response model is more general than the equivalent modal model. Having estimated the modal parameters of individual FRFs, derivation of the experimental mode shapes is relatively simple and animation of the experimental modes can be performed.

3.3. Pre-Test Planning Mathematical Background

3.3.1. Time and Frequency Domains Relationship

The steady-state response in the DOFs of a structure which is subjected to a number of external harmonic forces $\{f(t)\}=\{F(\omega)\}e^{i\omega t}$ will be at a frequency equal to the excitation frequency, ω, and can be expressed as $\{x(t)\}=\{X(\omega)\}e^{i\omega t}$. After substitution of these expressions into the equation of motion, (3.3.1-1), the relationship between the amplitudes of the external forces and the amplitudes of displacements is obtained as shown in expressions (3.3.1-2) and (3.3.1-3). Here, the structural damping is used in order to keep forthcoming equations simpler, but the whole discussion is equally valid for the case of more general viscous damping.

$$[M]\{\ddot{x}(t)\}+i[D]\{x(t)\}+[K]\{x(t)\}=\{f(t)\} \tag{3.3.1-1}$$

$$\left(-\omega^2[M]+i[D]+[K]\right)\{X(\omega)\}e^{i\omega t}=\{F(\omega)\}e^{i\omega t} \tag{3.3.1-2}$$

$$\{X(\omega)\}=[\alpha(\omega)]\{F(\omega)\} \tag{3.3.1-3}$$

where $[\alpha(\omega)]=\left(-\omega^2[M]+i[D]+[K]\right)^{-1}$ (3.3.1-4)

is the receptance matrix of the system, whose general term $\alpha_{jk}(\omega)$ can be written as a function of the natural frequencies and mode shapes of the system in the following form:

$$\alpha_{jk}(\omega)=\sum_{r=1}^{N}\frac{\phi_{j,r}\phi_{k,r}}{\omega_r^2-\omega^2+i\eta_r\omega_r^2} \tag{3.3.1-5}$$

Assuming that the system is being excited at a frequency, which is equal to the natural frequency of mode r, ω_r, then considering only the most significant term in the series in expression (3.3.1-5) results in:

$$\alpha_{jk}(\omega_r)\approx\frac{\phi_{j,r}\phi_{k,r}}{i\eta_r\omega_r^2} \tag{3.3.1-6}$$

Taking this result back into expression (3.3.1-3) for the amplitudes of vibration, it can be seen that the term $\frac{\phi_{i,r}\phi_{j,r}}{i\eta_r\omega_r^2}$ can be associated with a displacement quantity because it is directly proportional to the displacement amplitude vector, i.e.,

$$X(\omega_r) \propto \frac{\phi_{i,r}\phi_{j,r}}{i\eta_r\omega_r^2} \tag{3.3.1-7}$$

Displacement, velocity and acceleration, respectively, can be expressed as the following:

$$x(t) = X(\omega_r)e^{i\omega_r t} \tag{3.3.1-8}$$

$$\dot{x}(t) = i\omega_r X(\omega_r)e^{i\omega_r t} \tag{3.3.1-9}$$

$$\ddot{x}(t) = -\omega_r^2 X(\omega_r)e^{i\omega_r t} \tag{3.3.1-10}$$

Substituting (3.3.1-7) into the expressions for displacement (3.3.1-8), velocity (3.3.1-9) and acceleration (3.3.1-10), the following relationships for vibration amplitudes of these quantities are obtained:

$$\textit{Displacement Amplitude} \propto \frac{\phi_{i,r}\phi_{j,r}}{\omega_r^2} \tag{3.3.1-11}$$

$$\textit{Velocity Amplitude} \propto \frac{\phi_{i,r}\phi_{j,r}}{\omega_r} \tag{3.3.1-12}$$

$$\textit{Acceleration Amplitude} \propto \phi_{i,r}\phi_{j,r} \tag{3.3.1-13}$$

The damping values in expression (3.3.1-7) have been omitted in expressions (3.3.1-11) to (3.3.1-13) due to the difficulty of predicting damping parameters at the stage of a preliminary theoretical analysis. Since damping can only reduce structural response at resonant frequencies, this omission of damping assumes maximum response of the structure during measurements. If, however, for any reason the damping needs to be included in the planning of modal tests, it is recommended to specify the same value of damping coefficient to every mode. Inclusion of different damping coefficients in this analysis will give different weighting to modes in

consideration and it would consequently make the whole analysis sensitive to damping values which are extremely difficult to predict.

3.3.2. Definitions for the Average Values of Displacement, Velocity and Acceleration Amplitudes

In the previous section it was shown how to interpret modal constants of a mode regarding displacement, velocity and acceleration, assuming vibration in that mode only. However, in many practical situations, the excitation force is of an impulsive or random type and this excites many modes into vibration. In the case of a general transient excitation force, the response of the structure (the solution of the equation described in expression (3.3.1-1)) can be expressed as a linear summation of all the excited modes in the following form:

$$\{x(t)\} = \left\{ \sum_{j=1}^{N} \left(\xi_j \{\psi\}_j e^{(-\delta_j + i\omega_j)t} + \xi_j^* \{\psi\}_j^* e^{(-\delta_j - i\omega_j)t} \right) \right\} + \{x_p(t)\} \qquad (3.3.2\text{-}1)$$

where the vector $\{x_p(t)\}$ is a particular solution of the ordinary differential equation written in expression (3.3.1-1), and this vector is of the same form as the function of the excitation force $\{f(t)\}$.

Alternatively, the solution can be written in the following form:

$$\{x(t)\} = \sum_{j=1}^{N} A_j \left| \{\psi\}_j \right| e^{-\delta_j t} \{\cos(\omega_j t + B_j \angle(\psi_j))\} + \{x_p(t)\} \qquad (3.3.2\text{-}2)$$

where the coefficients A_j and B_j (or complex coefficients $\xi_j = A_j + iB_j$) are determined from the initial conditions described in the following expressions:

$$\{x(t_0)\} = \{x_0\} \qquad (3.3.2\text{-}3)$$

$$\{\dot{x}(t_0)\} = \{\dot{x}_0\} \qquad (3.3.2\text{-}4)$$

When a structure is forced to vibrate under one excitation force pattern, the amplitude of vibration for each DOF in the time domain is a function of some parameters of the structure (mass, stiffness and damping) and the particular excitation force. The amplitudes of vibration in the time domain are determined by

the natural frequencies and mode shapes which are simple functions of the structural and geometrical properties (mass, stiffness and damping) of the structure under investigation. This shows that for a particular excitation there will be one pattern of amplitudes of vibration in the time domain which is determined by the contributions of all the modes in the frequency domain. Therefore, in order to predict the average response at a DOF for displacement of the structure for a general excitation which would excite modes over a wide frequency range, the Average Driving DOF Displacement (ADDOFD) level can be defined as the average sum of all contributing modes as shown in the following expression:

$$ADDOFD(j) = \sum_{r=1}^{m} \frac{\phi_{jr}^2}{\omega_r^2} \qquad (3.3.2\text{-}5)$$

Similarly, the Average Driving DOF Velocity (ADDOFV) parameter is defined by:

$$ADDOFV(j) = \sum_{r=1}^{m} \frac{\phi_{jr}^2}{\omega_r} \qquad (3.3.2\text{-}6)$$

and it should be noted that the ADDOFV coefficient is the same as the Average Driving Point Residue (ADPR) coefficient, described in detail in reference [33].

Finally, the Average Driving DOF Acceleration coefficient (ADDOFA) describes the average acceleration of the response and the parameter can be defined by the following expression:

$$ADDOFA(j) = \sum_{r=1}^{m} \phi_{jr}^2 \qquad (3.3.2\text{-}7)$$

The reason for assigning the label 'average' to all the three above-defined parameters is because there are several modes which contribute to the whole response signal. Usually, when the structure is excited by an impulsive force, not all modes contribute to the response because some of the modes from the excitation frequency range are not excited for some reason (such as a poor choice of the excitation position).

The ADDOFD, ADDOFV and ADDOFA parameters define the 'average' amplitudes of the imaginary response caused by an hypotetically impulsive excitation which

would act on all DOFs simultaneously and therefore would excite all modes from the excitation frequency range.

3.4. Optimum Suspension Positions

Determination of the optimum suspension positions is a process of finding an arrangement such that particular boundary conditions can be achieved during testing. In many practical situations, the boundary conditions sought during testing are free-free and these are best approximated by suspending the structure on soft springs. The major difficulty is to find positions on the structure where these suspension springs should be attached, since any connection to the structure can interfere with its response and produce different dynamic parameters to those which should apply for the true free-free boundary conditions.

3.4.1. Testing for Free-Free Boundary Conditions

The free-free boundary conditions are the most common type of boundary conditions in practice. Theoretically, under these boundary conditions the structure is not connected to any other object and it is clear that this cannot be achieved in practice, apart from few situations where some form of non-contact force field is established to position test piece (e.g. magnetic field). Another situation where theoretically free-free boundary conditions could be achieved is testing in the zero gravity space. These special situations of achievable free-free boundary conditions without connection of the test piece to other objects are extremely rare and limited that their significance has a pure academic character.

In order to simulate free-free boundary conditions using some form of connection of the test piece to other objects, it would be necessary that each attachment location is situated on or very close to the nodal lines of all excited modes during testing. The nodal line of a mode is defined as a set of all DOFs inside geometrical domain of the structure which have zero amplitudes of vibration. When the structure is excited, several modes contribute to the time response, but since these modes contribute at different frequencies and they may have arbitrary phase difference between them (which is determined by the initial conditions, (3.3.2-3) and (3.3.2-4)), there is no guarantee that it is possible to find locations on the structure which have a total response equal to zero. If such locations existed then they would be the optimum suspension locations to achieve free-free boundary conditions. Hence, locations

which have minimum total response seem to be the optimum choice for accomplishment of free-free boundary conditions. Since the 'average' amplitude of total response (in terms of displacements) is defined by ADDOFD, this parameter can be used to find optimum suspension locations.

The optimum suspension locations for modal testing are generally to be found in the regions of a structure where the average displacement is the lowest, i.e. in those regions which are defined by low values of the ADDOFD coefficient. Unfortunately, as far as a suspension locations are concerned, there are physical limitations that restrict how and where the structure can be suspended and, usually, the number of possibilities for practical suspension attachments is small.

$$Optimum \quad suspension = \min_{j}(ADDOFD(j)) \qquad (3.4.1\text{-}1)$$

The use of the ADDOFD function to find optimum locations is conservative since it assumes the worst case scenario, which is that all modes contribute to the total response. The probability of this happening in practice is low and any degrees-of-freedom which have a low value of the ADDOFD coefficient when all modes are contributing can have only even lower values if some modes are not excited, as is the case in many practical situations.

3.5. Optimum Driving Positions

3.5.1. General Requirements for Optimum Excitation Positions

There are two main types of excitation for structures in respect to the input of excitation energy: (i) the non-destructive impact from an external source and (ii) the non-destructive attachment to an external source. Apart from these excitations with physical connections to the structure, there are some other excitation techniques which do not require physical contact between the test structure and the source of excitation and these include: (i) excitations by magnetic field and (ii) excitations by sound waves or air pressure.

The process of energy transfer from an excitation source to a structure's modes is a rather complicated process but there are a few major features which characterise it. Whether an excitation is impact- or continuous force-like, the excitation must not cause any permanent damage to the tested structure, not even in the vicinity of the

impact locations. The most common damage which occurs during a modal test is when a hammer excitation is used to excite high-frequency modes. In order to avoid double-hit effects and to have short enough impact times to excite the high-frequency modes, it is necessary to use a hard metal tip on the hammer. The structure should be checked during the test to make sure there are no permanent deformations caused by the metal tip of the hammer. Another example of possible damage during modal testing is the use of a shaker on lightly damped structures near resonant frequencies. This can cause such large deformations at frequencies close to and at resonances that these can consequently cause permanent damage to structures.

Process of Energy Transfer during Excitation

The exact process of energy transfer from the excitation source to each mode of the structure involves complex energy transformations during the vibration process. When a structure is excited by an impact, for instance, a certain amount of energy is transferred from the excitation source to the structure. If we assume that there is no loss of energy in plastic deformations at the excitation position, or in sound and heat during the impact process, then all energy input to the structure will be transferred into strain and/or kinetic energy at the vicinity of the excitation position. This kinetic and strain energy will initiate vibrations of the adjacent degrees-of-freedom and that will consequently cause generation of mechanical waves and their distribution throughout the domain of the whole structure. These waves will reflect at the boundaries of the structure and will interact among themselves until some kind of steady-state wave transmission pattern is established. In the frequency domain the general response of the structure can be separated into several frequency responses or modes. Since the speed of both the longitudinal and transverse waves in most practical materials is quite high, this will make the transmission time of the both waves a short period of time, it can be assumed that the distribution of energy throughout the domain of a structure and the establishment of all modes is almost instantaneous.

There are many factors which determine the distribution of energy into the modes, such as: (i) the level of damping of the structure, (ii) the elastic properties of the structure, (iii) the mass distribution, (iv) the homogeneouisity of the density and elastic properties throughout the domain, (v) the isotropy of the structural

properties, (vi) any known or unknown imperfections such as cracks, pre-stress levels and deformations and (vii) other factors like current temperature, etc..

In reality, it is impossible to predict effects of all these factors accurately in order to optimise the excitation position for a modal test, but it is known that one of the factors which determines the amount of energy received by each mode is the relative position of an excitation source to each mode shape. It is known that if a source of excitation is close to or at a nodal line of a mode, then little or no energy will be transferred to that mode which, consequently, will not be registered in the measured response. Other commonly-observed effects of the excitation position upon the whole vibration process during a modal test are so-called 'double-hit' by a hammer or interference caused by interaction between the shaker and the structure.
Several new techniques to select an optimum driving position for the excitation of as many modes as possible within a specified frequency range are presented in the following sections.

3.5.2. Hammer Excitation

Apart from a general requirement to avoid excitation positions near any nodal lines on the structure, there is a common experience that regions of high average velocity should be avoided since hitting in the vicinity of these positions can cause the so-called 'double-hit' effect. Therefore, the ADDOFV parameter can be of help when deciding where not to excite a structure using a hammer, and regions of high values of this parameter should be avoided.

3.5.3. Shaker Excitation

The general requirement for avoiding excitation close to any nodal lines applies also for excitation using a shaker, but it is also necessary to minimise the interference of a shaker with a structure during vibration testing. Since a shaker is, in fact, essentially a simple mass-spring-damper attached to the test structure, the least interference of the shaker will have or would occur if the shaker is attached to a region where the average acceleration, the ADDOFA parameter, has a minimum value. Therefore, the ADDOFA parameter can be used when deciding where not to attach a shaker to a structure.

3.5.4. Optimum Driving Point (ODP) Technique

The Optimum Driving Point (ODP) technique is designed to identify positions which are close to or on the nodal lines of any mode within a specified frequency range. Hence, the values of the modal constants for degrees-of-freedom which are close to or on nodal lines of a mode will be close to zero. In order to describe the position of any DOF in respect to the position of nodal lines of all modes, modal constants for all selected modes at each DOF are multiplied together and the resulting value is a coefficient called the ODP parameter for each DOF. Mathematically, the ODP method is based on the following expression:

$$ODP(i) = \prod_{r=1}^{m} \left\| \phi_{i,r} \right\| \qquad (3.5.4\text{-}1)$$

The DOFs which have ODP value close to zero are the DOFs which are close to or on a nodal line and, consequently, should be avoided as possible excitation positions. Contrary to the above-mentioned DOFs, the positions which have values of the ODP parameter which are different to zero are those which should be considered as possible excitation positions since they are not close to the nodal lines of any mode in the specified frequency range.

3.5.5. Non-Optimum Driving Point (NODP) Technique

The NODP technique is based on a similar principle for assessment of the optimum driving point to that used for the ODP technique: the method defines a parameter for each DOF which describes how close that DOF is to a nodal line of any mode within a specified frequency range. This method selects the minimum absolute value of the modal constants for all selected modes for a DOF and defines that value as the NODP parameter for that DOF. Mathematically, the method is based on the following expression:

$$NODP(i) = \min_{r} \left(\left\| \phi_{i,r} \right\| \right) \qquad (3.5.5\text{-}1)$$

It can be seen from the above expression that this parameter does not average all the modal constants but shows only the lowest-valued from all modes under consideration. The values of this parameter do not show how good a particular position is as a driving point, but they show how poor each DOF is in that role.

Therefore, if a DOF has a low value of the NODP parameter, this means that this DOF is not suitable as a possible driving position. In contrast, if a DOF has a high value of NODP, this does not necessarily mean that this DOF is automatically the best driving position. This is the reason for naming this method the Non-Optimum Driving Point (NODP), because it shows which points are **not** optimum rather than assessing an average value for all modes under consideration.

3.5.6. Determination of the Optimum Driving Positions

The ODP and NODP parameters essentially consider only positions of the nodal lines of all modes under consideration in order to discriminate DOFs as potentially good or bad excitation positions. These techniques do not consider the actual energy transfer from the excitation source to a test piece in order to select the optimum excitation location. Although it is very important that the excitation position is not set close to or on any of the nodal lines, there are some additional effects which have to be taken into account when selecting this position. If a hammer excitation is to be used, then there is a possibility of a double-hit if the excitation is applied inside a high-velocity region of a structure. If, however, a shaker is used for excitation, then there is a requirement for the interference of the shaker with the structure being tested to be minimised. Since a shaker can be considered as a simple mass-spring-damper attached to the test structure, it is clear that the least interference would be caused if the shaker is attached to the structure in the region where the average acceleration is lowest.

ODP-Based Methods

ODP-based methods use the ODP technique and any of the three average response parameters defined in section 3.3.2 to evaluate the optimum driving positions by using the following expressions:

$$ODP-D(j)=\frac{ODP(j)}{ADDOFD(j)}=\frac{\prod_{r=1}^{m}\left|\phi_{j,r}\right|}{\sum_{r=1}^{m}\frac{\phi_{j,r}^2}{\omega_r^2}} \qquad (3.5.6\text{-}1)$$

$$ODP-V(j)=\frac{ODP(j)}{ADDOFV(j)}=\frac{\prod_{r=1}^{m}\left|\phi_{j,r}\right|}{\sum_{r=1}^{m}\frac{\phi_{j,r}^2}{\omega_r}} \qquad (3.5.6\text{-}2)$$

$$ODP-A(j)=\frac{ODP(j)}{ADDOFA(j)}=\frac{\prod_{r=1}^{m}\left\|\phi_{j,r}\right\|}{\sum_{r=1}^{m}\phi_{j,r}^2} \qquad (3.5.6\text{-}3)$$

NODP-Based Methods

NODP-based methods use the NODP technique and any of the three average response parameters defined in section 3.3.2 to evaluate the optimum driving positions by using the following expressions:

$$NODP-D(j)=\frac{NODP(j)}{ADDOFD(j)}=\frac{\min_r\left(\left\|\phi_{j,r}\right\|\right)}{\sum_{r=1}^{m}\frac{\phi_{j,r}^2}{\omega_r^2}} \qquad (3.5.6\text{-}4)$$

$$NODP-V(j)=\frac{NODP(j)}{ADDOFV(j)}=\frac{\min_r\left(\left|\phi_{j,r}\right|\right)}{\sum_{r=1}^{m}\frac{\phi_{j,r}^2}{\omega_r}} \qquad (3.5.6\text{-}5)$$

$$NODP-A(j)=\frac{NODP(j)}{ADDOFA(j)}=\frac{\min_r\left(\left|\phi_{j,r}\right|\right)}{\sum_{r=1}^{m}\phi_{j,r}^2} \qquad (3.5.6\text{-}6)$$

3.5.7. Application of the ODP and NODP Techniques

Both the ODP and NODP techniques have been applied to several test case structures in order to identify the optimum driving point(s) for modal testing. A simple plate structure was used to demonstrate the application of the proposed methods for the optimisation of modal testing. It should be noted that in majority cases presented here regions indicated in RED are not the optimum as defined by the methods used.

Simple Plate

The geometry of the simple plate used as a test case can be seen in Figure 3.5.7-1. We shall assume that a modal test is to be performed on the structure and that all modes in the range 0-200 Hz should be measured. Preliminary analysis predicts several modes in that range, and these are given in Figure 3.5.7-1. Since the prediction of the preliminary mode shapes could be incomplete, i.e. not all modes from the frequency range might be predicted, another two modes with higher natural frequencies were included in the analysis to allow for the possibility of inaccurate predictions. All mode shapes used in the analysis are out-of-plane modes.

The Average Displacement, Velocity and Acceleration Estimates

Estimates of the average displacement, velocity and acceleration quantities are indicated by the values of the ADDOFD, ADDOFV and ADDOFA parameters, and are given in Figures 3.5.7-2, -3 and -4, respectively. All three contour diagrams indicate that the edges of the plate, and particularly the corners have higher average response levels than elsewhere, while the inner area of the plate has low average response level. There is a significant difference between the contours for the average displacement, velocity and acceleration parameters in the size of the central region of low response values. It can be seen from the pictures that the average acceleration contours have the largest area of low signal values, while the average displacement contour has the smallest area. It should be noted here that the optimum suspension position of the structure is considered to be in the area of the lowest average displacement values, which is clearly defined in Figure 3.5.7-2. The average velocity contours can help to identify the regions where the possibility of the double-hit by a hammer

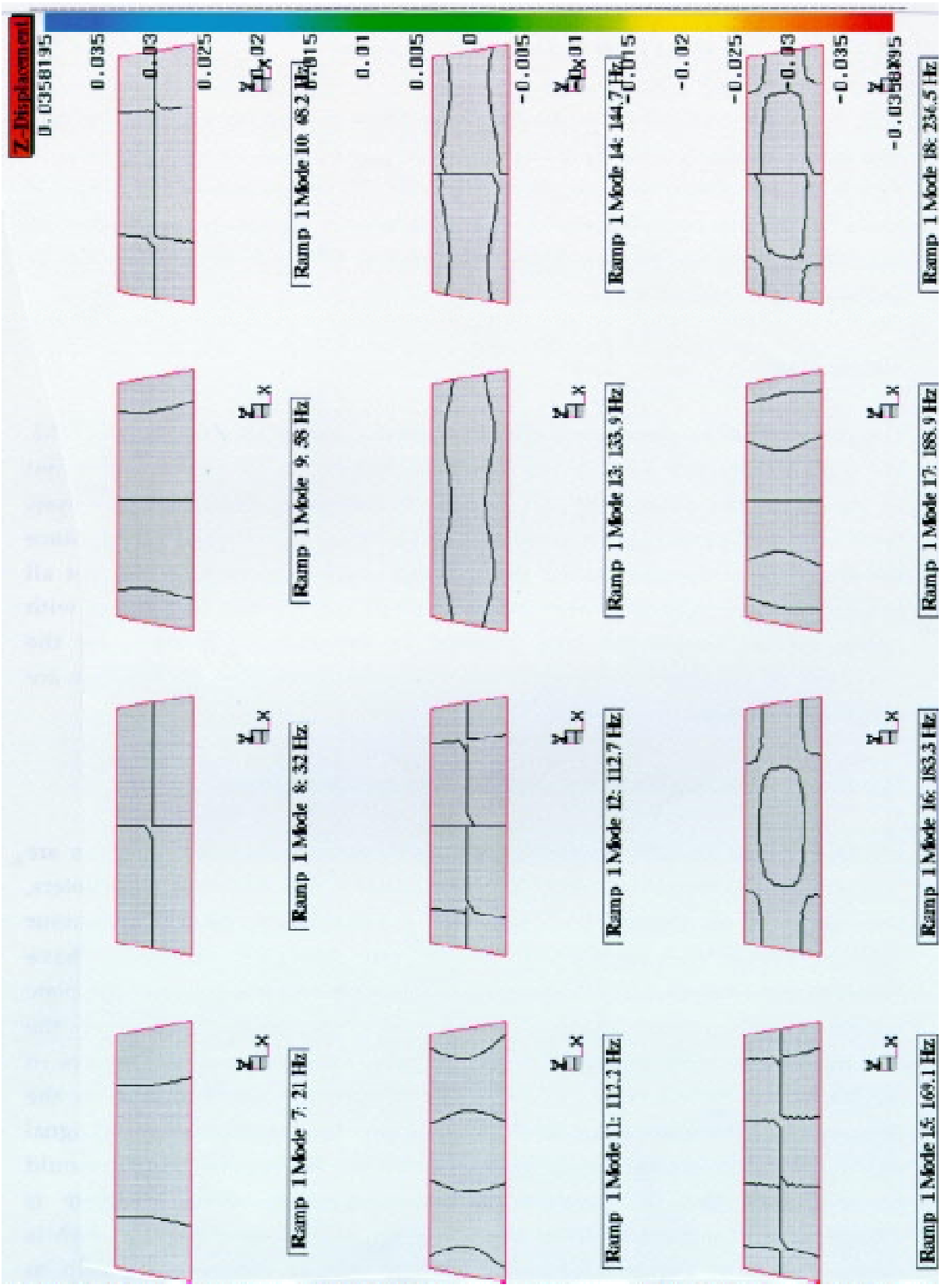

Figure 3.5.7-1. Mode Shape Nodal Lines of Simple Plate.

excitation is high and should be avoided. The average acceleration contours can help to find the best place to attach a shaker to excite the structure as well as suitable places for transducer locations where the average response signal strength is high, in order to minimise the noise-to-signal ratio and to improve the accuracy of the test.

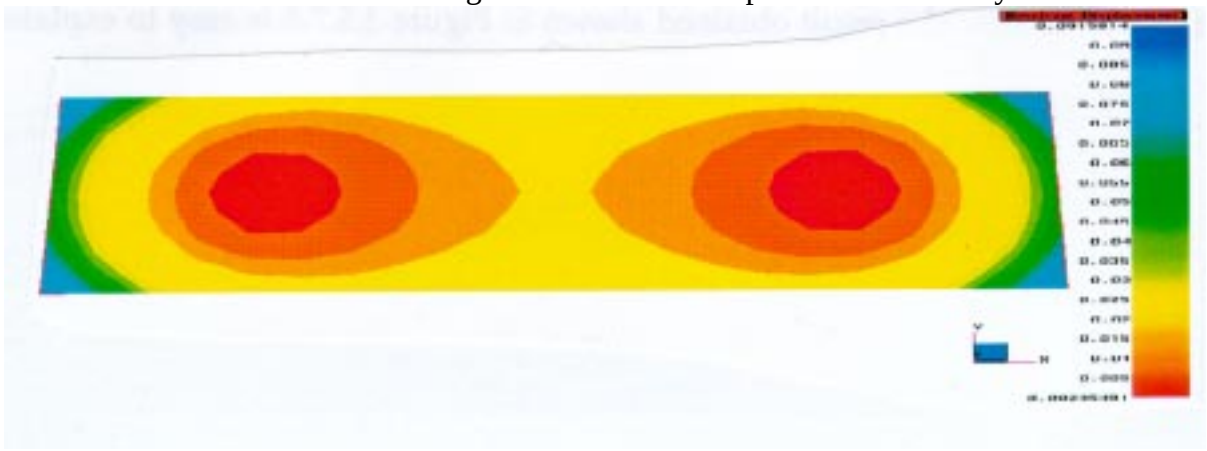

Figure 3.5.7-2. ADDOFD of Simple Plate.

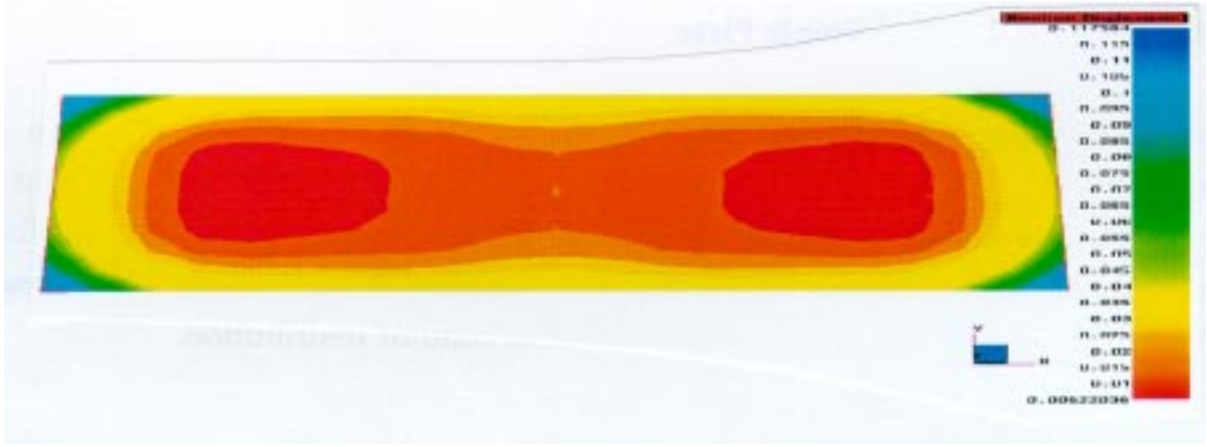

Figure 3.5.7-3. ADDOFV of Simple Plate.

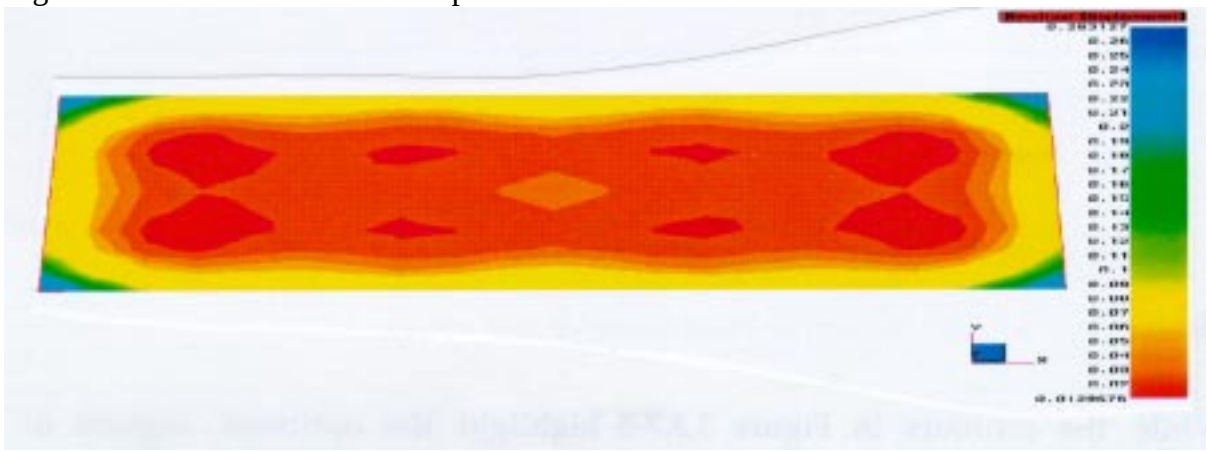

Figure 3.5.7-4. ADDOFA of Simple Plate.

The Optimum Driving Point (ODP) Application

The ODP method was applied to this structure in order to identify the optimum excitation positions. Since this method considers only the nodal lines of the included modes, the result obtained shown in Figure 3.5.7-5 is easy to explain.

Figure 3.5.7-5. ODP of Simple Plate.

After inspection of the nodal lines shown in Figure 3.5.7-1, it can be seen that there are no nodal lines which pass near the corners of the structure and the values of the modal constants are highest at these corners. However, the linear contour scaling in Figure 3.5.7-5 has been changed to a logarithmic scaling in Figure 3.5.7-6 and this gives a rather different contour distribution.

Figure 3.5.7-6. ODP of Simple Plate (logarithmic scale).

While the contours in Figure 3.5.7-5 highlight the optimum regions of the structure for excitation, those in Figure 3.5.7-6 highlight the regions of the structure which are

the worst for excitation. The result presented in Figure 3.5.7-6 can also be explained by analysing the nodal lines given in Figure 3.5.7-1 where it can be seen that almost all modes have some nodal lines passing near the regions indicated in Figure 3.5.7-6. It can therefore be concluded that the scaling of the ODP result can give a rather different picture of the ODP distribution throughout the structure domain, and both linear and longitudinal scaling is recommended in practical situations.

The ODP parameter was also used in conjunction with the average displacement, velocity and acceleration in order to help select the optimum driving positions, as suggested in section 3.5.6. The ODP-D results are given in Figures 3.5.7-7 and -8, for linear and logarithmic scaling, respectively.

Figure 3.5.7-7. ODP-D of Simple Plate.

Figure 3.5.7-8. ODP-D of Simple Plate (logarithmic scale).

Figures 3.5.7-9 and -10 show the ODP-V , while Figures 3.5.7-11 and -12 give the ODP-A parameter; in both cases, both linear and logarithmic scales of the results are shown. However, by analysing all the results given in Figures 3.5.7-7 to -12, it can be seen that there is no significant difference in any presented results from the original ODP parameter values.

Figure 3.5.7-9. ODP-V of Simple Plate.

Figure 3.5.7-10. ODP-V of Simple Plate (logarithmic scale).

Figure 3.5.7-11. ODP-A of Simple Plate.

Figure 3.5.7-12. ODP-A of Simple Plate (logarithmic scale).

The Non-Optimum Driving Point (NODP) Application

The NODP method was applied to this test case and the results are given in Figures 3.5.7-13 and -14 for linear and logarithmic scales, respectively.

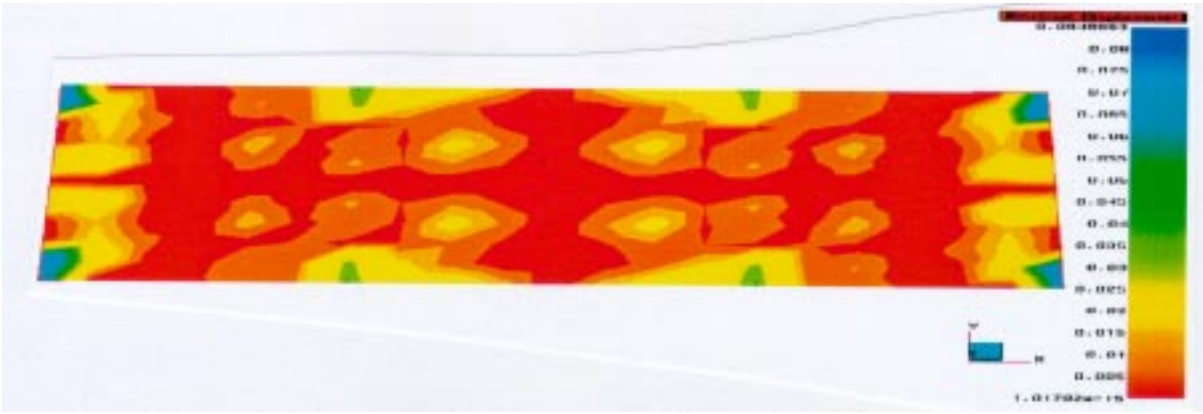

Figure 3.5.7-13. NODP of Simple Plate.

Figure 3.5.7-14. NODP of Simple Plate (logarithmic scale).

The linear scale contours of the NODP parameter values indicate several regions of the structure where the NODP parameter values are different to zero. The regions of the structure where the NODP values are close to zero are the regions which are definitely not suitable for excitation. This parameter indicates the regions of the structure which should not be selected as excitation positions but the rest of the structure, in which the values of the NODP parameter are greater than zero, should not be taken as necessarily being good excitation positions. As expected, the log scale of the NODP parameter results indicates that the two central lines are of very low value compared with the rest of the structure.

Application of the NODP method in conjunction with the average displacement, velocity and acceleration parameters was carried out in order to determine the optimum excitation positions using these criteria. Division of the NODP parameter by the ADDOFD parameter gives new contours, as shown in Figures 3.5.7-15 and -16 for linear and log scales, respectively.

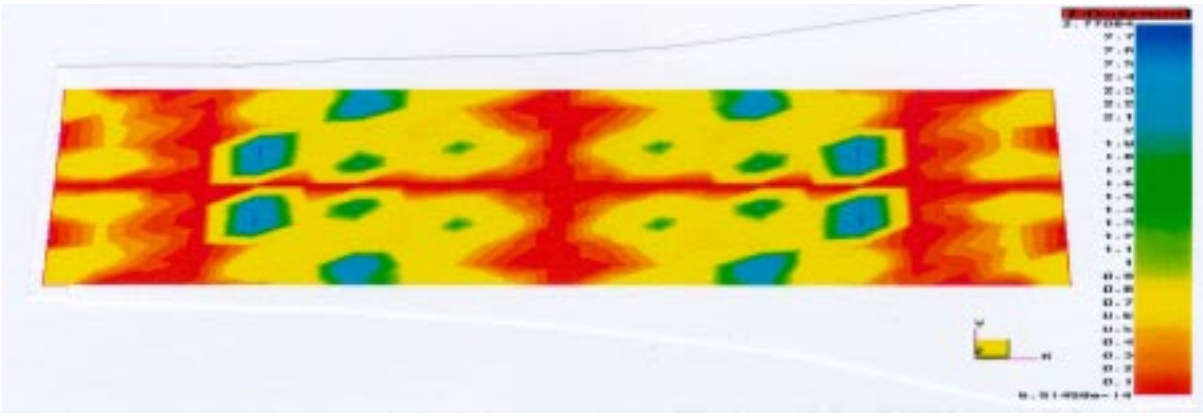

Figure 3.5.7-15. NODP-D of Simple Plate.

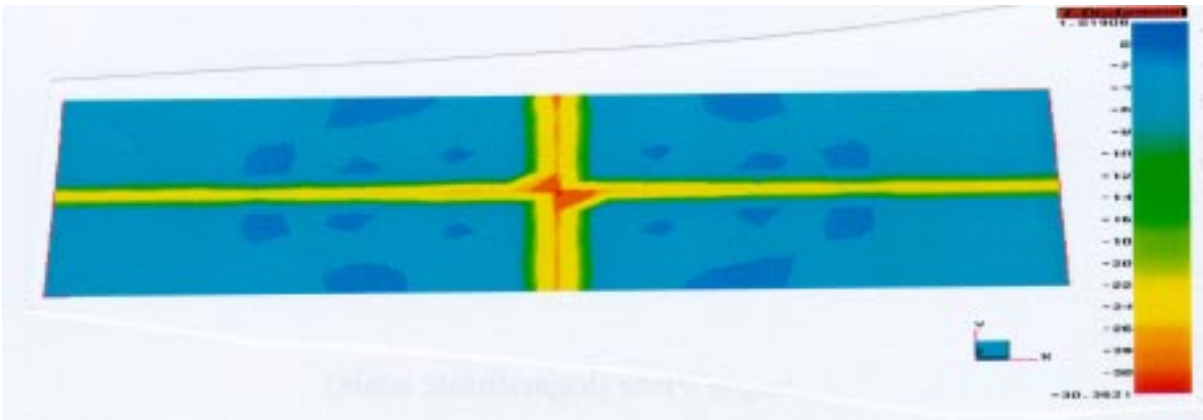

Figure 3.5.7-16. NODP-D of Simple Plate (logarithmic scale).

Analysing the nodal lines of all modes given in Figure 3.5.7-1, it can be concluded that there are no nodal lines near the indicated excitation locations; furthermore, considering the distribution of the average displacement value, it can be concluded that the ADDOFD values are low at these locations. The log scale of NODP-D plots indicate again the regions of the structure where the concentration of nodal lines is high for the included modes, and the excitation position should not be placed close to these central regions of the structure, as shown in Figure 3.5.7-16.

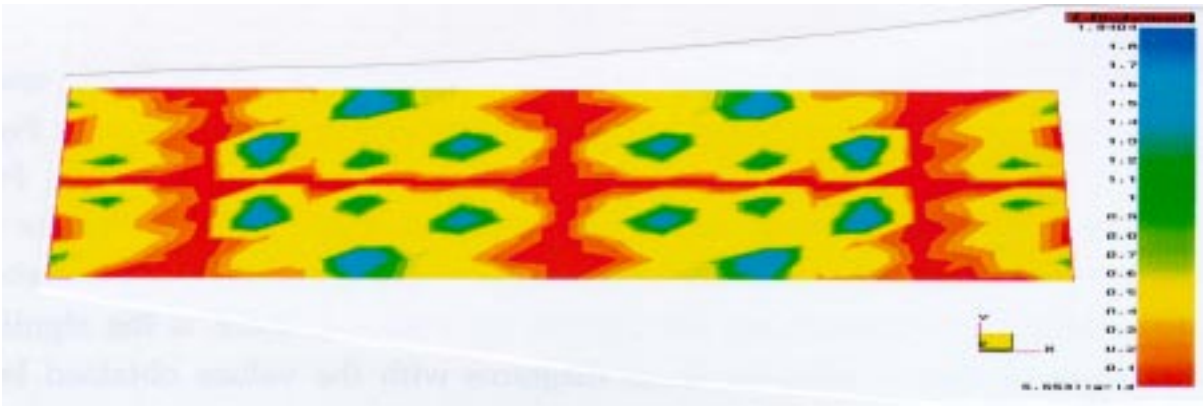

Figure 3.5.7-17. NODP-V of Simple Plate.

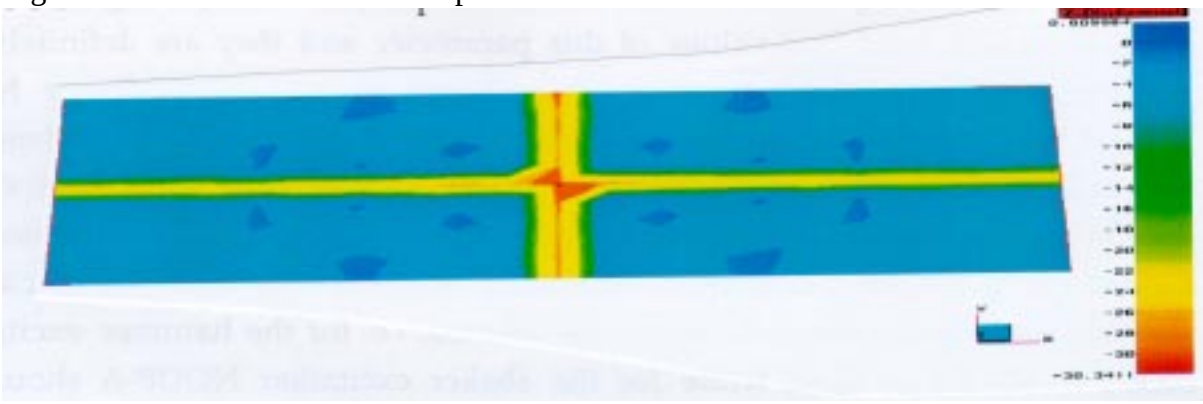

Figure 3.5.7-18. NODP-V of Simple Plate (logarithmic scale).

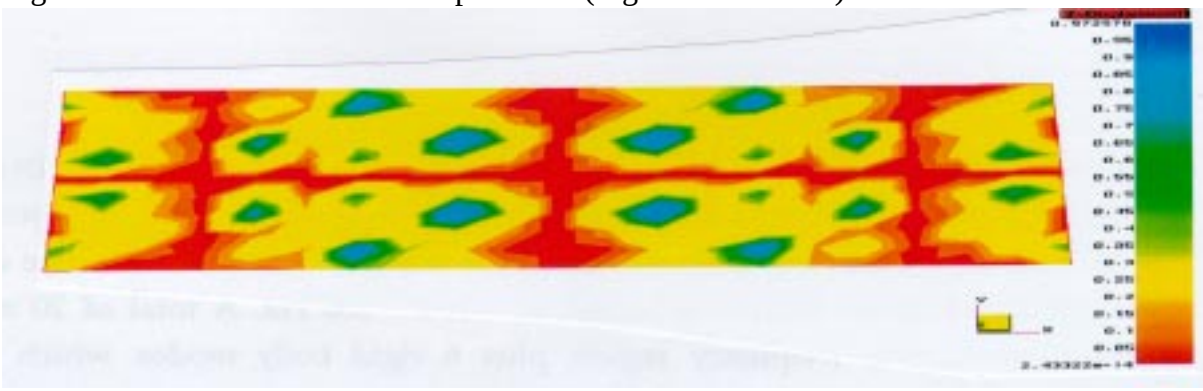

Figure 3.5.7-19. NODP-A of Simple Plate.

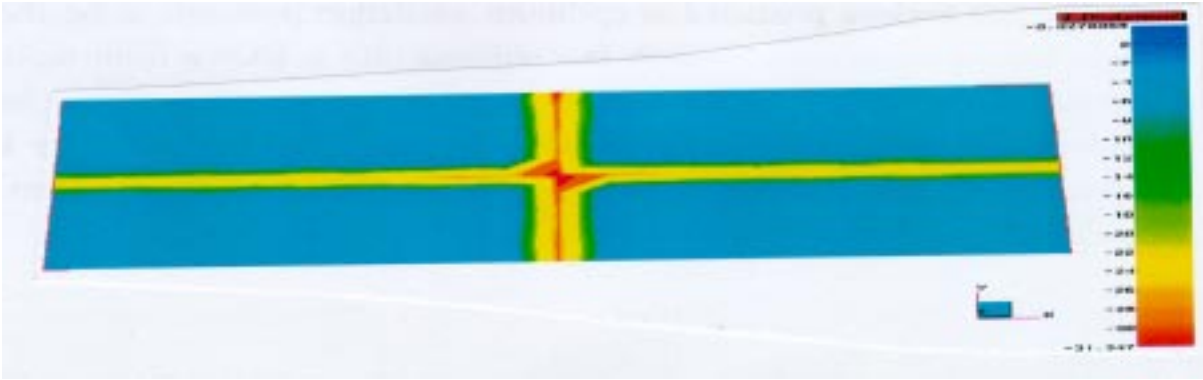

Figure 3.5.7-20. NODP-A of Simple Plate (logarithmic scale).

The NODP-V parameter is shown in Figures 3.5.7-17 and -18 for linear and log scaling respectively, produced almost identical results to those shown in Figures 3.5.7-15 and -16 for NODP-D. Also, the NODP-A parameter as shown in Figure 3.5.7-19 and 3.5.7-20 indicates very similar results to those given in Figures 3.5.7-15 to -18. Although the contours obtained by dividing the NODP parameter by three different parameters are similar but not identical, there is the significant difference of how to compare these diagrams with the values obtained by the ODP method. As explained earlier, the NODP values indicate regions of the structure which have low values of this parameter and they are definitely not suitable as potential excitation positions. Since neither the ODP nor NODP method consider the energy transfer from the excitation source to the structure, it is necessary to check several locations indicated by the NODP method as potentially good excitation positions, i.e. the locations which have non-zero values of the NODP parameter. Depending upon the type of the excitation method, the relevant diagram should be selected, i.e. for the hammer excitation, NODP-V should be used, while for the shaker excitation NODP-A should be selected for determination of the optimum driving location.

Engine Casing

Application of the ODP and NODP methods in order to choose the optimum excitation locations for a modal test produced results which were confirmed by a test carried out earlier. The natural frequencies and mode shapes of engine casing were calculated in the frequency region within 0 - 180 Hz. A total of 20 modes were found in this frequency region plus 6 rigid body modes which were excluded from the analysis. The ODP results are given in Figure 3.5.7-21 in a log scale. The two regions predicted as optimum excitation positions using the ODP method are the regions of extremely low stiffness (this is known from modelling of engine casing) and as such are not very suitable as excitation positions because impact within low stiffness region can result in mechanical damage to the component. This highlights a weakness of the ODP technique when it is individually used for selection of optimum excitation location.

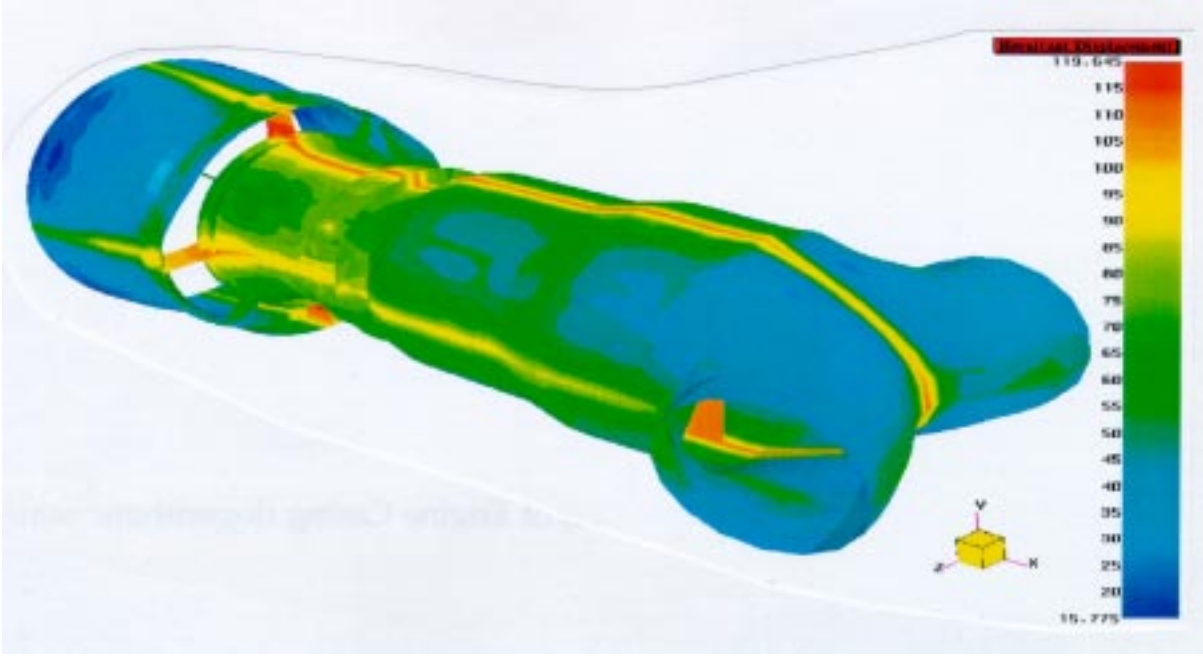

Figure 3.5.7-21. ODP of Engine Casing (logarithmic scale).

The NODP parameter was divided by the average velocity and the average acceleration and the results obtained are given in Figures 3.5.7-22 to 3.5.7-27. All results are shown in a logarithmic scale and for that reason, different directional components are shown separately. Figures 3.5.7-22, -23 and -24 show NODP-V in the X, Y and Z directions, respectively, while Figures 3.5.7-25, -26 and -27 show NODP-A in the X, Y and Z directions, respectively. After analysis of the contours of the above-mentioned pictures, it is apparent that the results obtained using the NODP method give rather different predictions for the optimum excitation location to those obtained by the ODP method. The full modal test on this structure had been carried out before the methods described above have been defined and the optimum excitation location was determined at the beginning of the experiment by trial-and-error.

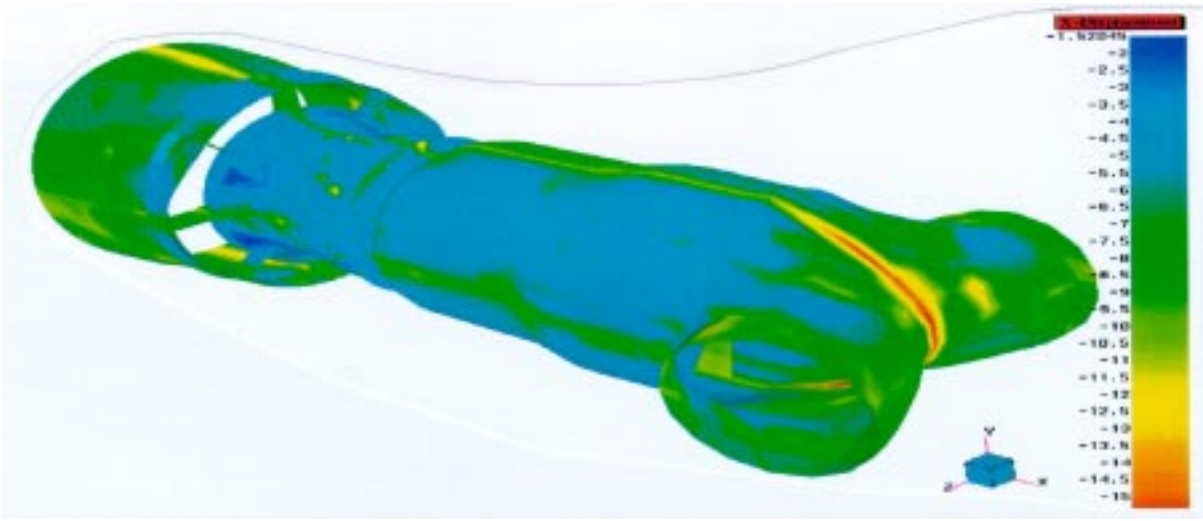

Figure 3.5.7-22. NODP-A (X component) of Engine Casing (logarithmic scale).

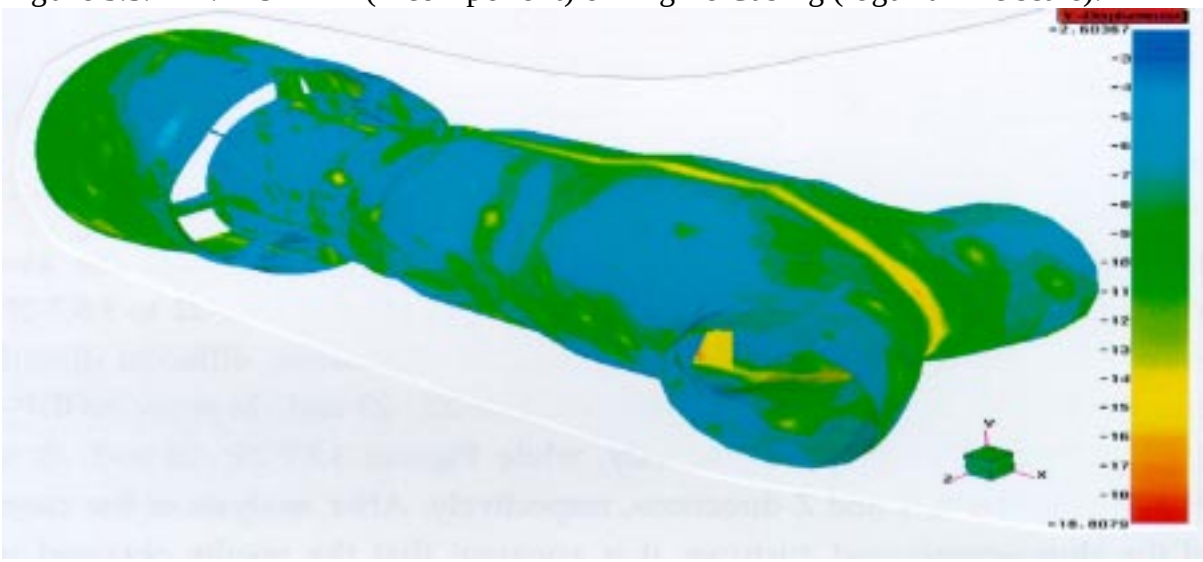

Figure 3.5.7-23. NODP-A (Y component) of Engine Casing (logarithmic scale).

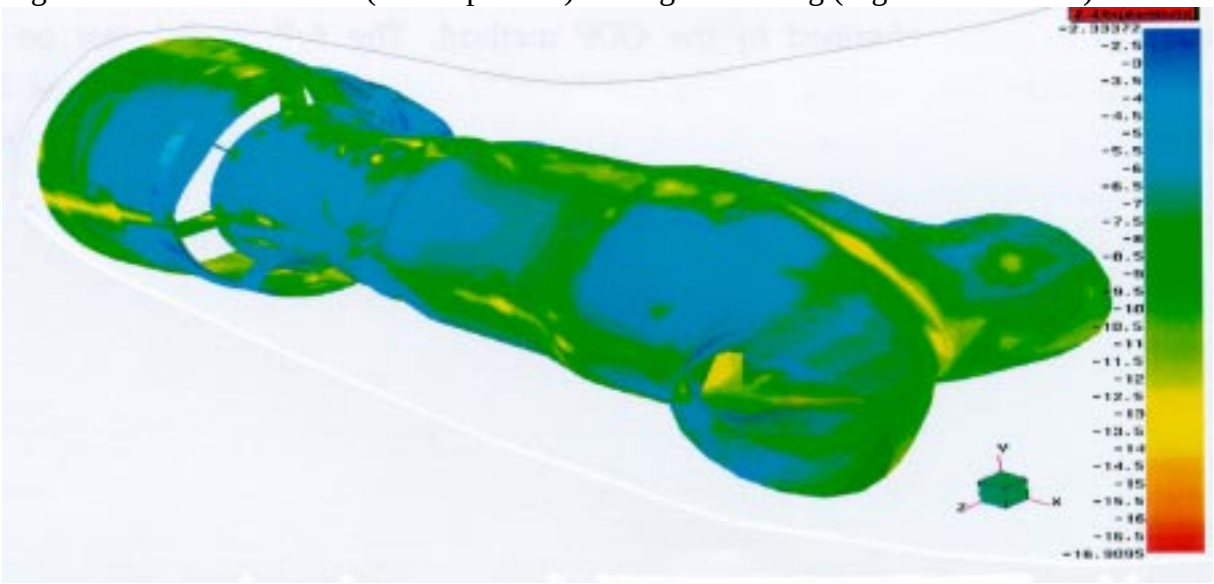

Figure 3.5.7-24. NODP-A (Z component) of Engine Casing (logarithmic scale).

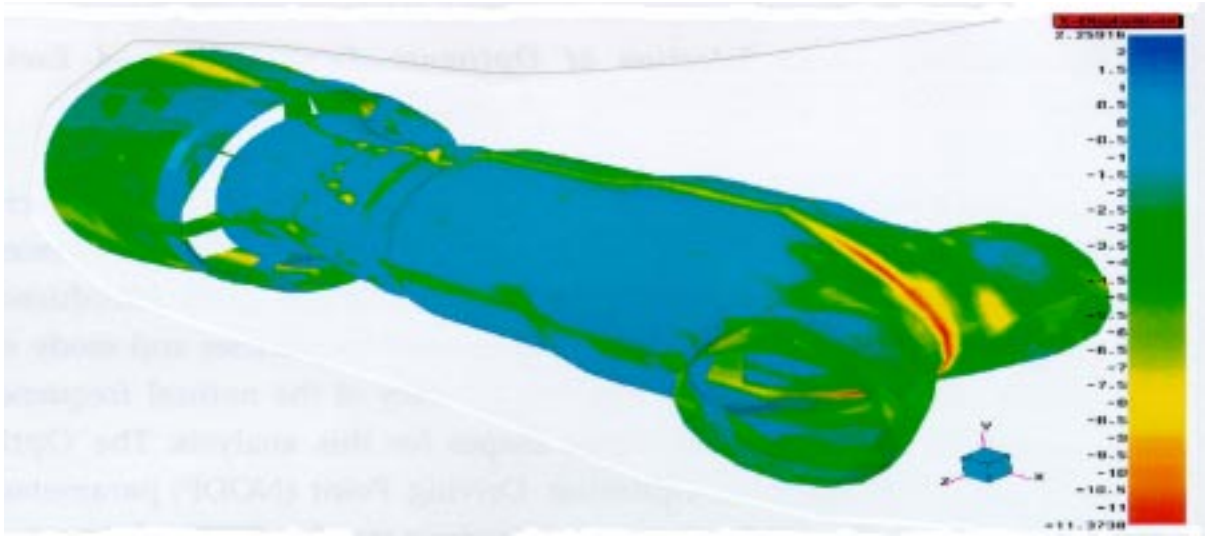

Figure 3.5.7-25. NODP-V (X component) of Engine Casing (logarithmic scale).

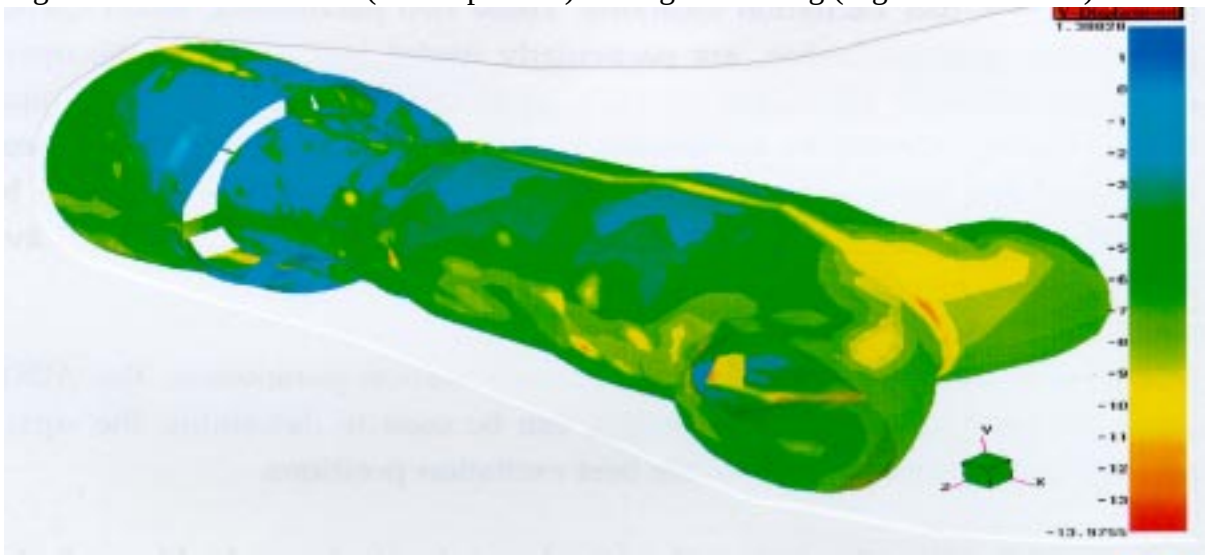

Figure 3.5.7-26. NODP-V (Y component) of Engine Casing (logarithmic scale).

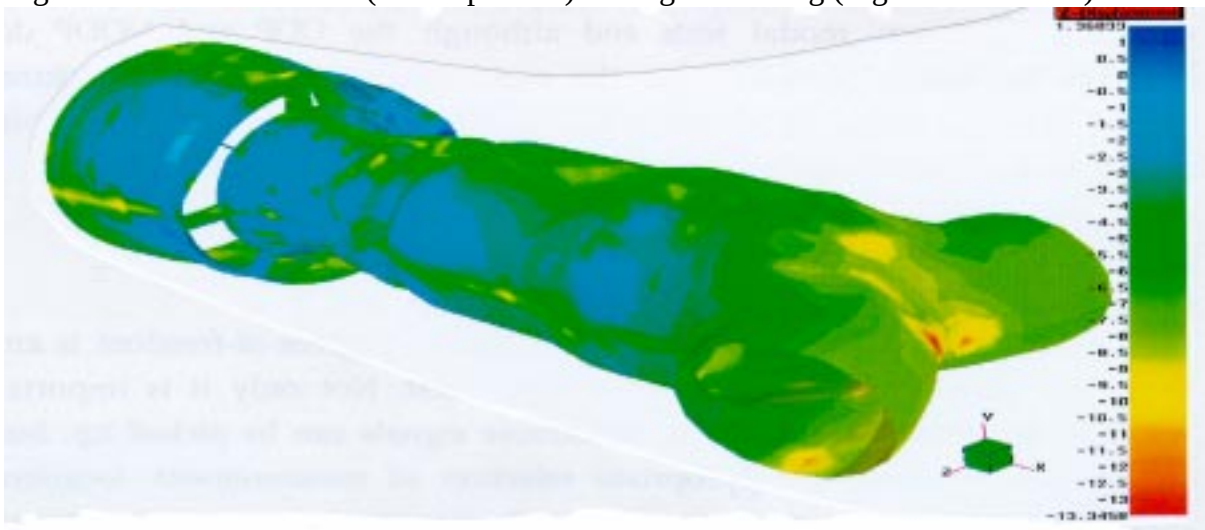

Figure 3.5.7-27. NODP-V (Z component) of Engine Casing (logarithmic scale).

3.5.8. Conclusions About Selection of Optimum Suspension and Excitation Locations

In this section two new methods for determining of the optimum excitation location and three new methods for estimation of the average displacement, velocity and acceleration of the vibrating structure have been introduced. All these methods assume that estimates of the natural frequencies and mode shapes are available prior to planning the test. The accuracy of the natural frequencies is not as important as is that of the mode shapes for this analysis. The Optimum Driving Point (ODP) and Non-Optimum Driving Point (NODP) parameters use information about the mode shapes to discriminate the DOFs of the structure into 'good' or 'bad' excitation locations. These two parameters, when divided by an average response value, are particularly useful indicators for the optimum excitation location. The methods have been applied to a simple plate and the Engine Casing in order to assess their effectivness. The Engine Casing structure was tested and the excitation location used for the test was one indicated by the NODP method, confirming that this method combined with the average response parameters can be used for real test cases.

The average displacement, velocity and acceleration parameters, the ADDOFD, ADDOFV and ADDOFA, respectively, can be used to determine the optimum suspension positions as well as the best excitation positions.

It is concluded that the proposed methods can be used as valuable tools for the design of optimum modal tests and although the ODP and NODP do not consider the energy transfer from the excitation source to the structure, the results obtained using these methods should be checked at the beginning of testing to confirm the optimum excitation location for the particular test.

3.6. Optimum Measurement Positions

Automatic selection of the required measurement degrees-of-freedom is another important part of the planning of a modal test. Not only it is important to measure the points where strong transducer signals can be picked up, but it is also crucial to make an appropriate selection of measurement locations for further use of modal test results, especially for correlation and updating. The final goal of the measurement location optimisation process is to select a number of measurement locations automatically with respect to some previously-determined criterion. This

might be defined as a linearly-independent truncated set of measured mode shapes, and / or the value of signal-to-noise ratio for measurement positions.

3.6.1. Definitions for optimum measurement positions

Before any evaluation of optimum transducer locations can be attempted, it is necessary to have some preliminary theoretical representation of the dynamic behaviour of the structure. These preliminary results usually come from a Finite Element Model (they are called "preliminary" because this might not be the final theoretical model of the structure) and this model will be referred to as the **preliminary theoretical model**. The full set of all the co-ordinates in this preliminary theoretical model will be referred to as **potential measurement points**. These are all the DOFs at the grid points in the preliminary theoretical model of the structure.

It is clear that some points cannot be measured simply because there is no access to them, at least with existing experimental techniques, and so there will be a subset of all the potential measurement points which consists of those DOFs which **are** accessible for measurement and these are called **possible measurement points**. Generally, this set only includes points on the surface of the model and only those which are actually accessible. It will be assumed that all the potential measurement positions that are inaccessible will be excluded from the selection of the optimum measurement positions.

3.6.2. Use of Average Displacement, Velocity and Acceleration

It is desirable to minimise the noise-to-signal ratio during the measurements in order to obtain a reliable set of experimental data. Once again, it is very clear that measurements close to or on nodal lines should be avoided since the strength of the response in these regions is low.

In the planning of modal tests it is also important to specify the right measurement quantity (acceleration, velocity or displacement) during the test. In most practical situations, acceleration is measured. Transducers (or accelerometers) are placed to measure the acceleration response which can be transformed analytically into either displacement, velocity or acceleration signals, but what is physically measured is the acceleration at the measurement locations. Therefore, the ADDOFA parameter should be used to identify the regions of the structure which have high response

levels and these regions should be considered as potentially good measurement locations.

In some situations, the actual measurement quantity is velocity, i.e. in the case of measurement being performed using a laser velocimeter. In this case, the same theory applies as for acceleration transducers, but the average velocity ADDOFV parameter is used rather than the average acceleration parameter, ADDOFA.

3.6.3. Effective Independence (EI) method

The Effective Independence transducer location optimisation technique was first proposed by Kammer in 1991, and is based on the following iterative process.

The initial mode shape matrix (only possible measurement DOFs are included in this matrix), $[\phi]_{Nxm}$, is used to calculate the following so-called 'Fisher Information Matrix', $[A]$:

$$[A]_{mxm} = [\phi]^T_{mxN}[\phi]_{Nxm} \tag{3.6.3-1}$$

and this matrix is then used to calculate so-called 'Prediction Matrix', $[E]$, of the mode shape matrix, as follows:

$$[E]_{NxN} = [\phi]_{Nxm}[A]^{-1}_{mxm}[\phi]^T_{mxN} \tag{3.6.3-2}$$

This Prediction Matrix is a symmetric and an **idempotent** matrix, i.e. it possesses the following features:

$$trace([E]) = rank([E]) = rank([\phi]) = m \tag{3.6.3-3}$$

$$[E]^2 = [E] \tag{3.6.3-4}$$

$$\sum_{i=1}^{N}\sum_{j=1}^{N} e_{ij}^2 = m \tag{3.6.3-5}$$

$$0 \le e_{ii} \le 1 \quad for\ all\ i \tag{3.6.3-6}$$

$$-0.5 \le e_{ii} \le 0.5 \quad for\ all\ i \ne j \tag{3.6.3-7}$$

The prediction matrix was originally developed in linear regression theory as a tool for selection of influential observations and for examination of sensitivity of observations and variables.

Every diagonal element of the prediction matrix, $[E]$, represents the contribution of its corresponding degree-of-freedom to the global rank of the truncated mode shape matrix, $[\phi]$. The diagonal element which has the smallest value in the prediction matrix determines the DOF which has the smallest contribution to the representation of mode shape matrix, $[\phi]$. That DOF is removed and the prediction matrix is calculated again in order to check the rank of the now-reduced mode shape matrix, $[\phi]$. This iterative process of removing the least-contributing DOF at every iteration is continued until the rank of the mode shape matrix ceases to be equal to the number of modes in $[\phi]$.

This procedure can be CPU-time consuming for large systems (those with over 1000 DOFs) and in these cases, several DOFs can be removed for each calculation of the prediction matrix $[E]$ in order to decrease the CPU time consumption, but it is clear that this algorithm does not generally produce the optimum measurement DOFs.

3.6.4. ADDOFV(A)-EI Method

The Effective Independence method is a very powerful tool for selection of the optimum measurement DOFs in order to identify the measured modes with as much linear independence as possible. The actual optimisation using the EI method seeks to find as few DOFs as possible, regardless of their position or other specific properties that they might possess. Since the EI method does not consider any other requirement for selection of measurement DOFs during the optimisation procedure, apart from their contribution to the global rank of the truncated mode shape matrix, a considerable number of the DOFs selected using the EI method will have a low response as predicted by the ADDOFV(A) method. In order to overcome this problem of selecting the measurement DOFs with low response, a modified method called the Average Driving DOF-Effective Independence (ADDOFV(A)-EI) method is created to select as few measurement DOFs (with the higher response by ADDOFV(A) measure) as possible to identify the measured modes as linearly independently as possible.

The actual algorithm of the ADDOFV(A)-EI method does not differ very much from the algorithm of the basic EI method. The principal goal of the ADDOFV(A)-EI method is the same as for the EI method, i.e. the truncated mode shape matrix has to be of full rank. The main difference between the EI and ADDOFV(A)-EI methods is in the selection of the least contributing DOF to the rank of the truncated mode shape matrix, the ADDOFV(A) of all DOFs is taken into consideration in order to remove the DOFs with low response first. This is achieved by multiplication of the ADDOFV(A) value of each DOF with the corresponding diagonal values of the prediction matrix, as shown in the expression below:

$$\left[E^{addofv(a)}\right]_{NxN} = [E]_{NxN}\, diag([ADDOFV(A)]) \qquad (3.6.4\text{-}1)$$

or $$e_{ii}^{addofv(a)} = e_{ii}\, ADDOFV(A)(i) \quad i = 1, N \qquad (3.6.4\text{-}2)$$

The optimum measurement DOFs are selected by removing the DOF with the lowest $e_{ii}^{addofv(a)}$ value at each iteration until the rank of the mode shape matrix ceases to be equal to the number of modes in the mode shape matrix. For large systems (those with 1000 DOFs and over), several DOFs can be removed for each calculation of $e_{ii}^{addofv(a)}$ matrix in order to decrease the CPU-time, but this procedure would probably produce a different result to the one when only one DOF is removed at a time.

By combining the two methods together, each DOF with a low response value (as defined by ADDOFV(A) method) would have the chance of removal greatly increased compared with the basic EI method so the final selection of measurement DOFs should consist of those with the higher responses.

3.6.5. Application of the EI and ADDOFV(A)-EI Methods

The EI and ADDOFV(A)-EI methods were applied to several test cases and this section contains results of these studies.

Clamped Disk

A shell model of a disk (shown in Figure 3.6.5-1), which was clamped at the outer radius, was run using MSC/NASTRAN to extract 10 natural frequencies and mode shapes. The number of DOFs of the full model was 1284. The total ADDOFV sum of all the selected measurement DOFs and the condition number of the truncated mode shape matrix were monitored during the elimination process in order to compare DOF selection for both EI and ADDOFV(A)-EI methods. The higher the value of the ADDOFV sum for selected DOFs, the better the selection of measurement DOFs from an average response consideration. The smaller the condition number of the truncated mode shape matrix, the better the selection of measurement DOFs from mode shape linear independence consideration. There are different levels for the critical condition number defined in the literature, but it will be accepted here that any value of the condition number below 10^3 represents a well-conditioned matrix; the values between 10^3 and 10^7 can be considered as poorly conditioned matrix but are still acceptable in a numerical sense and any value higher than 10^7 represents a near-singular or a singular matrix. The values of these two parameters (the condition number and the ADDOFV sum) have to be balanced to obtain the optimum selection of measurement DOFs, but there is a priority to keep the condition number as small as possible compared with the ADDOFV sum for selected measurement DOFs. The values of all these parameters are given in Table 3.6.5-1 for different numbers of measurement DOFs.

No. of measured DOF	EI ADDOFV sum 10^{-4}	ADDOFV-EI ADDOFV sum 10^{-4}	EI Condition Number	ADDOFV-EI Condition Number	EI Rank	ADDOFV-EI Rank
100	13.9937	15.3304	1.238	1.704	10	10
50	7.22242	7.55616	1.256	1.694	10	10
30	4.37002	4.47722	1.322	1.675	10	10
20	2.90501	3.05140	1.477	2.03	10	10
15	2.11996	2.30500	1.568	2.233	10	10
10	1.44001	1.47900	2.192	4.527	10	10

Table 3.6.5-1. Clamped disk, 10 Modes, EI and ADDOFV-EI selection of measurement DOF.

The actual positions of 15 and 10 selected measurement DOFs for both EI and ADDOFV-EI methods are given in Figures 3.6.5-1, -2, -3 and -4. The contours given in Figures 3.6.5-1, -2, -3 and -4 are ADDOFV values and it is clear that all selected DOFs have high response values. Analysing the values of parameters from Table 3.6.5-1, it can be concluded that there is not much difference in average response according to the ADDOFV method and that truncated mode shape matrices are well conditioned for both selections.

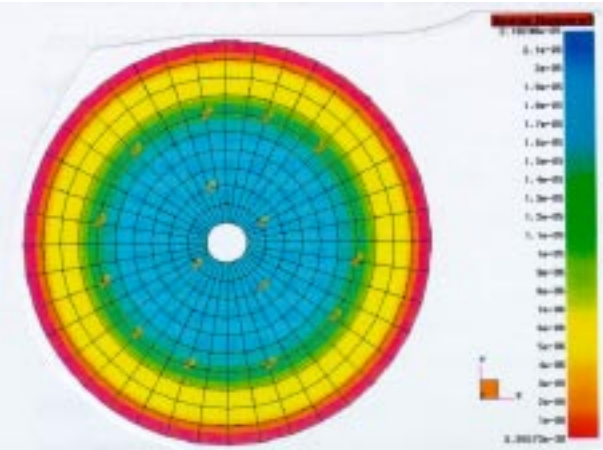

Figure 3.6.5-1. 15 DOFs by EI.

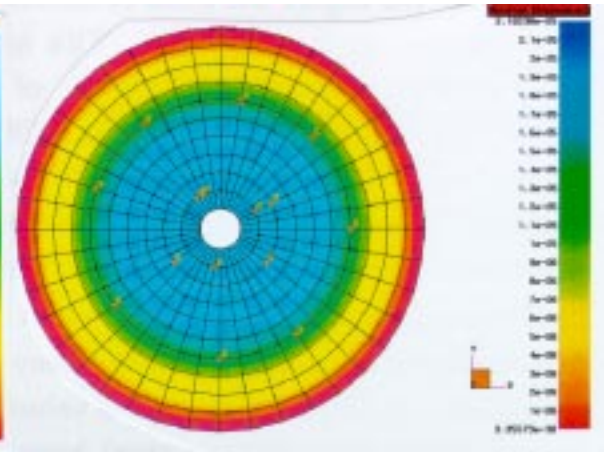

Figure 3.6.5-2. 15 DOFs by EI-V.

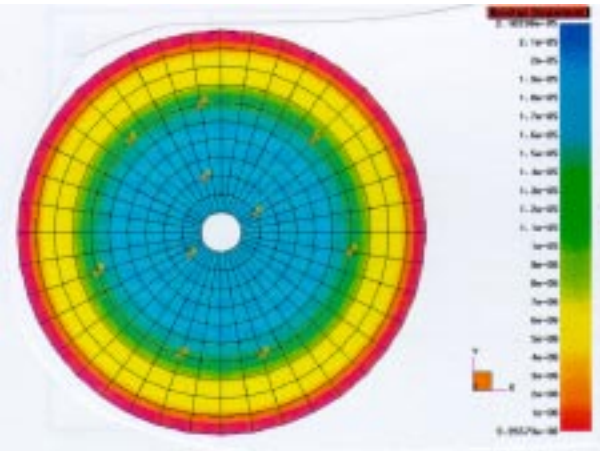

Figure 3.6.5-3. 10 DOFs by EI.

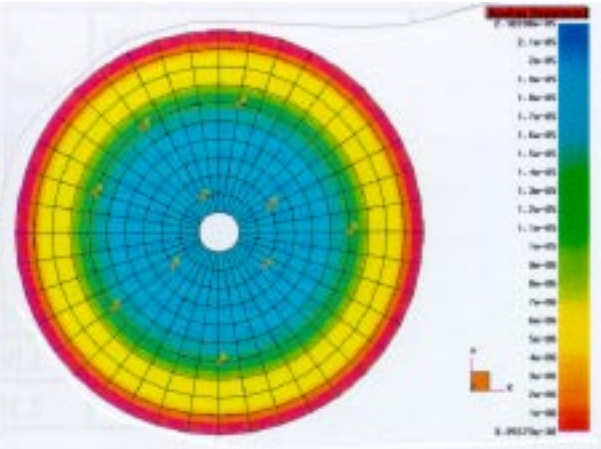

Figure 3.6.5-4. 10 DOFs by EI-V.

Simple Beam Structure (Lloyd's Register Correlation Benchmark)

The Lloyd's Register Correlation Benchmark [34] is a simple cantilever beam firmly screwed to a square base plate and is shown in Figure 3.6.5-5. The structure was to be tested with free-free boundary conditions in the frequency range up to 12800 Hz.

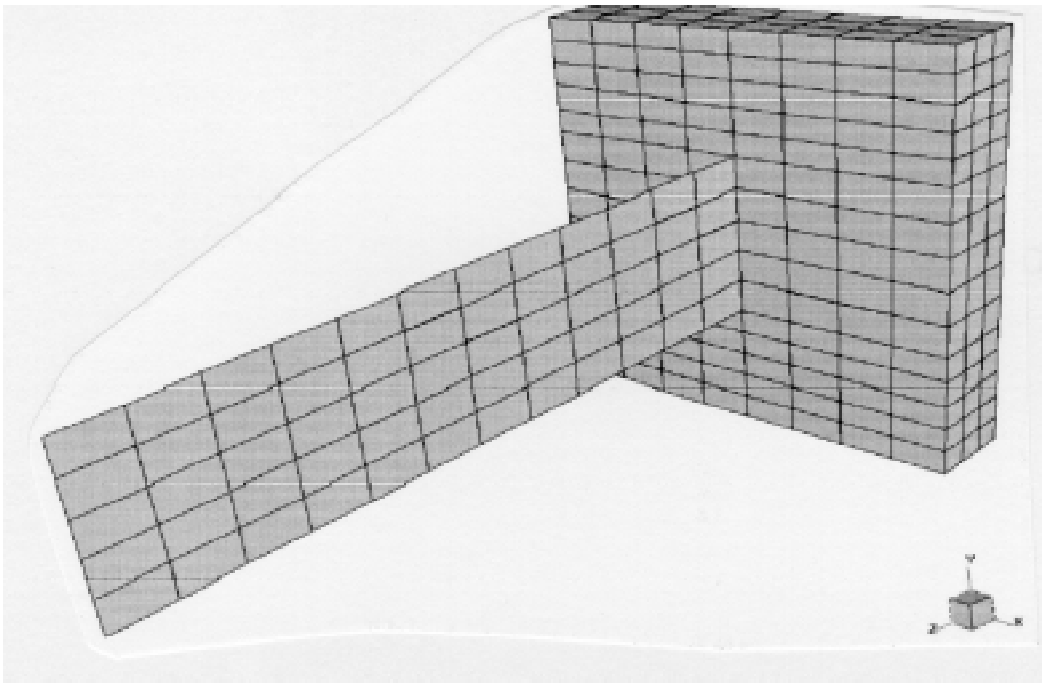

Figure 3.6.5-5. Lloyd's Register Correlation Benchmark FE model.

A preliminary assessment of the data requirements was carried out before the test was conducted using the EI and ADPR-EI methods to determine the optimum measurement locations. It was predicted by preliminary FE analysis that 20 modes were expected to be within the specified test frequency range. The EI method selected 30 measurement DOFs to identify 20 linearly-independent modes and the distribution of the measurement locations is given in Figure 3.6.5-6. The ADPR-EI method selected 40 measurement DOFs to measure 20 linearly-independent modes and that distribution is given in Figure 3.6.5-7. The reason for the selection of 10 more DOFs using the ADPR-EI method, by comparison with the EI method, is to retain the conditioning of the truncated mode shape matrix of the same order of magnitude. The ADPR-EI method selects the measurement locations of high average response rather than taking into account solely the contribution of each DOF to the rank of the mode shape matrix. After detailed analysis and comparison of both selected sets, it was decided to measure 38 DOF for the full modal test, as shown in Figure 3.6.5-8.

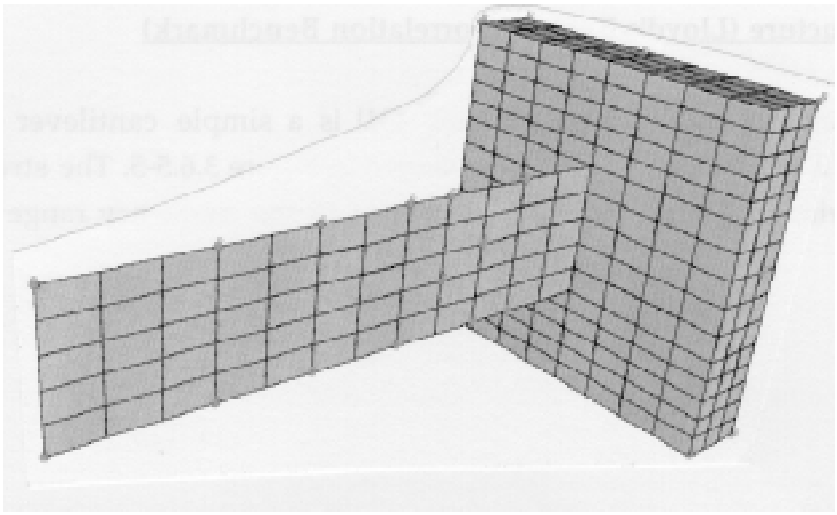

Figure 3.6.5-6. 30 DOFs selected by EI for 20 modes.

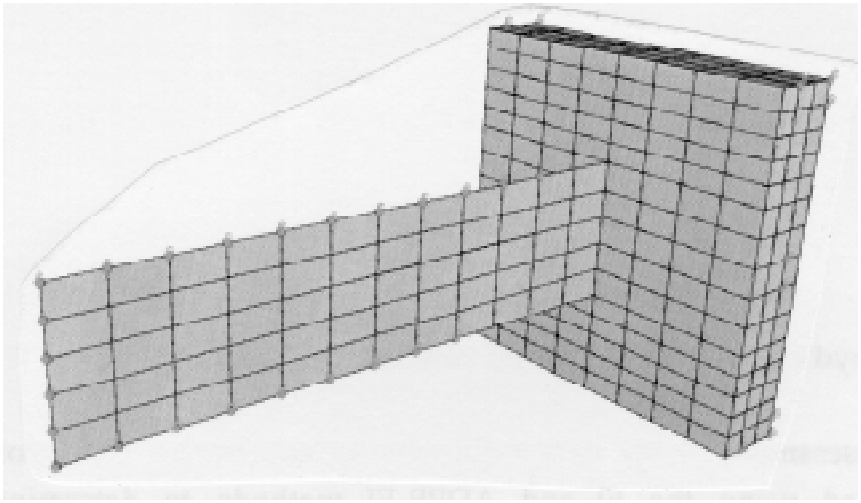

Figure 3.6.5-7. 40 DOFs selected by EI-V for 20 modes.

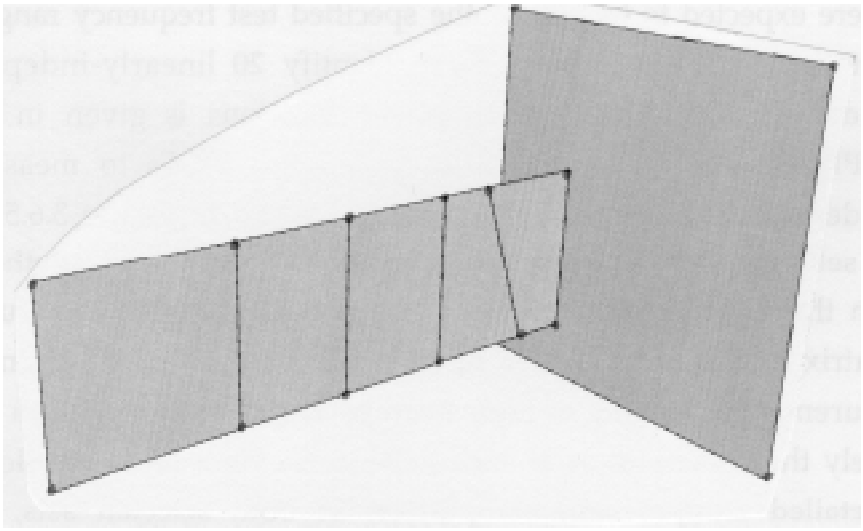

Figure 3.6.5-8. Experimental mesh of Correlation Benchmark (38 DOFs).

Engine Nozzle Structure

The FE model of an engine Nozzle structure and its first several mode shapes are shown in Figure 3.6.5-9. It can be seen that only the few first modes seem to be accurate due to the quite coarse mesh of the model. Clearly, there is a major problem when selecting measurement locations for a structure of such complicated geometry. A complete planning of a modal test was performed for this structure and after the ADDOFV-EI method was applied, the obtained measurement locations (shown in Figure 3.6.5-10) seemed quite different from something that engineering intuition and experience might suggest. Then it was decided to make a set of measurements at locations obtained by applying ADDOFV-EI (shown in Figure 3.6.5-11) and a separate set of measurements at locations obtained in consultation with experimentalists, as shown in Figure 3.6.5-12. After modal analysis was performed on the experimental FRFs - there were about 30 FRFs measured at locations selected using ADDOFV-EI and about 72 FRFs measured at locations manually selected using intuition and experience - the AUTOMACs on these separate data sets were calculated. It can be seen quite clearly that the smallest off-diagonal values in the AUTOMAC table is achieved using a data set at locations selected by the ADDOFV-EI method as shown in Figure 3.6.5-13. The AUTOMAC table obtained using data set at locations selected manually clearly indicates that some modes were not identified properly and that an aliasing problem is present, as shown in Figure 3.6.5-14. This example demonstrates the effectiveness of this new combined method even though the initial data used for these calculations were of limited accuracy. It should be noted that ADDOFV coefficient was used in the selection procedure since the measurements were performed by a laser vibrometer which measures velocity at the surface locations.

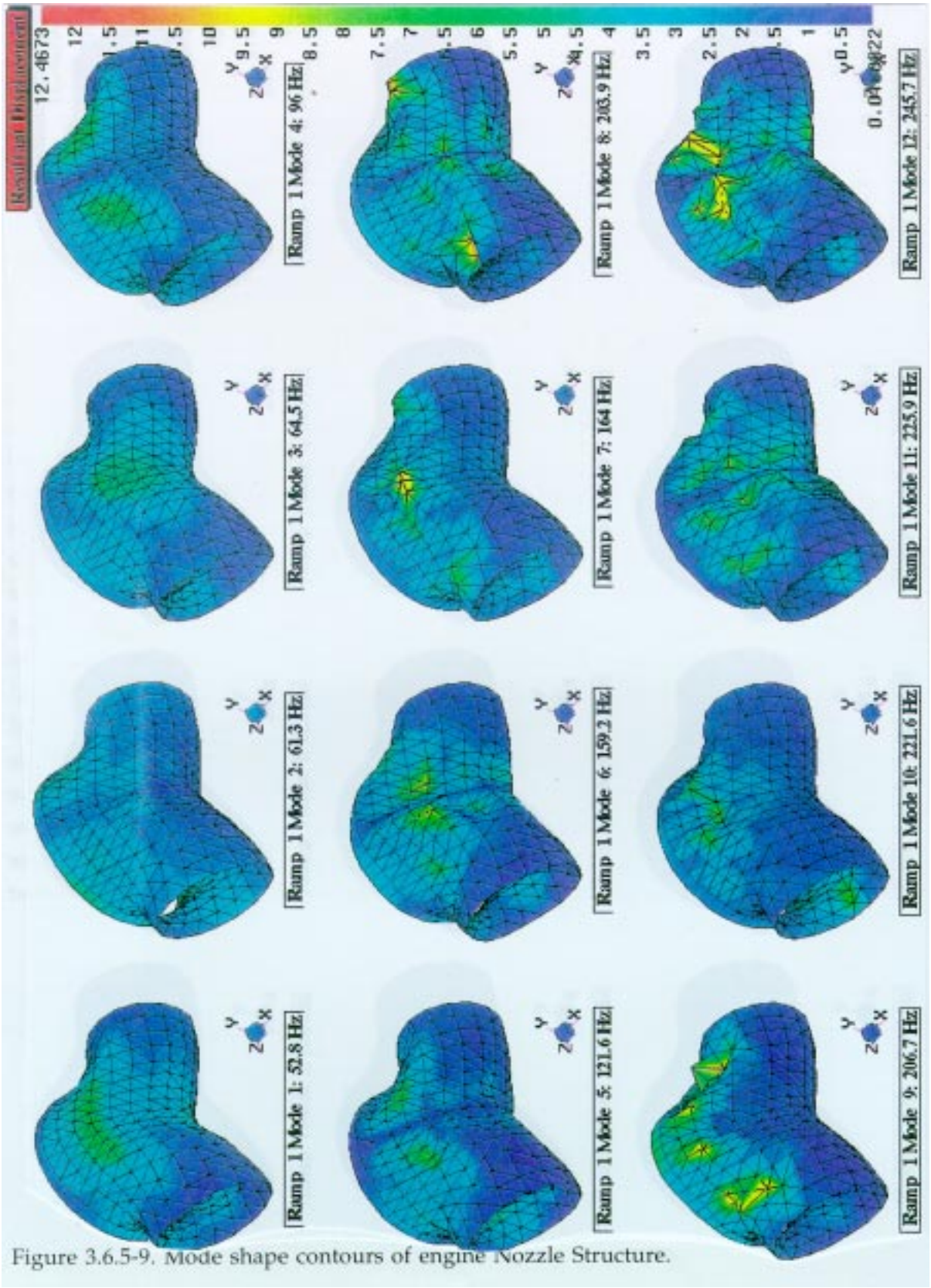

Figure 3.6.5-9. Mode shape contours of engine Nozzle Structure.

Figure 3.6.5-9. Mode shape contours of engine Nozzle Structure.

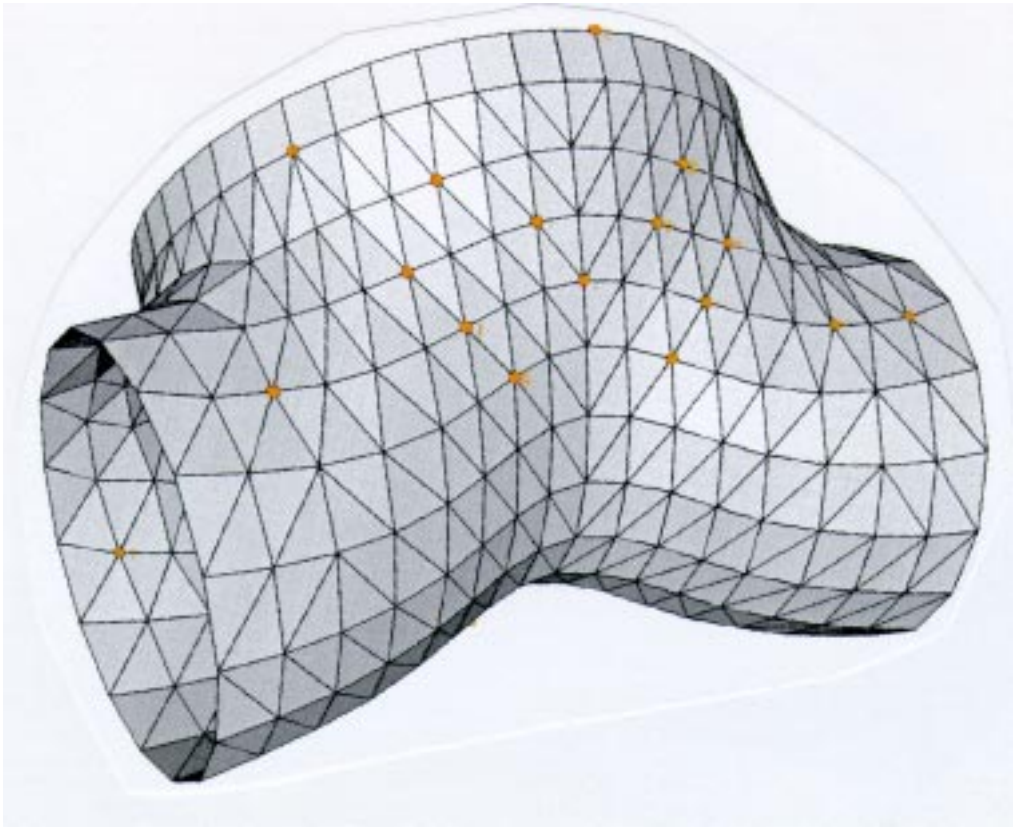

Figure 3.6.5-10. 30 DOFs selected by EI-V for 12 modes.

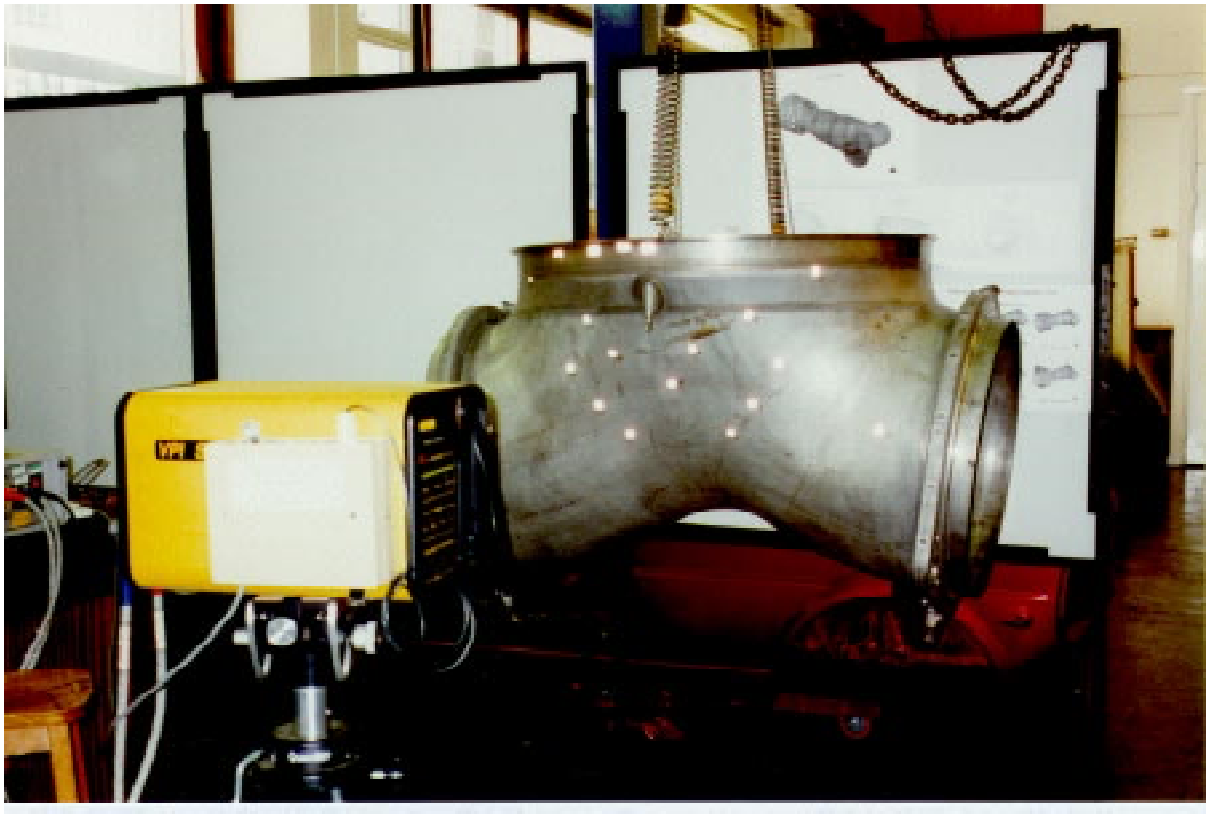

Figure 3.6.5-11. Measurements on engine Nozzle using laser vibrometer.

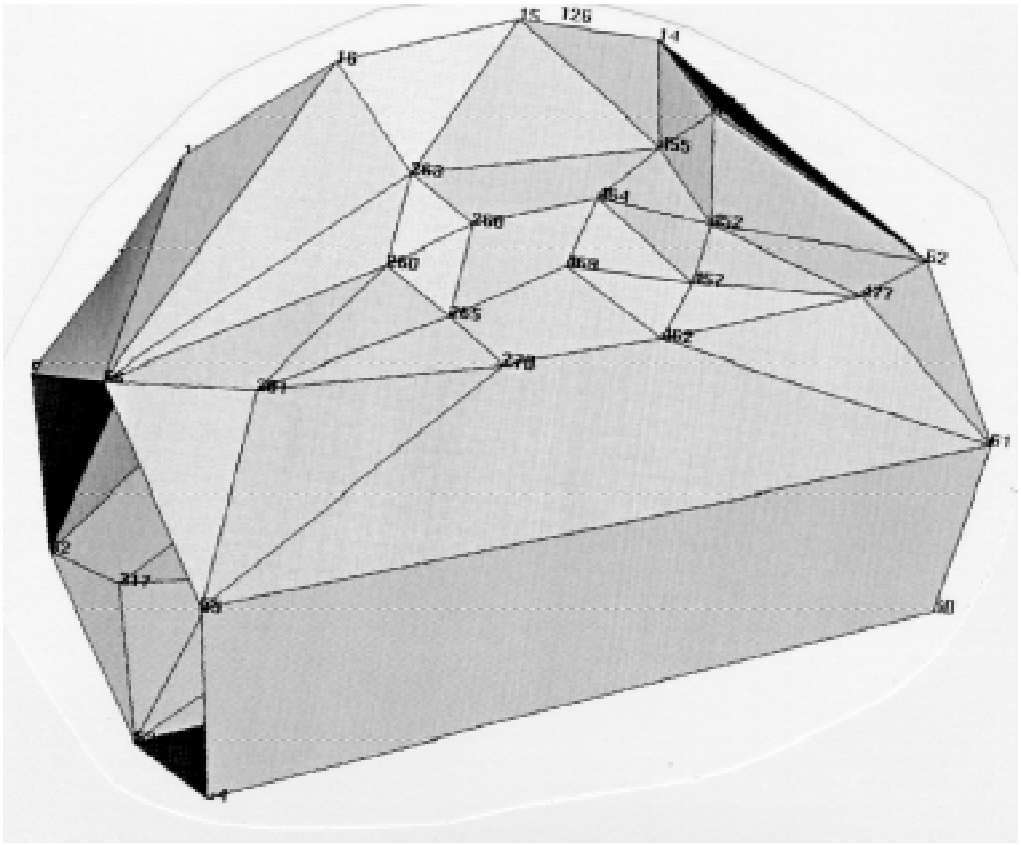

Figure 3.6.5-12. Experimental mesh (102 DOFs).

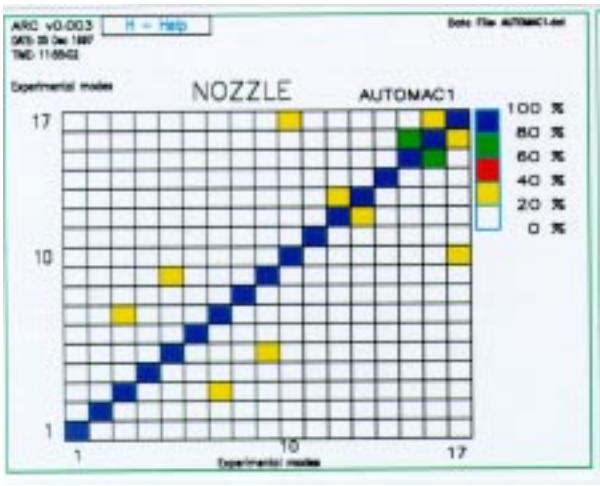

Figure 3.6.5-13. AUTOMAC on 30 DOFs selected by EI-V.

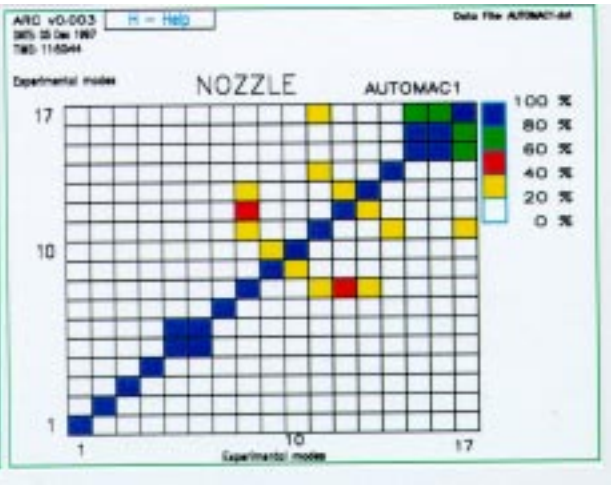

Figure 3.6.5-14. AUTOMAC on 72 DOFs selected using experience and intuition.

3.6.6. Conclusions for Selection of Optimum Measurement Locations

Two useful and efficient techniques for the automatic selection of optimum measurement DOFs have been presented. The EI method was used as a base to develop a new technique, the "combined ADDOFV(A)-EI method", which automatically have been measurement locations of high average response. Both techniques were applied to a few test cases and the results obtained demonstrated the capabilities of the methods. The major weakness of the basic EI method is that it can include in the selection some DOFs which have low values of the average response (locations close to or on nodal lines), but as a result, the EI method can be used to select a smaller number of measurement DOFs than the ADDOFV(A)-EI method, which also takes into consideration the values of the average responses of the potential measurement locations.

In order to use both techniques properly, it is recommended that the selection of measurement DOFs obtained by the ADDOFV(A)-EI method be used but that double the number of measurement DOFs (compared with the number of modes to be measured) should be selected. Following this logic of modal test planning, more accurate FRFs should be measured, but the conditioning of the truncated mode shape matrix should be in line with the value obtained by the EI method selection since more measurement DOFs are selected.

3.7. Reliability of Pre-Test Planning: Why/When does it work?

In order to plan a modal test successfully, it is necessary to know the frequency range in which measurements need to be performed and this information is determined from the relationship between the frequency-domain and the final time-domain analysis, as discussed in Chapter 2. Also, this analysis requires knowledge of natural frequencies and mode shapes of a structure and this requirement poses a major threat to the accuracy and reliability of pre-test planning. Analysts who wish to use these techniques have to be aware of limitations of the pre-test planning in terms of its accuracy and reliability.

It has been demonstrated on a few practical examples using real experimental data that pre-test planning can work and does work if used sensibly and according the rules described in this chapter. The Nozzle example demonstrates that even if preliminary predictions of the FE model are not particularly accurate, pre-test

planning will still produce some sensible answers for the optimum suspension, excitation and measurement positions. The real question is how much pre-test planning is really dependent on the accuracy of the preliminary data?

A major strength of all pre-test planning techniques lies in their simplicity of mathematical formulation. These techniques use neither the spatial or response properties of the structure, they use only the modal properties (the natural frequencies and mode shapes), and the importance of the natural frequencies can be neglected by comparison with mode shapes. All pre-test planning techniques assess positions of nodal lines for the selected modes. Methods for determination of the optimum suspension and excitation positions use all the modes averaged, rather than as individual properties and that is the major strength of these techniques. Experience shows that preliminary predictions tend to have higher accuracy for the mode shapes rather than for the natural frequencies.

For instance, for a simple cantilever beam such as the Lloyd's Register structure that is clamped at one end, the predicted mode shapes will be several pure bending and torsional modes. However, since the structure has a quite crude connection at the base plate, it is unlikely that the connection is completely symmetrical and consequently the mode shapes will not be pure bendings and torsions. In fact, a very detailed modal analysis shows that the actual mode shapes of the structure are combinations of bending and torsions.

Since the pre-test planning techniques use the mode shapes averaged rather than individually, even if the predicted mode shapes are not distributed very accurately by comparison with the actual mode shapes, the average information should have a higher degree of accuracy than the individual modes. This is a major reason for an enhanced reliability and accuracy of the pre-test planning. Also, experience shows that distribution of mode shapes is dependent on stiffness and mass, but it is more dependent on the geometry of the model, and since in most practical situations the geometry is known quite accurately, there is a high probability that most sensible models produce a sensible averaged information that can be used in the pre-test planning.

3.8. Closing Remarks

This chapter has presented a number of new techniques for the planning of modal tests. These techniques are designed in such a way that the level of accuracy required of the preliminary data used for predictions is minimised. There are several different conditions for a more reliable modal test: the optimum suspension, excitation and measurement positions. Data requirements are incorporated into the overall strategy for pre-test planning but this topic will be discussed further in the following sections. It has been demonstrated on several real engineering structures that these techniques can be used as a valuable tool for planning of modal tests.

4.0 Model Correlation

4.1. Introduction

This chapter presents the basis for an automatic correlation algorithm for structural dynamic models, which can be used during a model updating procedure in order to pair matching experimental and theoretical model CMPs (correlated mode pairs) automatically. Also, a method of modal complexity assessment is presented. Evaluation of modal complexity of experimental modes is a useful check on experimental data in order to assess consistency of the data. A new criterion for mode shape comparison (SCO) is introduced. The method is based on the SEREP reduction method and does not require any additional data to the natural frequencies and modes from theoretical model.

In addition, this chapter presents a new method for the determination of the number of modes required for accurate regeneration of FRFs using the modal summation approach. Theoretical FRFs are rarely computed by direct inversion of the dynamic stiffness matrix because of the CPU requirements for this calculation. Instead, they are regenerated using the modal summation approach, including only a limited number of modes and simply neglecting the influence of the higher modes. Using the modal FRF regeneration approach, the analyst always faces the question: "How many modes should be included for the FRF regeneration summation in order to minimise the influence of omitted higher modes?". This chapter presents a new method which provides an answer to this question.

4.2. Standard Correlation Methods

Validation of theoretical structural dynamic models is usually performed by comparison of theoretically-predicted with experimentally measured dynamic characteristics of structures. When a successful modal test of a structure is completed, correlation between theoretical and experimental sets of data is undertaken and if the agreement is satisfactory, the theoretical model of the structure is validated and considered to be suitable for use in further analysis (transient response, assembled structure analysis, fluid-structure interaction analysis, etc.). However, if satisfactory agreement is not obtained, then some modifications must be made to the theoretical model in order to improve correlation with the corresponding experimental results. This model correlation consists of

mode shape pairing between theoretical and experimental data sets and comparison of the values of corresponding natural frequencies and mode shapes.

Theoretical and experimental sets of modal data consist of a number of natural frequencies and mode shapes on the corresponding meshes for each model. A major practical problem in the correlation process is the incompatibility between these two meshes resulting from the experimental data set incompleteness, i.e. the limited number of measurement points in a limited measured frequency range.

Generally, assessment of the degree of correlation between two sets of data is performed both numerically and visually.

4.2.1. Numerical Comparison of Mode Shapes

Numerical comparison between two sets of modal data consists of the calculation of different correlation coefficients which give quantitative values of similarities between two mode shapes. All numerical correlation methods use the orthogonality properties of mode shapes in order to exploit the differences between them. The most commonly-used one for indication of CMPs is the MAC (Modal Assurance Criterion) [7], which calculates the least-squares deviation about a straight line of the plot of two arbitrarily-scaled mode shapes, and the NCO (Normalised Cross-Orthogonality) [8], which is basically the MAC coefficient weighted by a partitioned global mass or stiffness matrix. A good correlation between two modes is observed for MAC and NCO values close to 1 and a poor correlation corresponds to values close to zero. Since mode shapes are orthogonal with respect to the full mass or stiffness matrix, and the measured set of DOFs is never complete, it is impossible to specify absolute limits for indication of good or poor correlation based on the MAC or NCO correlation coefficients.

$$MAC(i,j)=\frac{\left|\{\psi_X\}_i^T\{\psi_A\}_j^*\right|^2}{\{\psi_X\}_i^T\{\psi_X\}_i^*\cdot\{\psi_A\}_j^T\{\psi_A\}_j^*} \qquad (4.2.1\text{-}1)$$

$$NCO(i,j)=\frac{\left|\{\psi_X\}_i^T[M_A]\{\psi_A\}_j^*\right|^2}{\{\psi_X\}_i^T[M_A]\{\psi_X\}_i^*\cdot\{\psi_A\}_j^T[M_A]\{\psi_A\}_j^*} \qquad (4.2.1\text{-}2)$$

Other correlation coefficients which are used in practice include the slope of the best straight line through the points of the plot of two identically-scaled mode shapes; the MSF (Modal Scale Factor) [2].

$$MSF(i,j) = \frac{\{\phi_X\}_i^T \{\phi_A\}_j^*}{\{\phi_A\}_j^T \{\phi_A\}_j^*} \qquad (4.2.1\text{-}3)$$

4.2.2. Visual Comparison of Mode Shapes

Visual comparison between two sets of modal data includes a process which involves the analyst's non-quantitative visual assessment of any kind of graphically-presented data. It usually consists of simultaneous animation of one mode shape from each of the two sets and direct comparison of their natural frequencies. This method basically consists of a visual comparison of the patterns of two different mode shapes and a non-quantitative analyst assessment of differences or similarities between two mode shape patterns. A problem arises when one experimental mode appears to match two or more theoretical modes. Although this can happen for several reasons, as will be discussed later, a more detailed inspection is necessary in order to identify the CMPs.

It is important to stress here that during this process the analyst compares experimental and theoretical meshes too and, to some extent, the analyst uses additional information about the structure in connection with the experimental mesh. This additional information includes the geometry of the structure which is already known to the analyst. A good example of this is a very coarse experimental mesh of an aircraft engine casing, which hardly resembles an approximation to the shape of the engine itself. During the animation comparison process, the analyst uses his/her prior knowledge of the geometrical shape of a structure which is visually assigned to the experimental mesh of the structure. It is interesting that visual linearisation for the points on the mesh is assumed as true as it is viewed on the screen, but which is generally unknown, because it was not measured. This is where some extra information about the experimental mode shapes can be introduced, and can disrupt the visual pattern comparison for geometrically complex mode shapes.

Other visual impressions of the mode shapes depend on the type of the elements used for the experimental mesh, e.g. an experimental mesh of a structure modelled by shell elements and another mesh of the structure modelled by beam elements can give rather different impressions about the shape of the same mode. An extreme situation would arise if a analyst for model updating were supplied with grid point positions, the global mass and stiffness matrices and a number of measured frequency response functions (FRFs) with the task of updating the initial model, but the contractor does not want to disclose details of the structure to the analyst. There are many such examples in industry, and the visual correlation would be difficult if not impossible, in this situation.

4.2.3. Problem of Complex Mode shapes

It can be seen that in expressions (4.2.1-1) and (4.2.1-2) it is assumed that both mode shapes are complex. In most practical situations, the theoretical mode shapes are real if the damping has not been included in the model as it is not in most practical cases, whereas the experimental mode shapes are always complex because of inevitable damping effects in any real structure. If, however, correlation is performed between real and complex mode shapes, this will in general decrease the correlation parameter values, since the correlation coefficient is a simple scalar product between two vectors divided by their magnitudes.

This incompatibility of mode shapes can be overcome by realising complex mode shapes, and this section describes a method which assess the modal complexity of complex mode shapes.

Assessing the Modal Complexity of Experimental Mode Shapes

Because of difficulties associated with the modelling of non-proportional damping and non-linearity, such effects are generally omitted and theoretical modes come out of the analysis as numerically real values. Since it is likely that the influence of damping or non-linearity (material, geometrical) will exist in practice, these effects will influence the measurements and, after modal analysis, the extracted modes will generally be complex.

The best way to assess the degree of modal complexity of an experimental mode shape is to plot real and imaginary values for each DOF in the complex plane

(Figure 4-1). Ideally, if a mode shape is 100 percent real, the vectors would all lie on a single line in the complex plane. The more these vectors diverge from a single line, the more the mode shape is complex. Figure 4-1 shows an experimental mode shape which is almost real, while Figure 4-2 shows a more generally complex mode.

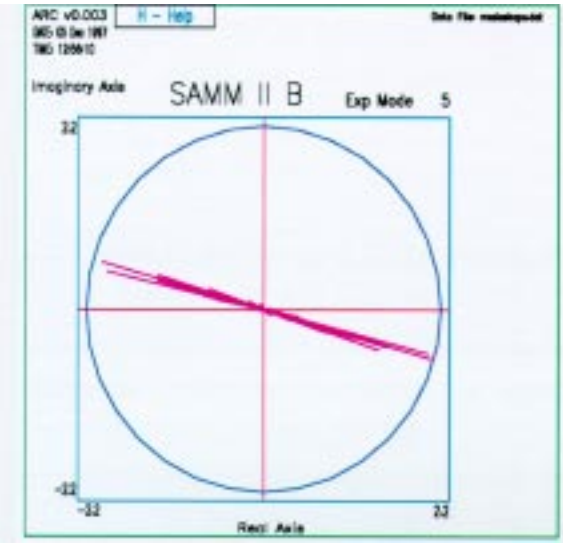

Figure 4.1. Experimental mode shape in the complex plane.

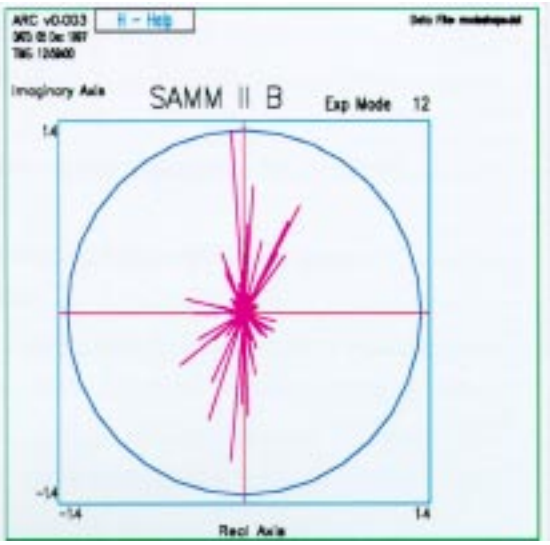

Figure 4.2. Heavily complex experimental mode shape.

The **Maximum Complex Area (***MCA***)** [35] of a mode is defined as the area of a polygon generated by constructing the envelope around the extremities of the tips of the eigenvector elements plotted in the complex plane, with only obtuse angles permitted outside the resulting polygon (Figure 4-3). It is clear that the more complex a mode is, the larger the maximum complex area of the mode (*MCA*) will be.

A mode is defined as maximally complex if it has properties defined by expression (4.2.3-1) for the same order of DOFs, i.e. the moduli are the same and equal to the maximum eigenvector value and phase angles between eigenvectors are the same.

$$\Delta\left(\angle\phi_{i-1,i}\right)=\Delta\left(\angle\phi_{i,i+1}\right)=360/n \quad \text{and} \quad \left|\phi_{i,1}\right|=\ldots=\left|\phi_{i,n}\right|=\max_{j}\left(\left|\phi_{i,j}\right|\right) \quad (4.2.3\text{-}1)$$

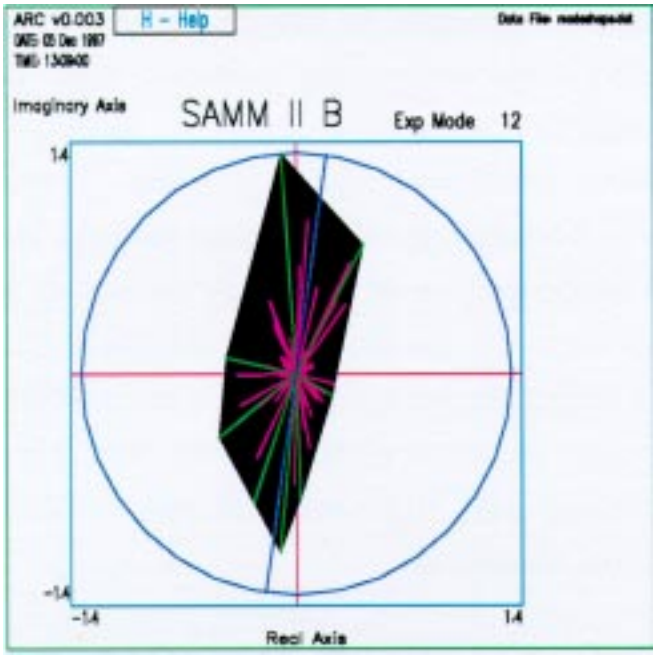

Figure 4.3. The maximum complex area of a complex mode shape.

In order to quantify the **Modal Complexity Factor (***MCF2***)** [35] of the **ith** mode shape, the following coefficient is defined as the ratio of the maximum complex area (MCA) of the mode to the maximum complex area of that mode when it is maximally complex as defined by expression (1).

$$MCF2(i) = \frac{MCA(i)}{MCA(i - \text{maximally complex by (4.2.3 - 1)})} \; x\,100 \quad [\%] \qquad (4.2.3\text{-}2)$$

The modal complexity factor can vary between 0 and 1. Real modes would have modal complexity factor 0 and a maximally-complex mode would have a *MCF2* value of 1. A very high value of the *MCF2* coefficient of a lightly damped structure for some experimental modes indicates probable error, either in the measurements or in the modal analysis.

4.2.4. Realisation of Complex Mode Shapes

After checking the *MCF2* coefficient values for the experimental mode shapes, and if these values are not very high, the mode shapes can be realised using one of the existing techniques which can be found in [36].

In this section, a simple method for realisation of complex mode shapes will be described. Most existing realisation techniques tend to realise complex mode shapes

in such a way that the correlation between complex and the corresponding real mode shapes is retained as high as possible. Generally, this approach is not recommended here since this assumes that there is a fair correlation between the experimental and theoretical modes and that the correlated mode pairs are known, what may not be the case. Another reason for questioning these approaches is that they tune the experimental mode shapes to the corresponding theoretical mode shapes (if these are known at that stage), but these theoretical mode shapes may not be completely accurate (that is why the correlation and updating are being performed in the first place). Hence, these approaches are essentially based on some assumptions that are incompatible with model validation technology and therefore are not recommended to be used in the application of model validation.

An extremely simple approach for realisation of complex modes will be described here. The most important feature of this realisation method is that there is no reference to any theoretical data in the realisation process. A lightly-damped and a complex mode shape is shown in Figure 4-2. In order to realise this complex mode shape it is necessary to ensure that the maximum possible values of complex modal parameters are retained when the mode shape is realised. The realisation process involves projecting complex plane modal parameter vectors of each DOF to a common single straight line. It is then necessary to find the angle of the line which would have a maximum value of the sum of all projections of modal parameters to that line. This problem can be solved by simple optimisation of projected value to a single line as a function of the angle of that line. Applying this procedure, it is possible that some modal parameters are perpendicular to the realisation line, and therefore their contribution to the mode shape would be completely lost. This is a major reason for optimising the value of the lengths of modal parameters during realisation process, since this will ensure that most contributing modal parameters are least distorted. All DOFs that have small modal parameter values are less important in the realisation process because the accuracy of modal parameters is approximately proportional to their values. A heavily complex mode shape and its realisation line are shown in Figure 4-3.

There is no realisation process that can retain all the properties of a complex mode shape; they all distort and cause some inaccuracies in the realised mode shapes. The effects of the realisation process are dependent on the technique used, but the major advantage of the realisation approach presented here is that these distortions of

mode shapes are minimised even though the theoretical mode shapes are never used for realisation.

4.3. Reduction of Theoretical Model to the Number of Measured DOF

In order to overcome the incompleteness problem in correlation, either (i) a reduction of the theoretical model to the size of the experimental mesh, or (ii) an expansion of the measured model to the size of the theoretical model, has to be performed. The experimental data set is incomplete in measured DOFs and number of measured modes (measured frequency range). Generally, expansion of modal data is successful only if a significant number of DOFs of the theoretical model have been measured [12],[13]. Most reduction processes reduce the size of the model but do not generally retain the properties of the initial model, except in the SEREP reduction process, [32]. This process reduces the size of the original model while retaining the exact modal properties and is not dependent on the choice of master DOFs [14]. The SEREP transformation was explained in section 2.4.3. and this reduction process will be used for defining new correlation technique.

4.4. Minimum Test Data Requirements for Correlation

It has already been noted that in order to have a unique least-squares solution to equation (2.4.3-3), the **necessary** and **sufficient** condition is the full rank of the measured mode shape submatrix, shown in equation (2.4.3-5). In practice, there are two different requirements embodied in this condition. The first of these is that the number of measured DOFs must be equal to or greater than the number of measured modes, and the second is that the **choice** of these measured DOFs must be such that it provides linear independence of the measured incomplete modes. There are a number of automatic measurement DOF selection methods, as explained in the previous chapter.

A sufficient requirement for selection of the minimum number of measurement points is a well-conditioned truncated theoretical mode shape matrix, $[\phi]_{nxm}$. Numerically, the equation (2.4.3-5) requirement means that the smallest singular value of the truncated mode shape matrix must be greater than the floating-point threshold value of the computer (see expressions 2.2.1-4 and 2.2.1-5).

Another type of check is an assessment of the ratio of the largest to the smallest singular values (condition number) of the theoretical mode shape matrix $[\phi]_{nxm}$ as explained in section 3.6.5. The larger the ratio, the worse the choice of the measurement DOFs.

4.5. SEREP-based Normalised Cross Orthogonality Correlation Technique

The Modal Assurance Criterion (MAC) is the most commonly-used correlation coefficient for assessing linear (in)dependence of mode shapes. However, this technique has been found inappropriate for some applications, and a SEREP theoretical mass reduced cross-orthogonality (SCO) correlation coefficient, as defined in equation (4.5-1), can be used instead [37].

$$SCO(i,j) = \frac{\left|\{\psi_{X,i}\}_n^T([\phi_A]_{nxm}^{+T}[\phi_A]_{mxn}^{+})\{\psi_{A,j}\}_n^*\right|^2}{\{\psi_{X,i}\}_n^T([\phi_A]_{nxm}^{+T}[\phi_A]_{mxn}^{+})\{\psi_{X,i}\}_n^* \cdot \{\psi_{A,j}\}_n^T([\phi_A]_{nxm}^{+T}[\phi_A]_{mxn}^{+})\{\psi_{A,j}\}_n^*} \qquad (4.5\text{-}1)$$

It is possible to use either a SEREP mass or stiffness reduced matrix from equations (2.4.3-10) or (2.4.3-11), based on experimental rather than theoretical modal data, but since the measurement accuracy for experimental mode shapes is generally not high (the experimental modes contain noise and that makes solution of equation (2.4.3-4) ill-conditioned), and because the theoretical mass matrix is usually known more accurately than the theoretical stiffness matrix, the most appropriate solution for SEREP-based correlation coefficient is to use only the theoretical mode shapes as given in equation (4.5-1).

This correlation coefficient has an advantage over the MAC in that it is more sensitive to the actual similarity or dissimilarity between the mode shapes. The SEREP mass matrix reduced normalised Cross Orthogonality (SCO) correlation coefficient will generally have a higher value for two similar mode shapes than the MAC correlation coefficient, and conversely for two dissimilar mode shapes, SCO will have a lower value than MAC. Another interesting feature of the SCO correlation coefficient is that no actual theoretical mass or stiffness matrices are required, i.e. no extra data are required other than those used for the standard MAC calculation.

Although realisation of complex mode shapes is proposed in the correlation procedure, SCO can handle complex modes. It should be noted here that in some cases of comparison of real and complex modes, the correlation results can change when realised complex mode shapes are used rather than original complex mode shapes. The influence of realisation process on the correlation results is limited in most practical test cases, although it is recommended to check the correlation results both before and after the realisation process.

4.6. Natural Frequency Comparison

Comparison of the natural frequencies between two models is usually performed by fitting the best straight line through a plot of the natural frequency points. This comparison technique cannot help to select the CMPs, and so a new technique that can be used for selection of CMPs is proposed here.

A **Natural Frequency Difference (NFD)** correlation coefficient gives an assessment of the differences between all combinations of natural frequencies, i.e. all potential CMPs.

$$NFD(i,j) = \frac{\left|\omega_i - \omega_j\right|}{\min(\omega_i, \omega_j)} x\,100 \quad [\%] \qquad (4.6\text{-}1)$$

A typical plot of the NFD matrix is given in Figure 4-4. It is important to note that this correlation coefficient should be used only as an additional piece of information when selecting CMPs, and not as the sole indicator. The larger the NFD value for two mode shapes is, the less likely the pair is to be a CMP.

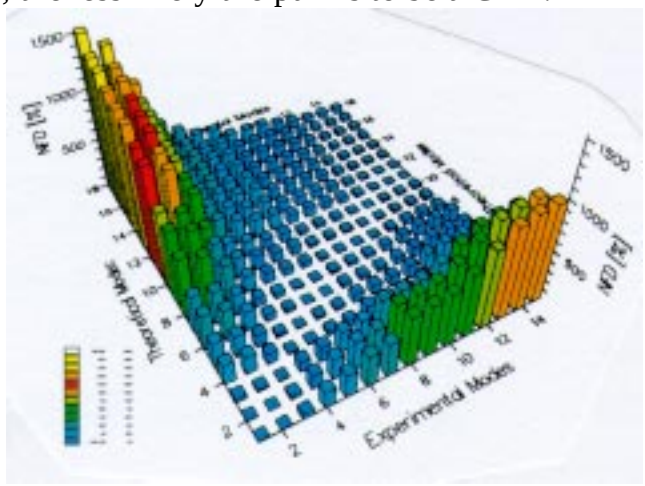

Figure 4.4. Natural Frequency Difference table.

4.7. Automatic Correlation Procedure

The automatic correlation procedure seeks to select CMPs automatically, based on statistical processing of some of the above-mentioned correlation coefficients. Figure 4-5 shows the automatic correlation steps schematically.

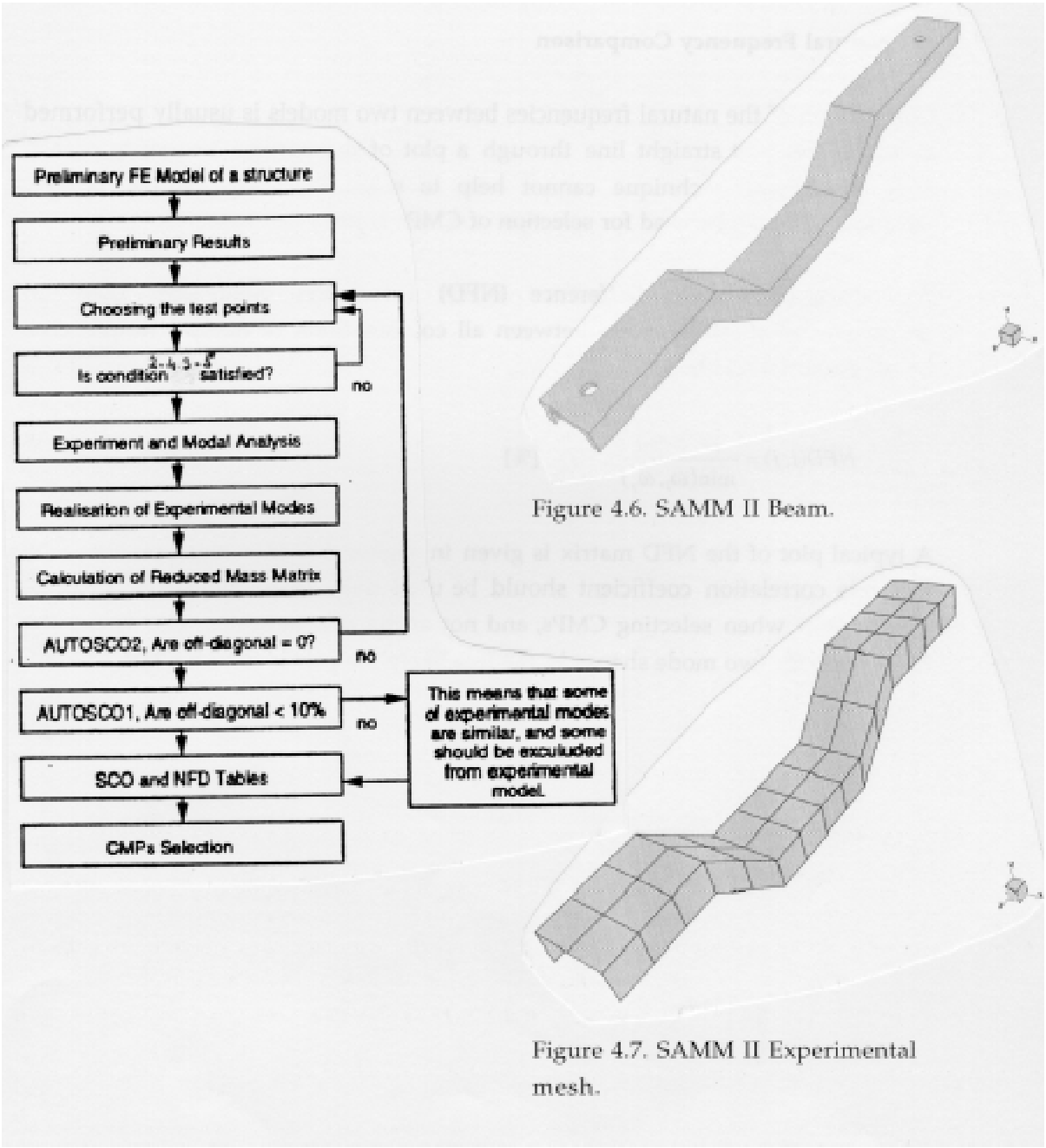

Figure 4.5. Automatic Correlation Procedure.

The procedure begins with the planning of a modal test on the structure. The first step is to generate a model of the structure and to extract the eigensolution in the required frequency range. Then, using any of the existing measurement point selection methods, the minimum data requirements can be established, i.e. the number of measured DOFs has to be greater than the number of measured modes, and the rank of the reduced mode shape matrix - determined by particular choice of DOFs - must be equal to the number of measured modes.

The second step in the algorithm is realisation of complex experimental mode shapes. In section 4.2.3 it was shown how to assess the complexity of the measured mode shapes. Generally, for a structure which is not very heavily damped, the modal complexity factor should not be very high. It is difficult to set a limit for critical modal complexity, but if the value of this coefficient is very high for some modes, those should be plotted in the complex plane and checked (Figures 4-1, 4-2 and 4-3). This checking is actually part of the modal analysis procedure and gives a general assessment of the reliability of the measured modal data. After this check, the experimental mode shapes should be realised using the techniques given in section 4.2.4, taking care to note that any realisation process is approximate.

The third step in this algorithm is the auto correlation of theoretical data on the equivalent experimental mesh in order to assess the independence of the theoretical mode shapes. Auto (self) correlation of theoretical mode shape data using the SCO formulation will give a perfect correlation result: all diagonal terms are 1 and all off-diagonal terms are zero (Figure 4-8(d)). The reason for this is that because of the normalisation of the mode shapes by the SEREP-reduced mass matrix, and because these mode shapes are orthogonal since they come from theoretical analysis, a perfect check is obtained and this diagram shows how the actual correlation picture should ideally be if the experimental mode shapes are exactly equivalent to the corresponding theoretical ones. Additionally, an auto correlation of the theoretical mode shapes, but confined to the DOFs corresponding to the experimental mesh, using the MAC correlation coefficient can be performed in order to assess the performance of the minimum test data requirement procedure which was used in the pre-test phase.

The fourth step in the algorithm is an auto correlation of the experimental mode shapes using the SCO correlation check in order to assess the independence of the experimental mode shapes. Ideally, the resulting SCO matrix should have all off-

diagonal terms identically zero. If any of the off-diagonal terms in the SCO matrix are not zero, this will indicate a linear dependence or similarity between the corresponding pair of modes. In most cases, the reason for this is either an error in the modal analysis which occurred during the modal parameter extraction process or because there are not enough measured DOFs. If it was found that some of modes in the experimental model were "generated" by the modal analysis procedure, these modes should be deleted from the experimental set. The second reason should not normally occur if the test data requirements were planned appropriately according to step 1.

The fifth step in the algorithm is the preliminary selection of CMPs which is based on the SEREP Cross Orthogonality (SCO). In the case of an ideal correlation, some terms of the SCO matrix should be equal to 1 and the rest of the matrix terms should be equal to zero, indicating perfect mode pairing. Because of discrepancies between theoretical and experimental models, high values in the SCO matrix indicate good agreement and low values indicate poor agreement between mode shapes. Generally, the SCO matrix will be similar to the MAC matrix with the improvement that the similarity between two modes will be represented with the higher SCO values than the MAC values, and dissimilarity between mode shapes will be represented with the lower SCO values than the MAC values, as explained in section 4.5.

The last step in the algorithm is the final selection of the CMPs using both SCO and NFD correlation tables. The SCO table is scanned first and if there are any uncertainties about the selection of particular CMPs, the NFD table is used in order to clarify the possibility of those CMPs. Generally, any two modes whose NFD value is greater than 100 % should not be taken as a possible CMP.

4.8. Test Case Study

The SAMM II B structure (shown in Figure 4-6) was used to demonstrate the use of the automatic correlation procedure. The measurements were performed at the 105 DOFs on the mesh shown in Figure 4-7. The minimum test data requirement, i.e. condition (2.4.3-5), is satisfied and the SEREP reduction process is well-conditioned, checking the singular values of reduced mode shape matrix $[\phi_A]_{nxm}$.

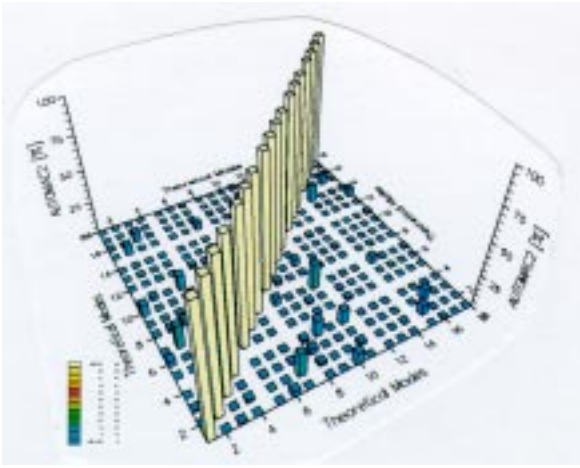

Figure 4.8(a). AUTOMAC1

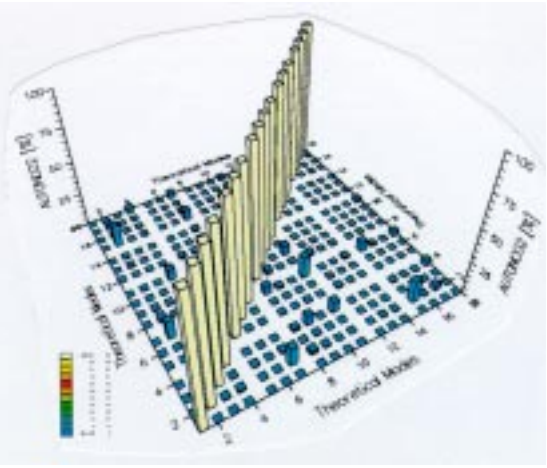

Figure 4.8(b). AUTONCO1(K)

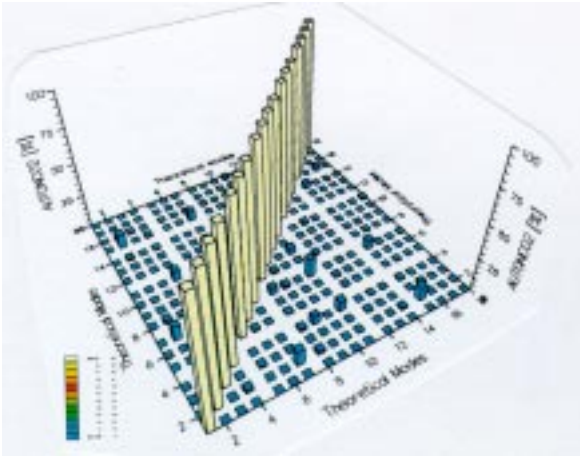

Figure 4.8(c). AUTONCO1(M)

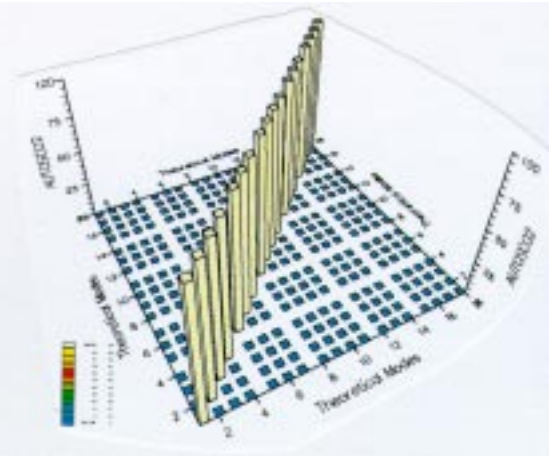

Figure 4.8(d). AUTOSCO1

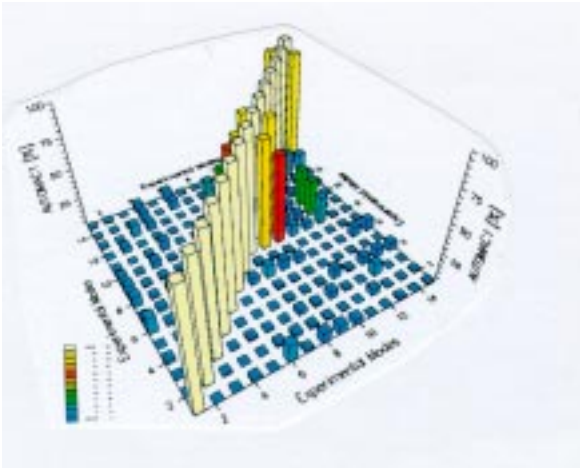

Figure 4.9(a). AUTOMAC2

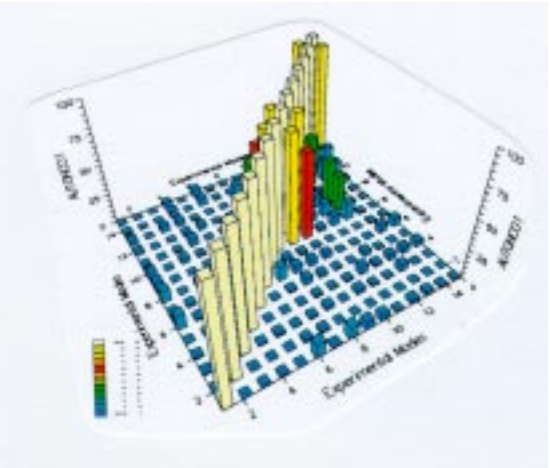

Figure 4.9(b). AUTONCO2(K)

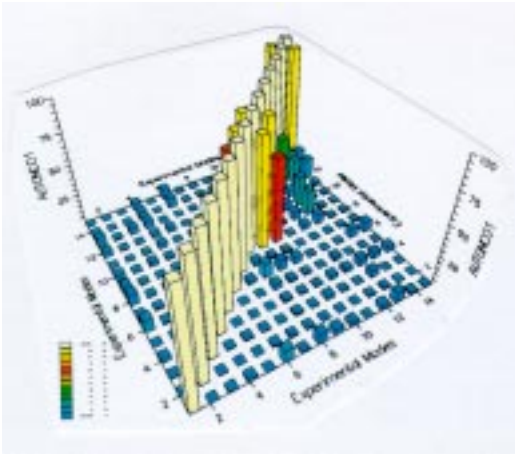

Figure 4.9(c). AUTONCO2(M)

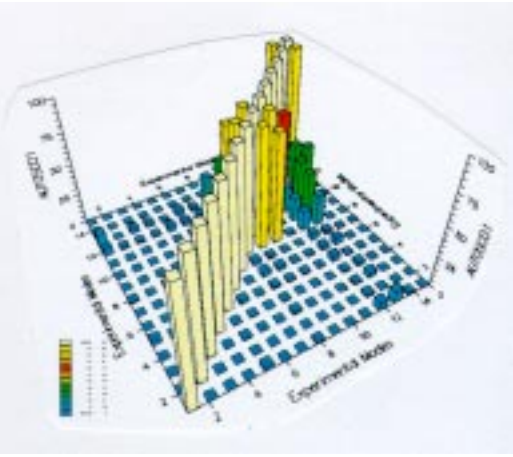

Figure 4.9(d). AUTOSCO2

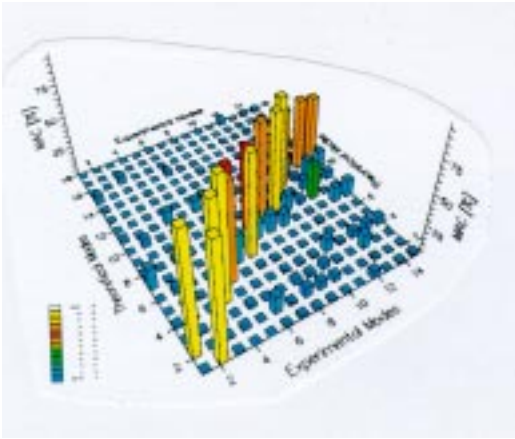

Figure 4.10(a). MAC

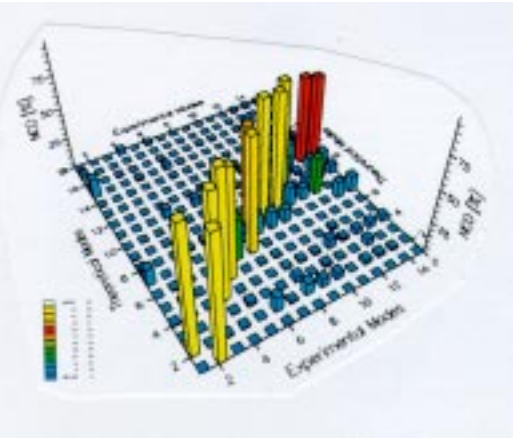

Figure 4.10(b). NCO(K)

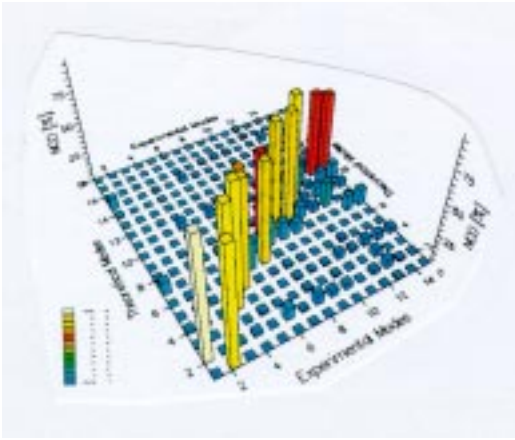

Figure 4.10(c). NCO(M)

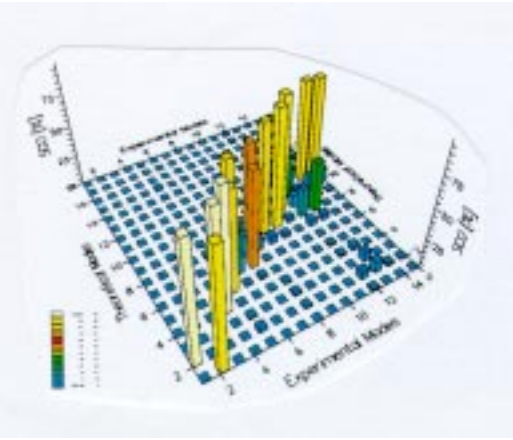

Figure 4.10(d). SCO

As was described in the previous section, and after realisation of experimental mode shapes, auto correlation of theoretical modes was performed using the DOFs on the experimental mesh. The Auto MAC result is shown in Figure 4-8(a), the NCO result using the truncated theoretical stiffness matrix is shown in Figure 4-8(b), the NCO result using the truncated theoretical mass matrix is shown in Figure 4-8(c) and, finally, the SCO result is shown in Figure 4-8(d). Comparing these four graphs it is clear that little improvement is gained by using the NCO formulation over the MAC, but the ideal situation is observed using the SCO correlation formulation where the off-diagonal terms are actually zero, and that is not the case with the MAC and NCO correlation techniques.

Auto correlation analysis was performed on the experimental modes using different correlation formulations (MAC, NCO and SCO), and the results are shown in Figures 4-9(a), 4-9(b), 4-9(c) and 4-9(d). Inspecting each of these tables, it can be seen that there are some similarities between experimental modes 8, 9 and 10. Comparing their natural frequencies, it is easy to realise that modes 8 and 9 were "created" during the modal analysis process and that they should be excluded from experimental model. Again, the SCO formulation gave a better assessment of the correlation between mode shapes since it detected the similarity between modes 8, 9 and 10 with higher values.

Finally, theoretical and experimental modes were compared using the MAC, NCO mass and stiffness based formulations, and the SCO correlation techniques. Results are shown in Figures 4-10(a), 4-10(b), 4-10(c) and 4-10(d), respectively. The NCO gives slightly improved results over the MAC. Also, it is possible to detect by close inspection that the NCO mass-based formulation generally gives a little better results than the NCO stiffness-based results. This is due to a more accurate mass matrix estimation in the theoretical model than the stiffness matrix. Improvement from MAC to SCO is obvious, both for correlated pairs and uncorrelated pairs of modes. This shows that generally for two modes which are similar, the SCO correlation values will be higher than the MAC correlation values, and vice versa if they are orthogonal: the SCO values will be lower than MAC values.

4.9. Comparison of Response Properties

Correlation at response level is a basic comparison of two sets of FRFs. Two corresponding FRFs are simply overlaid and their resemblance is observed.

Unfortunately, there are a few disadvantages associated with this comparison technique, the main one is that it is almost impossible to quantify comparison between two curves in such a way that it could be useful in most practical situations. It is possible to find the area between two corresponding FRFs, but then a small differences in natural frequencies will imply very low degree of correlation between the two FRFs where in fact, both FRFs could be regenerated using the same modal constants. The major problem for this quantification process is the inability to separate natural frequencies and modal constants in the comparison process.

Another disadvantage of this type of correlation is the residual problem on the theoretical FRFs. A very useful method for control of the residual effect on regenerated FRFs is presented in section 4.10.1.

These two disadvantages should not dissuade analysts from performing comparisons at the response level, because there are some advantages that should be mentioned here. A major advantage and reason for using this comparison approach is that this type of comparison can show correlation at response level between two FRFs, and in some cases it is impossible or inappropriate to perform modal analysis (due to heavy damping), then this comparison technique can be very useful.

4.10. Calculation of Frequency Response Functions (FRFs)

Predicted Frequency Response Functions (FRFs) of a system can be generated using either the direct or the modal superposition approaches.

The direct approach consists of direct inversion of the dynamic stiffness matrix of the system for every frequency point of interest, as shown in the following expression:

$$[\alpha(\omega)] = \left[\mathrm{K} + i\mathrm{D} - \omega^2 \mathrm{M} \right]^{-1} \qquad (4.10\text{-}1)$$

The direct approach generates **exact** values for the FRFs but is computationally very expensive since an inversion of the dynamic stiffness matrix is required for every frequency point. These inversions become particularly expensive as the number of

degrees-of-freedom increases and that makes this approach for generation of the predicted FRFs unsuitable and, at some stage of model size, practically impossible.

The modal approach for regeneration of predicted FRFs is based on expression (4.10-2) below in which the general form of structural damping in the system is assumed.

$$\alpha_{j,k}(\omega) = \sum_{r=1}^{N} \frac{\left(\phi_{j,r}\right)\left(\phi_{k,r}\right)}{\omega_r^2 - \omega^2 + i\eta_r\omega_r^2} \qquad (4.10\text{-}2)$$

The modal approach will generate exact values for the FRFs only if all the natural frequencies and modes are available for inclusion in expression (4.10-2). It is extremely rare for all the natural frequencies and modes to be calculated for a theoretical system: instead, only modes from a limited frequency range are calculated. Now, if an incomplete set of modes is used for the FRF generation in expression (4.10-2), the FRF value becomes **approximate**, as shown in the following expression:

$$\alpha_{j,k}(\omega) \approx \sum_{r=1}^{m} \frac{\left(\phi_{j,r}\right)\left(\phi_{k,r}\right)}{\omega_r^2 - \omega^2 + i\eta_r\omega_r^2} \qquad (4.10\text{-}3)$$

Since the values of the FRF around a resonance are influenced mostly by the modal parameters of that mode only, the more so closest to the resonance, an acceptable approximation of the FRF around the resonance can be obtained when only a limited number of modes are included. This modal approach using an incomplete set of modes, expression (4.10-3), is the most commonly-used approach for FRF regeneration in practice. Figure 4-11 shows a plot of two FRFs regenerated using different numbers of terms in the series, (4.10-3).

Generally, a similar value of damping is used for each mode in expression (4.10-3), unless the damping is modelled explicitly, which is rarely the case for theoretical systems. Figure 4-12(a) shows three FRFs which were regenerated each with different value for the modal damping. Figure 4-12(b) shows an expanded region of the Figure 4-12(a) in which the sensitivity of the FRFs' values to damping can be seen more clearly.

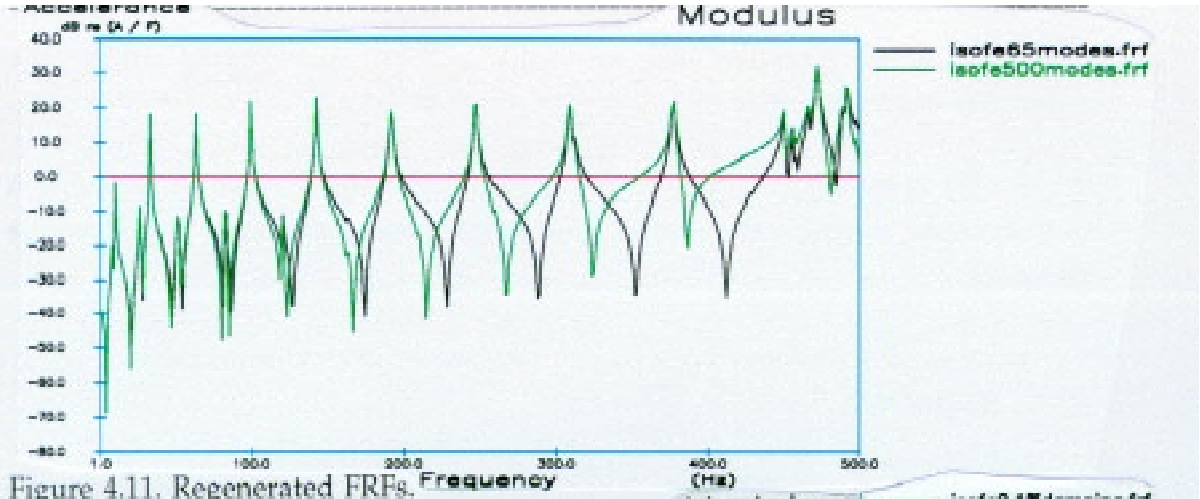

Figure 4.11. Regenerated FRFs.

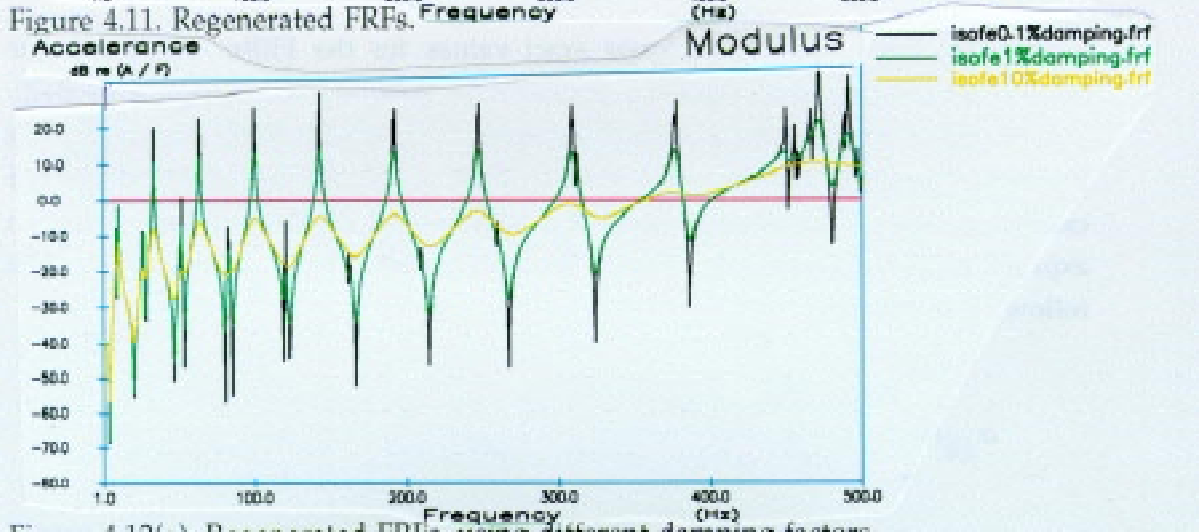

Figure 4.12(a). Regenerated FRFs, using different damping factors.

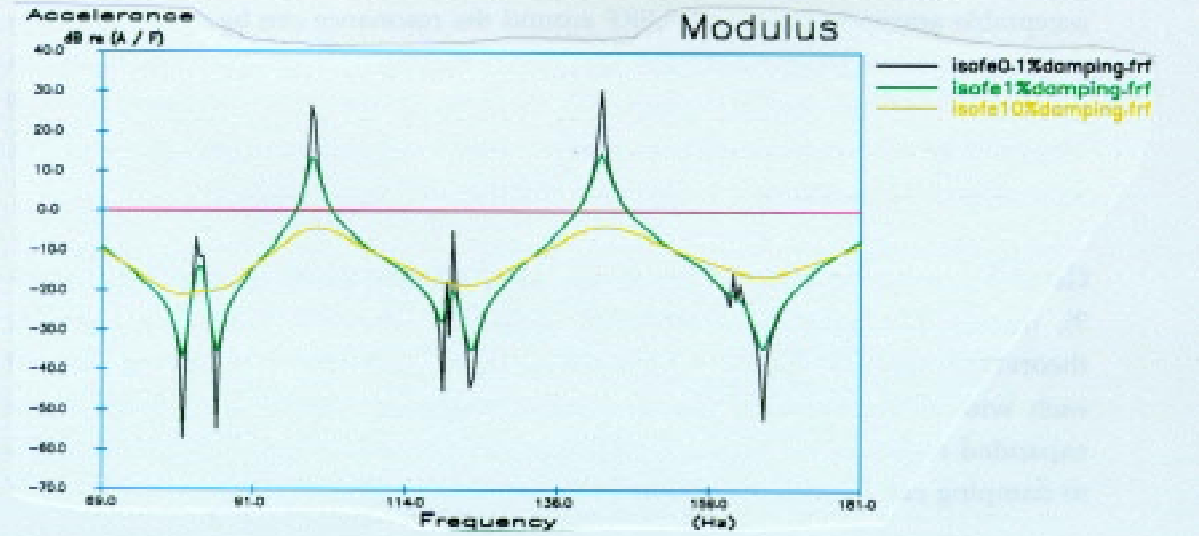

Figure 4.12(b). Expanded regions of FRFs from Figure 4.12(a).

The FRFs are continuous curves, i.e. continuous complex functions of a real variable (excitation frequency, ω), and in order to display them, two plots must be presented. Since the values of the FRFs around the resonances are larger by several orders of magnitude than the values away from resonance, and particularly around antiresonances, a sufficient number of frequency points is necessary in order to obtain a consistent shape of the FRFs around the resonances. This means that for the same values of modal parameters and damping but different frequency increments, the shape of the FRFs could appear rather different, as shown in Figure 4-13. In order to have all resonances shown consistently on the FRF plots, the frequency increment must be significantly smaller than the difference between the two closest natural frequencies, although some resonances can disappear with an increase of the damping value. Once the frequency increment is refined so that all resonances are clearly shown, one can notice that the positions of maximum resonance values also depend on the frequency increment. The smaller the frequency increment, the larger the values that will be obtained at the resonances, until this converges to stable values for a small value of frequency increment.

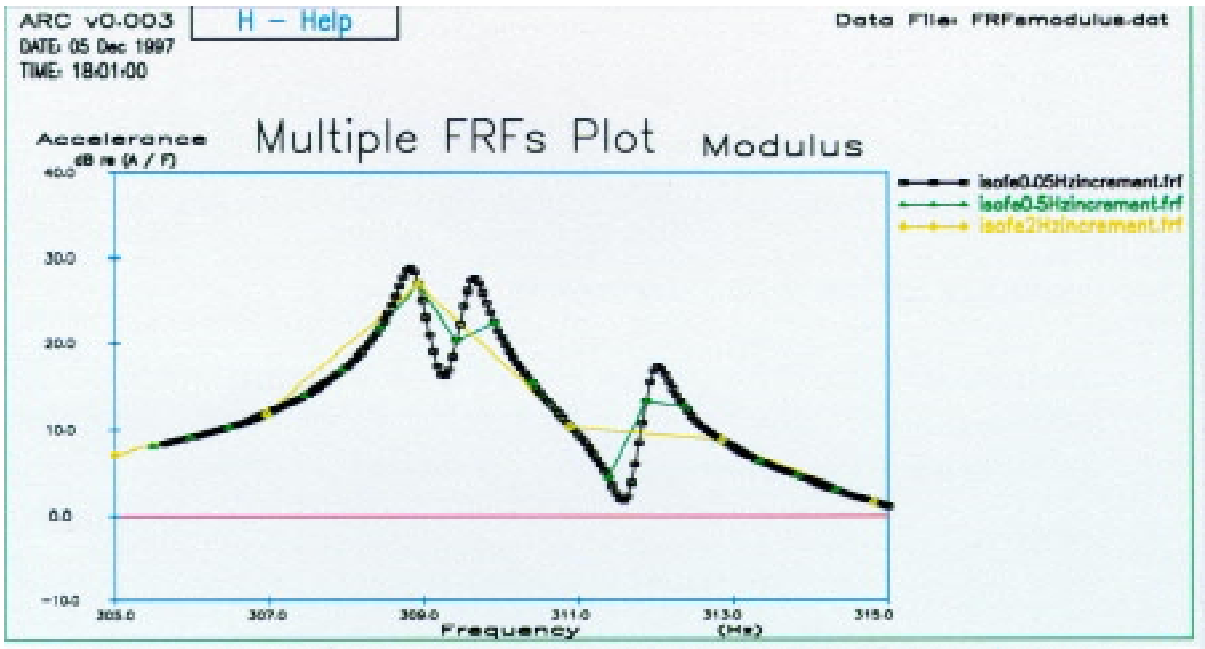

Figure 4.13. Regenerated FRFs using different frequency increment.

4.10.1. Finding The Residual Effects For The System - The "Forest" Technique

Each FRF of an MDOF system which has a number of resonances in a specified frequency range can be approximated by the same number of SDOF FRF components, as shown in Figure 4-14. The values of each SDOF FRF are smaller at frequencies away from its resonance frequency. This means that for any FRF in the frequency range between ω_1 and ω_2, there is a final frequency ω_3, which is larger than ω_2, for which the influence of all modes whose natural frequencies are higher than ω_3 to the MDOF FRF become negligible.

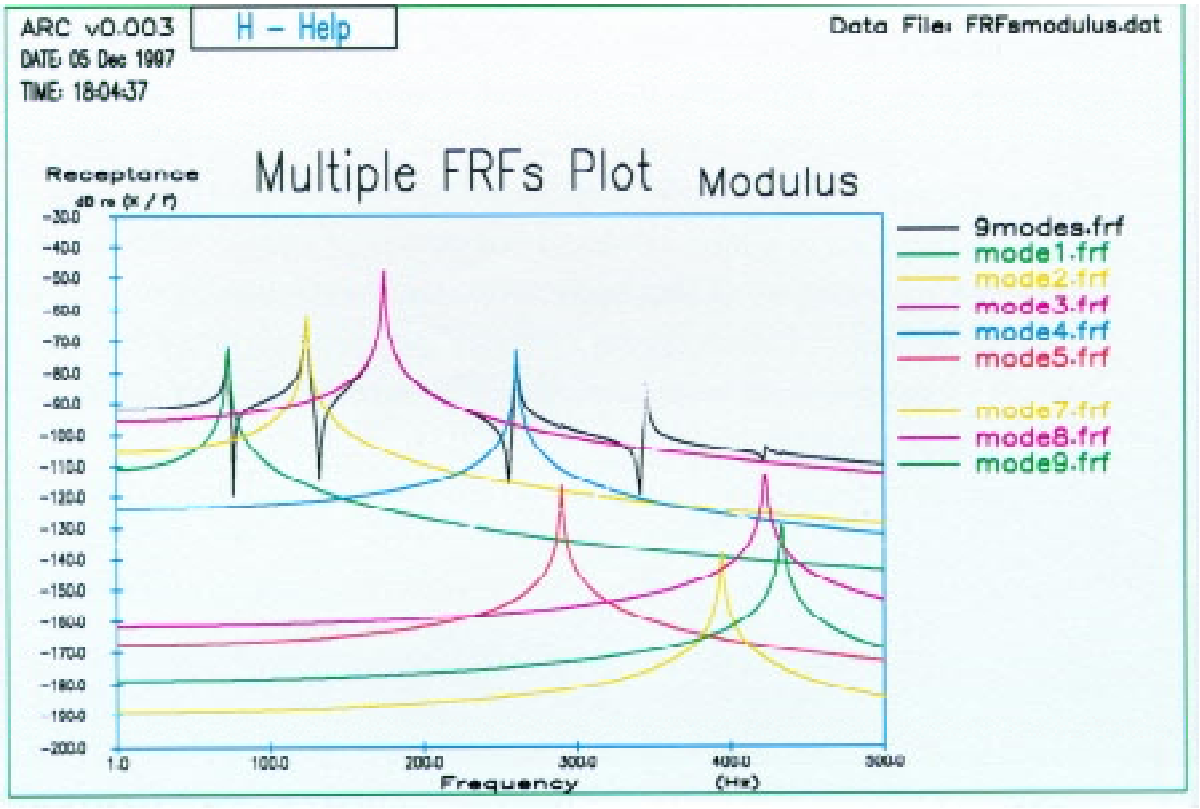

Figure 4.14. FRF and its SDOF components.

Analysing the SDOF FRF expression which is given by the equation (4.10.1-1), it can be seen that the absolute value of the basic FRF around its resonance depends on the values of eigenvector elements $\left(\phi_{j,r}\right)$ and $\left(\phi_{k,r}\right)$, and the given damping value.

$$\alpha_{j,k}(\omega) = \frac{\left(\phi_{j,r}\right)\left(\phi_{k,r}\right)}{\omega_r^2 - \omega^2 + i\eta_r\omega_r^2} \qquad (4.10.1\text{-}1)$$

Generally, the larger the values of the parameters $\phi_{j,r}$, or the modal constants ${}_rA_{j,k}$ (which are their products), the larger will be the values of the corresponding SDOF

FRFs and the higher will be the influence of the higher modes. Now, it will be **assumed** that the values of all eigenvectors are of the same order of magnitude for all modes. This assumption is reasonable on the grounds that it means that all deformations of the structure are of the same order of magnitude. Usually, the lower modes have larger maximum mode shapes vector values, $\phi_{\max}$, than do the higher modes, although maximum mode shape vector value, $\phi_{\max}$, does not strictly decrease for higher modes.

The "FOREST" technique (Finding of the Residual Effects for the System) for determination of the residual effects for FRF calculations is based on the principle that inclusion of all modes in the frequency range between ω_1 and ω_3 would reproduce the FRFs in the smaller frequency range between ω_1 and ω_2 with a required accuracy. Assuming that all modes of the theoretical model are calculated over the frequency range between ω_1 and ω_2, and that all the required FRFs were regenerated in that frequency range for specified damping levels and frequency increment, it is not known what is the actual influence of the higher modes on those FRFs. Since the influence of each higher mode depends on its natural frequency and modal constant, it will be assumed here that there can be considered to be a mode, whose natural frequency is ω_3 and whose modal constant value is equal to the maximum modal constant value of all other DOFs for all calculated modes from the frequency range between ω_1 and ω_2, which obeys the following expression (4.10.1-2):

$$\left| \frac{\phi_{\max}^2 \varepsilon_\phi}{\omega_3^2 - \omega_2^2 + i\eta\omega_3^2} \right| \leq \left| \alpha_{\min} \right| \varepsilon_\alpha \qquad (4.10.1\text{-}2)$$

This expression states that, in the worst case, the first of the "higher" modes which is excluded from the FRF regeneration has the maximum influence on the FRFs in the frequency range between ω_1 and ω_2 which is less than the minimum value of these FRFs regenerated using only the modes in the frequency range between ω_1 and ω_2 and multiplied by the required accuracy factor, ε_α. Since the maximum eigenvector amplitude, $\phi_{\max}$, is chosen by considering all DOFs, although only for modes within the frequency range between ω_1 and ω_2, another accuracy coefficient, ε_ϕ, is required in order to eliminate the possibility of larger maximum amplitudes for the higher modes above the frequency ω_2.

The values of the two accuracy factors, ε_α and ε_ϕ, can vary as shown in the following expressions (4.10.1-3) and (4.10.1-4).

$$0 < \varepsilon_\alpha \leq 1 \tag{4.10.1-3}$$

$$1 \leq \varepsilon_\phi < \infty \tag{4.10.1-4}$$

The problem given in expression (4.10.1-2) is a polynomial inequality of the 4th order, where proper solution is of the following form:

$$\omega_3^2 \geq \frac{\omega_2^2 + \sqrt{F\left(1+\eta^2\right) - \eta^2\omega_2^4}}{1+\eta^2} \tag{4.10.1-5}$$

where the coefficient F is defined by:

$$F = \left(\frac{\phi_{\max}^2 \varepsilon_\phi}{\left|\alpha_{\min}\right| \varepsilon_\alpha} \right)^2 \tag{4.10.1-6}$$

The required condition for a reasonable solution of the inequality (4.10.1-2) is of the following form:

$$Cond(II) = \frac{\varepsilon_\phi \phi_{\max}^2}{\eta\omega_2^2 \left|\alpha_{\min}\right| \varepsilon_\alpha} \geq 1 \tag{4.10.1-7}$$

The $Cond(II)$ value has some physical meaning for the FOREST technique. The higher the value of $Cond(II)$, the better the accuracy of the regenerated FRFs. If the value of $Cond(II)$ is less than 1.0, then the inequality (4.10.1-2) does not have a reasonable solution for the specified accuracy parameters ε_α and ε_ϕ, i.e. the inequality is already satisfied for the quoted accuracy parameters and their values should be changed so that a more reasonable solution can be obtained. From the inequality (4.10.1-7), it is possible to find the maximum allowed values for the accuracy parameters which are given by the following expression:

$$\frac{\varepsilon_\alpha}{\varepsilon_\phi} \le \left(\frac{\varepsilon_\alpha}{\varepsilon_\phi} \right)_{\max} = \frac{\phi^2_{\max}}{\eta \omega_2^2 \left| \alpha_{\min} \right|} \tag{4.10.1-8}$$

Expression (4.10.1-8) determines the accuracy which the regenerated FRFs have in the frequency range between ω_1 and ω_2 using only the modes from that frequency range and the specified accuracy for the FOREST calculation must be smaller than this value.

4.11. "FOREST" Accuracy Diagram

In the previous section, the FOREST technique was defined by expression (4.10.1-2) and a solution for finding the required frequency ω_3 for the specified accuracy of the regenerated FRFs was presented. It was also shown that this solution has the form of a polynomial equation of the 4th order with a unique solution. Another way of defining the problem of the influence of the higher modes is to find the accuracy of the regenerated FRFs for the specified frequency ω_3, i.e. using expression (4.10.1-2) the following expression is obtained which defines the accuracy of the regenerated FRFs:

$$\frac{\varepsilon_\alpha}{\varepsilon_\phi} = \left| \frac{\phi^2_{\max}}{(\omega_3^2 - \omega_2^2 + i\eta\omega_3^2)\,\alpha_{\min}} \right| \tag{4.11-1}$$

The above expression defines the accuracy of the regenerated FRFs in the frequency range from ω_2. The curve defined by expression (4.11-1) is called the "FOREST Accuracy Diagram". A typical plot of the "FOREST Accuracy Diagram" is shown in Figure 4-15. Using this diagram it is relatively easy to find the required frequency value ω_3 for the specified accuracy ratio value $\left(\frac{\varepsilon_\alpha}{\varepsilon_\phi} \right)$ and it is not necessary to solve the polynomial equation of the 4th order. This accuracy curve is dependent on several factors, i.e. damping value, maximum amplitude of the mode shapes, minimum receptance value of the regenerated FRFs and the frequency ω_2 and the choice of the DOFs for which the FRFs need to be regenerated. However, one question remains unanswered, and that is: "What value of accuracy ratio $\frac{\varepsilon_\alpha}{\varepsilon_\phi}$ should be considered as reasonable?". It is clear that the higher the frequency limit ω_3 , the smaller will be the influence of the higher modes excluded and the more expensive

are the calculations required to extract the necessary modes. Considering the shape of the accuracy curve (see Figure 4-15) it can be seen that after some frequency value ω_3 the accuracy actually changes very little and any calculation of the modes above that frequency is not necessary. In order to find the optimum value of the frequency ω_3 it is recommended that the first derivative of expression (4.11-1) be considered and then that the frequency ω_3 be selected as the first derivative value approaches zero. This would mean that above the selected frequency, ω_3, the change in the accuracy value is insignificant. The first derivative of the accuracy function is defined by the following expression:

$$\frac{d\left(\frac{\varepsilon_\alpha}{\varepsilon_\phi}\right)}{d(\omega_3)} = -\frac{2\left|\phi^2_{\max}\right|\left[\omega_3\left(\omega_3^2-\omega_2^2\right)+\eta^2\omega_3^3\right]}{\left|\alpha_{\min}\right|\left[\left(\omega_3^2-\omega_2^2\right)^2+\eta^2\omega_3^4\right]^{\frac{3}{2}}} \qquad (4.11\text{-}2)$$

A typical plot of the first derivative of the FOREST accuracy function is shown in Figure 4-16.

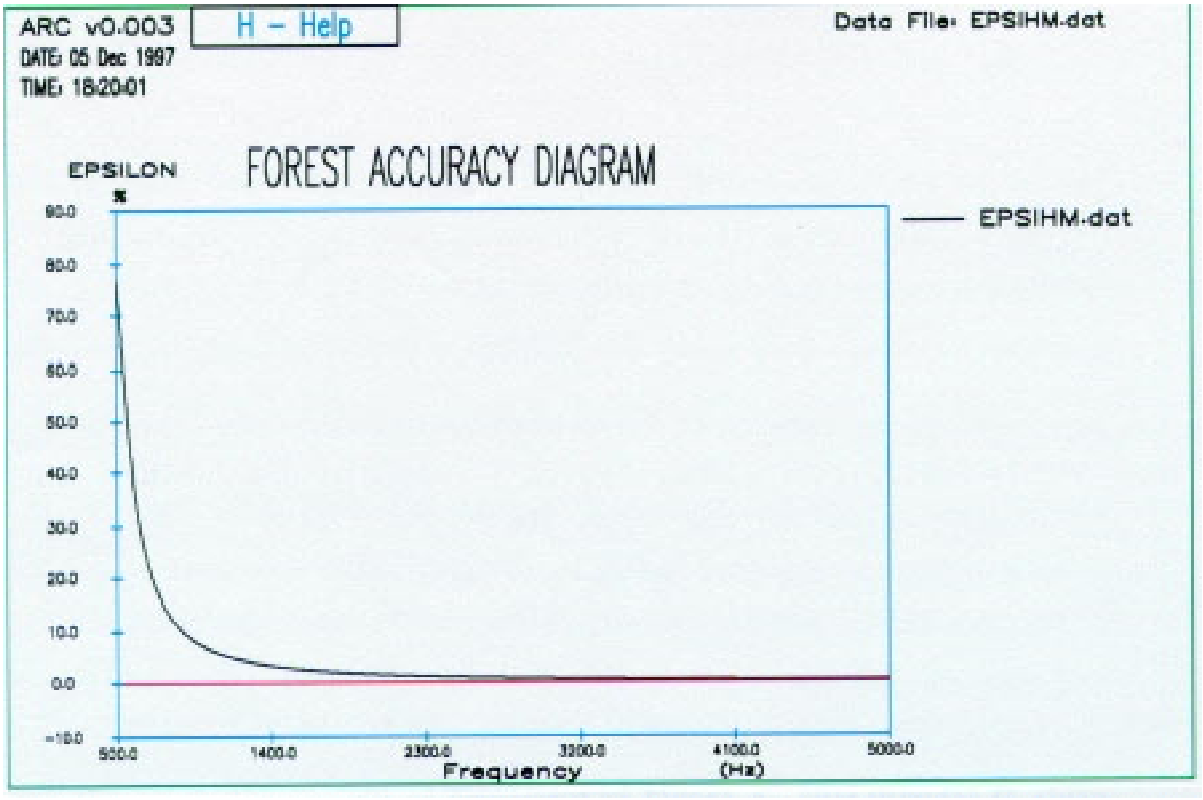

Figure 4.15. 'FOREST' Accuracy Diagram.

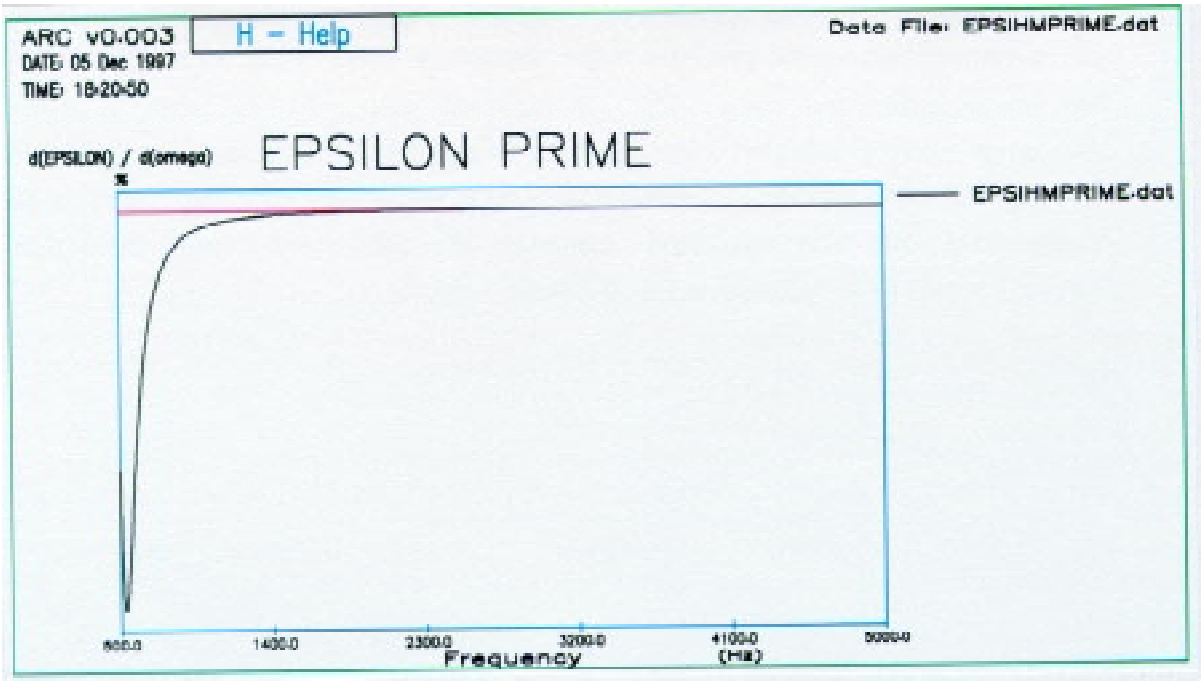

Figure 4.16. First derivative curve of 'FOREST' accuracy diagram.

4.11.1. Application Of The FOREST Technique

Figure 4-17 shows schematically the separate steps for application of the FOREST technique and each separate step is described in detail below.

In the first step it is necessary to calculate all modes from the frequency range in which the required FRFs need to be regenerated with a specified accuracy. This is necessary in order to find the maximum value of the eigenvector elements for all the translational DOFs, $\phi_{\max}$.

Then, in the second step, the required FRFs need to be regenerated using all the calculated modes from the first step with a specified damping value and frequency increment. This is necessary in order to find the minimum value of the required FRFs in the next step.

In the third step, the minimum value of all regenerated FRFs from the first step must be found, together with the maximum value of all the eigenvector elements for the translational DOFs. The residual effects are different for each FRF and the minimum value of each regenerated function determines the sensitivity of that function to the residual effects. Generally, for two different functions, the minimum

values of the FRFs will be different and, consequently, the FOREST technique performed for the same damping and accuracy parameters values would predict a larger frequency limit, ω_3, for the FRF which has lower minimum value. This is expected since an FRF with a lower minimum value is actually more sensitive to the residual effects. If the FOREST technique is to be applied to a system for which more than one FRF needs to be regenerated, then the minimum value of the FRFs ($\alpha_{\min}$) must be found considering all FRFs regenerated in the second step.

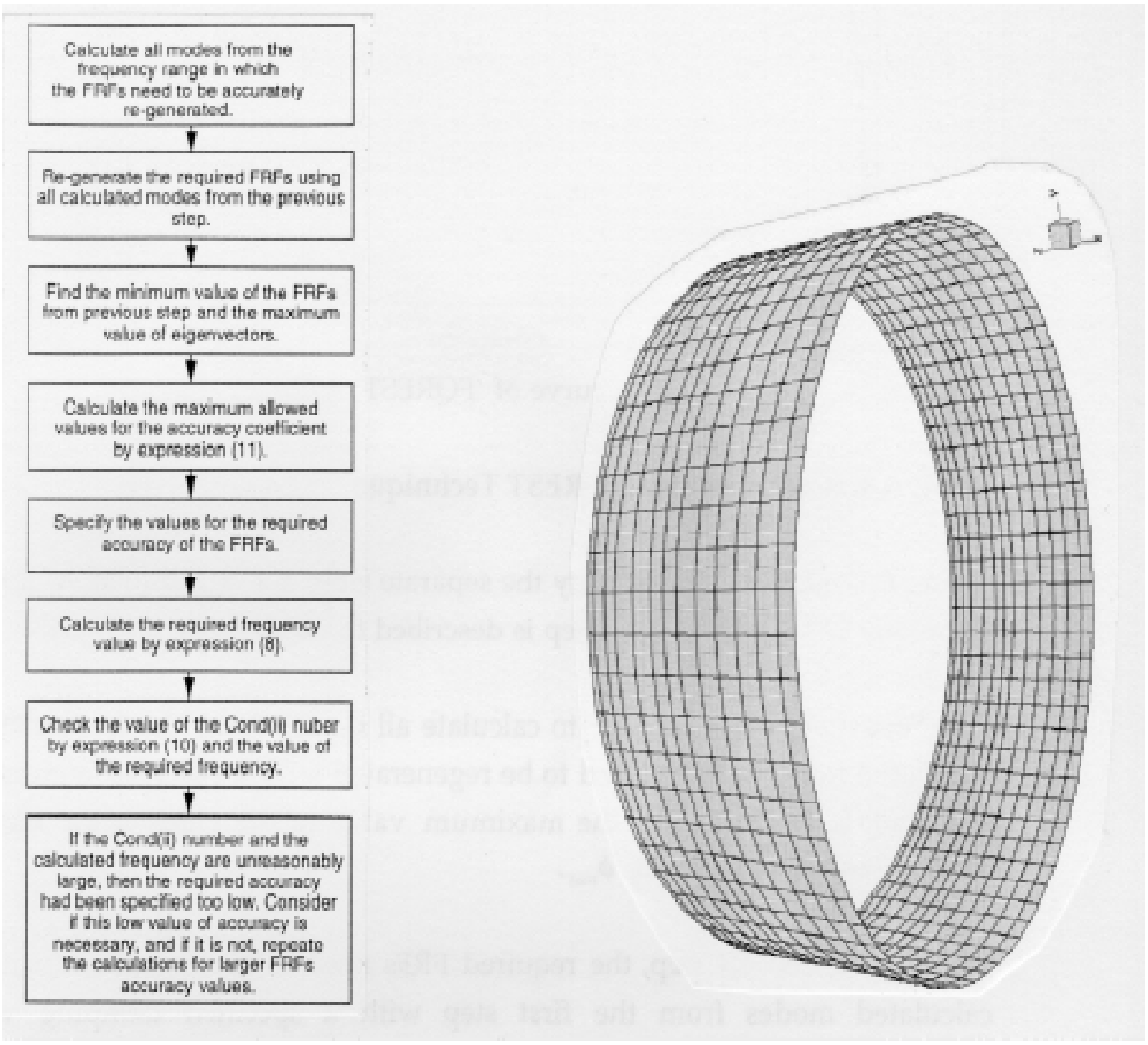

Figure 4.17. Application of FOREST Technique. Figure 4.18. Casing FE model.

The fourth step consists of calculating of the maximum allowed accuracy values from expression (4.10.1-8). The maximum allowed accuracy is, in fact, the accuracy of the regenerated FRFs using only those modes from the frequency range between ω_1 and ω_2.

In the fifth step, the required accuracy for the regenerated FRFs is specified, and this must be less than the maximum allowed accuracy calculated in the fourth step. This is necessary in order to obtain a realistic solution for the required cut-off mode frequency, ω_3. Normally, the accuracy parameters are specified as two different quantities, ε_α for the minimum value of the FRFs, $|\alpha_{\min}|$, and ε_ϕ for the maximum eigenvector value of the translational DOFs, $\phi_{\max}$. Usually, ε_α is specified as a percentage of the $|\alpha_{\min}|$ value, i.e. 1 to 5 % is recommended, and ε_ϕ is specified as a multiple of the $\phi_{\max}$ value.

The required frequency value, ω_3, is calculated from expression (4.10.1-5) in the sixth step.

The seventh step includes calculation of the *Cond*(*II*) number and checking the values of *Cond*(*II*) and frequency ω_3. If the values of *Cond*(*II*) and ω_3 are unreasonably large, due to specifying too small an accuracy value in the fifth step, it should be considered whether this high accuracy is necessary and, if it is not, then new calculations should be performed from the fifth step.

4.11.2. Application of the FOREST Accuracy Diagram

After supplying a minimum receptance value, $\alpha_{\min}$, maximum amplitude value, $\phi_{\max}$, damping value, η, and the frequency, ω_4, the expressions (4.11-1) and (4.11-2) can be used to calculate the "FOREST Accuracy Diagram" (see Figure 4-15) and the derivative of the accuracy function (see Figure 4-16) in the frequency range between ω_2 and ω_4. This frequency, ω_4, represents the upper limit of interest which is usually more than 10 times of the ω_2 frequency value. In order to select the optimum frequency value, ω_3, both diagrams should be considered, noting that the optimum frequency ω_3 value is where the derivative curve of the accuracy function approaches zero, i.e. that means that there is no significant change in the accuracy of the regenerated FRFs.

4.12. FOREST Test Case Study

A structure whose model has 9542 DOF (see Figure 4-18) was used as a test case study for application of the FOREST technique. It is clear that for this size structure a direct FRF regeneration approach is practically impossible. Figure 4-11 shows the point FRFs for point 1 regenerated by the modal approach using 65 and 500 modes.

The influence of the residuals on the FRF which was regenerated using 65 modes is very high, but calculation using 500 modes is quite expensive, so the FOREST technique will be applied in order to find an optimal accuracy-dependent required number of modes.

The FOREST technique is applied in the following steps:

1. 65 modes are known to exist in the frequency range between 0 and 500 Hz, in which range the point FRF for point 1 needs to be regenerated with a given accuracy.

2. The point FRF is regenerated in the frequency range between 0 and 500 Hz using all 65 modes calculated from the previous step, for the specified damping value of $\eta = 0.003$ and a frequency increment of 1 Hz.

3. The minimum receptance value of the FRF is $\alpha_{\min} = -140\,dB$ and the maximum value of the eigenvector elements is $\phi_{\max} = 0.476\,(kg)^{-\frac{1}{2}}$.

4. The maximum allowed ratio for the accuracy coefficient is $\left(\frac{\varepsilon_\alpha}{\varepsilon_\phi}\right)_{\max} = 0.774$.

5. The specified accuracy parameters are $\varepsilon_\alpha = 5\%$ and $\varepsilon_\phi = 2$, or $\left(\frac{\varepsilon_\alpha}{\varepsilon_\phi}\right) = 2.5\%$, well below the maximum allowed values.

6. The required frequency is $\omega_3 = 1565.7\ Hz$.

7. The condition number, $Cond(II)$ is equal to 30.9, and this is considered to be reasonable as well as the value of the required frequency, $\omega_3 = 1565.7\ Hz$, which is about three times the value of the upper limit frequency $\omega_2 = 500\ Hz$.

Now, calculating all modes in the frequency range between 0 and $\omega_3 = 1565.7\ Hz$ it is found that there are 378 modes which must be included for the FRF regeneration to attain the specified accuracy. Figure 4-19 shows the same FRF but regenerated using 65, 378 and 500 modes. It is clear that little improvement is obtained if modes after the FOREST predicted frequency, ω_3 are included.

The "FOREST Accuracy Diagram" was generated in the frequency range between 500 and 5000 Hz. The FOREST accuracy function for this case is shown in Figure 4-15 and the derivative of the FOREST accuracy function is shown in Figure 4-16. By considering these curves it is relatively easy to conclude that the optimum frequency value ω_3 is around 1500 Hz.

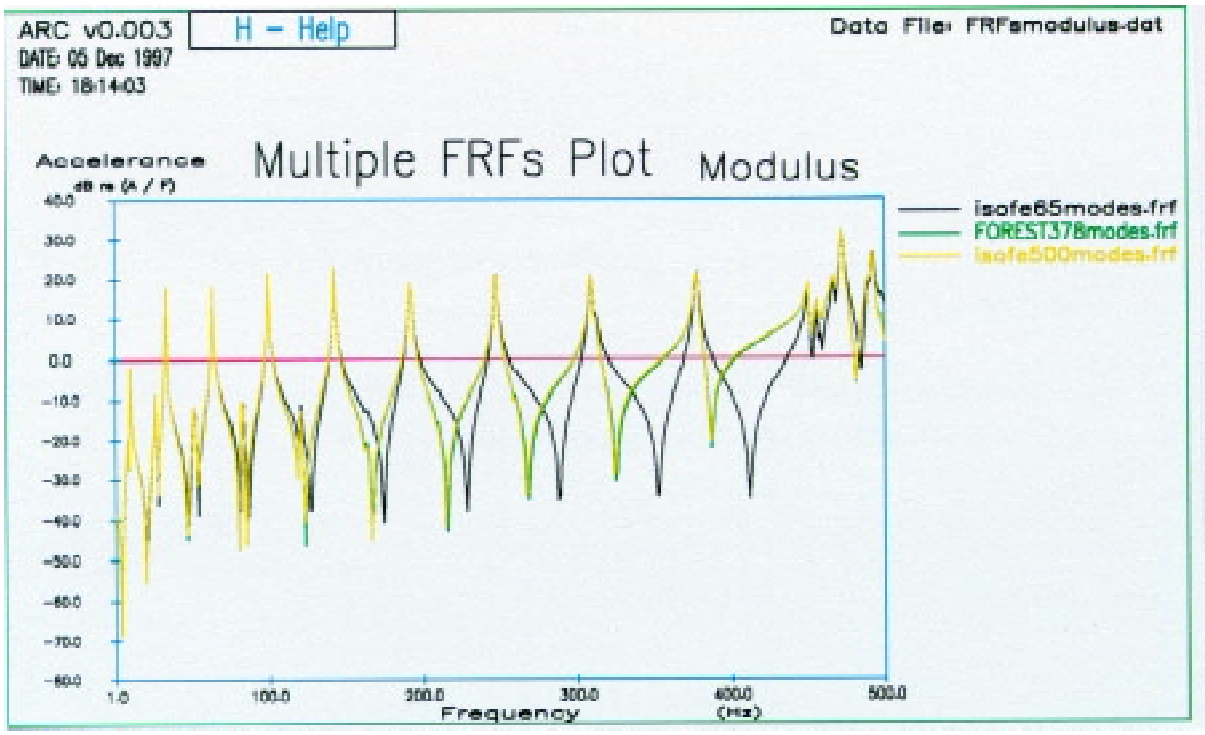

Figure 4.19. FRFs regenerated using 65, 378 and 500 modes.

4.13. Co-ordinate Modal Assurance Criterion (COMAC)

Co-ordinate Modal Assurance Criterion (COMAC) has been in use for a number of years, first introduced by Lieven 1988 [11]. COMAC is mathematically derived from the MAC, the only difference is that MAC is the scalar product between two mode shapes for all DOFs, whilst the COMAC is the scalar product between two vectors that represent two DOFs for a number of selected corresponding mode shapes. This definition implies that the knowledge of the CMPs is necessary for calculation of this correlation coefficient and therefore this correlation procedure is more significant as a refined correlation tool for assessment of global correlation. Its major

advantage is that it shows the correlation between two DOFs for number of modes, and if it is found that there is little agreement for some DOF pairs, then they should be checked and possibly removed from data sets if appropriate.

Mathematically, the COMAC correlation coefficient is defined in the following expression:

$$COMAC(DoF_i, DoF_j) = \frac{\left[\sum_{r=1}^{m} \left|\phi_{i,r}\phi_{j,r}^{*}\right|\right]^2}{\left(\sum_{r=1}^{m}\phi_{i,r}\phi_{i,r}^{*}\right)\left(\sum_{r=1}^{m}\phi_{j,r}\phi_{j,r}^{*}\right)} \qquad (4.13\text{-}1)$$

where index r represents the correlated mode pairs from each set of data. Application of this method is demonstrated in Figure 4-20 using SAMM II B structure test case.

A useful application of this correlation coefficient will be described in weighting of updating equation later in the text.

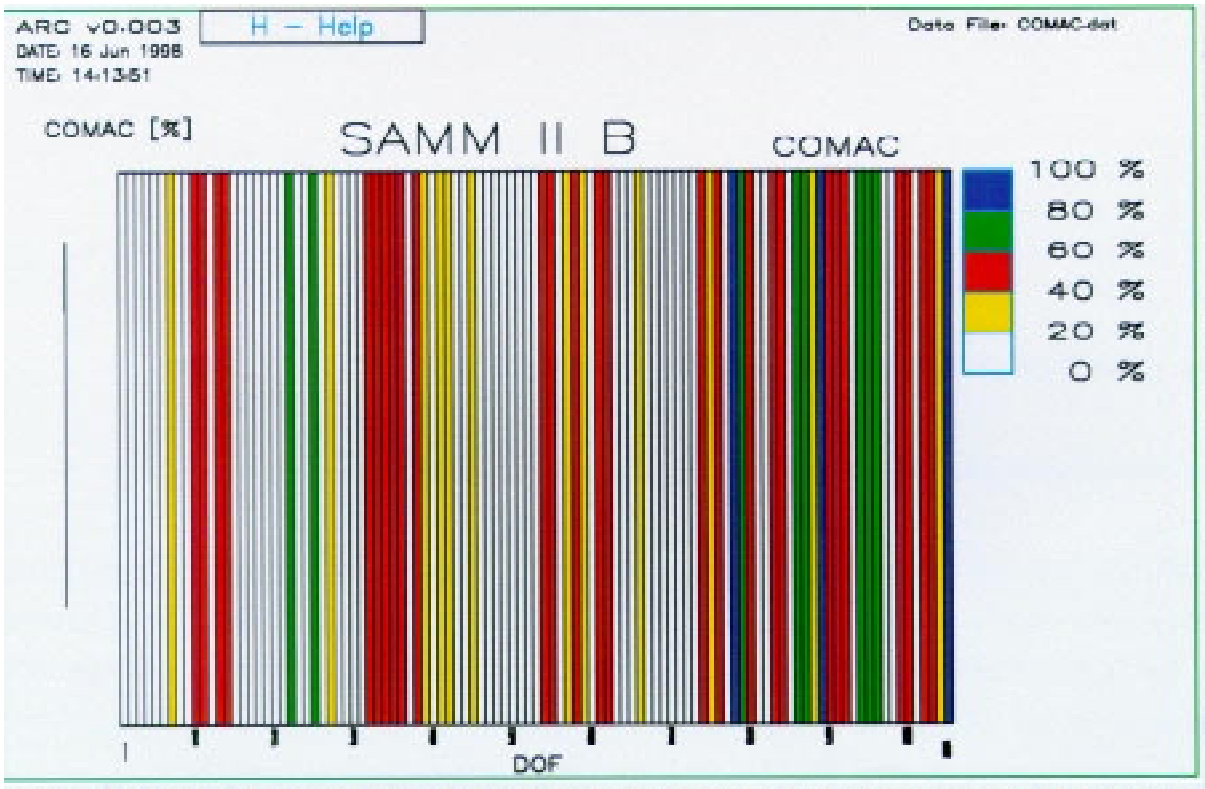

Figure 4.20. A typical COMAC results.

4.14. Conclusion

A new correlation procedure which can be used during model updating as an automatic tool for mode pairing is presented in this paper. The method combines the minimum data requirements necessary for successful application of a correlation coefficient based on SEREP reduction of the theoretical model. The advantages of the SEREP-based correlation coefficients over MAC or NCO are demonstrated. The SEREP Cross Orthogonality (SCO) correlation technique is more sensitive than MAC or NCO techniques, i.e., it will show similarities with higher values than MAC or NCO for similar modes, and vice-versa it will have lower values for independent modes.

Also, a method for assessment of the modal complexity of experimental modes has been presented which helps to assess global quality of experimental data. In addition, a useful realisation process has been described that can be used prior to correlation and updating.

The FOREST technique is a simple method for determining the required number of modes for the modal summation approach to FRF regeneration with a specified accuracy or for determining the accuracy which will be obtained with a specified number of modes. The method is simple to use and does not require any complicated calculations. The method was originally developed to be used for model correlation purposes in FRF-based updating methods and, since the rotational DOFs cannot be easily measured experimentally the method considers only translational DOF.

5.0 Error Location Theory

5.1. Introduction

Error location is probably the most difficult part of the model validation. Error location can be defined as the process of finding and isolating the parts in the model of the structure which it is believed are responsible for the observed discrepancies between the theoretical predictions and the measurements. Unfortunately, there is no simple direct procedure which can localise the error in the structural model on the basis of experimental data. Instead, most existing updating procedures localise errors in the model and update the model simultaneously. In order to localise the error in the model properly, all possible model definition parameters should be selected as updating parameters, and this means that for a system with N degrees-of-freedom, the maximum number of updating parameters is $N(N+1)$, assuming completely dense system matrices, and excluding damping in order to simplify the problem. This would further mean that the measured data requirement should have at least the same amount of information as the number of updating parameters, i.e. all natural frequencies and mode shapes should be measured at all co-ordinates, in order to be able to solve the updating and error location equation uniquely.

In practice, it is not possible to overcome the experimental data incompleteness problem: it is theoretically possible to measure frequency responses up to 100 kHz, but practically this value drops to about 5-20 kHz due to the limitations given in section 3.2. Also, the number of measurement positions is limited by access and time constraints, and it can never match the number of theoretical DOFs. Since numerical methods are approximate methods - see Chapter 2 - only a limited number of modes from equations 2.4-4 and 2.4-5 will converge to numerically-accurate solutions of these equations (this does not mean that the converged accurate solutions are in good agreement with experimental modes).

This discussion leads to the inevitable conclusion that there are some constraints (lack of experimental data and imperfection of theoretical models) which make the error location almost impossible to solve exactly using any deterministic approach. Even if these limitations are somehow resolved, error location using experimental data cannot be guaranteed because a particular theoretical model may be of such a configuration that it can never represent the experimental behaviour accurately.

This does not mean that the error location problem cannot be tackled - in fact there are several approaches for selecting updating parameters - and these methods are discussed in more detail in this chapter.

5.1.1. Identification Approach

It has been said in previous sections that measured data are incomplete in respect of the number of measured modes as well as in respect of the number of measurement points. However, if it was possible to measure all natural frequencies and all modes, then it would be possible to perform a simple identification of the spatial properties of the system (the global mass and stiffness matrices) from the modal properties (the natural frequencies and mode shapes) using the orthogonality equations (2.4-6) and (2.4-7) [38][39][40][22]. Unfortunately, the measurement frequency range is limited, as defined by equation (3.2-4), and usually the maximum practical measured frequency limit is below 50 kHz in practice. By solving a special eigenvalue problem for a symmetric system matrix $[A]$ it is possible to obtain the following expression [29]:

$$[A] = \sum_{r=1}^{N} \{\psi\}_r \lambda_r \{\psi\}_r^T \qquad (5.1.1\text{-}1)$$

where vectors $\{\psi\}_r$ are found by solving the special eigenvalue problem:

$$([A] - \lambda_r [I])\{\psi\}_r = \{0\} \qquad (5.1.1\text{-}2)$$

and vectors $\{\psi\}_r$ are normalised according the following expression:

$$[\psi]^T [\psi] = [I] \qquad (5.1.1\text{-}3)$$

By analysing the right hand side of expression (5.1.1-1), it can be concluded that since all eigenvector elements, $\psi_{r,j}$, have the same order of magnitude values, and the eigenvalue λ_r is consistently rising as the mode number increases, the values of the system matrix terms are numerically dominated by the higher frequency modes. This means that from the identification point of view, eigenvector with low eigenvalues are not of much use since they do not contribute any significant amount to the system matrix element values. Unfortunately, due to reasons given earlier

using expression (3.2-4), it is not possible to measure the higher frequency modes: even if it was possible to measure the FRFs in the high frequency range, the measured FRFs become very unfriendly for modal parameter identification since damping becomes more influential for the higher modes.

One might think that, after measuring a certain (practically reasonable) number of modes (e.g. 10) at the same number of locations (i.e. 10), and after performing modal analysis of the measured FRFs, the identification approach (expressions (2.4-6) and (2.4-7)) would certainly lead to mass and stiffness system matrices of size 10x10 which would be of full rank. However, these matrices cannot be used for further analysis (static, general dynamic etc.) since the actual value of each of the stiffness matrix element would be just a fraction of the real stiffness value which is mainly dominated by the higher frequency modes, although the eigensolution would not change from the values which were initially used to construct these matrices.

5.2. Causes of Discrepancies in Model Validation

5.2.1. Introduction

Most discrepancies in real correlation test cases are blamed on some unspecified errors in the finite element model. Experience also shows that there is a tendency for theoretical analysts to explain discrepancies through inaccurate measurement data, whilst the experimentalists would hold the theoretical model responsible for the discrepancies. Although the experimental data are used to validate the finite element models - not vice versa - this does not mean that all discrepancies are due to imperfect finite element models. The experimental data are of limited accuracy and it is absolutely crucial to check whether measured data are repeatable and also any other non-linearities must be detected if they exist. Usually, most engineering structures are designed so that they should retain more or less the same dynamic characteristics throughout their working life. Moreover, it is expected that two structures coming from the same production series would be identical and consequently would have identical dynamic properties. Unfortunately, this is not the case in practice and it is not unusual to come across examples that demonstrate significant difference in dynamic properties for two structures thought to be identical. Clearly, it can be concluded that both the experimental data and theoretical modelling share responsibilities for discrepancies observed in

correlation, although the degree of responsibilities are generally different as is explained in the following sections [41].

In order to ilustrate the above discussion, an example is selected to demonstrate potential difficulties when trying to explain descrepancies between test and predicted data. An assembled stucture is shown in Figure 5.2.1-1. The structure is assembled from several pieces and it is bolted to a large steel block in order to simulate clamped boundary conditions. Comparison between measured and predicted FRFs is shown in Figure 5.2.1-2. Clearly, the two models are quite different and initially the majority of descrepancies were thought to be caused by inappropriate modelling of structural joints. However, later on it was shown that the individual components had certain descrepancies even though they all are one-piece components.

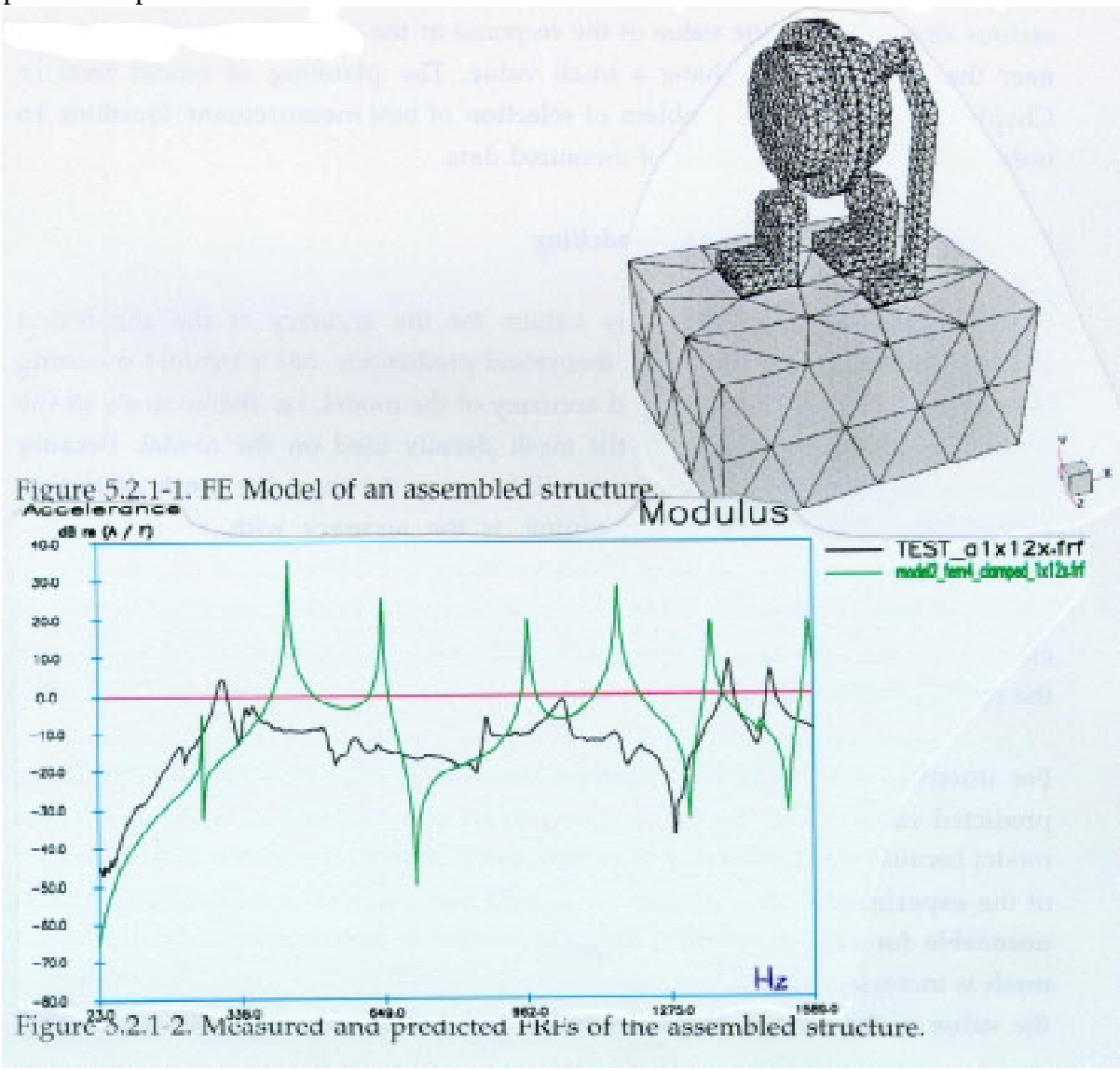

Figure 5.2.1-1. FE Model of an assembled structure.

Figure 5.2.1-2. Measured and predicted FRFs of the assembled structure.

5.2.2. Errors in Experimental Data

Generally, the accuracy of the measured natural frequencies is higher then the accuracy of the mode shapes. The accuracy of measured FRFs varies for different frequency values, [2] - it is higher around resonances and lower around anti-resonances due to different signal-to-noise ratios - and also the accuracy depends on measurement position for the same reason. If, for instance, a measurement position is located near the nodal line of a mode, then the response signal around natural frequency of that mode will have a low value and inevitably the relative accuracy of the measured FRF will be smaller than relative accuracy of FRFs for points which are located away from the nodal lines of that mode. However, it should be stressed here that this loss of relative accuracy is not so serious since the absolute value of the response at the measured position located near the nodal line will have a small value. The planning of modal tests in Chapter 3 deals with the problem of selection of best measurement locations in order to improve the accuracy of measured data.

5.2.3. Errors in Finite Element Modelling

It is not possible to prescribe any values for the accuracy of the theoretical predictions. The term ‘accuracy of theoretical predictions’ has a twofold meaning here. The first one is the converged accuracy of the model, i.e. the accuracy of the dynamic properties in respect to the mesh density used on the model. Because this error is so common in practice it will be given the name the **mesh distortion related error** [31]. The second meaning is the accuracy with respect to the experimental values observed in the correlation. In most practical situations it is observed that in order to improve correlation significantly it is necessary to change the configuration of the model and therefore this type of error is called the **configuration related error**.

For instance, if a measured frequency value is 15.1 Hz and the corresponding predicted value is 25.5 Hz, the first suspect for this discrepancy is the theoretical model because the discrepancy is so high that if there is any doubt in the accuracy of the experimental data on this scale then the whole experimental data set is unreliable for validating the theoretical model. If, however, the density of the mesh is increased several times to a number of DOFs where there is no change to the value of the natural frequency which is now 23.3 Hz, then this means that there is

something more fundamentally wrong with the model, i.e. the configuration of the model is the next suspect for the correlation discrepancies.

Mesh Distortion Related Errors

In order to generate either mass or stiffness matrices for a finite element it is necessary to perform integration over the domain of that element as indicated in expressions (2.3.1-3) and (2.3.1-4). The global and local co-ordinate systems are related non-linearly via the Jacobian matrix and in the case of an extremely distorted element, the Jacobian matrix can become singular and therefore this can influence the values of structural matrix. This problem can be overcome by dividing distorted elements into several less distorted elements and an example of the influence of the mesh on the eigenvalue solution is given below [42]. The structural component shown in Figure 5.2.3-1 is modelled using two different meshes. Model 'A' has 20,000 DOFs, whilst the second model 'B' shown in Figure 5.2.3-2 has 45,000 DOFs. Figures 5.2.3-3 and -4 shows the two theoretical FRFs re-generated from models 'A' and 'B' on the same plot with the corresponding experimental FRF. This example clearly demonstrates vulnerability of finite element modelling to this type of error.

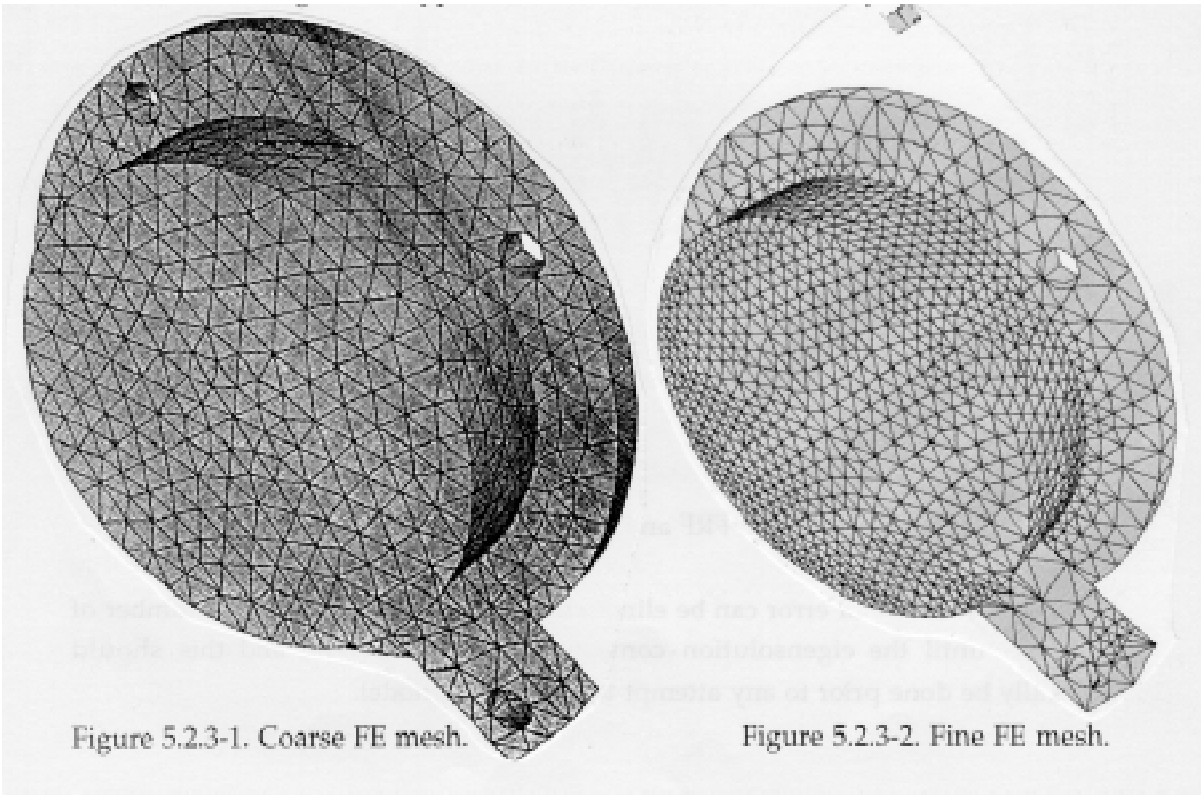

Figure 5.2.3-1. Coarse FE mesh.

Figure 5.2.3-2. Fine FE mesh.

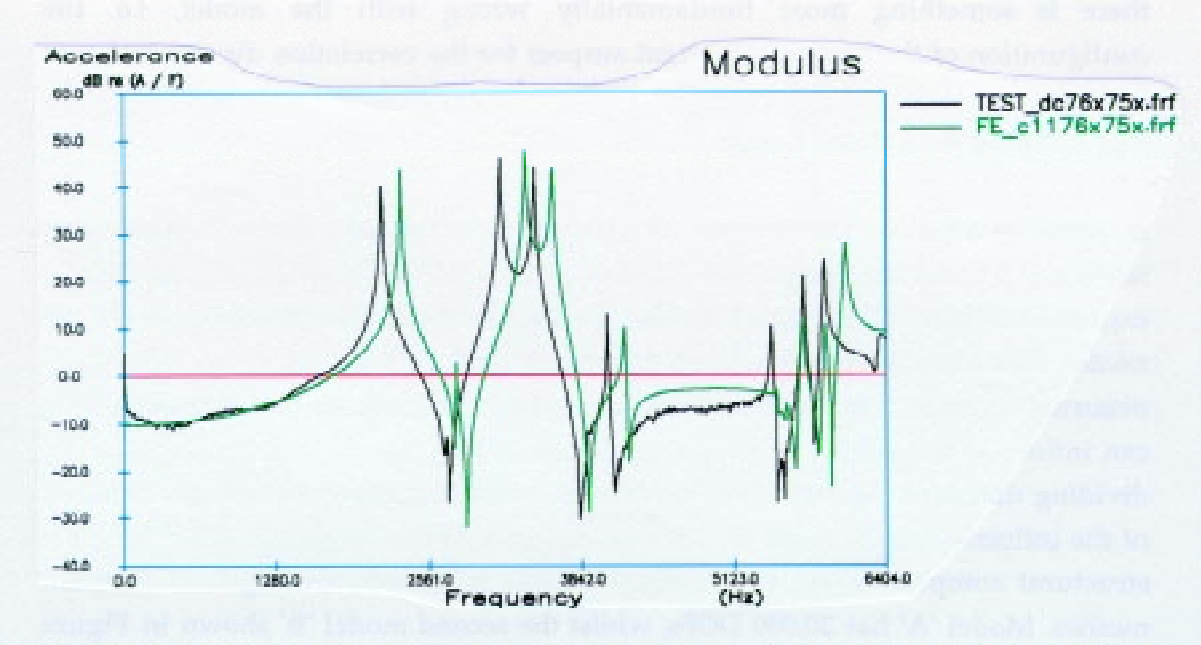

Figure 5.2.3-3. Coarse FE Model FRF and the corresponding experimental FRF.

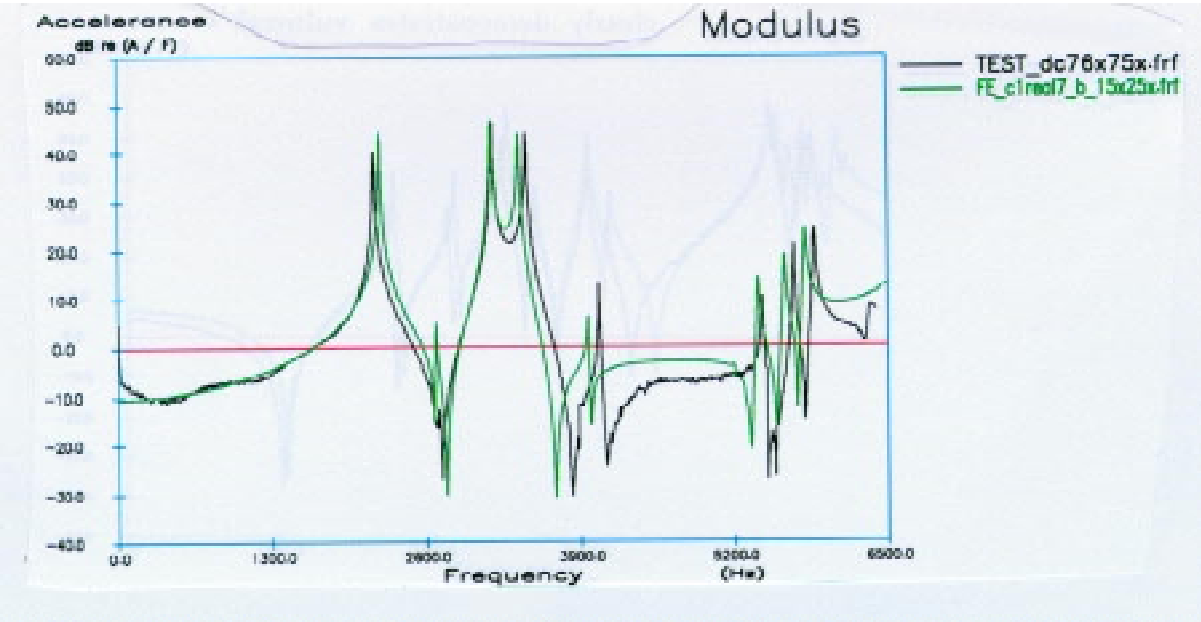

Figure 5.2.3-4. Fine FE Model FRF and the corresponding experimental FRF.

However, this type of error can be eliminated by simply increasing the number of elements until the eigensolution converges to a stable value, and this should generally be done prior to any attempt to update the model.

Configuration Related Errors

Errors of this type are the most common ones found to be responsible for discrepancies observed in practice. When any uncertainty that could exist between the model and the real structure is resolved, i.e. material properties, geometrical representation of the structure, physical properties of some elements etc., and if the discrepancies are still larger than the uncertainty of the accuracy of the experimental data, then the model is likely to be of the wrong configuration. The term 'wrong configuration' is a very broad term and could mean any of several different imperfections that model possesses. If, for instance, a simple plate is modelled, then it is very unlikely to expect that the model could be of wrong configuration, but if there is a crack inside the structure that is not included in the model, then even such simple model could be of wrong configuration.

Another inevitable example of wrong configuration is modelling of structural joints. Structural joints are regions where two components of a structure are permanently connected. There are several reasons why structural joints are difficult to model. It is almost impossible to find a precise description of structural joints. Practical inspection of structures will disclose that there is often an unspecified inconsistency between the description of structural joints in technical drawings and in reality. It is extremely difficult to determine contact areas between the two parts that are connected by a structural joint. Moreover, it is possible that the contact area is not consistent during vibration. This type of structural joint will almost inevitably introduce some non-linear effects in the dynamic behaviour of structures.

Modelling of structural joints is critical for the accuracy of the theoretical predictions. There are two approaches for modelling structural joints: (i) one employes a simplification of the joints and (ii) the other one involves detailed modelling of the joints. Oversimplification of structural joints is almost certain to lead to an inadequate representation of real connections and consequently this will affect the accuracy of the predicted dynamic characteristics. In contrast to the simplification approach, a particularly detailed modelling of structural joints is unlikely to improve the accuracy of the theoretical predictions because the very details of structural joints are unknown and consequently these inaccuracies are transferred to the model. The recommended approach for modelling of structural joints is to have a proper balance between these two approaches: neither an extremely simplified nor an extremely detailed model.

5.3. Updating Parameters Definition

There is no restriction to what could be an updating parameter and anything that makes changes to the theoretical model predictions can be selected, as the following expression indicates:

$$\lambda_r, \{\phi\}_r = function(p_1, .., p_l), \quad r = 1, .., N \tag{5.3-1}$$

All updating parameters can be divided into two groups; one is for the whole matrix correction and the other group is selective updating parameters. There are two different types of selective updating parameter, one is the spatial-type and another is the design-type. Also, there is a particular general spring-like updating parameter which is the most basic updating parameter.

5.3.1. Whole Matrix Updating Parameters

A whole-matrix updating parameter can be defined as the a simple correction to the entire system matrices, as indicated in the following expressions:

$$[K_U] = [K_A] + [\Delta K_U] \tag{5.3.1-1}$$

$$[M_U] = [M_A] + [\Delta M_U] \tag{5.3.1-2}$$

The main disadvantage of this type of updating parameter is that there is no control over which particular elements are selected for updating. Also, after updating, the original connectivity of the model could be lost. Since the whole matrix correction would destroy the initial connectivity of the global mass or stiffness matrices, this procedure has a particular disadvantage in the application for updating of large finite element models because it will make the system matrices dense and consequently difficult or practically impossible to handle.

5.3.2. Spatial-type Updating Parameters

The spatial-type parameters are defined as the products of an updating coefficient and a macro element matrix which has the same format as its corresponding assembled spatial system matrix (mass, stiffness or damping). This is, in effect, a linearisation of the updating equation through an assumption of linear distribution of errors in the model. The changes to the initial matrices are defined as follows, for the global mass matrix, for example:

$$[\Delta M_U] = \sum_{r=1}^{p_M} p_r [M_r^e] \tag{5.3}$$

and for the global stiffness matrix as,

$$[\Delta K_U] = \sum_{r=1}^{p_K} p_r [K_r^e] \tag{5.4}$$

where $[M_r^e]$ and $[K_r^e]$ are macro-element matrices for mass and stiffness updating parameters, respectively. Macro elements, $[M_r^e]$ or $[K_r^e]$, can possess the same connectivity as the initial model, i.e. no extra elements would be introduced, or if their connectivity is generally different from that of the initial matrices then extra elements would be created and the initial connectivity would be destroyed. The updated mass and stiffness matrices would then be defined by the following equations:

$$[M_U] = [M_A] + p_1[\Delta M_1^e] + \quad \ldots + p_{p_M}[\Delta M_{p_M}^e] \tag{5.5}$$

$$[K_U] = [K_A] + p_1[\Delta K_1^e] + \quad \ldots + p_{p_K}[\Delta K_{p_K}^e] \tag{5.6}$$

An advantage of this type of updating parameter definition is that it is very general, but a disadvantage is that there is limited physically-meaningful explanation for this kind of change of the structural model.

5.3.3. Design-type Updating Parameters

The third updating parameter type is the design-type, and is defined as any design input parameter of the initial model. There is no restriction on what the updating parameter could be as long as it provides the desired changes to the eigensolution of the system. Examples of this updating parameter are: material properties of each finite element, geometrical properties of finite elements, thickness of the shell elements, beam element diameter, area, moments of inertia, torsion constant, etc.. The main disadvantage of this type of updating parameter is that there is a limited number of them and they may not provide enough variables to update a structure successfully since they cannot change the configuration of a model. However, an advantage of this type of updating parameter is that they represent physical changes in the structure, which are physically meaningful.

5.3.4. General Spring-like Updating Parameters

The general spring-like updating parameter is a simple spring element that connects two degrees-of-freedom. If the whole-matrix correction is one extreme type of updating parameter that does not allow any selection of finite elements, the general spring-like element is the most basic updating parameter that represents the connection between two individual DOFs. Model updating is basically the process of changing the values in the global stiffness or mass matrices, but there are some minimum requirements that have to be fulfilled when modifying these matrices. The global mass and stiffness matrices are symmetric and therefore any updating changes have to be symmetric in order to keep the updated system matrices symmetric. Another important condition is the reciprocity between two DOFs. This means that if there are two DOFs that belong to a updating parameter, then any change to the stiffness or mass values in the global matrices have to be of the same values for both DOFs.

The change of the global mass or stiffness matrix can be represented symbolically in the following expression:

$$\begin{bmatrix} k_{1,1}-k^U_{1,1} & k_{1,2} & k_{1,3}+k^U_{1,3} & k_{1,4} \\ k_{2,1} & k_{2,2} & k_{2,3} & k_{2,4} \\ k_{3,1}+k^U_{3,1} & k_{3,2} & k_{3,3}-k^U_{3,3} & k_{3,4} \\ k_{4,1} & k_{4,2} & k_{4,3} & k_{4,4} \end{bmatrix} = \begin{bmatrix} k_{1,1} & k_{1,2} & k_{1,3} & k_{1,4} \\ k_{2,1} & k_{2,2} & k_{2,3} & k_{2,4} \\ k_{3,1} & k_{3,2} & k_{3,3} & k_{3,4} \\ k_{4,1} & k_{4,2} & k_{4,3} & k_{4,4} \end{bmatrix} + \begin{bmatrix} -k^U_{1,1} & k^U_{1,3} \\ k^U_{3,1} & -k^U_{3,3} \end{bmatrix} \qquad (5.3.4\text{-}1)$$

In fact, the matrix $\begin{bmatrix} -k^U_{1,1} & k^U_{1,3} \\ k^U_{3,1} & -k^U_{3,3} \end{bmatrix}$ represents the most basic change to the global stiffness matrix, and also there are additional conditions as shown in the following expression:

$$k^U_{1,1} = k^U_{3,3} \qquad (5.3.4\text{-}2)$$

$$k^U_{1,3} = k^U_{3,1} \qquad (5.3.4\text{-}3)$$

The reciprocity condition is described in expression (5.3.4-2) whilst expression (5.3.4-3) describes the symmetry condition. Also, the global matrices have to be diagonally dominant, and that is described in the following expression:

$$\left|k^U_{1,1}\right| \geq \left|k^U_{3,1}\right| \qquad (5.3.4\text{-}4)$$

A simple spring element is defined by $k^U_{1,1} = k^U_{3,1}$ which is the simplest physically meaningful updating parameter.

The bandwidth of a sparse matrix is defined as the largest number of coupled DOFs for any column or row in the matrix. This coupling of DOFs is determined by the type of finite elements used in the model, i.e. a simple spring couples two DOFs, whilst the higher the order of the finite element formulation the larger the number of coupled DOFs. Generally, it can be assumed that all DOFs connected by one finite element are fully coupled amongst themselves, whilst the bandwidth of the matrix will depend on inter-elemental connections in the model.

By introducing the spring-like element it becomes possible to change the configuration of the model, i.e. it is possible to couple two DOFs that belong to one

finite element additionally if the original finite element is not capable of representing the experimental results accurately.

5.3.5. Limitations of Updating Parameters Value

Apart from the above-mentioned properties of the finite element, i.e. symmetry, reciprocity and diagonal dominance, there are some other requirement that have to be fulfilled if the model is considered to be properly defined. The stiffness matrix must not be numerically singular or near-singular or ill-conditioned. These requirements are used to derive the limitations for the updating parameter values during model updating process.

It is important to stress here that there are two possible causes for singularity of stiffness matrix. One reason for such singularity could be due to boundary conditions which enable the structure to move freely in one or more generalised directions. In this case, we expect to find the same number of rigid-body-modes (RBMs) as the number of unconstrained generalised directions for the whole structure. Another reason for singularity of the stiffness matrix could be due to inadequate representation of some parts of structure or simply due to crude formulation of stiffness matrix for some elements, or any other reason. The singularity of the stiffness matrix described here is assumed not to be caused by existence of RBMs in model.

Singularity of the stiffness matrix

Any DOF is considered to be singular if [29]

$$\frac{k_{i,j}}{k_{max}} \leq \varepsilon_{sing} \qquad (5.3.5\text{-}1)$$

where $k_{i,j}$ is the term in the i-th row and j-th column and k_{max} is the largest term in $[K]$. The minimum permitted value for the constant ε_{sing} is defined below

$$\varepsilon_{sing} = 10^{-8} \qquad (5.3.5\text{-}2)$$

In practice, if the stiffness matrix appears to be singular, then it is likely that that DOF does not have any stiffness, or the stiffness is so large that this condition is not satisfied.

Ill-conditioning of the stiffness matrix

Ill-conditioning of the stiffness matrix is defined by the following condition [29],

$$\frac{k_{i,i}}{d_{i,i}} \leq \varepsilon_{K-cond} = 10^5 \qquad (5.3.5\text{-}3)$$

where d_{ii} is defined by the decomposition process of the symmetric stiffness matrix according the following expression:

$$[K] = [L][D][L]^T \qquad (5.3.5\text{-}4)$$

where $[L]$ is lower triangular factor matrix and $[D]$ is a diagonal matrix. The stiffness matrix is considered to be ill-conditioned if the condition defined by (5.3.5-3) expression is not satisfied. The ill-conditioning of the stiffness matrix can be caused by: (i) low stiffness in rotation, (ii) very stiff beam, (iii) mechanisms or (iv) other reasons.

5.4. Selection of Updating Parameters

The previous discussion in this chapter leads to the conclusion that exact error identification is practically impossible, due largerly to the data requirement problem, although even in the case of knowledge of all the required data, the updating equations would be so large that practically it would not be possible to solve them. It is possible for any updating method to find a simple relationship between the amount of available experimental data and the maximum number of updating parameters so that it is possible to select only a limited number of updating parameters which is almost never equal to the number of measured parameters in order to keep the updating equation well-conditioned. This leaves the analyst to choose a limited number of updating parameters which have higher priority for updating according to the selection based on his/her engineering judgement and experience. We can conclude that there is never enough data to perform a total error localisation in the general case because of the problem

encountered in measuring the higher frequency modes [40][43]. Instead, a limited number of updating parameters is selected by the analyst in those parts of the structure which are believed to be most uncertain in order to improve correlation with the experimental data rather then to locate all modelling errors. This also leaves a certain amount of possibility for the updating process to fail to improve correlation due to reasons of inappropriate selection of updating parameters and this also makes the updating process case-dependent and the final solution to be non-unique [44][45].

5.4.1. Classification of Methods for Initial Selection of Updating Parameters

Initial selection of updating parameters can be divided in to two basic approaches and these are: (i) an empirical approach and (ii) a sensitivity-based approach. Both approaches are manual, i.e. selection is carried out manually by the analyst.

Empirically-based initial selection of updating parameters

This type of initial selection of updating parameters is based on a knowledge of the finite element model of the structure and approximations built into the initial model. In most practical cases, the analyst will compare technical drawings of a structure with the structure itself, and after thorough inspection of the structure an initial finite element model will be generated. Using this process the analyst can select several regions of the structure that are not approximated (i.e. modelled) as accurately as the reminder of the model. These regions of the structure are then selected in a few updating parameters according to the level of approximation in the initial model. It is important to notice here that no other knowledge than the level of approximation of the initial model is used for this type of selection of updating parameters.

Sensitivity-based initial selection of updating parameters

This type of initial selection of updating parameters is based on knowledge of the dynamic behaviour of the initial finite element model. When the dynamic properties of the initial model are calculated, it is possible to determine the regions of the initial model that are taking most of strain deformation for a number of mode shapes. The dynamic properties under consideration (i.e. natural frequencies and mode shapes) are clearly highly sensitive to any changes of the model in these high

strain energy regions and therefore these regions are selected as updating parameters.

5.4.2. Important Factors in Selection of Updating Parameters

A critical stage of the model updating process is the actual selection of updating parameters, and a real question that the analyst faces is which regions of initial model to select as updating parameters. The two approaches described above are very different and in different situations different approaches should be used. It is not possible to draw a line between empirical and sensitivity-based updating parameter selection approaches; instead it is important to understand how they relate to and influence the whole course of the model updating process.

The empirical updating parameter selection approach is a fundamentally correct and appropriate method to detect the genuine errors in an initial model. A major advantage of this approach is that it is based on an empirical knowledge of the initial model and the structure itself. The method is expected to select the regions of structure which have the largest errors providing that sufficient knowledge about the initial model and structure is available. Unfortunately, this condition may not be easy to meet in real practical situations, i.e. sometimes it is not possible to inspect a structure, or even if the structure is available it may be impossible to inspect every detail or some regions of structure may be extremely difficult to assess. Also, an initial finite element model of a structure may be very complicated, assembled from several sources that were generated by different people or the initial model may be based on technical drawings that may not be exactly identical to built structure. This process of assessment of both structure and initial model is extremely dependent on human factors (the analyst's experience) and it can not be easily quantified.

The sensitivity-based updating parameters selection approach selects the regions of a structure that are most strained for a number of modes under consideration. Using this method for selection, the most sensitive parts of the structure are expected to be selected rather than the regions where errors are expected to be found. A major advantage of this method is that it is straightforward to use automatically and the user input in the selection process is limited.

It is difficult to advise which method of selection of updating parameters is more suitable in the general case. If, for instance, only the empirical selection approach is

used but the dynamic properties under consideration are not sensitive to the selected updating parameters, there is little chance of a successful final result. If, however, only the sensitivity-based selection approach is used, then there is a possibility that accurately modelled regions of a structure are selected as updating parameters and this will reduce the confidence in the final updated model. A proper balance of the two methods is recommended, i.e. select both sets independently and overlay them in order to select updating parameters.

5.5. Objective Function Diagrams

Most updating techniques are, in effect, procedures of optimisation of a defined objective function, which is usually a global correlation function between the dynamic properties of the analytical and the experimental models. It was already noted that there might not exist a theoretical model, based on a particular formulation (e.g. Finite Element Method), which can represent behaviour of the structure exactly. Instead, the analyst will try to find a model which is the closest to describe the behaviour of the structure. Updating procedures are capable of refining the structural model in order to bring the discrepancies between the predictions and the experiment to a minimum possible level.

Errors in the structural model are distributed throughout the model. No matter how simple a structure’s geometry is and how structural model is refined, the theoretical model of the structure has a finite accuracy in a finite frequency range.

If we consider the simple beam structure shown in Figure 5.5.1. and its corresponding finite element model shown in Figure 5.5.2., it is generally thought that the finite element model should be able to predict the dynamic behaviour of the structure very accurately. The correlation between measured and predicted FRFs is shown in Figure 5.5.3. and it can be seen that the discrepancies between the two models increase for higher frequencies. One would expect that prediction of such a simple structure with such a fine model should be more accurate than is indicated in Figure 5.5.3. A natural question after analysing the correlation is: "What are the parameters in the model that are responsible for these discrepancies and how to detect them?". This particular model consists of solid elements and the mesh can be considered to be very fine so that any further refinement of the mesh would not be likely to improve correlation significantly. Also, there are no other likely design

parameters in the model, i.e. geometry or material properties, to be blamed for correlation discrepancies.

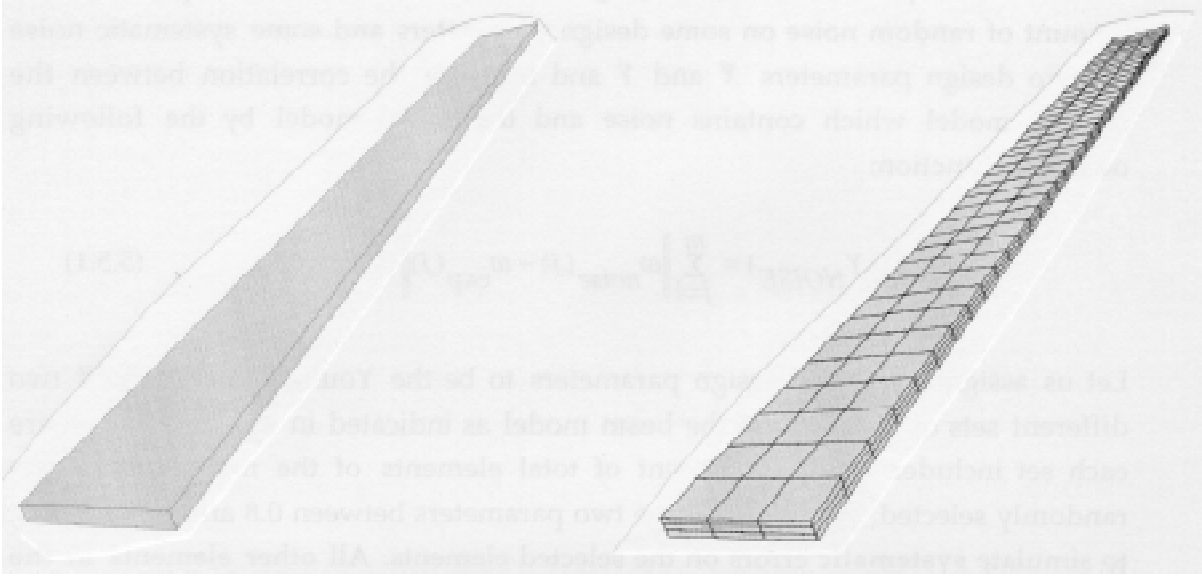

Figure 5.5-1. Simple Beam geometry.

Figure 5.5-2. Simple Beam FE mesh.

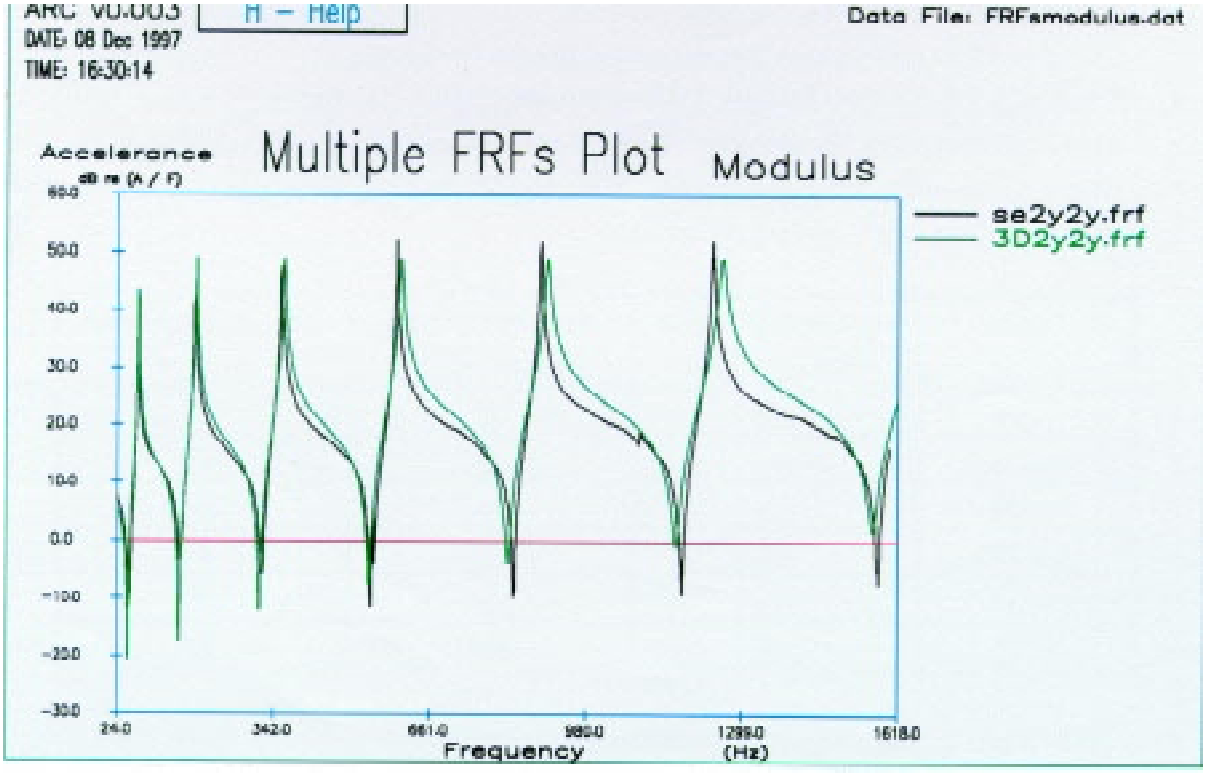

Figure 5.5-3. Predicted and mesured FRF of the simple beam.

In order to examine the error distribution and its implication on the objective function in the finite element model more closely, let us assume that the true errors in the model are distributed as random noise of certain amplitude on all possible finite element design parameters. Let us take one model and define that model as an experimental model (**target model**) and then we will put a certain amount of random noise on some design parameters and some systematic noise on two design parameters X and Y and measure the correlation between the current model which contains noise and the target model by the following objective function:

$$OF(X_{NOISE}, Y_{NOISE}) = \sum_{j=1}^{m} \left\| \omega_{noise}(j) - \omega_{\exp}(j) \right\| \qquad (5.5.1)$$

Let us assign these two design parameters to be the Young's Modulus of two different sets of elements of the beam model as indicated in Figure 5.5.2, where each set includes about 30 percent of total elements of the model which are randomly selected. We will vary the two parameters between 0.8 and 1.2 in order to simulate **systematic** errors on the selected elements. All other elements in the model will receive a certain amount of **random** noise in order to keep the study as realistic as possible, [1]. This random noise on all other elements can be introduced to any design parameter of the finite elements.
Figures 5.5.4, 5.5.4(a), 5.5.4(b), 5.5.4(c), 5.5.4(d) and 5.5.5. show objective function topology diagrams for different level of systematic and random noise as well as different numbers of 'experimental' data available for generation of the objective function diagrams.

Figure	Systematic Noise Variation [%]	Random Noise Amplitude [%]	No. of Measured Modes
5.5.4	±20.	0.	50
5.5.4(a)	±20.	±2.	45
5.5.4(b)	±20.	±5.	40
5.5.4(c)	±20.	±10.	40
5.5.4(d)	±20.	±15.	35
5.5.5	±20.	±30.	30

Table 5.5.1. List of Objective Function Case Studies.

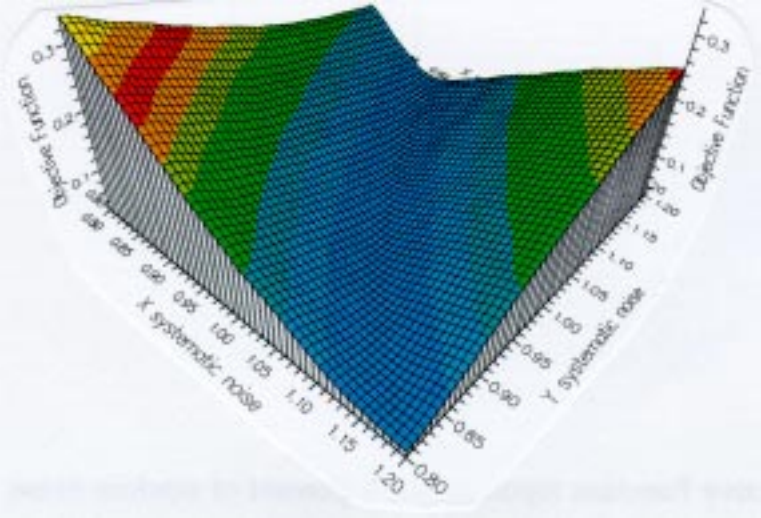

Figure 5.5.4. Objective Function topology without random noise.

In a case of 50 'experimental' modes available and complete absence of random noise the objective function diagram is given in Figure 5.5.4., and it can be seen that the topology of objective function diagram is globally convex and smooth, and clearly there are no local variations in the topology whilst an unique global minimum of the objective function is clearly defined and visible.

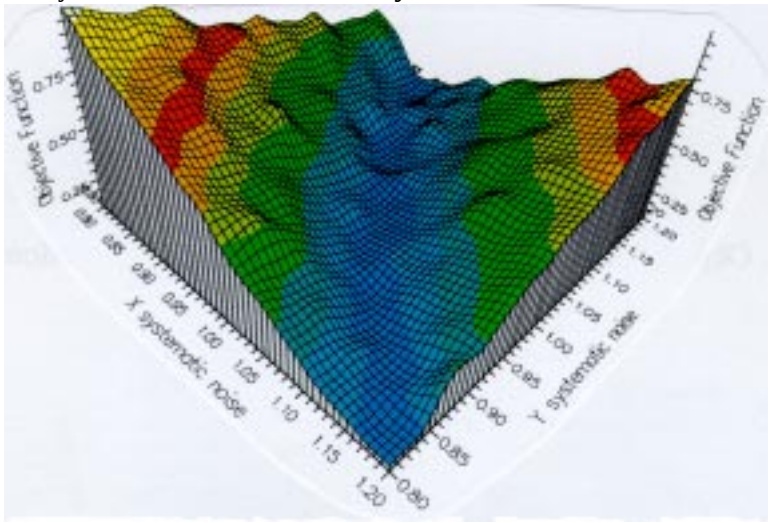

Figure 5.5.4(a). Objective Function topology for 2. percent of random noise.

In a case of 40 'experimental' modes available and 2. percent of random noise the objective function diagrams begin to show some local variations as shown in Figure 5.5.4.(a), although it can be said that the topology is still globally convex but without clear global minimum. Figures 5.5.4(b) to (d) also show objective function diagrams for different amounts of experimental data and different values of amplitude of random noise.

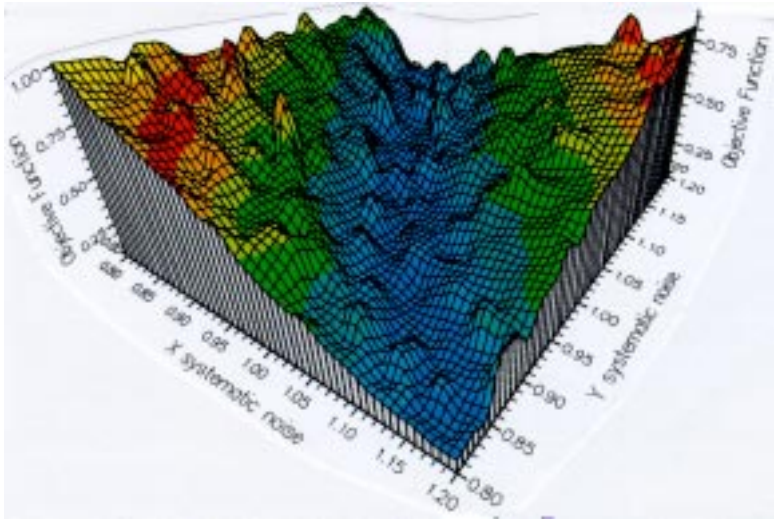

Figure 5.5.4(b). Objective Function topology for 5. percent of random noise.

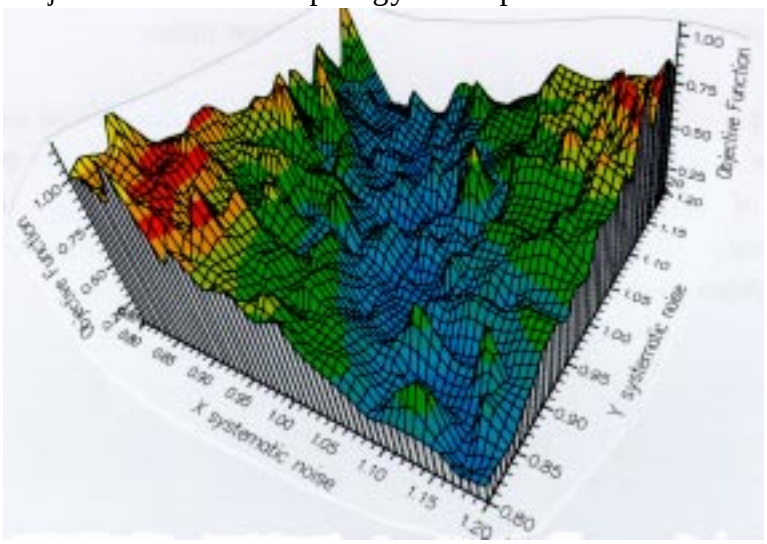

Figure 5.5.4(c). Objective Function topology for 10. percent of random noise.

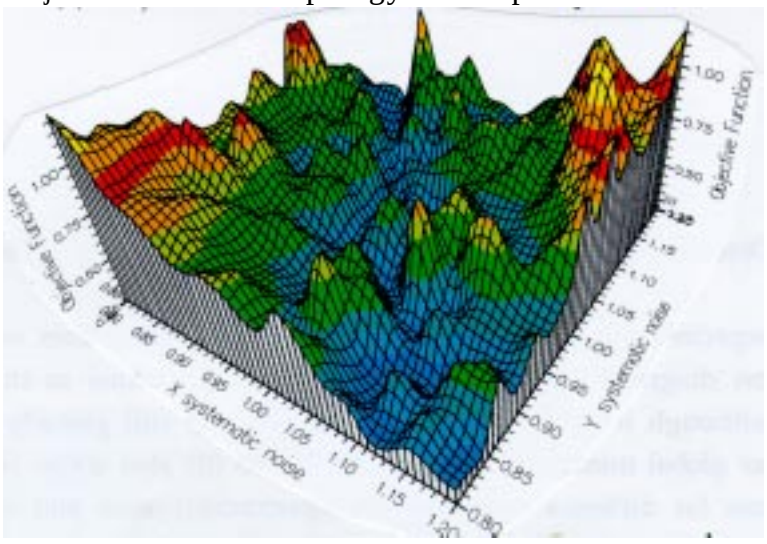

Figure 5.5.4(d). Objective Function topology for 15. percent of random noise.

As the number of 'experimental' modes is reduced to 15 and the variation of random noise is increased to 30 percent, the objective function topology ceases to have any global convexity, as shown in Figure 5.5.5.. The objective function in this case has large local variations and consequently it has many local minima. This case represents the majority of real engineering situations in which the location of errors in the model are unknown and the amount of experimental data is insufficient. Also, this case does not have unique global minimum since the random errors are of the same order of magnitude as the systematic noise.

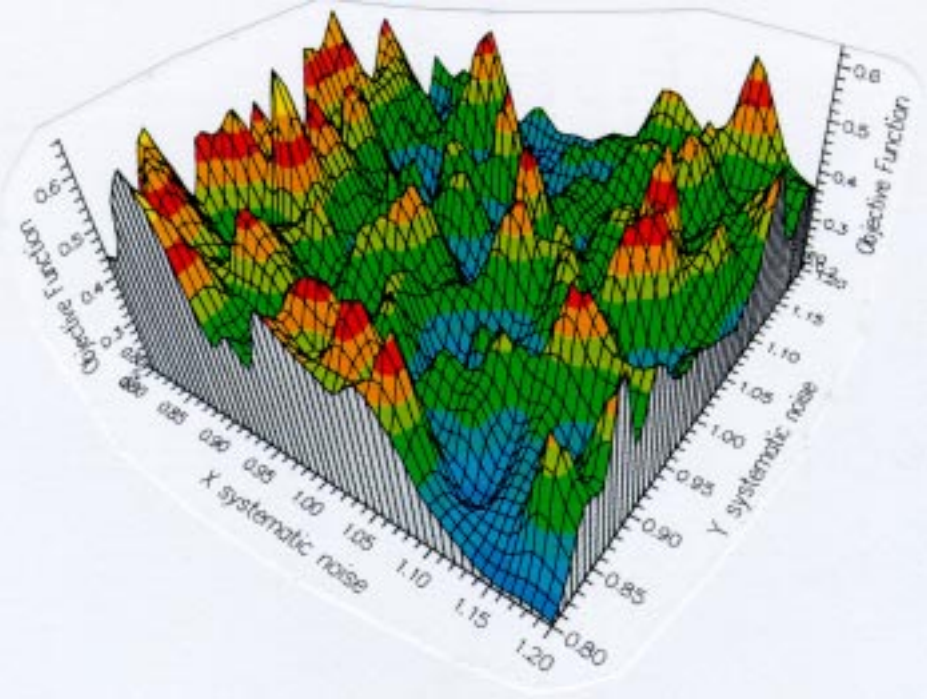

Figure 5.5.5. Objective Function topology for 30 percent of random noise.

It is clear that as the number of experimental data decreases, the objective function topology becomes more complicated and consequently the updating becomes more difficult. The updating procedure is effectively to find the global minimum of the objective function and it is easy to notice by analysing these objective function topology diagrams that finding the global minimum of the objective function is mathematically a very difficult task [46]. Most of the existing mathematical procedures find only the nearest local minimum of the objective function and some of them find any (not necessarily the local) minimum of the objective function. By studying these diagrams, the problem of convergence of the updating procedure can be fully appreciated.

If the initial model position is at point A in Figure 5.5.6. then the sensitivity matrix represents gradient vectors on the surface of the objective function diagram and updating parameters values are determined by finding point B on the horizontal plane which determines the target model. This position, B, determines a new model (point C) for which correlation is assessed and a new sensitivity matrix is calculated in order to go into a further search for the updated model (point D). This process can easily fail to converge due to many different reasons.

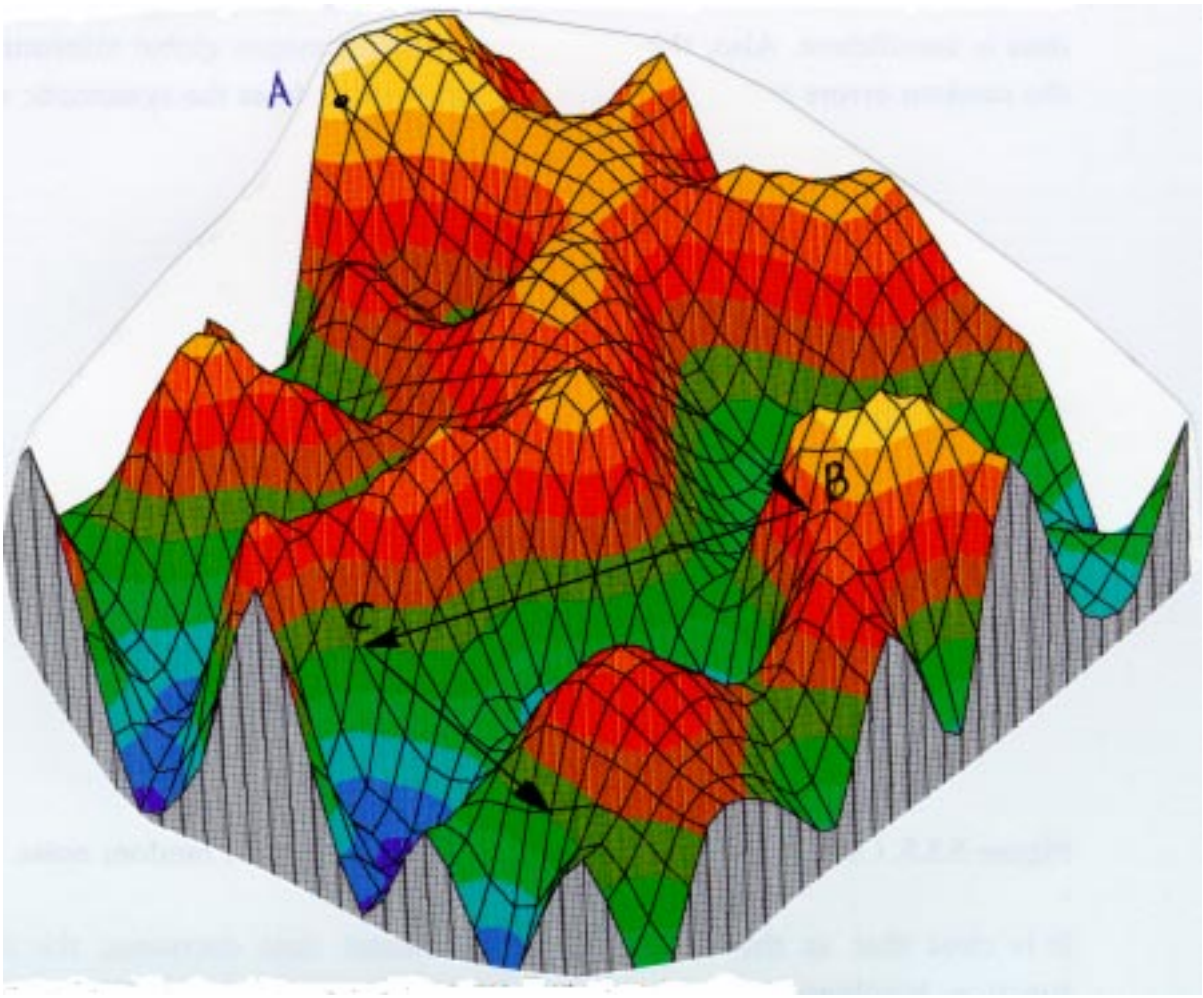

Figure 5.5.6. Search algorithm on Objective Function topology.

When considering the topology of the objective function diagrams, it can be noted that there are two major features which are important for updating and these are: (i) the global shape of the topology of the objective function diagram and (ii) local variations on the surface of the objective function. In an ideal case where a huge amount of experimental data were available, the topology of the objective function diagram would not have significant local variations and it would have a clear

convex (or concave, depending on the reference point) shape. In most practical cases where an incomplete set of experimental data is used for updating, the global convex shape cannot be recognised due to the dominance of the large local variations. One way of making the topology of objective function globally more convex is by including experimental data which have higher residuals (here residuals means the difference between measured and predicted values) in the updating equation. Completely the opposite approach is to use only experimental data which have low residuals in order to improve the convergence process of the updating process, but in fact this localises the objective function topology and provides only minor improvement to the initial model. It can be concluded that it is equally important to include even experimental mode shapes which do not initially correlate well with any modes from the theoretical model in order to make the objective function diagram globally more convex, although this can numerically destabilise the updating process. This also leads to a conclusion that it is important to find positions which would detect possible discrepancies between the experimental and theoretical models, rather than measure only at positions which would indicate low degree of disagreement and make the objective function diagram globally less convex with large local variations.

5.5.1. Random Errors Distribution Theory

It has been demonstrated in the previous section that the amount of experimental data available has an important role in the whole updating process. The fewer experimental data that are available, the more complicated the objective function diagram is. These diagrams provide good visual representation of the updating process. One approach for complete updating is to generate the objective function diagram using as much experimental data as possible and then simply to find regions of minimum value of the objective function. Unfortunately, this process requires a huge calculation effort, even for a very simple finite element model with a small number of DOFs.

Random errors distribution theory assumes that every parameter in a finite element model is inaccurate and that the errors of the parameters are random values which are limited. These limits have different values for different parameters and the analyst should be able to select groups of finite element parameters of equivalent error limits. For instance, the node positions are probably uncertain up to 0.05 % of the largest dimension of a structure while the stiffness values of some elements are

uncertain up to 50 % of the original values. In this example, it is clear that the dominant uncertainty comes from the stiffness values and they are the ones that should be selected as updating parameters. This quantification process of the determination of the uncertainty limits for different updating parameters is also dependent on the correlation results. The better the correlation result, the more difficult it is to determine the error limits for different finite element parameters. As the correlation improves, it is possible to arrive at a stage where correlation could be explained by the mistuning effect for some structures rather than any errors in a model. In most practical situations this possibility can be ruled out since the agreement between the predicted and measured properties is so low that the mistuning effect is not considered to be a reasonable explanation for discrepancies.

Determination of uncertainty limits is a part of the empirical selection of updating parameters [1] and the random errors distribution theory is used to explain and to understand that selection process which is visualised through objective function diagrams.

5.6. Conclusions

The clear conclusion of the above discussion is that it is generally impossible to update a structure uniquely when only a limited amount of experimental data are available and instead only a partial error localisation can be attempted. In order to localise errors further, the elements which are found to be responsible for discrepancies should be refined, i.e. these elements should be separated into a number of parameters in order to allocate errors more accurately. Also, this process would increase the number of updating parameters and consequently the data requirements for updating would increase proportionally. Objective function diagrams clearly show what impact data requirements have on model updating success. Also, these diagrams show the complexities and difficulties which lie behind the updating task in general. Nevertheless, since direct model identification is impossible, because the inaccessible higher modes contribute mostly to stiffness matrix, model updating is currently the best available approach for obtaining theoretical models of improved accuracy.

6.0 Model Updating

6.1. Introduction

Model updating can be defined as the process of correcting an original finite element model in order to improve correlation with experimental data. Once experimental data are collected, an initial correlation is performed and the updating parameters are selected, and it becomes necessary to choose an updating approach that will minimise the discrepancies between the experimental and the updated models. There are several different mathematical updating procedures developed specifically to minimise discrepancies between the two models. These procedures are based on different assumptions and mathematically they may be quite different, but they all have one common feature and that is minimisation of an objective function.

Until recently, model updating was considered to be the complete procedure for finding an accurate model of a particular system in structural dynamics. The problem of finding this accurate model has been considered from a broad perspective using both empirical and theoretical knowledge about the dynamic behaviour of linear structures, in which even the accuracy of experimental data was questioned. By combining existing research methods and theories from this area, several conclusions were drawn in the previous chapters. One is that it is impossible to carry out a complete identification of structural model parameters; and this influenced the course of research in the area of model validation. Much previous work has concentrated solely on model updating considering correlation and data requirements as being of secondary importance. Structural dynamic researchers are continuously producing yet more new updating approaches, but little or no attention is paid to areas that are considered to be outside the research scope but in fact appear to be fundamental, such as the selection of updating parameters and experimental data requirements [47].

This chapter provides an introduction to existing updating formulations and their incorporation in the model validation process together with the new methods for correlation, updating parameter selection and data requirements presented earlier. Although model updating is an important part of the model validation process, it is not possible to quantify its relative role in comparison with the other parts of the model validation process. Model updating provides a mathematical procedure for model parameter identification of already-selected updating parameters and

measured experimental data. Most updating approaches are, in effect, linearisation of a complicated mathematical function, i.e. dynamics properties are approximated as linear function of updating parameters. The model updating task is to find the global minimum of an objective function which is defined mainly by selected updating parameters and measured experimental data and partly by mathematical formulation of an updating method. Whether the final updating equation is overdetermined or underdetermined, the search algorithm will be decided by the mathematical formulation of the updating method.

6.1.1. Definition of The Updated Model

Defining **the** updated model of a structure is as difficult as the updating process itself. If m experimental mode shapes have been measured at n DOFs, then a mathematical definition of **the** updated model is contained in the following expression:

$$\lambda_r^A = \lambda_r^E, \quad r = 1,\ldots,m \tag{6.1.1-1}$$

$$\phi_{j,r}^A = \phi_{j,r}^E, \quad r = 1,\ldots,m; \quad j = 1,\ldots,n \tag{6.1.1-2}$$

or a more complete requirement is that the responses must satisfy the following:

$$\alpha_j^A(\omega) = \alpha_j^E(\omega), \quad 0 \le \omega \le \infty; \quad j = 1,\ldots,n \tag{6.1.1-3}$$

The above expressions are necessary conditions for an updated model to be **the** updated model but whether they are sufficient is not known. This depends on the relative amount of experimental data available and that in turn is determined by the modal test planning procedure. Moreover, the modal test planning procedure assumes that at least the frequency range for the experiments is known and is determined by the final use of the updated model. For instance, if the updated model is to be used for general linear transient response predictions then there is a simple relationship between the minimum transient analysis time step and the frequency range in which the dynamic behaviour of the updated model should be validated. This procedure is described in section 2.2.3. If, however, the updated model is to be used for a linear static analysis then there is no need to attempt to correlate high-frequency responses; it is important that there is good correlation of FRFs in the low-frequency range only.

The requirement (6.1.1-3) may seem a complete condition for two models to be equivalent (equivalent FRFs). However, it is still only a limited number of FRFs that are included in (6.1.1-3) and therefore this condition is only extended from the conditions (6.1.1-1 and -2) for correlation of damping values.
Since it is possible to measure only a limited amount of experimental data, it can be concluded that defining **the** updated model is not possible. Instead, it is recommended to define the final use of the updated model and from that to identify the frequency range for the validation process. Even if measurement of an unlimited amount of data were possible, it is hard to believe that any numerical model which consists of mass, stiffness and damping matrices would be able to reproduce all the experimental data exactly. Although it is a highly sensitive area for discussion, it will be concluded here that **the** updated model does not exist and instead that it is only possible to identify **an** updated model that is very close to something that we consider as **the** updated model. Defining the criteria for determination of minimum data requirements for updating is the next step forward in the updating process itself.

6.2. Classification of Updating Methods

Existing updating methods can be classified into two major groups according the form of the experimental data they use, [47], and these are: (i) methods that use modal domain data and (ii) methods that use frequency domain data. The aim of this thesis is not to review all existing methods, or to list them here for educational purposes, but rather to concentrate on the in-depth research of some methods that currently seem to be most promising for use on large finite element models.

6.2.1. Modal-domain updating methods

Modal-domain updating methods can be further subdivided into (a) direct and (b) iterative updating methods.

Direct modal-domain updating methods do not require an iterative process to find the updated model and this feature avoids excessive computation and the possibility of divergence. A major weakness of this type of updating method is that although it reproduces the measured data exactly and there is no possibility of selection of

updating parameters, i.e. only whole-matrix updating is possible. The exact reproduction of the measured data is a weakness because if there is any noise in the measured data the noise will be reproduced too. One particular problem with these methods is that they require a full set of the measured mode shapes and as a result these methods will not be selected for further research of updating of large finite element models.

Iterative modal-domain updating methods use some iterative procedure to minimise a particular objective function which is defined using some correlation parameters. A major weakness of these updating methods is that they require the iterative process to update the initial model and there is no guarantee of convergence. Another problem is that they require accurate pairing of the correlated modes at every iteration. The main strength of these methods is that they allow a wide choice of updating parameters and experimental data as well as selective weighting on both. These methods do not require inclusion of damping in the model. Also, the most important feature of these methods is that they do not require complete mode shapes for updating and, and as result, they will be selected for further research of updating of large finite element models.

6.2.2. Frequency-domain updating methods

Frequency-domain updating methods use the measured frequency response function data directly so there is no need for modal analysis on the experimental data. The main weakness of these methods is that they require damping to be considered and this is very difficult to model accurately. Another difficulty with these methods is that they require residual-free regenerated FRFs during the updating process and the FOREST technique was specifically designed to tackle this problem. The process of selection of frequency points can be difficult if the initial correlation of natural frequencies is not particularly close. The selection of different updating parameters is allowed. These methods are generally considered to be not as effective as the iterative modal domain updating methods, but they could be used for updating of large finite element models.

6.3. Application of Linear Regression Theory to Model Updating

Linear regression theory [48][9][49] has an important application in most model updating approaches and therefore a thorough understanding of this theory is

crucial. The basic equation of most model updating approaches is the same as the standard linear regression equation, i.e. of the following form:

$$[S]_{N_o x l}\{\Delta p\}_l + \{\varepsilon\}_{N_o} = \{\Delta W\}_{N_o} \tag{6.3-1}$$

where $[S]_{N_o x l}$ is the matrix of predictors, [50], $\{\varepsilon\}_{N_o}$ is a vector of unknown random disturbances, $\{\Delta W\}_{N_o}$ is the vector of observations and $\{\Delta p\}_l$ is a vector of updating parameters. The number of rows in the updating equation is N_o - the number of observations, while the number of columns is l - the number of updating parameters. The ratio between the number of observations, N_o, and the number of updating parameters, l, will determine whether the updating equation is overdetermined or underdetermined. The updating equation will be overdetermined if the following condition is true:

$$N_o > l \tag{6.3-2}$$

whereas the underdetermined updating equation is defined for the following condition,

$$N_o < l \tag{6.3-3}$$

and a determined updating equation is defined when the following is satisfied,

$$N_o = l \tag{6.3-4}$$

although the case of the determined updating equation is not equivalent to either the overdetermined or underdetermined case, and has some properties of both processes. Mathematically, there is a fundamental difference in the processes of solving and interpretation between overdetermined and underdetermined updating equations and therefore these two cases will be considered separately, [51][49].

Overdetermined Updating Equation

When the number of observations is larger than the number of updating parameters in the updating equation then the updating equation is said to be overdetermined. There is not always an exact solution for (6.3-1) such that all equations are satisfied. Instead, a solution of the (6.3-1) equation is defined as a vector of updating

parameters, $\{\Delta\hat{p}\}_l$, such that the following norm of the residual vector, $\{\Delta r\}$ is minimised:

$$\{\Delta r\}^T\{\Delta r\} = \left(\{\Delta W\}_{N_o} - [S]_{N_o xl}\{\Delta p\}_l\right)^T\left(\{\Delta W\}_{N_o} - [S]_{N_o xl}\{\Delta p\}_l\right) \qquad (6.3\text{-}5)$$

It is important to mention here that an overdetermined updating equation has a unique solution under some conditions, i.e. there is only one solution of equation (6.3-1) which minimises the residual vector. The least-squares procedure for finding the solution vector in this case, $\{\Delta\hat{p}\}_l$, and the necessary conditions for the existence of the unique solution, will be described in section (6.3.1).

Underdetermined Updating Equation

When the number of independent observations is smaller than the number of updating parameters then the updating equation is said to be underdetermined and there are an infinite number of different vectors, $\{\Delta\hat{p}\}_l$, which make the updating equation (6.3-1) fully satisfied. The problem encountered in this case is that there is no unique solution of the updating equation and that requires a special treatment for estimating updating parameters. One method which determines a unique solution of an underdetermined equation is the Singular Value Decomposition, [9]. A solution of equation (6.3-1) found using the Singular Value Decomposition method is particularly interesting in model updating because it defines a solution vector, $\{\Delta\hat{p}\}_l$, that has a minimum norm amongst all possible solutions. The Singular Value Decomposition method and its application in model updating will be described in more detail in section (6.3.2).

6.3.1. Least-Squares Method

The standard least-squares problem is defined in expression (6.3-1) for the case of an overdetermined system of equations. The least-squares of vector $\{\Delta p\}_l$ is obtained by minimising the norm of the residual vector defined in (6.3-5). Taking the first derivative of (6.3-5) with respect to $\{\Delta p\}_l$ yields the so-called normal equations:

$$\left([S]^T[S]\right)\{\Delta p\} = [S]^T\{\Delta W\} \qquad (6.3.1\text{-}1)$$

The system of linear equations (6.3.1-1) has a unique solution if, and only if, the inverse of $([S]^T[S])$ exists. In this case, the least-squares estimate of $\{\Delta p\}_l$ is

$$\{\Delta\hat{p}\} = ([S]^T[S])^{-1}[S]^T\{\Delta W\} \tag{6.3.1-2}$$

This least-squares estimate $\{\Delta\hat{p}\}_l$ has several features if, and only if, certain assumptions described hold [48], and these features are:

(i) $$\mathrm{E}[\{\Delta\hat{p}\}_l] = \{\Delta p\}_l \tag{6.3.1-3}$$
that is, $\{\Delta\hat{p}\}_l$ is an unbiased estimate for $\{\Delta p\}_l$.

(ii) $$Var(\{\Delta\hat{p}\}) = \sigma^2([S]^T[S])^{-1} \tag{6.3.1-4}$$
$\{\Delta\hat{p}\}_l$ is the best linear unbiased estimate for $\{\Delta p\}_l$, that is, among the class of linear unbiased estimates, $\{\Delta\hat{p}\}_l$ has the smallest variance.

(iii) $$\{\Delta\hat{p}\} \propto N_l(\{\Delta p\}, \sigma^2([S]^T[S])^{-1}) \tag{6.3.1-5}$$
where $N_l(\mu, \Sigma)$ denotes an l-dimensional normal distribution with mean μ and variance Σ.

The vector of fitted (predicted) values is given by:

$$\{\Delta\hat{W}\} = [S]\{\Delta\hat{p}\} = [S]([S]^T[S])^{-1}[S]^T\{\Delta W\} = [P]\{\Delta W\} \tag{6.3.1-6}$$

where the so-called 'prediction' matrix,

$$[P] = [S]([S]^T[S])^{-1}[S]^T \tag{6.3.1-7}$$

has the following properties:

(iv) $$E[\{\Delta\hat{W}\}] = [S]\{\Delta p\} \tag{6.3.1-8}$$

(v) $$Var(\{\Delta\hat{W}\}) = \sigma^2[P] \tag{6.3.1-9}$$

(vi) $$\{\Delta\hat{W}\} \propto N_{N_o}([S]\{\Delta p\}, \sigma^2[P]) \tag{6.3.1-10}$$

The vector of ordinary residuals, $\{\Delta e\}$, which is defined as

$$\{\Delta e\} = \{\Delta W\} - \{\Delta \hat{W}\} = \{\Delta W\} - [P]\{\Delta W\} = ([I] - [P])\{\Delta W\} \tag{6.3.1-11}$$

has the following properties [48]:

(vii) $$E[\{\Delta e\}] = \{0\} \tag{6.3.1-12}$$

(viii) $$Var(\{\Delta e\}) = \sigma^2([I] - [P]) \tag{6.3.1-13}$$

(ix) $$\{\Delta e\} \propto N_{N_o}(\{0\}, \sigma^2([I] - [P])) \tag{6.3.1-14}$$

An unbiased estimate of σ^2 is given by

(x) $$\hat{\sigma}^2 = \frac{\{\Delta e\}^T\{\Delta e\}}{N_o - l} = \frac{\{\Delta W\}^T([I] - [P])\{\Delta W\}}{N_o - l} \tag{6.3.1-15}$$

The above results (i)-(x) are valid only if the following assumptions hold [48].

1. Linearity assumption: This assumption is implicit in the definition of equation (6.3-1) which says that each observed response value ΔW_i can be written as a linear function of the i-th row of $[S]$, $\{S\}_i^T$, that is,

$$\Delta W_i = \{S\}_i^T\{\Delta p\} + \varepsilon_i, \quad i = 1,\ldots,N_o \tag{6.3.1-16}$$

2. Computational assumption: In order to find a unique estimate of $\{\Delta p\}_l$ it is necessary that $([S]^T[S])^{-1}$ exists, or equivalently that:

$$rank([S]) = l \tag{6.3.1-17}$$

3. Distributional assumption: The statistical analyses based on least-squares (e.g., the t-test, the F-test, etc.) assume that

(a) $[S]$ is without errors, (6.3.1-18)

(b) ε_i does not depend on $\{S\}_i^T$, $i = 1,\ldots,N_o$, and (6.3.1-19)

(c) $$\{\varepsilon\} \propto N_{N_o}(\{0\}, \sigma^2[I]) \tag{6.3.1-20}$$

4. Implicit assumption: All observations are equally reliable and should have an equal role in determining the least-squares results and influencing conclusions.

Not all of these assumptions are required in all situations. For example, for (6.3.1-3) to be valid, the following assumptions must hold: (6.3.1-16), (6.3.1-17), (6.3.1-18) and part of (6.3.1-20), that is, $E[\{\varepsilon\}]=\{0\}$. On the other hand, for (6.3.1-4) to be correct, assumption (6.3.1-19), in addition to the above assumptions, must hold.

6.3.2. Singular Value Decomposition

The singular value decomposition (SVD) of matrix $[S]$ is defined in the following expression [9]:

$$[U]^T_{N_o xN_o}[S]_{N_o xl}[V]_{lxl}=[\Sigma]_{pxp} \tag{6.3.2-1}$$

where $[\Sigma]_{\text{pxp}} = diag[\sigma_1,\sigma_2,...,\sigma_p]$ (6.3.2-2)

$$p=min(N_o,l) \tag{6.3.2-3}$$

and $\sigma_1 \geq \sigma_2 \geq ... \geq \sigma_p > 0$ (6.3.2-4)

The values $\sigma_j, \quad j=1,...,p$ are the singular values of $[S]$. The matrices $[U]$ and $[V]$ satisfy the following condition:

$$[U]^*[U]=[V]^*[V]=[I] \tag{6.3.2-5}$$

Using the (6.3.2-5) condition it is straightforward to find the pseudo-inverse to be given by

$$[S]^+_{lxN_o}=[V]_{lxl}\begin{bmatrix}\Sigma^{-1}_{\text{pxp}} & 0\\ 0 & 0\end{bmatrix}_{lxN_0}[U]^T_{N_o xN_o} \tag{6.3.2-6}$$

The **condition number** of a matrix $[S]$ is defined [52] as

$$cond([S]) = \frac{\max\limits_{\{x\}} \frac{\|[S]\{x\}\|}{\|\{x\}\|}}{\min\limits_{\{x\}} \frac{\|[S]\{x\}\|}{\|\{x\}\|}} \tag{6.3.2-7}$$

which, in the case of known singular values of the full rank matrix $[S]$, becomes

$$cond([S]) = \kappa = \frac{\sigma_{max}}{\sigma_{min}} \tag{6.3.2-8}$$

The condition number of a matrix can be used to assess how close the matrix is to singularity. Matrices with small values of the condition number are said to be well-conditioned while matrices with large condition number are said to be ill-conditioned. It is difficult to define the exact value of the condition number that separates well- and ill-conditioned matrices, but for a sufficient number of digits of computation these values are: (i) $\kappa < 10^5$ defines well-conditioned matrices, (ii) $10^5 < \kappa < 10^8$ defines ill-conditioned matrices and (iii) $10^8 < \kappa$ defines numerically **singular** matrices [29][9]. These values should be taken as the order of magnitude only rather than as exact values. The condition number is generally used for assessment of the accuracy of solutions that are dependent on some inverse matrices rather than as a tool for pure assessment of singularity of a matrix. For more reliable and accurate ways of determination of the singularity and the rank of a matrix, the singular value decomposition method is used as described below.

The rank of a matrix $[S]$ is defined by the number of non-zero singular values of the matrix, that is,

$$rank([S]) = r, \quad \sigma_{max} \geq \ldots \geq \sigma_r \geq \sigma_{r+1} = \ldots = \sigma_p = 0 \tag{6.3.2-9}$$

When a matrix contains noisy data it is possible to have some singular values which are not identically zero but which are small enough to be taken as zero singular values of the matrix. In this situation it is necessary to define the numerical limit for determination of the singular values and the smallest value for determination of the singular values is the computer threshold value, $A_{THRESHOLD}$, as defined in (2.2.1-3) [52]. The threshold values for 8- and 16-digit machines are given in expressions (2.2.1-4) and (2.2.1-5). Therefore all singular values of a matrix that have the values

smaller than the appropriate threshold value will be considered to be zero and consequently will not be counted for the rank of the matrix, i.e.,

$$\sigma_1 \geq \sigma_2 \geq \ldots \geq \sigma_r > A_{THRESHOLD} > 0 \qquad (6.3.2\text{-}10)$$

The singular value decomposition has an important role in solving the underdetermined least-square problem since the solution found using the SVD is unique in the sense that it represents the **minimum norm solution**. Proof of this statement can be found in several sources, [9][49][53][48].

6.3.3. Solutions of Overdetermined and Undetermined Linear Systems

There are two major versions of the final updating equation (6.3-1) and these are: (i) **overdetermined** updating equations as described by (6.3-2) and (ii) **underdetermined** updating equations as described by (6.3-3). The solution procedures for these two types require the use of mathematically different methods and tools. Each of these two major types can be further divided into two subgroups in respect of the **rank** and **conditioning** of the matrix of predictors in the updating equation. Whilst determination of whether an updating equation is overdetermined or underdetermined is clearly defined, it is not so straightforward to determine whether a matrix is of full rank, ill-conditioned or singular. Each of these different cases is considered below and an appropriate solution procedure is developed and proposed. There is a strong argument for a complete understanding of different mathematical methods employed for solving the updating equation due to the need for physical explanation of the obtained results and estimation of their accuracy.

Solving of overdetermined updating equations

The least-squares method is mainly used for solving overdetermined updating equations. However, these equations can become ill-conditioned or singular and in these situations an appropriate method has to be used in order to find the most accurate solution.

Normal equations

The general least-squares solution (6.3.1-2) is obtained by resolving the normal equations (6.3.1-1). This procedure will produce a unique solution for the updating parameters if the following conditions hold; (6.3.1-16), (6.3.1-17), (6.3.1-18) and (6.3.1-20). All these conditions are generally fulfilled in model updating theory and practice. The linearity condition (6.3.1-16) is applicable to small values of updating parameters. The normal distribution assumption (6.3.1-20) is in line with modal testing results as described in section 3.0. The matrix of predictors is measured without any noise, as required in the condition (6.3.1-18). The only condition that partially determines the accuracy of the solution is the rank of the matrix of predictors requirement (6.3.1-17). Unfortunately, the fulfilment of this condition does not guarantee an accurate solution of the least-squares problem using the normal equations. To explain this let us consider expression (6.3.1-2) which gives the solution based on normal equations. The solution is mainly dependent on the existence of the $\left([S]^T[S]\right)^{-1}$ matrix and its conditioning. There is a very basic relationship between the condition of the $[S]$ and $\left([S]^T[S]\right)$ matrices as stated in the following expression [9],

$$cond\left([S]^T[S]\right) = \left\{cond([S])\right\}^2 \qquad (6.3.3\text{-}1)$$

It turns out that the matrix $\left([S]^T[S]\right)$ often has a high condition number, so that no matter how the normal equations are actually solved, errors in the data and roundoff errors introduced during the solution are excessively magnified in the computed coefficients. The normal equations are not a recommended approach for the general least-squares problem. The most reliable methods are based on matrix factorisation using orthogonal matrices, such as **Orthogonal Factorisation** approach, **Householder Transformations** or **Singular Value Decomposition** [9]. Nevertheless, there are situations where the normal equations offer an advantage and it is tempting to use the normal equations when there are many more observations than updating parameters.

To summarise the importance of the condition number in solving a system of linear equations: relative numerical accuracy in the solution is proportional to relative accuracy in the coefficient matrix or the right-hand side, with constant of

proportionality as large as the condition number. This means that relative accuracy of the solution is of the following form [52]:

$$\varepsilon(\{\Delta p\}) = C cond([S])\varepsilon(\Delta W)\varepsilon_{mach} \tag{6.3.3-2}$$

where C is a special constant (which is usually not larger than 1) and ε_{mach} is a binary computer constant determined by the number of bits, [52]. Suppose that the condition number of the sensitivity matrix is $cond([S]) = 10^6$ and that we have a binary computer with 24 bits in the fraction, then the numerical accuracy of the solution of a system of linear equations would be $\varepsilon(\{\Delta p\}) \approx 10^6 2^{-24} = 10^{-2}$, but the accuracy of the solution using the normal equations would be $\varepsilon(\{\Delta p\}) \approx 10^{12} 2^{-24} = 10^4$. The second approach in this example would lead to a completely inaccurate solution and consequently it would probably cause divergence of the updating analysis.

Solving of underdetermined updating equation

Solving of underdetermined linear equations requires a totally different approach to that of solving overdetermined linear equations. An underdetermined system of linear equations has an infinite number of solutions, i.e. there is no unique solution to the problem. Therefore, it is necessary to impose some other criteria in addition to the updating equation in order to determine a unique solution. The most common condition imposed upon the solution is that the norm of the updating parameters is minimised, as described in the following equation:

$$J = min\|\{\Delta p\}\| \tag{6.3.3-3}$$

Solution of the underdetermined system of linear equations using the SVD approach will minimise the norm of the updating parameters [9]. The pseudo-inverse of the sensitivity matrix can be found using the SVD as described in equation (6.3.2-6). The proper use of the SVD involves a tolerance reflecting the accuracy of the original data and the floating point arithmetic being used. Increasing the tolerance leads to larger residuals but gives results that are less likely to be sensitive to errors in the observation data. Decreasing the tolerance leads to smaller residuals and gives results that are more sensitive to the observation data. Neglecting singular values, σ_i, less than the tolerance has the effect of decreasing the condition number. Since the condition number is an error magnification factor, this results in a more reliable

determination of the updating parameters. The cost of this increased reliability is a possible increase in the size of the residuals.

6.4. Assessment of the Rank and the Conditioning of Updating Equation

In the previous section it was explained how to solve a general type of updating equation, i.e. overdetermined or undetermined. If the updating equation is underdetermined then the SVD algorithm must be employed and by choosing a proper tolerance for the minimum acceptable singular value it is possible to solve the general updating equation even if the equation is ill-conditioned or singular. If the updating equation is overdetermined but ill-conditioned or singular, then in this case the SVD has to be used in order to solve the updating equation with limited accuracy.

However, the SVD is not the only method of dealing with ill-conditioned or rank-deficient overdetermined updating equations. Another way of dealing with these situations is by proper selection of the updating parameters so that singularities of the updating equation are removed and/or the conditioning is improved [54]. The minimum requirements for finding an accurate pseudo-inverse of the matrix of predictors is that the matrix is of full rank and well-conditioned. If, however, the matrix of predictors is rank-deficient or ill-conditioned, that means that some columns in the matrix are linearly dependent or almost linearly dependent, respectively. If this is the case, then identifying linearly-independent subsets of columns in the matrix would enable the analyst to find a better fit for the updating parameters by simply excluding those columns (this is equivalent to excluding some of the corresponding updating parameters) of the matrix that are responsible for the rank-deficiency or the ill-conditioning.

Generally, in the problem of least-squares, this exclusion of linearly-dependent columns does not guarantee that the residual will be reduced but it does give a somewhat more stable and accurate solution. The fact that residuals are not affected can be explained by ill-conditioning and/or singularity of the matrix of predictors where the particular least-square problem does not have a unique solution, i.e. even though the system is overdetermined it has an infinite number of solutions that will produce similar residuals. In these instances, the solution of the ill-conditioned least-square problem tends to have large variances of extracted parameters and this poses a major threat to physical justification of the obtained results. Therefore, it is

necessary to find an algorithm which can be used to identify a subspace of linearly independent columns from the matrix of predictors.

6.4.1. Identifying the Column Space of the Matrix of Predictors

Identifying the column space of the matrix of predictors is an extremely difficult process. Many publications have explored the problem and several procedures have been recommended for solving this problem and can be found in [55]. The recommended methods are based on either the QR factorisation or the SVD and they involve interchange strategy for identification of independent columns. Unfortunately, none of these procedure[1] is guaranteed to succeed in finding the column space of an ill-conditioned matrix in the general case, [55]. Hence, a new procedure which consists of a continuing process for assessment of the contribution of each column to the conditioning of the matrix is constructed to resolve the problem of identifying the column space of a matrix.

The final goal of this process of identification of the best subspace of a matrix is to identify a set of columns of the matrix such that the condition of the matrix will have a known value. Therefore, the value for the condition number is defined so that when the matrix has a condition number less than or equal to that value, the process of identification of the column space will be stopped. The condition number of the matrix is calculated using the SVD approach as described in (6.3.2-8) expression.

The following procedure can be employed for the identification of linearly-independent subspace of the overdetermined matrix of predictors:

(i) calculate the condition number for the following matrices,

$$\kappa_i = cond\left(\left[S_{(i)} \right]_{N_0 x (l-\xi-1)} \right) \quad i = 1,\ldots, l-\xi \tag{6.4.1-1}$$

where the $\left[S_{(i)} \right]_{N_0 x (l-\xi-1)}$ matrix is obtained by excluding the *i*-th column from the $[S]_{N_0 x (l-\xi)}$ matrix and the parameter ξ is the number of already excluded columns.

(1) [1] Q Zang, G Lallement, R Fillod, J Piranda "A Complete Procedure for Adjustment of a Mathematical Model from the Identified Complex Modes" IMAC5, London, England 1987 (pp 1183 - 1190)

(ii) Then the minimum value of all calculated condition numbers is found,

$$\kappa_{min} = min(\kappa_i), \quad i = 1,...,l - \xi \tag{6.4.1-2}$$

and the *i*-th column which, when excluded from the matrix $[S]_{N_0 x(l-\xi)}$ most improves the condition number, is permanently excluded from the matrix of predictors.

(iii) The ξ coefficient is updated as $\xi = \xi + 1$ and if the following condition is satisfied,

$$\kappa_{min} \leq K \tag{6.4.1-3}$$

then the process of selection of independent column subspace of the matrix of predictors is terminated since the required conditioning is obtained. If, however, condition (6.4.1-3) is not satisfied, then the whole procedure is repeated from steps (i) to (iii) until the required conditioning is achieved.

6.4.2. Selection of Updating Parameters using Identification the Column Space of the Matrix of Predictors

The process of identification of the stable part of the column space of a matrix has been developed specifically for dealing with singular or ill-conditioned matrices of predictors of the updating equation. For instance, the finite element model of the simple beam in Figure 6.4.2-1 needs updating and it is known that the greatest uncertainty is located at the clamped end of the beam. The updating of the model is performed by selecting the two elements at the clamped end of the beam numbered 1 and 13. When the updating equation is formed using the sensitivities of the eigenvalues only [50], it is found that the two columns in the sensitivity matrix are almost identical or linearly dependent. When the inversion of the sensitivity matrix is attempted, it is found that the matrix is heavily ill-conditioned or even singular. The reason for this situation is because the finite element model of the structure is symmetric along the axial line and the selected elements 1 and 13 have almost identical sensitivities apart from sensitivities of torsional modes which also have very close values.

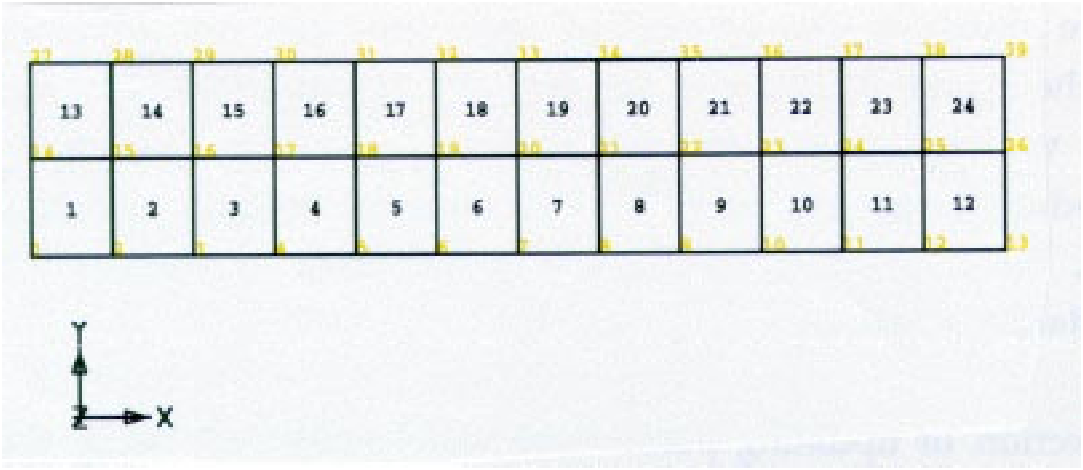

Figure 6.4.2-1. FE model of a simple beam structure clamped at the left end.

There are two ways to deal with this situation. First, if this ill-conditioning is ignored, and the updating equation is solved nevertheless, the accuracy and reliability of the solution will be low. The second approach is to eliminate one column from the sensitivity matrix using the identification of the column space of the sensitivity matrix. This procedure will select one of the two elements and reduce the size of the sensitivity matrix, solve the updating equation for the selected updating parameter and in the next iteration both originally-selected elements can be used for further updating. Numerically, this procedure is justified by improved accuracy of the solution at each iteration, but physically, the selection process is difficult to justify. Both elements have the same empirical uncertainty level and there is no reason why one element should be selected and the other one removed, even though this is the case only for one iteration. However, model updating is a numerical method that is based on the use of an initial model which is not accurate in terms of correlation because this model does not represent the real structure, e.g. the finite element model is initially symmetric but the real structure is not symmetric. The perfection of the finite element model could be a potential source of these singularities or ill-conditioning of the updating equation. The actual ‘simple’ beam structure is not symmetric and it can be identified how the stiffness of the clamped part of the beam is distributed. However, it appears that our updating parameter selection procedure is insensitive to which updating parameter is selected, and in effect, the updating procedure does not discriminate between the two elements because the model is completely symmetrical. This also can be explained as a defect of the updating method.

This method of selection of updating parameters appears to be in conflict with the engineering modelling approach. However, by analysing the experimental mode

shapes in more detail, it can be noticed that they are not perfectly symmetrical because the actual structure is not perfectly symmetrical. The fact that this information was not taken into the updating equation is a direct consequence of the updating equation being equally sensitive to both updating parameters. Therefore, the solution in this case is in inclusion of eigenvector sensitivities in the updating equation.

A few test cases of selection of updating parameters were performed using the identification of the column space of the sensitivity matrix. The sensitivity matrix was assembled by generating 20 eigenvalue sensitivities (first 20 rows) and 600 eigenvector sensitivities (other 600 rows), therefore the sensitivity matrix was heavily overdetermined but not well conditioned due to poor choice of updating parameters. This matrix is shown in Figure 6.4.2-1(a) and 6.4.2-1(b). It can be seen from Figures 6.4.2-1(a) and (b) that sensitivities of eigenvalues are larger for several order of magnitudes than sensitivities of eigenvectors.

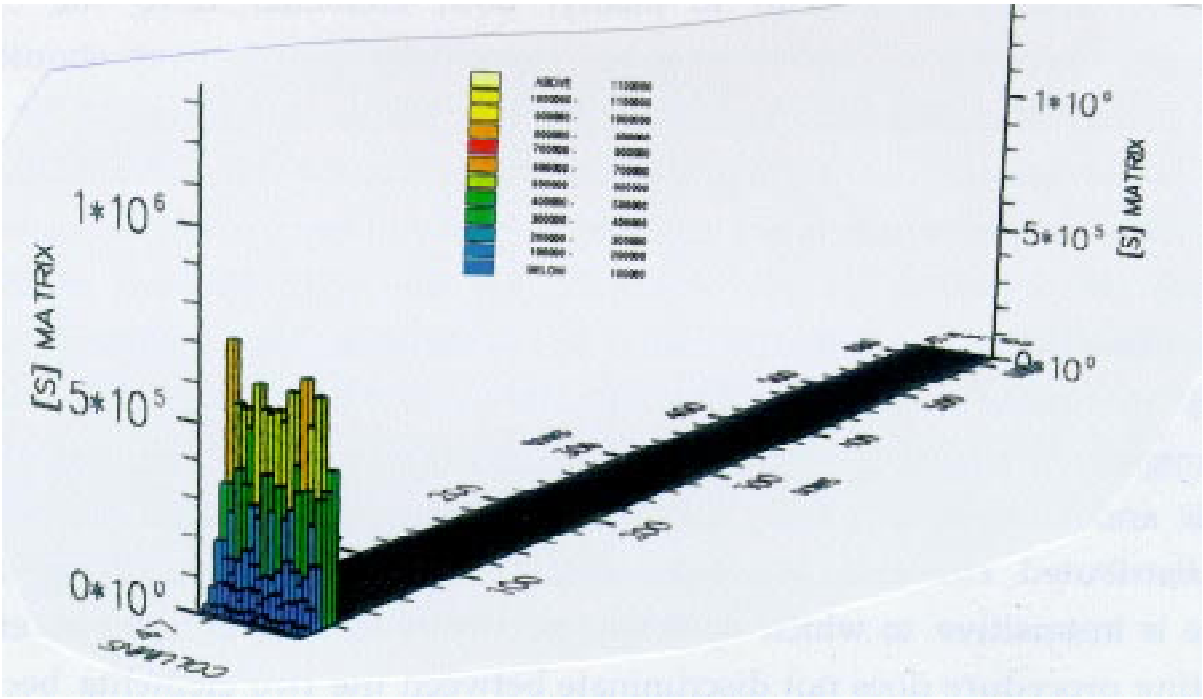

Figure 6.4.2-1(a). Sensitivity matrix, 20 eigenvalues sensitivities, 600 eigenvector sensitivities, 48 updating parameters (linear scale of absolute values).

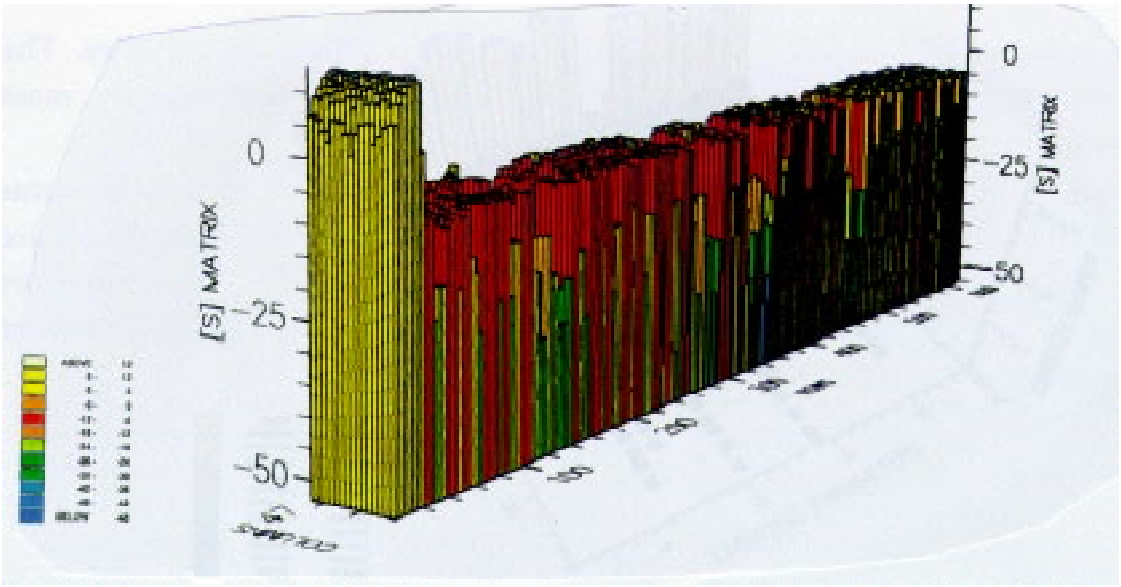

Figure 6.4.2-1(b). Sensitivity matrix, 20 eigenvalues sensitivities, 600 eigenvector sensitivities, 48 updating parameters (logarithmics scale of absolute values).

In one test case all elements of the simple beam were initially selected for updating of both mass and stiffness. Initially, the number of updating parameters was 48 and the sensitivity matrix was heavily singular. When the selection procedure was applied, the condition number of the sensitivity matrix steadily decreased until, after about 20 elements were removed, the condition number was reduced to a value below 10^5. The complete iteration process of the selection is shown in Figure 6.4.2-2.

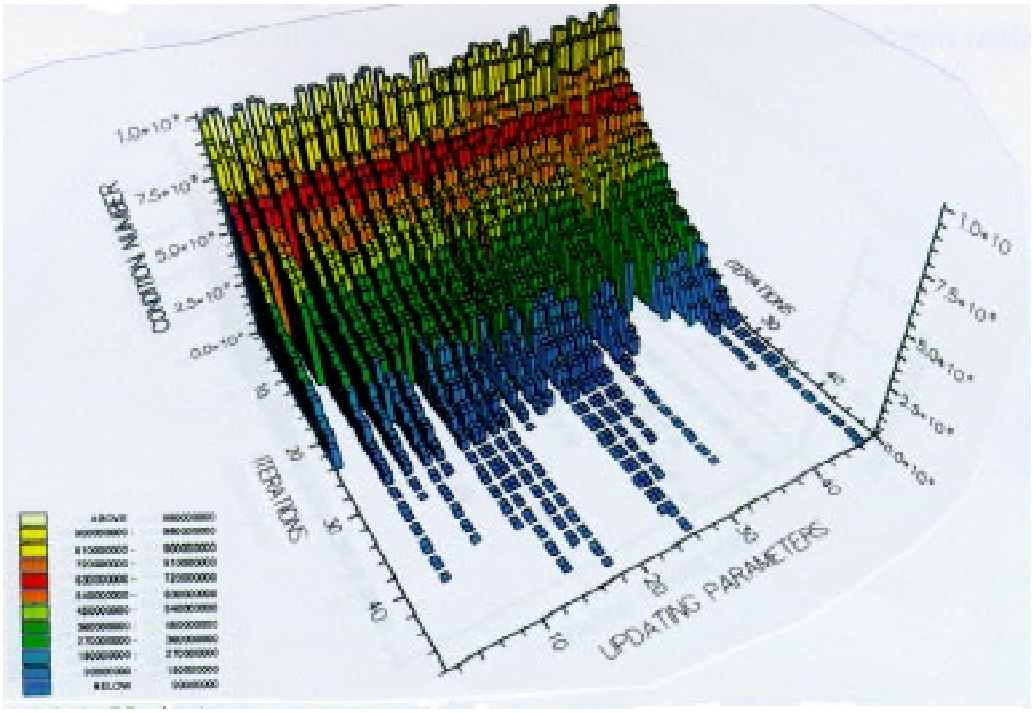

Figure 6.4.2-2. Updating parameter selection process for the sensitivity matrix

consistsing of 20 eigenvalue sensitivities and 600 eigenvector sensitivities. The initial number of updating parameters was 48 (24 stiffness and 24 mass elements).
A similar test case was performed for updating of the mass and stiffness elements of the same beam structure separately, and the result of that selection procedure is shown in Figure 6.4.2-3 and Figure 6.4.2-4, respectively. The iteration chart shows that, for reasonable conditioning of the sensitivity matrix, at least half of all symmetrical elements must be removed.

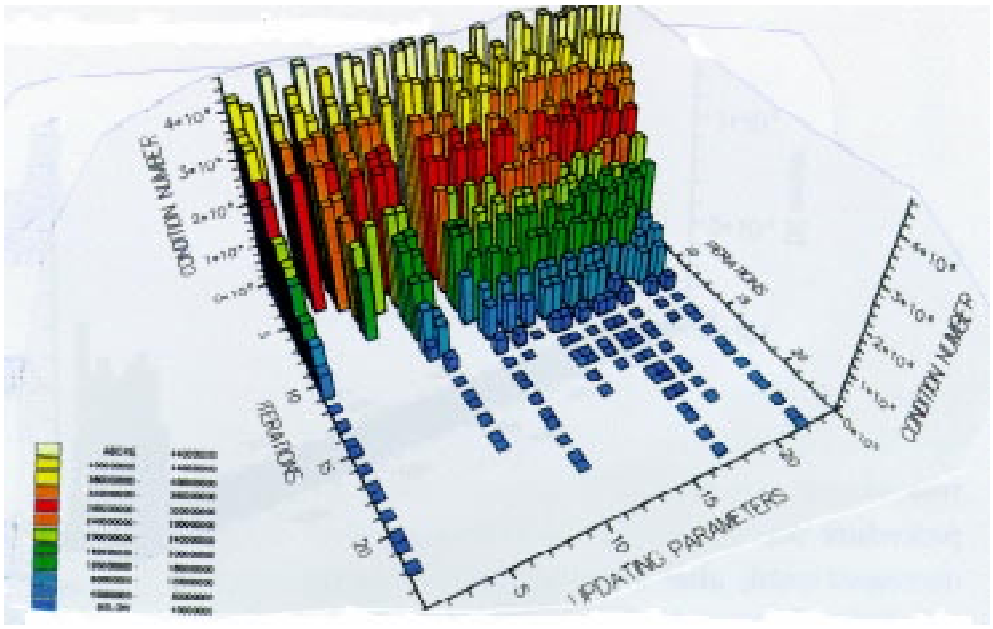

Figure 6.4.2-3. Updating parameter selection process for the sensitivity matrix consistsing of 20 eigenvalue sensitivities and 600 eigenvector sensitivities. The initial number of updating parameters was 24 stiffness elements.

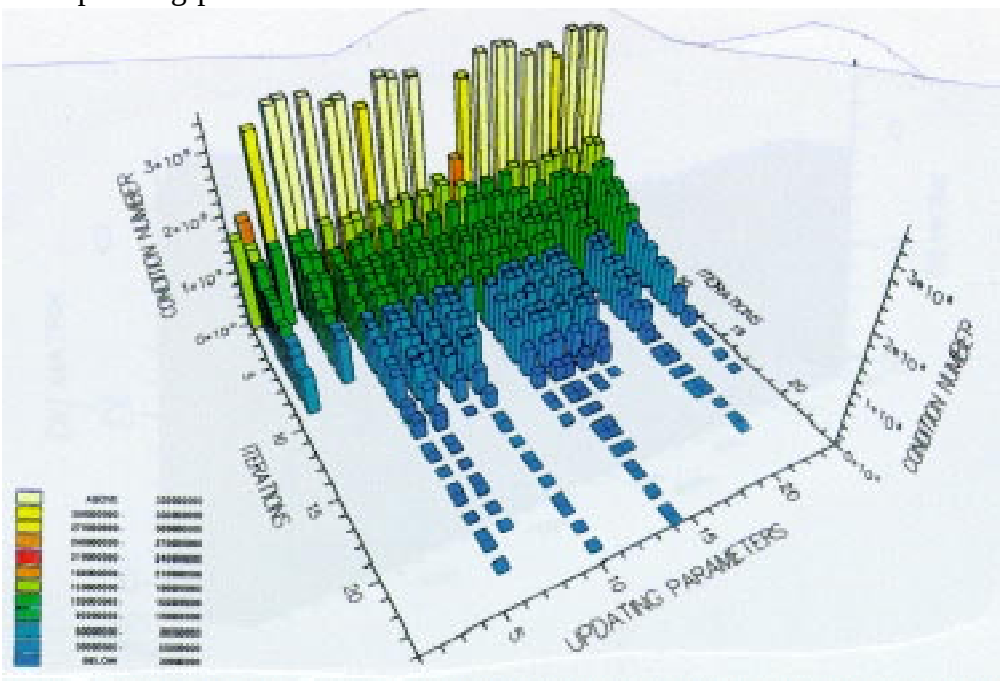

Figure 6.4.2-4. Updating parameter selection process for the sensitivity matrix

consistsing of 20 eigenvalue sensitivities and 600 eigenvector sensitivities. The initial number of updating parameters was 24 mass elements.

Use of $cond\left([S]^T[S]\right)$ for selection of updating parameters

One might think that in the process of finding the column space of the matrix of predictors it is possible to use $[S]^T[S]$ rather than the $[S]$ matrix (see expression (6.3.3.-1)) in order to decrease the computational time required for calculation of the singular values of the matrix. Figure 6.4.2-5 shows the difference of the condition number estimates using the $[S]^T[S]$ and $[S]$ matrices, and it is clear that expression (6.3.3.-1) holds only for well-conditioned matrices. When the $[S]$ matrix is ill-conditioned, then $[S]^T[S]$ has twice as bad conditioning as the $[S]$ matrix and the estimate of the singular values of ill-conditioned and even worse conditioned matrices are different. Because of this, the process of selection of updating parameters is best performed using the $[S]$ matrix rather than the $[S]^T[S]$ matrix.

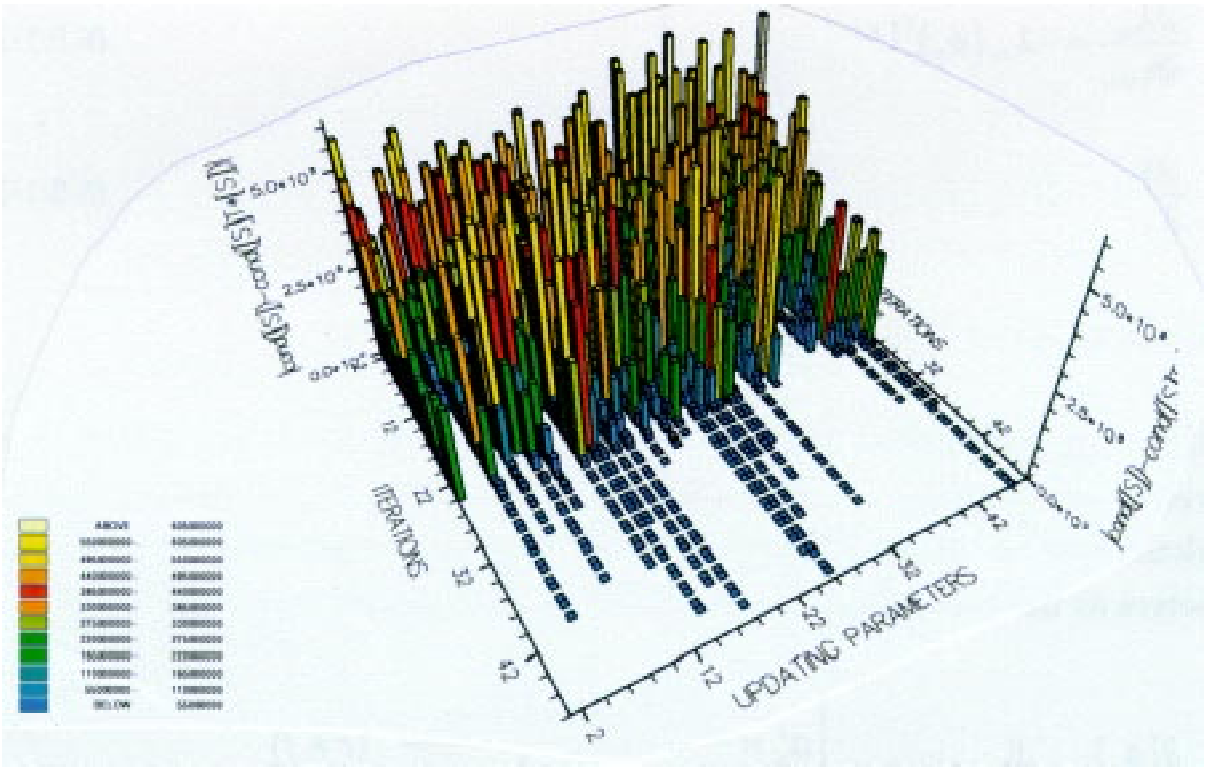

Figure 6.4.2-5. Updating parameter selection process for the matrix $[S]^T[S]$, where the sensitivity matrix consistsing of 20 eigenvalue sensitivities and 600 eigenvector sensitivities. The initial number of updating parameters was 48 (24 stiffness and 24 mass elements).

6.5. Calculation of the Sensitivity Matrix

The sensitivity matrix consists of two different types of sensitivities; (i) eigenvalue sensitivities and (ii) eigenvector sensitivities. Definitions of both sensitivities are given in the two following sections, respectively.

6.5.1. Calculation of Eigenvalue Sensitivities

By differentiating expression (2.4-4) with respect to an updating parameter, it can be shown that eigenvalue sensitivity is given by the following expression:

$$\frac{\partial \lambda_{Ar}}{\partial p_i} = \{\phi_A\}_r^T \left[\frac{\partial [K_A]}{\partial p_i} - \lambda_{Ar} \frac{\partial [M_A]}{\partial p_i} \right] \{\phi_A\} \tag{6.5.1-1}$$

For mass or stiffness updating parameters defined as in expression (5.3) and (5.4), respectively, the eigenvalue mass or stiffness sensitivities are given in the following expressions, respectively:

$$\frac{\partial \lambda_{Ar}}{\partial p_{(M)i}} = -\lambda_{Ar} \{\phi_A\}_r^T [M_A]_i \{\phi_A\}_r \tag{6.5.1-2}$$

$$\frac{\partial \lambda_{Ar}}{\partial p_{(K)i}} = \{\phi_A\}_r^T [K_A]_i \{\phi_A\}_r \tag{6.5.1-3}$$

6.5.2. Calculation of Eigenvector Sensitivities

Calculation of eigenvector sensitivities is more complicated than calculation of eigenvector sensitivities. Fox and Kapoor (1968) derived the following expression for calculation of eigenvector mass and stiffness sensitivities for updating parameters as defined in expressions (5.3) and (5.4), respectively:

$$\frac{\partial \{\phi_A\}_r}{\partial p_{(M)i}} = \sum_{j=1}^{N} \alpha_{rj}^i \{\phi_A\}_j \quad \begin{cases} \alpha_{rj}^i = -\dfrac{\lambda_{Ar} \{\phi_A\}_j^T [M_A]_i \{\phi_A\}_r}{\lambda_{Ar} - \lambda_{Aj}} & (r \neq j) \\ \alpha_{rj}^i = -\dfrac{1}{2} \{\phi_A\}_j^T [M_A]_i \{\phi_A\}_r & (r = j) \end{cases} \tag{6.5.2-1}$$

$$\frac{\partial\{\phi_A\}_r}{\partial p_{(K)i}} = \sum_{j=1}^{N} \beta_{rj}^i \{\phi_A\}_j \quad \begin{cases} \beta_{rj}^i = \dfrac{\{\phi_A\}_j^T [K_A]_i \{\phi_A\}_r}{\lambda_{Ar} - \lambda_{Aj}} & (r \neq j) \\ \beta_{rj}^i = 0 & (r = j) \end{cases} \tag{6.5.2-2}$$

Even though expressions (6.5.2-1) and (6.5.2-2) define exact eigenvector sensitivities, in order to obtain exact numerical values of eigenvector sensitivities it is necessary to include all mode shapes in the above expressions.

However, in most practical situations, it is not possible to calculate all mode shapes and therefore this approach for eigenvector sensitivities calculation is not recommended. Instead, it is recommended to use Nelson's (1976) approach [50] which requires knowledge of only particular eigenvector and its corresponding eigenvalue for calculation of that eigenvector sensitivity. However, the approach is mathematically not a simple one but a major advantage of this method is that it maintains the sparseness of structural matrices in the calculation of eigenvector sensitivities. The complete eigenvector sensitivity comprise two parts:

$$\frac{\partial\{\phi_A\}_r}{\partial p_{(M)i}} = \{\xi\}_r + \delta_r \{\phi_A\}_r \tag{6.5.2-3}$$

where coefficient δ_r can be calculated using the following expression:

$$\delta_r = -\{\phi_A\}_r^T [M_A] \{\xi\}_r - \frac{1}{2} \{\phi_A\}_r^T \frac{\partial [M_A]}{\partial \{\phi_A\}_r} \{\phi_A\}_r \tag{6.5.2-4}$$

Calculation of vector $\{\xi\}_r$ is defined by the following expression:

$$\begin{bmatrix} [[K_A] - \lambda_r [M_A]]_{11} & 0 & [[K_A] - \lambda_r [M_A]]_{13} \\ 0 & 1 & 0 \\ [[K_A] - \lambda_r [M_A]]_{31} & 0 & [[K_A] - \lambda_r [M_A]]_{33} \end{bmatrix} \begin{Bmatrix} \{\xi\}_1 \\ \xi_k \\ \{\xi\}_3 \end{Bmatrix} = \begin{Bmatrix} \{f\}_1 \\ f_k \\ \{f\}_3 \end{Bmatrix} \tag{6.5.2-5}$$

where DOF k is chosed at the location where $|\{\phi_A\}_r|$ is a maximum.

The vector $\{f\}_r$ is defined by the following expression:

$$\{f\}_r = -\left[\frac{\partial[K]}{\partial p} - \lambda_r \frac{\partial[M]}{\partial p} - \{\phi_A\}_r^T \left[\frac{\partial[K]}{\partial p} - \lambda_r \frac{\partial[M]}{\partial p}\right]\{\phi_A\}_r[M]\right]\{\phi_A\}_r \qquad (6.5.2\text{-}6)$$

Since it is not possible to calculate all mode shapes for the majority of practical engineering applications, and particularly for large FE models, it is recommended to use Nelson's method for calculation of eigenvector sensitivities.

6.5.3. Use of Eigenvector Sensitivities

The sensitivity matrix of the FE model shown in Figure 6.4.2-1 consists of 620 rows of which first 20 rows are eigenvalue sensitivities and the other 600 rows are eigenvector sensitivities. There are 12 updating parameters (stiffness values of elements 1,2,..12), i.e. columns of sensitivity matrix. The rank of the sensitivity matrix is 12 since the selection of updating parameters is such that all columns of the matrix are linearly independent because the condition number of this matrix is $cond([S]_{620\,x12}) = 139.58$. In this case, for a well-conditioned sensitivity matrix, it is possible to calculate the prediction matrix of this sensitivity matrix in order to find the contribution of every row to the rank of the matrix, as shown in the following table.

Row No.	Modal Parameter	Contribution to rank
1	λ,	0.2814323739792 x E-6
2	λ,	0.1096905701970 x E-3
3	λ,	0.6778407900804 x E-3
4	λ,	0.1274363632337 x E-2
5	λ,	0.1983045010151 x E-2
6	λ,	0.4173508823678 x E-1
7	λ,	0.7826221123678 x E-1
8	λ,	0.2894185810461
9	λ,	0.8396950191003
10	λ,	0.4443564606393
11	λ,	0.9987059873396
12	λ,	0.3737190949353
13	λ,	0.5400648100049
14	λ,	0.6575566689807
15	λ,	0.9021244756341
16	λ,	0.8945524503730
17	λ,	0.9679739606158
18	λ,	0.9837471523141
19	λ,	0.9948488605076
20	λ,	0.9891939575761
21	ϕ,	0.1018738100120 x E-11
22	ϕ,	0.4942650084504 x E-11
23	ϕ,	0.9146244241179 x E-12
24	ϕ,	0.9782250424170 x E-12
25	ϕ,	0.3566062058370 x E-11
26	ϕ,	0.2305001845271 x E-11
27	ϕ,	0.1802376582287 x E-11
28	ϕ,	0.2742710557550 x E-11
29	ϕ,	0.1161861234673 x E-11
30...620	ϕ,...	< 0.9 x E-11

Table 7. Contribution of eigenvalue and eigenvector sensitivities to the rank of sensitivity matrix.

Also, in order to determine the contribution of the eigenvector sensitivities to the condition number of the sensitivity matrix, let us consider the following study on the same sensitivity matrix. If the first row of the sensitivity matrix is removed iteratively, and the condition number recorded for every new reduced matrix, then the following results are obtained:

No. of Eigenvalue Sensitivities in [S] matrix	cond([S])
19	139.58
18	139.58
17	139.58
16	139.61
15	139.62
14	139.79
13	276.24
12	276.32
11	24539032.61

Table 8. Condition number of the sensitivity matrix as function of number of eigenvalue sensitivities.

It is clear from Table 7 that contributions of the eigenvector sensitivities are negligible in comparison with the eigenvalue sensitivities. It is also interesting to note that sensitivities of higher eigenvalues are significantly more important than those of the lower eigenvalues. This observation is in line with conclusions obtained in section 5.1.1. where the identification approach was discussed.

Considering the results presented in Table 8 it can be concluded that conditioning of sensitivity matrix is independent of the inclusion of eigenvector sensitivities, i.e. the conditioning of the sensitivity matrix depends only on the number of eigenvalue sensitivities, the number of updating parameters and their selection. Another important conclusion from Table 8 is that the number of updating parameters should not exceed the number of experimental natural frequencies.

The above results suggest that the inclusion of experimental mode shapes in the sensitivity matrix is not important, but it would be wrong to generalise this statement and suggest that it is not necessary to estimate experimental mode shapes at all because they cannot be used for sensitivity calculations and updating. Experimental mode shapes must be estimated because CMPs are selected by considering correlation between mode shapes, and even though it appears that the experimental mode shapes do not have to be used in the updating equation directly, they still contribute to the updating equation through the selection of CMPs. However, it is possible to perform special weighting on the sensitivity matrix and increase the contribution of eigenvector sensitivities to rank and conditioning of the sensitivity matrix as explained in the following section.

6.5.4. Weighting of the Sensitivity Matrix (Updating Equation)

Some researchers [45][19] perform a special weighting of the sensitivity matrix by multiplying those rows which correspond to eigenvector sensitivities by large numbers. This process will definitely give an extra importance to these rows, but there is no physical justification for this particular weighting since the variance of the measured eigenvectors is several times larger than the variance of the eigenvalues. A statistically better weighting of the sensitivity matrix should be performed by dividing each row of the matrix by the corresponding variance of the variable used (eigenvalue or modal constant), but this weighting would further decrease the importance of eigenvector sensitivities in the sensitivity matrix.

Also, it may be useful to use the COMAC correlation coefficient for weighting the sensitivity matrix, i.e. eigenvector sensitivities can be multiplied by the COMAC value of the correponding DOF added to the value of a special constant $\varepsilon_{w-COMAC}$. This weighting will increase the influence of DOFs which have good correlation and decrease the influence of DOFs which have poor correlation measured by the COMAC value. The coefficient $\varepsilon_{w-COMAC}$ is a constant which is used to ensure that in case of low COMAC value for a particular DOF, the contribution of this DOF to the objective function is not completely diminished. For instance, let us consider two DOFs which have COMAC values of 2% and 95%, respectively. The numerical contribution to the objective function (error) of the first DOF (2 percent COMAC) is obviously much larger than the contribution of the second DOF (95 percent COMAC). However, the sensitivities of the first DOF are more likely to be less accurate than the sensitivities of the second DOF due to less accurate modal

constants of first DOF than the second DOF, which is measured by COMAC values. It is difficult to recommend a particular value for the special constant, $\varepsilon_{w-COMAC}$, but it should not be very small because, in this case, this weighting would remove influence of all major contributors to the objective function and the updating equation would rely solely on only well correlated parameters. Too large a value of the special constant, $\varepsilon_{w-COMAC}$, would diminish the influence of the COMAC coefficient and it would artificially force the updating solution to rely more on experimental mode shapes rather than experimental eigenvalues even though the variance on the measured mode shapes is larger than the variance on the measured eigenvalues. The recommended values for $\varepsilon_{w-COMAC}$ is to be in the range [0.1,100.].

6.6. Conclusions

Due to linear representation of the errors in the model, most model updating methods transform into a standard problem of least-squares. Several methods for solving a general updating equation have been examined in this chapter, and it can be concluded that in different situations different solution methods should be used. If there is large number of measured data and a small number of updating parameters, then the use of normal equations seems to be the most suitable one. However, if the quantity of experimental data is only slightly greater than the number of updating parameters, then the SVD method should be used.

Use of eigenvector sensitivities has been discussed and it can be concluded that eigenvector sensitivities can be neglected, unless a special and largely unjustified weighting is performed (mulitiplying of eigenvector sensitivity rows with large values), and in order to keep updating equation well conditioned the number of selected updating parameters should not exceed the number of experimental natural frequencies.

In any case, it is recommended to control conditioning and accuracy of the updating equation by proper selection of the updating parameters as it is specified in a new method for selection for these parameters.

7. Model Validation Case Studies

This chapter contains two practical model validation test cases. Each test case was carefully chosen to highlight the applicability of model validation technology to practical engineering problems. The first case study is a simple cantilever beam clamped at one end. Even though the structure is extremely simple, the unknown clamped boundary condition make this example an interesting one, particularly as it was selected as the benchmark for a validation study. The second case study is a large aerospace structure for which a well-defined validation criterion is specified. This case study was selected to be presented here because it is a typical industrial example, and the idea behind it is to show the real and practical challenges an analyst will face when applying model validation technology to industrial cases.

7.1. Model Validation of Lloyd's Register Structural Dynamics Correlation Benchmark

7.1.1. Introduction

The Lloyd's Register Structural Dynamics Correlation Benchmark structure consists of three separate components: a cantilever beam, a baseplate and the foundation. The cantilever beam is firmly screwed to the baseplate which is resting on the foundation. A detailed description of the benchmark can be found in Appendix 7A and in reference [4].

7.1.2. FE model

The finite element model used for the structure consists of a shell element model of the cantilever beam partially embedded into a brick element model of the baseplate, as shown in Figure 3.6.5-5. Connection between the shell and brick parts of the model is across the area shown in details in Figure 7-1. This overlap of shell elements inside the brick elements is necessary because the brick elements do not have rotational degrees-of-freedom and a simple connection between shell and brick elements would treat the system as a mechanism. The specified thickness of the two bottom layers of shell elements is 1 mm only while the top layer connected to beam has an equivalent thickness to that of the shell elements of the beam. The boundary conditions specified in the model are free-free, as specified in the original

specifications for the test case (Appendix 7A). The total number of degrees-of-freedom for the model used in this study is 6001.

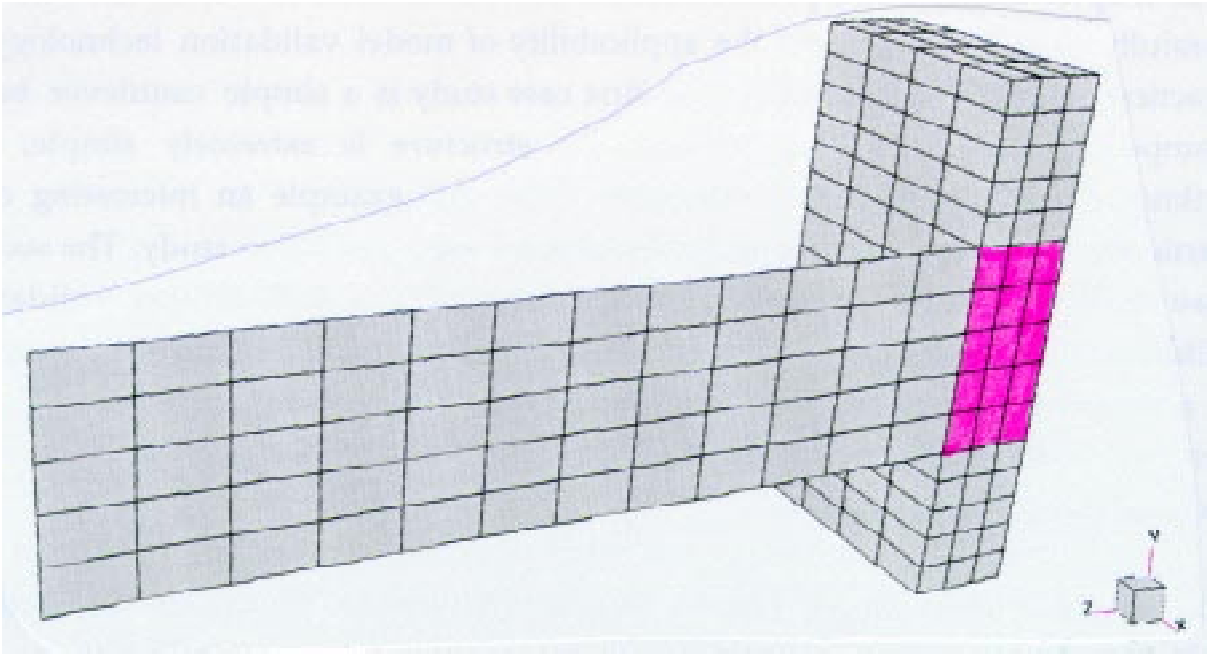

Figure 7-1. Structural joint modelling by embedding shell elements between brick elements.

The list of natural frequencies of the initial FE model is given in the following table:

Mode Number	Natural Frequency [Hz]
1 - 6	0.0
7	376.1
8	1258.0
9	1488.0
10	1534.9
11	3368.6
12	3949.0
13	4271.6
14	4543.4
15	4704.8

Table 1. List of natural frequencies of the initial benchmark model.

7.1.3. Experimental data

The experimental data consisted of seven natural frequencies and quantitative descriptions of the corresponding mode shapes. These data were supplied by Lloyd's Register who collected test results from three different companies which carried out the tests and also another set of natural frequencies was combined as the average results of all three supplied sets of data. Details of the original experimental data can be found in Appendix 7B. Close inspection of these data reveals that differences in the measured natural frequency sets measured by different companies are as high as 3 %. These differences could be considered as significant in terms of reliability of the measured data but it is impossible to comment any further since no any additional information was supplied. In this case, it was decided to use average results from the three data sets since any systematic and/or random measurement errors would be compensated in the average data set. As far as mode shapes are concerned, only a basic geometric description was supplied by Lloyd's Register and it will be necessary to assume that the experimental modes are symmetric. The mode shapes of the initial FE modes will be used as numerical values of experimental mode shapes for correlation purposes during updating process.

7.1.4. Correlation between experimental and initial FE results

Correlation between the experimental and initial FE models was performed by comparing natural frequencies of two modes (one from the experimental and one from the initial FE model) which have the same mode shape description. The following table gives more details of this correlation of natural frequencies between experimental and initial FE models.

Exp. Mode	Av. Exp. Freq. [Hz]	Initial FE Mode	Initial FE Freq. [Hz]	Relative Freq. Difference [%]
1	313	7	376.1	+20.2
2	1065	8	1258.0	+18.1
3	1210	10	1534.9	+26.9
4	1372	9	1488.0	+8.5
5	3019	11	3368.6	+11.6
6	3535	13	4271.6	+20.8
7	4250	14	4543.4	+6.9

Table 2. Correlation between Experimental and Initial FE models

7.1.5. Error localisation in FE model

Many errors in the initial FE model might be responsible for the discrepancies found between the experimental and the initial FE models described in the previous section. Some of these errors bear less and some more responsibility for the observed discrepancies, but since in the description of the model it is said that the baseplate and the beam are firmly screwed together it is probable that the main causes of inaccuracy of the initial model are errors in this region of the model. There are probably some other errors as well, but the amount of the discrepancies caused by the other errors can probably be neglected in comparison with correlation discrepancies caused by the joint between the baseplate and the beam. The obvious conclusion from the above discussion is that most of the errors are assumed to be concentrated at the joint between the baseplate and the cantilever beam and, consequently, the updating parameters will be selected in this region of the theoretical FE model.

7.1.6. Updating of FE model

The selected method for updating was Inverse Eigensensitivity method mainly due to the availability of only natural frequencies with quantitative description of experimental mode shapes only rather than any numerical values for them. Due to this lack of experimental data it was possible to use only eigenvalue sensitivities for model updating rather than combined sensitivity of both eigenvalues and eigenvectors.

Selection of updating parameters

Since there are seven modes in the experimental model, in order to have as good conditioning of the updating equation as possible, the number of updating parameters should be limited to five. Considering the mesh of the combined brick and shell FE model of the structure, the stiffnesses of two shell elements were assigned to each updating parameter, as shown in Figure 7-2. Several other updating parameters selection choices were used for updating, but for most of them convergence was not achieved while some converged to physically unreasonable results and as such were excluded from the studies.

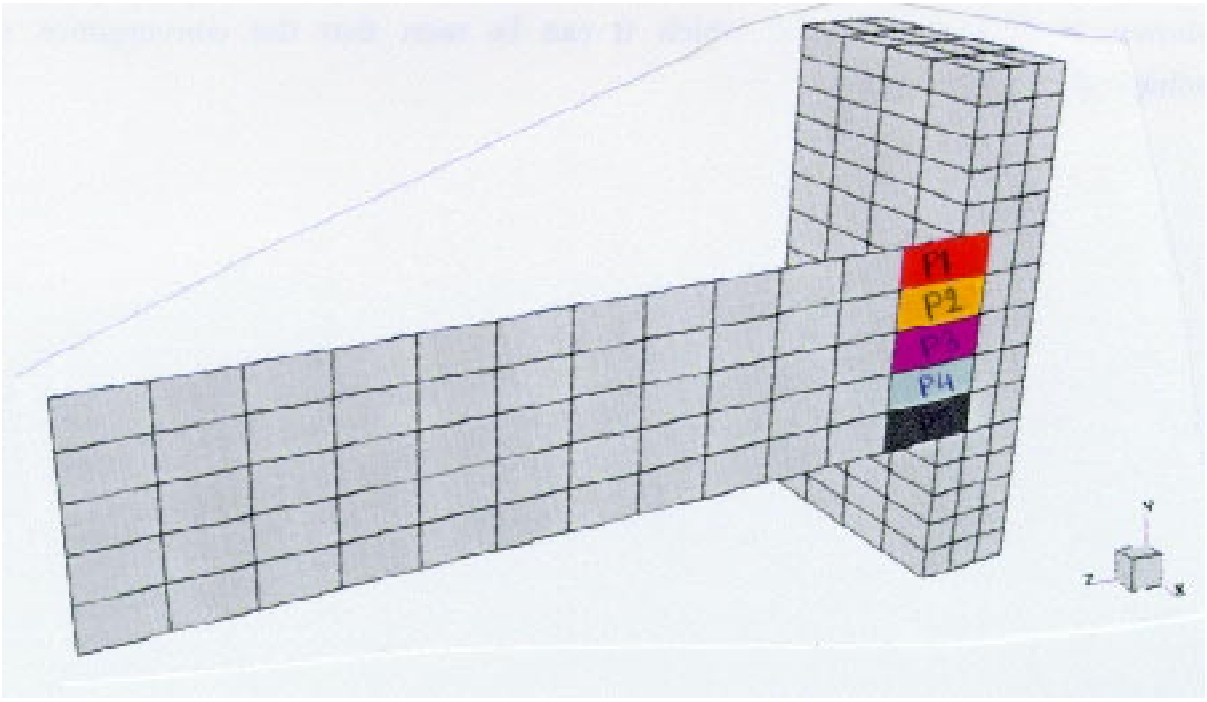

Figure 7-2. Selected updating parameters.

7.1.7. Convergence of updating parameters

Convergence of updating parameters is an important measure of the success of particular updating test case, and is a necessary but not sufficient condition for a successful updating result. Since in the case of this test case, updating is mathematically only an optimisation procedure, once convergence is achieved and the final updating parameters have converged to particular values, it is highly likely that the position described by the converged values of the updating parameters is

just a local minimum of the defined objective function. Even if the final values of updating parameters converge to a global minimum of the objective function, that result does not represent the true updated model because of the incompleteness of the objective function used in the updating formulation and the incomplete number of selected updating parameters.

It is very unlikely that if all elements in the initial model were selected, the same result would have been achieved as when only a limited number of updating parameters are selected. It is important to stress that selection of stiffnesses of all elements in the initial model as updating parameters was not possible due to the lack of experimental data, in this case seven natural frequencies. Convergence of the five selected updating parameters described in the previous paragraph is shown in Figure 7-3 from which it can be seen that the convergence was achieved in 15 iterations.

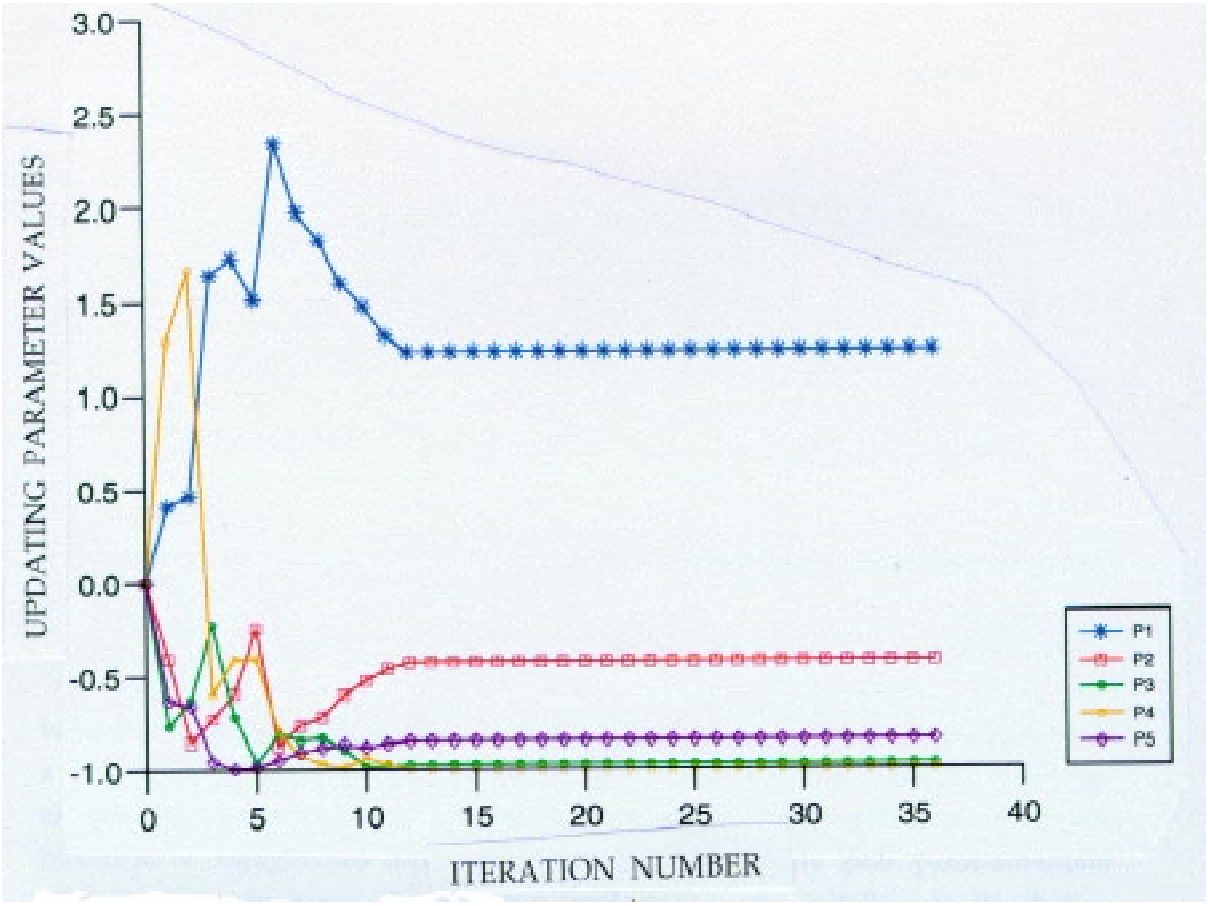

Figure 7-3. Convergence of updating parameters.

The values of the final stiffness correction or updating parameters is given in Table 3 below. All digits given in Table 3 are stable converged digits of the updating parameter values.

Updating Parameters	Stiffness Correction
P1	1.2324
P2	-0.42143
P3	-0.97382
P4	-0.999999899
P5	-0.84739

Table 3. The converged values of the updating parameter stiffness correction.

The values of the updating parameters in Table 3 should be multiplied by their corresponding elemental stiffnesses and then these resulting stiffnesses should be added to the structural stiffness matrix of the initial FE model in order to obtain the new stiffness matrix of the updated model. The values of the updating parameters should be interpreted as the additional stiffnesses of the initial values of the local elemental stiffnesses to the initial global stiffness matrix.

Considering the values from the above table, it can be concluded that there is a loss of stiffness at the joint on one side of the structure. This result could indicate that the actual connection between the two pieces is achieved via only one screw which is positioned at one side of the joint, but it should be borne in mind that this conclusion is highly speculative and is only a possibility which may not necessarily be the true explanation.

7.1.8. Correlation between experimental and updated FE model

Correlation between experimental and updated FE models is performed by comparing the natural frequencies of the two correlated mode shapes using the Modal Assurance Criterion to determine the degree of mode shape correlation.

The table below gives more details of the correlation results after model updating has been completed.

Exp. Mode	Exp. Freq. [Hz]	Upd. FE Mode	Upd. FE Freq. [Hz]	MAC [%]	Relative Freq. Difference [%]
1	313	1	312.1	98	-0.29
2	1065	2	1102.4	85	3.5
3	1210	3	1218.9	94	0.74
4	1372	4	1371.1	91	-0.07
5	3019	5	3087.9	90	2.3
6	3535	6	3560.7	77	0.73
7	4250	8	4219.6	90	-0.72

Table 4. Correlation between experimental and updated FE models

Although the MAC values decreased for some correlated mode pairs during updating, close inspection of mode shapes of the updated model indicates that the updated mode shapes are not symmetric as these mode shapes used for updating which originate from the initial FE model. Another indication that the updated mode shapes are not symmetric is because they originate from a model which is not symmetric, i.e. by considering the values of the updating parameters in Table 3 it can be seen that the updated model is not a symmetric one. If the results from the updating exercise are valid, i.e. if the model is not symmetric, then the experimental mode shapes should not be symmetric either. Since numerical values of the experimental mode shapes were not supplied, it is impossible to check whether they were symmetric or unsymmetric.

7.1.9. Conclusions for Validation of Lloyd's Register Correlation Benchmark

A significant improvement of correlation of natural frequencies has been achieved by changing the stiffnesses of structural elements selected as the updating parameters. Although the inverse-eigensensitivity method is used for updating, only eigenvalue sensitivities were used since only experimental natural frequencies are available. There is a possible physical explanation for the results obtained but the lack of experimental evidence makes it impossible to draw a firm conclusion. Nevertheless, the improvement of natural frequencies obtained by updating are from an average discrepancy of 15% before updating to an average of 0.6% after updating.

7.2. Model Validation of an Aerospace Structure (C-Duct)

7.2.1. Introduction

This second case study is the validation of a FE model of an aerospace structure, known as C-Duct in aerospace industry. Two C-Duct structures hold an aircraft engine between them when the engine is mounted onto the wing of the aircraft. The structure itself consists of many one-piece components which are assembled by several thousand rivets. The structure is shown in Figure 7-4. The overall measured mass of the structure is about 435 kg. It is necessary to validate an FE model of the structure to within 5 percent of natural frequency difference between the test and FE data.

7.2.2. FE model

The structure is modelled using shell and beam elements and concentrated masses and the final mesh has about 92,000 DOFs. The FE model is shown in Figure 7-5. Estimated mass of the FE model is 430 kg. The list of the initial FE model estimated natural frequencies is given in Table 5.

7.2.3. Modal Test Data

A free-free modal test was carried out in the range between 0 and 100 Hz. The structure was tested for non-linearity by exciting it using different force levels. It was found that the dynamic behaviour of the structure is linear within the 0 - 40 Hz frequency range, but not-linear for the higher frequencies. The list of measured natural frequencies is given in Table 5. The total number of measured FRFs is 90, and the measurement locations are shown in Figure 7-6.

It is important to stress here that planning of the modal test could not be performed because the initial FE model was not available at the time when the modal test was carried out. This particular validation exercise was done as part of a commercial project involving major engineering companies and as it is not unusual in these circumstances that such delays that can change the course of a validation exercise. However, several checks on modal test data have been done when the initial model was made available and it was concluded that a sufficient number of points has been measured.

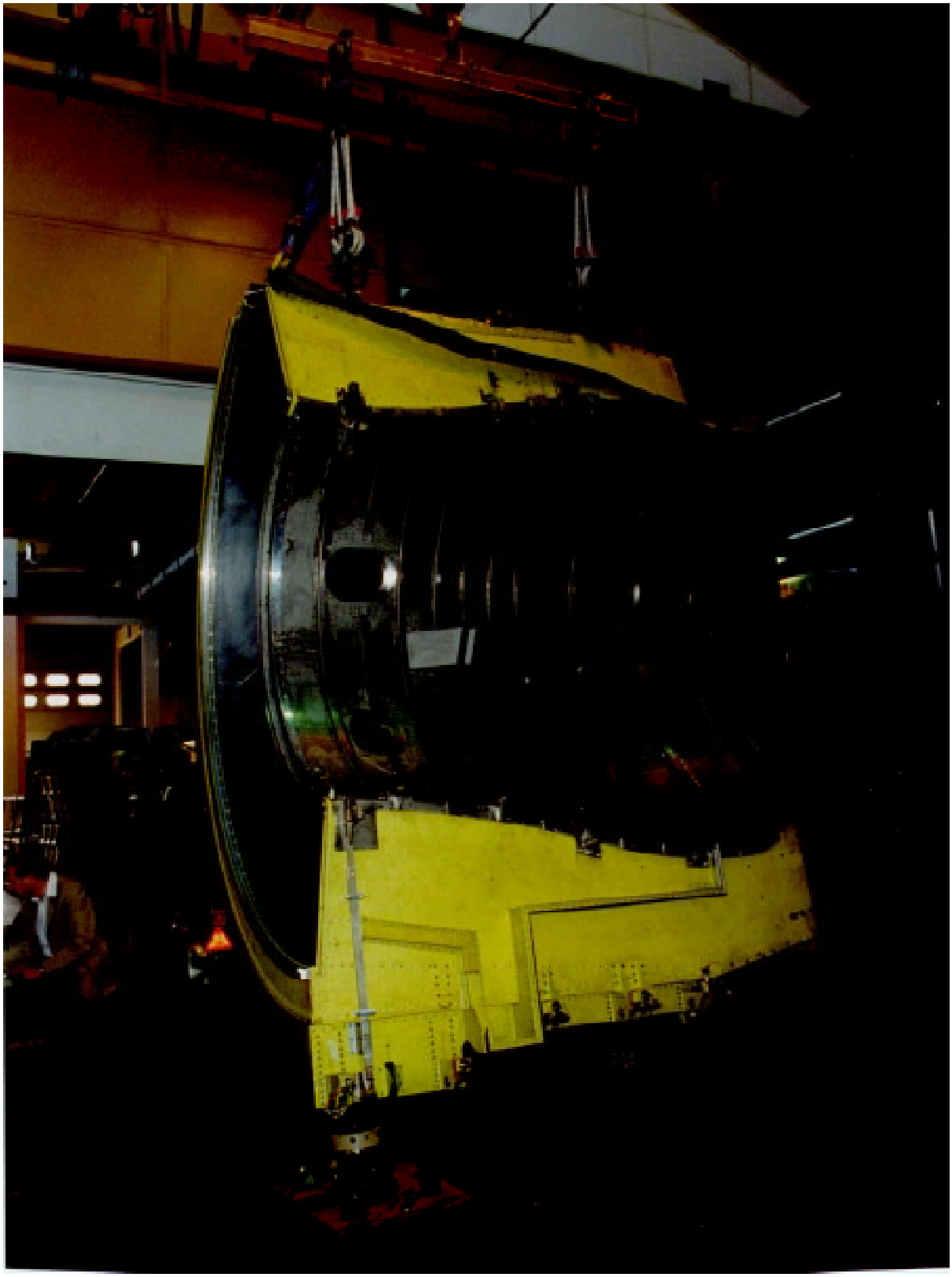

Figure 7-4. C-Duct structure during modal testing.

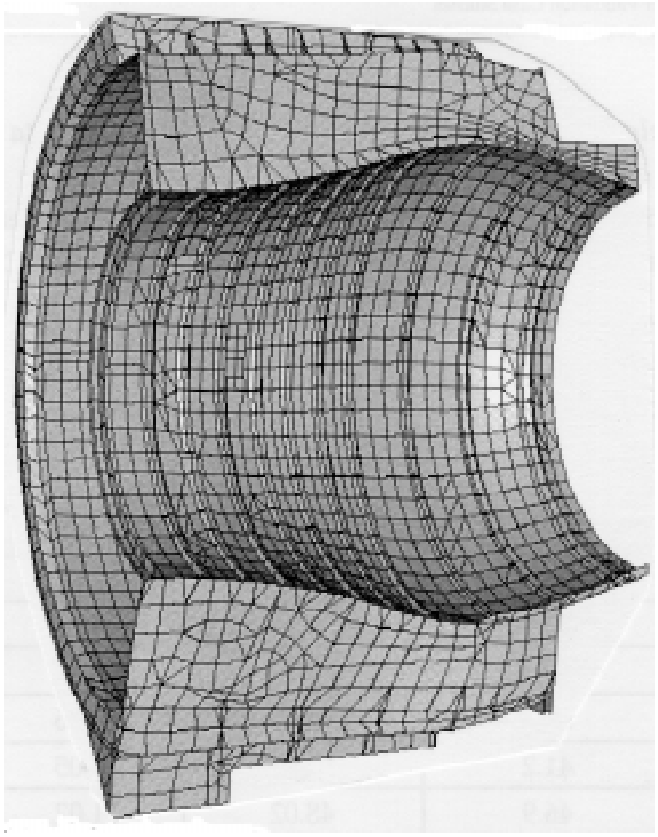

Figure 7-5. FE model of C-Duct structure.

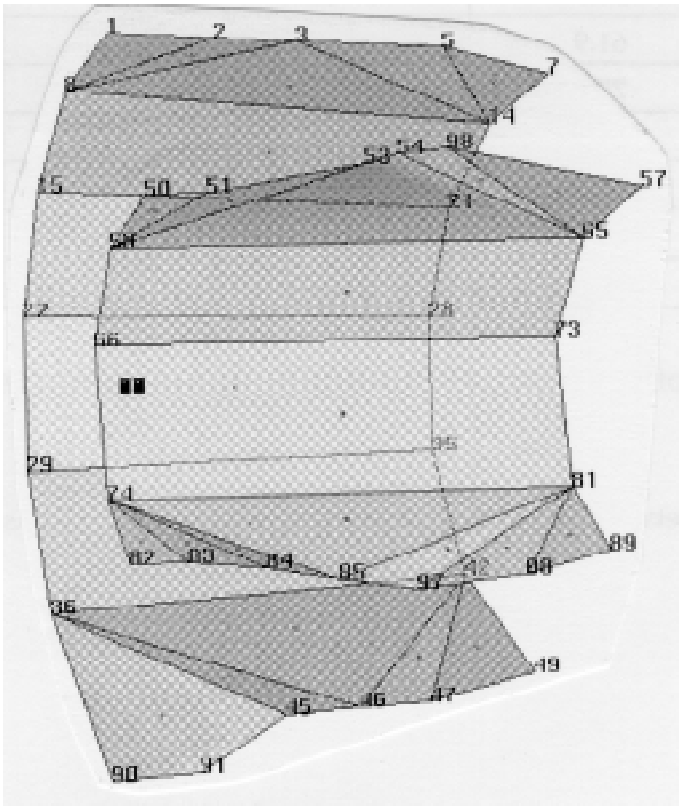

Figure 7-6. Experimental mesh of C-Duct structure.

7.2.4. Correlation between measured and the initial FE data sets

The following table gives details of the correlation between the initial FE model frequencies and the measured natural frequencies for the C-Duct structure.

Mode No.	Experimental Frequency [Hz]	FE Frequency [Hz]	$f_{FE}/f_{exp.}$
1	9.3	10.5	1.12
2	14.6	17.10	1.14
3	16.1	18.35	1.09
4	17.0	20.26	1.13
5	21.5	26.56	1.21
6	26.9	34.02	1.26
7	30.3	38.82	1.36
8	41.2	43.36	1.05
9	46.9	48.02	1.02
10	60.8	59.02	0.97
11	61.9	71.67	1.25
12	75.2	89.66	1.19
13	75.9	93.52	1.23
14	82.4	99.13	1.20
15	85.2	103.41	1.21
16	97.9	108.25	1.11

Table 5. List of experimental and the initial FE natural frequencies.

Correlation between the experimental and FE mode shapes is given in Figure 7-7.

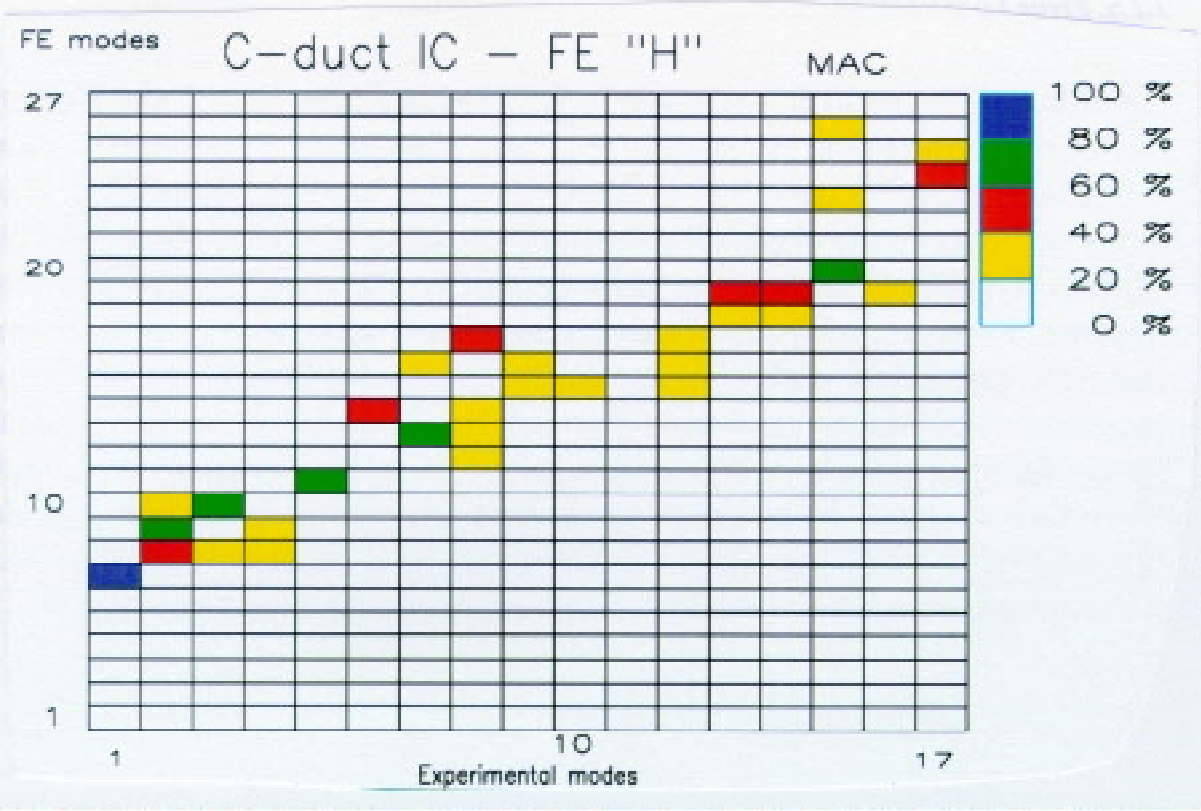

Figure 7-7. Initial mode shape correlation between the test and FE data sets.

After analysing the MAC matrix, a list of the 8 clearly-correlated mode pairs (CMPs) can be constructed as given in the following table (Table 6).

CMPs No.	Experimental Mode	Experimental Frequency [Hz]	FE Mode	FE Frequency [Hz]	MAC [%]	$\frac{f_{FE} - f_{exp.}}{f_{exp.}}$ [%]
1	1	9.2	7	10.5	90.	+14.7
2	2	14.5	9	18.3	62.	+25.8
3	3	16.1	10	20.3	70.	+25.9
4	4	17.0	8	17.1	27.	+0.03
5	5	21.5	11	26.5	75.	+23.3
6	6	26.9	14	43.4	44.	+60.9
7	7	30.2	13	38.8	68.	+28.2
8	8	35.3	17	71.7	52.	+102.7

Table 6. Correlated mode pairs for the initial FE model.

7.2.5. Error Localisation

The C-Duct finite element model can be classified as a large model, and has far more possible updating parameters than the amount of experimental data available. Since only eigenvalue sensitivities are used in updating equation, this means that the number of updating parameters must be limited to the number of experimental natural frequencies, which is eight in this case. By inspecting the structure, it can be concluded there are several regions which are relatively crude structural joints. Since each of these regions has quite complicated but uniform structural joints, this means that each type of structural joint can be represented by one updating parameter. It is also important to select regions of the model which have significant strain energy for the mode shapes which are to be used in updating, and the final selection of updating parameters is shown in Figure 7-8. Each updating parameter comprises a number of individual finite elements.

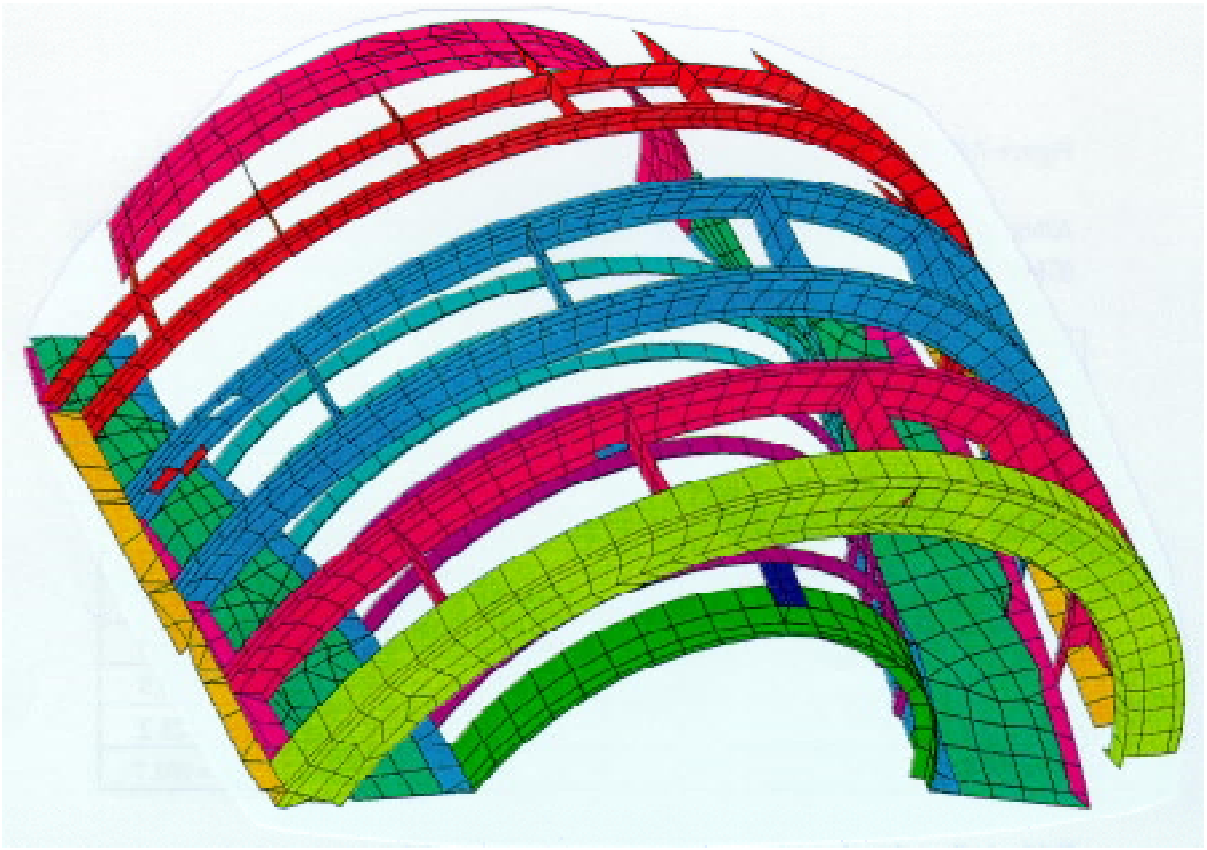

Figure 7-8. Selection of updating parameters for C-Duct FE model.

It was thought that the mass representation of the structure was properly defined by the initial FE model and therefore only stiffness correction is to be performed during updating. By considering the approximation of the initial FE model it was decided that a limit for possible perturbations (or values of the updating parameters) should be set to 60 percent of the initial stiffness value. This effectively meant that there was a limit on all updating parameters to vary only in the region [-0.6,0.6].

7.2.6. Model Updating

Model updating of the C-Duct structure was performed using the standard inverse eigensensitivity method but using only eigenvalue sensitivities. Eigenvector sensitivities were not used in updating equation due to the fact that their contribution to the rank of the sensitivity matrix is negligible and the computational effort necessary to calculate them is unreasonably expensive (see chapter 6).

7.2.7. Convergence of updating parameters

Several different initial selection of updating parameters were used during updating of the C-Duct case study. Identification of the column space of the stiffness matrix was used during updating in order to stabilise the search process and to ensure convergence or at least limit divergence. Only about 30 percent of all updating attempts converged to improved models. A few updating attempts were made for every single selection of updating parameters with different initial values given to the updating parameters. Successful iterative search attempts found several different updated models, one updated model for each iteration. Some of these updated models from the same iteration sequence are almost equivalent, but due to the nature of the searching algorithm there are usually quite a few different updated models for every iteration sequence. At the end, more that 300 updated models were found and it was necessary to establish some systematic selection process in order to determine the final updated model.

7.2.8. Selection of the final updated model

When selecting the final updated model several important factors were considered, but particular emphasis was paid to: (i) natural frequency difference of CMPs, (ii) MAC values of CMPs, (iii) values of updating parameters, (iv) global uniqueness of

CMPs in the MAC matrix (equivalent to uniqueness condition for AUTOMAC matrix) and any improvement in the correlation beyond the frequency range used in updating. After careful consideration of all major factors, the final updated model was selected and its correlation is given in the following table:

CMPs No.	Experimental Mode	Experimental Frequency [Hz]	FE Mode	FE Frequency [Hz]	MAC [%]	$\frac{f_{FE} - f_{exp.}}{f_{exp.}}$ [%]
1	1	9.2	7	8.9	67.	-3.0
2	2	14.5	8	14.7	52.	0.9
3	3	16.1	10	17.0	64.	3.6
4	4	17.0	9	15.8	41.	-7.4
5	5	21.5	11	22.6	81.	5.1
6	6	26.9	12	26.0	21.	-3.6
7	7	30.2	13	32.8	70.	8.5
8	8	35.3	14	33.9	38.	-4.2
9	9	40.8	15	45.9	45.	12.5

Table 8. Correlated mode pairs for the updated FE model.

The values of the updating parameters for the final updated model are given in the following table:

No. of Updating Parameter	Updating Parameter Value
1	-0.5918
2	-0.5583
3	-0.1908
4	-0.5889
5	-0.5915
6	-0.5902

Table 9. The final values of updating parameters for the updated model.

The MAC matrix for the final updated model is shown in Figure 7-9. It can be seen from both MAC matrix and Table 8 that some improvements were made even for some correlated CMPs that were not included in the updating process, such as CMP 9. This improvement in correlation beyond the frequency limit used in updating was a major reason for selecting the particular model to be the final updated model. It needs to be stressed here that all updated models including the final updated model indicate lower MAC values than the initial model when correlated to the test data even though uniqueness of CMP(s) has been improved. This particular effect is the consequence of not including eigenvector sensitivities in updating equation.

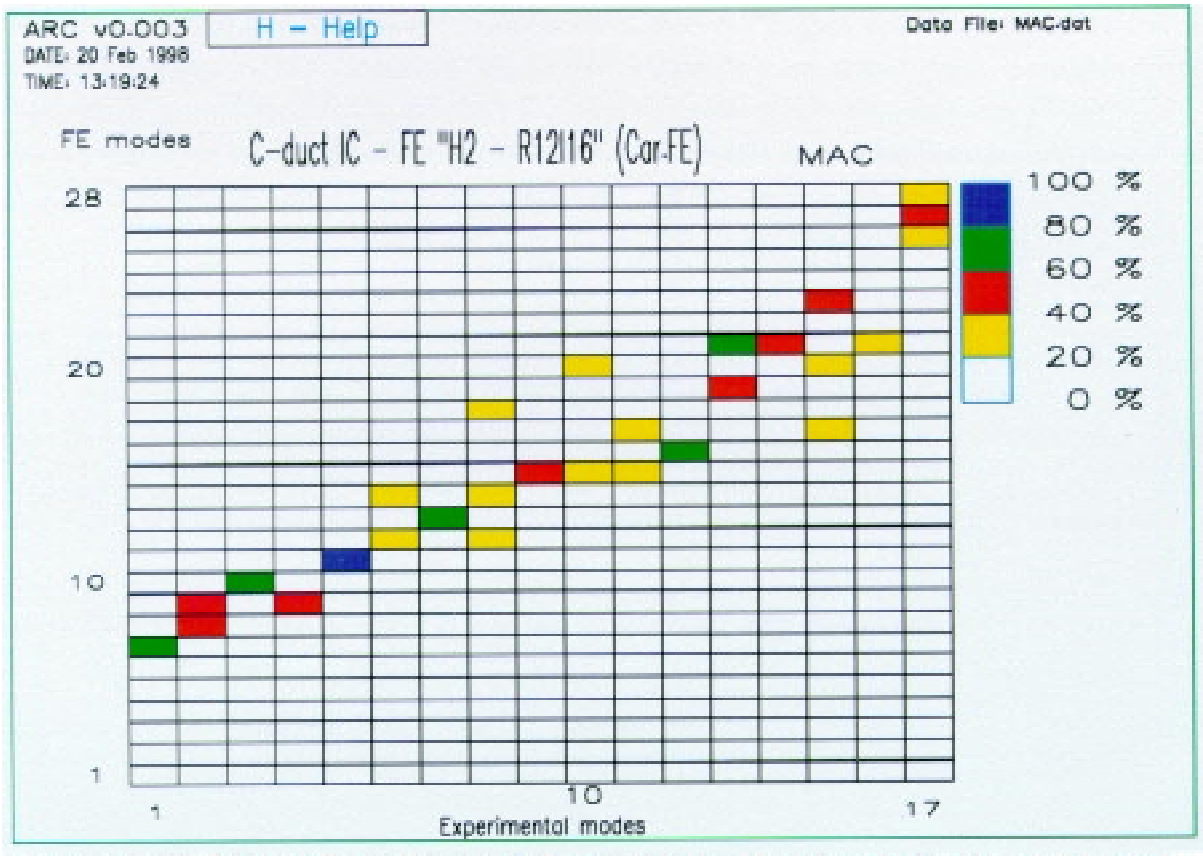

Figure 7-9. Correlation between measured and FE modes after updating.

7.2.9. Conclusions for Validation of C-Duct Structural Dynamic Model

Model validation of the initial structural dynamic model of C-Duct structure was performed. The objective of the exercise was to validate natural frequencies within 5 percent but this objective was difficult to achieve due to limits imposed on variations of the updating parameters. However, some mode shapes had higher importance and these mode shapes satisfied the initial criterion for frequency correlation. Eigenvector sensitivities were not used in the updating process due to the disproportionate calculation effort required to calculate them in respect of their contribution to the overall conditioning of the sensitivity matrix. After applying model validation to the C-Duct case study more than 300 improved models were generated, most of them showing close correlation to the experimental results even though every single improved model was different to the others. The selection process proved to be almost as difficult as any other part of model validation and therefore some additional criteria had to be employed to select one final improved model. The final updated model shows correlation even beyond frequency for which model validation was performed.

8.0 Conclusions and Suggestions for Future Work

This chapter presents the main conclusions and a summary of the specific contributions reported in this thesis. The Conclusions section below represents the overall conclusions for the use of model validation as presented in this thesis while more specific conclusions are given at the end of each chapter.

8.1. Conclusions

The main goal of the research reported in this thesis was to study the applicability of model validation to real engineering problems. Since the majority of real engineering problems involve quite complicated structures, see Figure 8.1-1 for example, these models are usually large in terms of their number of DOFs, and therefore a particular emphasis was given to applicability of model validation to 'large' theoretical models.

Before model validation of any structure is attempted, there should always exist well-defined criteria for the validated model. In practice, these criteria are usually given in terms of natural frequency and mode shape differences for a specified number of modes or over a specified frequency range. Validation criteria can be found from the final use of a validated model, i.e. if the validated model is to be used for prediction of general transient response then it is possible to define a frequency region within which the initial model needs to be validated (section 2.2.3).

Once validation criteria are found, then it is necessary to determine the minimum data requirements for validation. Data requirements have been defined separately for correlation and for model updating. In the case of correlation, it has been shown that it is possible to define the minimum data requirements (section 4.4), while in the case of model updating it was shown that defining data requirements is not so straightforward (section 5.1.1).

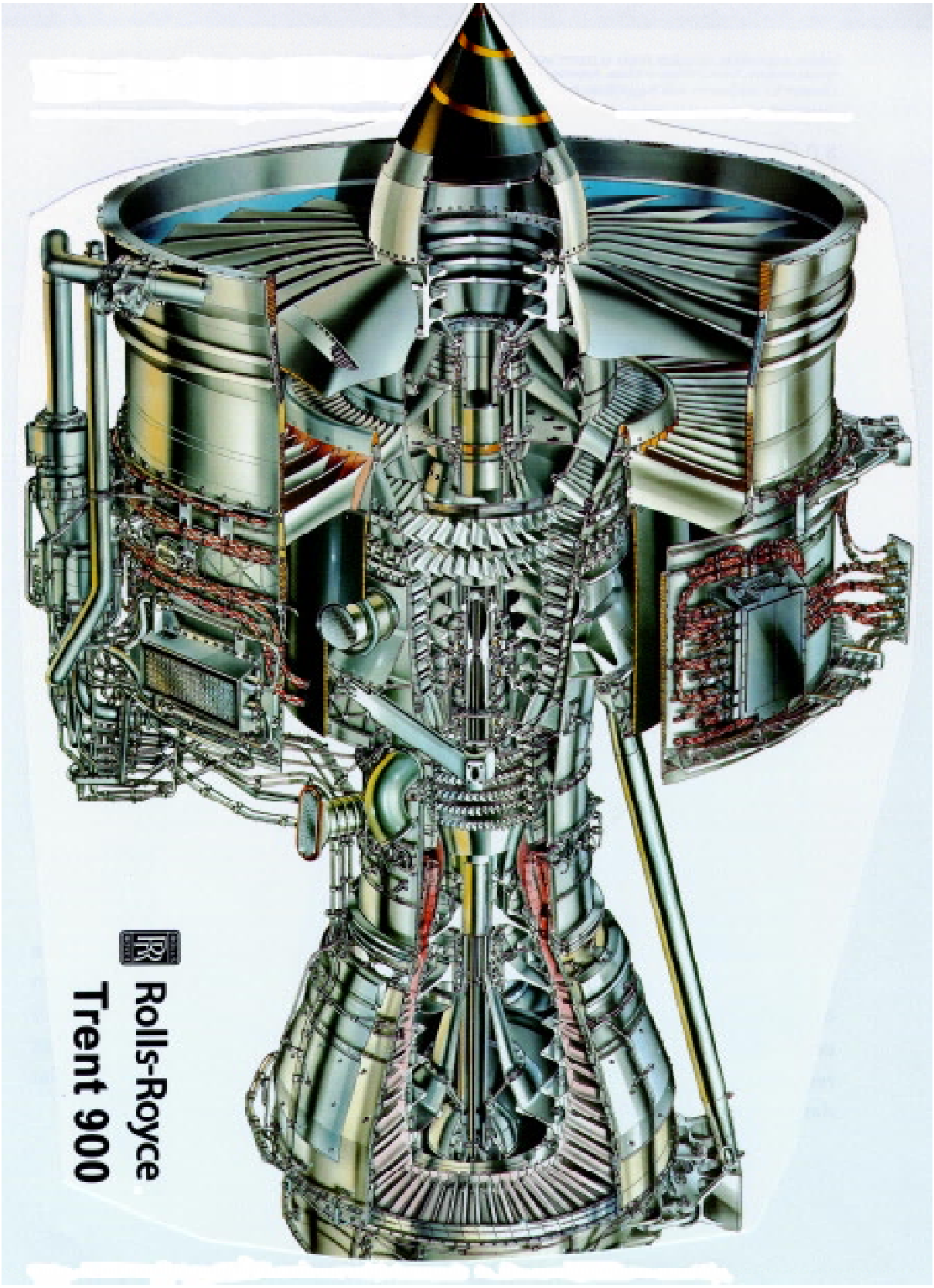

Figure 8.1-1. A typical structure which needs to be modelled accurately.

Data requirements for correlation were coupled with test planning to ensure that the necessary experiments can be optimised. Modal tests on complicated structures can be quite time-consuming and expensive. It is necessary to ensure that these tests are carried out with the minimum of effort while the measured data acquired are of the highest accuracy. During a modal test, it is necessary to select optimum suspension, optimum excitation location(s) and optimum measurement locations, as shown in Chapter 3.

Obviously, the test is a critical stage of the model validation process. The test should be carried out according to a test plan and the data requirements for correlation, but since the initial model used in test planning is of limited accuracy (that is the main reason for doing validation of the model), it is necessary to spend some time investigating the results produced by the test planning phase to make sure that the final modal test does not miss any important data.

Correlation is not just a simple comparison between experimental and theoretical models. Correlation is also used to determine the completeness of the measured data set. Although correlation is not as complicated as test planning or model updating, performing correlation automatically during updating is quite a complicated process. The main task of correlation is to produce a list of correlated mode pairs and this is critical information for the generation of the sensitivity matrix. Also, during the correlation process a picture of possible error locations can be drawn. Provided that the measured data set is complete, then all discrepancies due to errors somewhere in the model can be shown and identified during correlation process.

Accurate selection of the sites of the errors responsible for discrepancies shown in the correlation is a crucial requirement for a successful model validation. There are two main approaches for selection of error locations and defining model updating parameters. One approach is to select error locations according to knowledge about the initial model and likely approximations of the initial model. The second approach is to select error locations according to the strain energy distributions for the modes of interest.

Once the updating parameters are selected and defined and the initial correlation is known, then model validation enters a stage where the initial model is corrected and the final updated model is produced. There are many model updating techniques, but very few of them can be applied to real engineering problems successfully. The inverse eigensensitivity method was identified as one of the most promising for updating of large theoretical models and this method has been researched in-depth from a numerical stability and accuracy point of view. It is recommended to perform updating using well-conditioned over-determined updating equation through a special selection of updating parameters, as explained in section 6.4.2.

Use of eigenvector sensitivities has been discussed in particular detail and it was shown that the eigenvector sensitivities' contribution to the sensitivity matrix rank and conditioning is negligible in comparison with that of the eigenvalue sensitivities. This led to the conclusion that eigenvector sensitivities should not be used in updating, unless a special physically-unjustified weighting is introduced, not least because it is very expensive to calculate them. As only updating using over-determined equations is recommended, that means that the number of updating parameters should not exceed number of CMP(s) determined during correlation.

After several updating attempts are made, it is necessary to select the final updated model. Since model updating does not produce a unique solution, it is common practice to find several different updated models giving similar levels of correlation with the experimental model. The final updated model must be selected by consideration of some additional criteria which were not used in updating, such as correlation of FRFs for the higher frequencies etc.

8.2. List of Contributions to Model Validation

8.2.1. Contributions to Test Planning

In test planning, the following contributions have been made and are presented in this thesis:

(i) new methods for defining the average displacement, velocity and acceleration of an excited system, ADDOFD, ADDOFV and ADDOFA, respectively;

(ii) a new method for finding the optimum suspension locations based on the ADDOFD parameter;

(iii) new methods for analysing the distribution of the nodal lines of an excited system; Optimum Driving Point (ODP) and Non-Optimum Driving Point (NODP) parameters;

(iv) a new method for finding the optimum excitation locations; the ODP method, and guidance on how to use it;

(v) a new method for finding the non-optimum excitation locations; NODP method and guidance on how to use it;

(vi) a series of new coefficients based on ADDOFV, ADDOFA, ODP and NODP parameters for selection of the optimum excitation location; ODP-V, ODP-A, NODP-V and NODP-A and guidance on how to use them;

(vii) the existing Effective Independence (EI) method was used as the basis for development of new method for finding the optimum set of measurement locations. New methods use EI and the ADDOFV or ADDOFA parameters to select the best optimum locations to measure mode shapes as independently as possible but measuring only locations where the highest signal-to-noise ratio is to be found;

(viii) Whether a modal test is to be carried out using a hammer or a shaker for excitation, and whether the response is to be measured using accelerometers or a

laser velocimeter, a complete test planning strategy is developed and presented in this thesis;

(ix) all new methods were verified on many practical test cases, a few of which are included in this thesis.

8.2.2. Contributions to Correlation

In correlation, the following new methods and contributions have been made:

(i) a relatively new method for assessment of complexity of experimental mode shapes has been defined and explained in detail and a discussion about realisation of complex mode shapes is given;

(ii) a new correlation coefficient, the SEREP Cross-Orthogonality (SCO), based on the SEREP reduction process, is introduced with all the required and sufficient conditions for its successful use clearly defined;

(iii) a new coefficient for comparison of natural frequencies, Natural Frequency Difference (NFD), has been defined;

(iv) a new correlation procedure for selection of correlated mode pairs is presented. This correlation procedure is used in model updating approach as a tool for automatic selection of CMPs;

(v) a new method for determination of the necessary number of out-of-range modes for calculation of FRFs with controlled accuracy of antiresonances has been developed and presented, abbreviated as the FOREST technique.

8.2.3. Contributions to Error Location Methods

The following contributions to error location methods have been made:

(i) a detailed explanation of problems associated with solving model updating as an identification problem;

(ii) new limitations for updating parameter values have been presented and explained;

(iii) two different approaches for selection of model updating parameters have been introduced, empirically- and sensitivity-based selection methods;

(iv) a comprehensive study of distribution of error locations to the overall objective function based on random error distribution theory.

8.2.4. Contributions to Model Updating

In model updating the following contributions have been made:

(i) a new definition of the updated model is given;

(ii) a systematic selection of existing promising updating approaches to be used for validation of large finite element models;

(iii) a comprehensive study of all possible scenarios for solving the least-squares problem when applied in model updating using the Inverse Eigensensitivity method;

(iv) a new method for elimination of ill-conditioning of the sensitivity matrix and selection of updating parameters based on finding the best column space of the matrix;

(v) use and contribution of mode shape sensitivities for updating of large finite element models has been discussed.

8.3. Suggestions for Future Work

Model validation is reaching a stage at which it is becoming more and more actively used within industry, particularly for aerospace applications. Today, there are more and more situations within industrial practice when a company asks its supplier to provide a validated model of an ordered product. These products vary from simple components to aircraft engines or planes. One can almost certainly expect that the

need for model validation will increase in the future and therefore further developments are ensured, the only uncertainty being the way in which this technology will be developed. The latest developments suggest that there is an increasing trend towards the use of model validation for damage detection. This seems as an obvious and natural path that model validation application will follow. Also, further integration between experimental methods and theoretical predictions is expected, not only within the structural dynamics field, but further, combining fluid-dynamic effects with structural dynamics.

There are some encouraging findings and results presented in this thesis, but there are also some results (see section 5.2.1, Figure 5.2.1-2) which indicate that there is still some way to go before model validation can be used as a routine tool for industrial applications. Further development of model validation technology is necessary to bring it to a stage where every engineer with the minimum of specialist knowledge about model validation techniques can safely use this technology as a black-box routine. In order to ensure that further development of this technology brings it a step closer to wide industrial application the following areas need to be researched.

(i) **Integration of final use of the validated model and validation techniques, test planning, correlation and updating**. Every validation exercise is attempted with a specific goal - usually, this goal is to match particular modes for given the frequency tolerance - and this information must be used as the initial data for determining the minimum data requirements for correlation and updating. If the final user of the validated model knows what the validated model is intended for, then this knowledge should be converted into numerical form which can indicate the frequency range of validation and the required level of correlation in this frequency range. In practice, if a company requires model validation to be performed for a specific purpose, then the party who undertakes the validation task should be able to define the required level of correlation and the frequency range of validation. Nowadays, everyone wants their models to be validated within a specific frequency range but little or nothing is known about the reliability of these validated models when used for further analysis.

(ii) **Error location theory needs to be further developed and better understood than it is the case today**. Every validation exercise should be used to explain discrepancies so that model validation is also used as a tool for learning about improved modelling. As more sophisticated and perhaps new modelling techniques developed through model validation are used, the boundary of the expected validation level will move further. Today, it is standard practice **not** to expect more than 20 (certainly 30) modes in general to have an acceptable correlation. This boundary will move as model validation techniques improve, new modelling techniques are used and, obviously, as new measurement techniques are made available. It is important to understand physical changes made to the initial model whenever possible rather than just to take changes to the initial model blindly without properly understanding errors of the initial model.

(iii) **Determination of data requirements for model updating**. It was shown in Chapter 5 that it is virtually impossible to gather sufficient data for a complete identification of the structural model. However, it should be possible to find a relationship between the accuracy of the validated model (for a specific purpose, of course) and the data requirements. It is almost certain that the data requirements for model updating will be huge, although perhaps not unattainable as in the model identification case, but at least by knowing this relationship it will be possible to assess whether the current approaches used in model updating are feasible. Also, it would be interesting to explore the dependency of different updating formulations on the data requirements for model updating.

(iv) **Further study is needed of the validation data requirements of an assembled structure**. Clearly, single components must be validated within a higher frequency range than applied to the assembled structure. This approach of disassembling structure and validating single components first and then assembling the structure and validating every subassembly is a natural way of validation for complicated structures.

(v) **Development of new updating algorithms using stochastic optimisation techniques**. The objective function diagrams presented in Chapter 5 clearly show difficulties associated with model updating. Optimisation of objective functions which originate from model updating is extremely difficult to solve. So far no known search algorithm can even expect to find the global optimum of these

functions and therefore some more sophisticated optimisation procedures, such as Genetic Algorithms or Simulated Annealing, need to be explored for this purpose.

8.6. A Final Word

Model validation technology and the current know-how about it have been presented in this thesis. Some results are extremely encouraging even though some findings showed serious problems associated with model validation and its application. Clearly, there is still some way to go before this technology becomes mature for wide-scale application in industry but, in general, it can be said that application of model validation (by specialists) is readily available. Model validation is equally important as a field which drives and highlights the need for further development of experimental techniques.

A specific goal in this thesis was to make model validation more applicable as a tool for validation of models in practice. This has been achieved by a thorough understanding of current developments, by developing new techniques presented herein, and by applying model validation to many industrial applications.

References

[1] **Natke H G**
Updating Computational Models in the Frequency Domain Based on Measured Data: A Survey
Probabilistic Engineering Mechanics, Vol. 4, No. 1, 1988

[2] **Ewins, D J**
Modal Testing: Theory and Practice
Research Studies Press Ltd., 1984

[3] **T W Lim**
Actuator / Sensor Placement for Modal Parameter Identification of Flexible Structures
Modal Analysis, 8(3). 1993.

[4] **The Dynamic Testing Agency & NAFEMS**
International Conference - Structural Dynamics Modelling, Test, Analysis and Correlation
NAFESM, 1993

[5] **R J Guyan**
Reduction of Stiffness and Mass Matrices
AIAA Journal 3(2),380, 1965

[6] **D C Kammer**
Sensor Placement for On-Orbit Modal Identification and Correlation of Large Space Structures
Journal of Guidance, Control and Dynamics, 14(2),251-259, 1991

[7] **Allemang, R J and Brown, D L**
A Correlation Coefficient for Modal Vector Analysis
Proc. of the 1st Int. Modal Analysis Conf., pp 110-116, 1982

[8] **N A J Lieven and T P Waters**
Error Location using Normalised Orthogonality
12th IMAC, Honolulu, Hawaii, 1994

[9] **GH Golub, CF Van Loan**
Matrix Computations
Second Edition. The John Hopkins University Press. London 1993.

[10] **M I Friswell, J E Mottershead**
Finite Element Model Updating In Structural Dynamics

Kluwer Academic Publishers. ISBN 0-7923-3431-0. 1995.

[11] **N A J Lieven, D J Ewins**
Spatial Correlation of Mode Shapes, the Coordinate Modal Assurance Criterion (COMAC)
6th IMAC, Orlando, Florida, 1988

[12] **M Imregun, DJ Ewins**
An Investigation into mode shape expansion techniques
11th IMAC, Florida 1993

[13] **C O'Callahan, P Avitabile, I Lieu, R MAdden**
An efficient method of determining rotational degrees of freedom from analytical and experimental modal data
4th IMAC, Los Angeles, CA, February 1986

[14] **P Avitable, J O'Callahan, J Milani**
Comparison of system characteristics using various model reduction techniques
7th IMAC, Las Vegas, Nevada, February 1989

[15] **M Paz**
Dynamic Condensation
AIAA Journal, 22(5), 724-727, 1984

[16] **Sidhu, J, Ewins D J**
Correlation of Finite Element and Test Studies of a practical Structure
2nd IMAC, 1984

[17] **Baruch, M**
Optimisation procedure to Correct Stiffness and Flexibility Matrices using Vibration Tests
AIAA Journal, Vol. 16, No. 11, 1978

[18] **Berger H, Chaquin J P, Ohayon R**
Finite Element Model Adjustment using Experimental Modal Data
2dn IMAC, 1984

[19] **Link M**
Comparison of Porcedures for Localising and Correcting Errors in Computational Models using Test Data
9th IMAC, 1991

[20] **Link M, Zhang L**
Experience with Different Procedures for Updating Structural Parameters of Analytical Models using test Data

10th IMAC, 1992

[21] **Niedbal N, Klusowski E, Luber W**
Updating of Finite Element Model by Means of Normal Mode Parameters
13th International Seminar on Modal Analysis, K U Leuven, 1988

[22] **Collins J D, Hart G C, Hasselman T K, Kennedy B**
Statistical Identification of Structures
AIAA Journal, Vol. 12, No. 2, 1974

[23] **Chen J C, Wada B K**
Criteria for Analysis - Test Correlation of Structural Dynamic Systems
Journal of Applied Mechanics, 1975

[24] **Inman D J, Minas C**
Matching Analytical Models with Experimental Modal Data in Mechanical Systems
Control and Dynamic Systems, Vol. 37, 1990

[25] **Minas C, Inman D J**
Matching Finite Element Models to Modal Data
ASME Journal of Vibration and Acoustics, Vol. 112, 1990

[26] **R M Lin, D J Ewins**
Model Updating using FRF Data
15th International Modal Analysis Seminar, K U Leuven, Belgium, 141-163, 1990

[27] **K J Bathe**
Finite Element Procedures in Engineering Analysis
Prentice Hall, New Jersey, 1982

[28] **B M Irons, S Ahmad**
Techniques of Finite Elements
Ellis Horwood, Chichester, 1980

[29] **MSC/NASTRAN**
Handbook for Numerical Methods
The MacNeal-Schwendler Corporation, Los Angeles, 1990

[30] **NAFEMS**
A Finite Element Primer
National Agency for Finite Element Methods and Standards, 1986

[31] **O C Zienkiewicz, R L Taylor**
The Finite Element Method, Vol. 1

4th Edition, McGraw-Hill, London, 1988

[32] **D E Newland**
An Introduction to Random Vibrations and Spectral Analysis
2dn Edition, Longman Group Ltd., 1985

[33] **N Imamovic, D J Ewins**
Optimization of Excitation DOF Selection for Modal Test
15th IMAC, 1997.

[34] **N Imamovic**
preliminary FE Analysis Results of the Lloyd's Register Correlation Benchmark (Ref.: CIV/9334/jrm)
Imperial College Technical Notes. 1995.

[35] **M Imregun and DJ Ewins**
Complex Modes - Origins and Limits
13th IMAC, Nashville, Tennessee, 1995

[36] **S R Ibrahim**
Computation of Normal Modes from Identified Complex Modes
AIAA Journal, 21(3), 446-451

[37] **N Imamovic, D J Ewins**
An Automatic Correlation Procedure for Structural Dynamics
CEAS Conference 1995 in Manchester, England.

[38] **T Soderstrom, P Stoica**
System Identification
Prentice Hall Informational Series in Systems and Control Engineering, London, 1989

[39] **J D Collins, G C Hart, T K Hasselman, B Kennedy**
Statistical Identification of Structures
AIAA Journal, 12(2), 185-190, 1974

[40] **A Berman, W G Flannely**
Theory of Incomplete Models of Dynamic Structures
AIAA Journal, 9(8), 1481-1487, 1971

[41] **Mottershead J E, Friswell M I**
Finite Element Model Updating in Structural Dynamics
Kluwer Academic Publishers. ISBN 0-7923-3431-0, 1995.

[42] **O C Zienkiewicz, J Z Zhu**
A Simple Error Estimator and Adaptive Procedure for Practical Engineering Analysis
International Journal of Numerical Methods in Engineering, 24, 337-357, 1987

[43] **A Berman**
Limitations on the identification of discrete structural dynamic models
2nd International Conference on Recent Advances in Structural Dynamics, Southampton, 427-435, 1984

[44] **M I Friswell**
Candidate Reduced Order Models for Structural Parameter Estimation
Transaction of the ASME, Journal of Vibration and Acoustics, 112(1), 93-97, 1990

[45] **M link, O F Santiago**
Updating and Localizing Structural Errors Based on Minimisation of Equation Errors
International Conference on Spacecraft Structures and Mechanical Testing, ESA/ESTEC, Noordwijk, Holland, 1991

[46] **R Horst, P M Pardalos**
Handbook of Global Optimization
Kluwer Academic Publishers, 1995
The Netherlands

[47] **Mottershead J E, Friswell M I**
Model Updating in Structural Dynamics: A Survey
Journal of Sound and Vibration, 167(2), 1993.

[48] **S Chatterjee, A S Hadi**
Sensitivity Analysis in Linear Regression
John Wiley & Sons, Inc., 1988

[49] **T L Boullion, P L Odell**
Generalised Inverse Matrices
Wiley-Interscience 1971 USA

[50] **R B Nelson**
Simplified Calculation of Eigenvector Derivatives
AIAA Journal, 14(9), 1201-1205, 1976

[51] **R M Pringle and AA Rayner**
Generalised Inverse Matrices with applications to statistics
Griffin London 1971

[52] **D Kahaner, C Moler, S Nash**
Numerical Methods and Software
Prentice-Hall, Inc., 1989

[53] **N R Draper, H Smith**
Applied Regression Analysis
John Wiley & Sons, Inc., Second Edition, 1981

[54] **J E Mottorshead**
Theory of the Estimation of Structural Vibration Parameters from Incomplete Data
AIAAJournal, 28(7), 1326-1328, 1990

[55] **G Golub, V Klema, G W Stewart**
Rank Degeneracy and Least Squares Problem
Stanford University Publication, STAN-CS-76-559, 1976

[56] **O'Callahan, P Avitable, R Riemer**
System equivalent reduction expansion process(SEREP)
7th IMAC, Las Vegas, Nevada, February 1989

[57] ICATS Reference Manual
ICATS, Imperial College of Science & Technology
Exhibition Road, London SW7, 1988

[58] **D J Ewins**
A Survey to Assess the Reliability of Mobility Measurement Techniques
Imperial College of Science and Technology, London

[59] **W J Visser**
Updating Structural Dynamics Models Using Frequency Response Data
PhD, Imperial College, London. 1992.

[60] Notation for Modal Testing & Analysis
Version A1.01, January 1993, Imperial College, London

[61] **Bishop, R E D and Johnson, D C**
The Mechanics of Vibration
Cambridge University Press, 1960

[62] **JET Penny, MI Friswell, D S Garvey**
The Automatic Choice of measurement locations for dynamic testing
11th IMAC 30-36, Florida 1993

[63] **LMS International**
Large-Scale Modal Testing of a Space Frame Structure - from Pretest Analysis to FEA Model Validation
Sound And Vibration / Volume 25 / No. 3 / March 1991

[64] **D C Kammer**
Effect of Noise on Sensor Placement for On-orbit Modal Identification and Correlation of Large Space structures
Journal of Dynamical Systems, Measurement and Control - Transactions of ASME, 114(3), 436-443, 1992

[65] **M L M Duarte, D J Ewins**
High-Frequency Pseudo-Mode Approximation for the High-Frequency Residual Terms
Paper submitted to IMAC XIV

[66] **J A Brandon**
Strategies for Structural Dynamic Modification
Research Studies press Ltd., Somerset, England, 1990

[67] **I U Ojalvo**
Efficient Computation of Mode-Shape Derivatives for Large Dynamic Systems
AIAA Journal, 25(10), 1386-1390, 1987

[68] **T R Sutter, C J Camarda, J L Walsh, H M Adelmans**
Comparison of Several Methods for Calculating Vibration Mode Shape Derivatives
AIAA Journal, 26(12), 1506-1511, 1988

[69] **J H Wilkinson**
The Algebraic Eigenvalue Problem
Oxford University Press (Clarendon), London, 1965

[70] **S R Ibrahim**
Computation of Normal Modes from Identified Complex Modes
AIAAJournal, 21(3), 446-451, 1983

[71] **Y Ben-Naim**
Adaptive Model Updating by Selective Sensitivity: Overview and New Results
International Journal of Numerical Methods in Engineering, To be published.

[72] **A Berman**
System Identification of Structural Dynamic Models - Theoretical and Practical Bounds
AIAA Conference Paper 84-0929, 1984

[73] **S Cogan, G Lallement, Y Ben-Haim**
Updating Linear Elastic Models with Modal-Based Selective Sensitivity
12th IMAC, Honolulu, Hawaii, 1994

[74] **E Fissette, S Ibrahim**
Error Location and Updating of Analytical Dynamic Models using a force balance method
6th IMAC, Orlando, Florida, 1063-1070, 1988

[75] **G Golub, C Van Loan**
An Analysis of the Total Least Squares Problem
SIAM Journal of Numerical Analysis, 17, 883-893, 1980

[76] **W Gawronski, H G Natke**
On ARMA Models for Vibrating Systems
Probabilistic Engineering Mechanics, 1(3), 150-156, 1986

[77] **W Gawronski, H G Natke**
Order Estimation of AR and ARMA Models
International Journal of Systems Science, 19(7), 1143-1148, 1988

[78] **G Lallement, J Piranda**
Localisation Methods for Parameter Updating of Finite Element Models in Elastodynamics
8th IMAC, Orlando, Florida, 579-585

[79] **L Ljung**
System Identification - Theory for the User
Prentice Hall Information and Systems Sciences Series, Englewood Cliffs, 1987

[80] **J E Mottershead, C D Foster**
On the Treatment of Ill-Conditioning in Spatial Parameter Estimation from Measured Vibration Data
Mechanical Systems and Signal Processing, 5(2), 139-154, 1991

[81] **J E Mottershead, W Shao**
Correction of Joint Stiffnesses and Constraints for Finite Element Models in Structural Dynamics
Transaction of ASME, Journal of Applied Mechanics, 60(1), 117-122, 1993

[82] **J E Mottershead, E L Goh, W Shao**
On the Treatment of Discretisation Errors in Finite Element Model Updating
17th International Modal Analysis Seminar, K U Leuven, 1245-1262, 1992

[83] **H G Natke**
Updating Computational Models in the Frequency Domain based on Measured Data: A Survey
Probabilistic Engineering Mechanics, 3(1), 28-35, 1988

[84] **H G Natke**
On Regularisation Methods Applied to the Error Localisation of Mathematical Models
9th IMAC, Florence, Italy, 70-73, 1991

[85] **I U Ojalvo, T Ting**
Interpretation and Improved Solution Approach for Ill-Conditioned Linear Equations
AIAA Journal, 28(11), 1976-1979, 1989

[86] **I U Ojalvo**
Efficient Solution of Ill-Conditioned Equations Arising in System Identification
8th IMAC, Orlando, Florida, 554-558, 1990

[87] **H Rake**
Step Response and Frequency Response Methods
Automatica, 16, 519-526, 1980

[88] **Van Huffel, Vandewalle**
The Use of Total least Squares Techniques for Identification and Parameter Estimation
IFAC Conference on Identification and System Parameter Estimation, York, 1167-1172, 1985

[89] **Q Zhang, G Lallement**
Dominant Error Localisation in a Finite Element Model of a Mechanical Structure
Mechanical Systems and Signal Processing, 1(2), 141-149, 1987

[90] **A Berman, E J Nagy**
Improvement of a Large Analytical Model using Test Data
AIAA Journal, 17(8), 1168-1173, 1983

[91] **B Caesar**
Updating System Matrices using Modal Test Data
5th IMAC, London, England, 453-459, 1987

[92] **C Minas, D J Inman**
Correcting Finite Element Models with Measured Modal Results using Eigenstracture Assignment methods
6th IMAC, , 583-587, 1988

[93] **S W Smith, C A Beattie**
Secant-Method Adjustment for Structural Models
AIAA Journal, 29(1), 119-126, 1991

[94] **F-S Wei**
Structural Dynamic Model Modification using Vibration Test Data
7th IMAC, Las Vegas, Nevada, 562-567, 1989

[95] **F-S Wei**
Structural Dynamic Model Improvement using Vibration Test Data
AIAA Journal, 28(1), 175-177, 1990

[96] **F-S Wei**
Mass and Stiffness Interaction Effects in Analytical Model Modification
AIAA Journal, 28(9), 1686-1688, 1990

[97] **D C Zimmerman, M Widengren**
Correcting Finite Element Models using a Symmetric Eigenstructure Assignment Technique
AIAA Journal, 28(9), 1670-1676, 1990

[98] **K D Blakely, W B Walton**
Selection of Measurement and Parameter Uncertainties for Finite Element Model Revision
2nd IMAC, , 82-88, 1984

[99] **K Chen, D L Brown, V T Nicolas**
Perturbed Boundary Condition Model Updating
11th IMAC, Kissimmee, Florida, 661-667, 1993

[100] **M I Friswell**
The Adjustment of Structural Parameters using a Minimum Variance Estimator
Journal of Mechanical Systems and Signal Processing, 3(2), 143-155, 1989

[101] **S Lammens, W Heylen, P Sas, D Brown**
Model Updating and Perturbed Boundary Condition Testing
11th IMAC, Kissimmee, Florida, 449-455, 1993

[102] **S Li, H Vold, D L Brown**
Application of UMPA to PBC Testing
11th IMAC, Kissimmee, Florida, 223-231, 1993

[103] **N G Nalitolela, J E T Penny, M I Frisswell**
Updating Structural Parameters of a Finite Element Model by Adding Mass or Stiffness to the System
8th IMAC, , 836-842, 1990

[104] **N G Nalitolela, J E T Penny, M I Frisswell**
A Mass or Stiffness Addition Technique for Structural Parameter Updating
International Journal of Analytical and Experimental Modal Analysis, 7(3), 157-168, 1992

[105] **E Rothwell, B Drachman**
A Unified Approach to Solving ill-conditioned Matrix Problem
International Journal for Numerical Methods in Engineering, 28, 609-620, 1989

[106] **C N Felgenhauer, H G Natke**
On the Parameter Identification of Elastomechanical Systems using Input and Output Residuals
Ingenieur Archiv, 54(5), 378-387, 1984

[107] **C D Foster, J E Mottershead**
A Method for Improving Finite Element Models by using Experimental Data: Application and Implication for Vibration Monitoring
International Journal of Mechanical Sciences, 32(3), 191-203, 1990

[108] **M I Friswell**
Updating Physical Parameters from Frequency Response, Function Data
12th Biennial ASME Conference on Mechanical vibration and Noise, Montreal, Canada, DE-Vol 18-4, 393-400, 1989

[109] **M I Friswell**
Candidate Reduced Order Models for Structural Parameter Estimation
Transaction of the ASME, Journal of Vibration and Acoustic, 112(1), 93-97, 1990

[110] **M I Friswell, J E T Penny**
Updating Model Parameters from Frequency Domain Data via Reduced Order Models
Mechanical Systems and Signal processing, 3(5), 377-391, 1990

[111] **M I Friswell, J E T Penny**
The Effect of Close or Repeated Eigenvalues on the Updating of Model Parameters from FRF Data
Transactions of the ASME, Journal of Vibration and Acoustics, 114(4), 514-520, 1992

[112] **C P Fritzen, S Zhu**
Updating of Finite Element Models by Means of Measured Information
Computers and Structures, 40(2), 475-486, 1991

[113] **L Ljung**
System Identification: Theory for the User
Prentice Hall, 1987

[114] **J E Mottershead, R Stanway**
Identification of Structural Vibration Parameters by using a Frequency Domain Filter
Journal of Sound and Vibration, 109(3), 495-506, 1986

[115] **J E Mottershead, C D Foster**
On the Treatment of Ill-conditioning in Spatial Parameters Estimation from Measured Vibration Data
Mechanical Systems and Signal Processing, 5(2), 139-154, 1991

[116] **J E Mottershead, S Weixun**
On the Tuning of Analytical Models by using Experimental Vibration Data
4th International Conference on Recent Advances in Structural Dynamics, Southampton, UK, 432-443, 1991

[117] **A G Nalecz, J Wicher**
Design Sensitivity Analysis of Mechanical Systems in Frequency Domain
Journal of Sound and Vibration, 120(3), 517-526, 1988

[118] **H G Natke**
Updating Computational Modes in the Frequency Domain Based on Measured Data: A Survey
Probabilistic Engineering Mechanics, 3(1), 28-35, 1988

[119] **A Sestieri, W D'Ambrogio**
Why be Modal: How to Avoid the use of Modes in the Modification of Vibrating Systems
International Journal of Analytical and Experimental Modal Analysis, 4(1), 25-30, 1989

[120] **R S Sharp, P C Brooks**
Sensitivities of Frequency Response Function of Linear Dynamic systems to Variations in Design Parameter Values
Journal of Sound and Vibration, 126(1),167-172, 1988

[121] **S S Simonian**
Inverse Problems in Structural Dynamics - I. Theory
International Journal of Numerical Methods in Engineering, 17(3), 357-365, 1981

[122] **S S Simonian**
Inverse Problems in Structural Dynamics - I. Applications
International Journal of Numerical Methods in Engineering, 17(3), 367-386, 1981

[123] **M Brughmans, J Leuridan, K Blauwkamp**
The Application of FEM-EMA Correlation and Validation Technique on a Body-in-White
11th IMAC, Kissimmee, Florida, 646-654, 1993

[124] **M Brughmans, F Lembregts**
Using Experimental Normal Modes for Analytical Model Updating
8th IMAC, Kissimmee, Florida, 389-396, 1993

[125] **F Lembregts, M Brughmans**
Estimation of Real Modes From FRF's via Direct Parameter Identification
7th IMAC, Las Vegas, Nevada, 631-636, 1989

[126] **H Zeischka, O Storrer, J Leuridan, U Vandeurzen**
Calculation of Modal Parameter Sensitivity based on a FEM Proportionality Assumption
6th IMAC, Orlando, Florida, 1988

[127] **Y K Cheung, M F Yeo**
A Practical Introduction to Finite Element Analysis
Pitman Publishing Ltd., 1979

[128] **N Imamovic**
Correlation of a Structural Dynamics Model of RB211 524 H3 HP Rotor
Rolls-Royce Report No. VUTC/E2/94004

[129] **N Imamovic**
Notes on the interface between different FE packages in the Centre of Vibration Engineering
Rolls-Royce Tec. Notes No. E2001/NI/060694

[130] **N Imamovic**
Interface Programs for SJ30 Correlation Program - Users' Guide
Rolls-Royce Tec. Notes No. E2001/NI/240495

[131] **N Imamovic**
An Automatic Correlation Procedure for Structural Dynamics
Rolls-Royce Report No. VUTC/E2/95006

[132] **N Imamovic**
Methods for Selection of Measurement Points for Modal Testing - Average Driving Point Residue (ADPR) Method
Rolls-Royce Report No. VUTC/E2/95007

[133] **N Imamovic**
A Method to Determine the Residual Effects for FRF Calculations
Rolls-Royce Report No. VUTC/E2/95009.

[134] **N Imamovic**
Application of Model Correlation Methods to SAMM II B Structural Dynamic Analysis
Rolls-Royce Report No. VUTC/E2/95011.

[135] **N Imamovic**
Application of Model Correlation Methods to ISOGRID Fan Case Dynamic Analysis
Rolls-Royce Report No. VUTC/E2/95012.

[136] **G Chen, N Imamovic**
Modal test and Analysis of the Nozzle Substructure (Pegasus Project)
Rolls-Royce Report No. VUTC/E2/96012.

[137] **N Imamovic**
Determination of Optimal Excitation Positions for Modal testing - The ODP and NODP Techniques
Rolls-Royce Report No. VUTC/E2/96004.

[138] **N Imamovic**
Methods for Selection of Measurement DOF for Modal Testing - Effective Independence (EI) Method and ADPR-EI Method
Rolls-Royce Report No. VUTC/E2/96002.

[139] **N Imamovic**
Model Validation of Lloyd;s Register Structural Dynamics Correlation Benchmark (Ref.: CIV/9334/jrm)
Rolls-Royce Report No. VUTC/E2/96003.

[140] **G Chen**
Summary Report on Pegasus Carcase Model Validation Project
Rolls-Royce Report No. VUTC/E2/96013.

[141] **N Imamovic, D J Ewins**
A method to Determine the Residual Effects for FRF Calculations
NAFEMS 2nd International Conference on Structural Dynamics Modelling, Test, Analysis and Correlation, Lake District, England 1996.

[142] **N Imamovic, D J Ewins**
Automatic Selection of Parameters for Updating Procedures
16th ASME Conference on Mechanical Vibration and Noise. Sacramento, California. 1997.

[143] **N Imamovic, D J Ewins**
Application of an Automatic Correlation Procedure for Structural Dynamics in MSC / NASTRAN
MSC UK Users' Conference 1995.

[144] **L Davis**
Genetic Algorithms and Simulated Annealing
Pitman, ISBN 0-273-08771-1, 1987.

[145] **Mares C, Surace C**
Finite Element Model Updating Using a Genetic Algorithm
DTA NAFEMS 2nd International Conference on Structural Dynamics Modelling, 1996.

Appendix 7A

A Challenge to FE Analysts from Lloyd's Register

What is it?
The challenge is to solve a structural dynamics problem, shown opposite using the FE method, firstly with no knowledge of the real (test) behaviour, and secondly with hindsight, given the real behaviour.

Why do it?
Based on the experiences of a number of companies who have already solved this problem there are a number of educational and community benefits. The problem posed is deliberately "small" to avoid involving significant resources in the solution.

How do I go about it?
We ask you firstly to solve the problem and supply the undersigned with frequencies and modal descriptions for the range 0-5000 Hz (concentrating primarily on the cantilever modes).

Once completed, we will supply you with 3 independent sets of test results, and average test results, for key modes.

Then we ask you to update (if necessary) your model, as you see fit, in light of the test results and supply us with updated frequencies and modal descriptions.

Finally, we will collect and, publish, with your permission, all submitted results (unattributed) showing the correlation between analysis and test.

This should benefit yourself and the FE community by contributing to the debate on what is good correlation, and how good a reconciliation between FE analysis and test can be expected.

A few hints
Uncertainties to be addressed include the boundaries between the steel cantilever, steel base, rubber block and earth. The steel cantilever to steel base connection is a firmly screwed connection. The flat steel base rests on the flat rubber and may be assumed to remain in contact due to gravity. During testing very low levels of vibration were used to ensure, as far as possible, linear behaviour and no uplift of either steel base or rubber block.

Ed Note: The issues of Analysis, Test and verification are central to the DTA/NAFEMS conference to be held on 3-5 July 1996.

Further details
If you should require any further details please contact:

John Maguire, Lloyd's Register, 29 Wellesley Road, Croydon, Surrey CRO 2AJ, UK
Tel: 0181-681 4764
Fax: 0181-681 6814.

LLOYD'S REGISTER CORRELATION BENCHMARK (Ref: CIV/9334/jrm)
STRUCTURE FOR ANALYSIS / TEST / CORRELATION / UPDATING

Isometric View (not to scale):

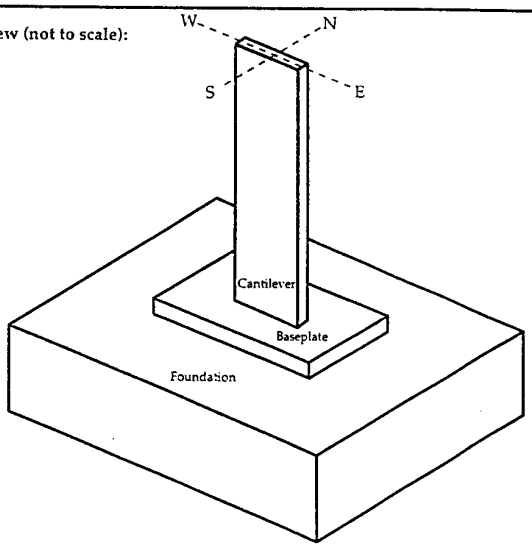

Notes:

1. Cantilever firmly screwed to baseplate, baseplate resting on foundation.
2. Each item centrally located upon the item below.
3. Assume fully rigid boundary beneath foundation.

Geometric Details:

Cantilever = 14.1mm (NS) x 60mm (EW) x 239.5mm (high)
Baseplate = 150mm (NS) x 150mm (EW) x 30mm (high)
Foundation = 248mm (NS) x 248mm (EW) x 122mm (high)

Mass Details:

Cantilever = 1.574 kg (steel)
Baseplate = 5.307 kg (steel)
Foundation = 8.374 kg (moulded rubber)

Material data:

Cantilever = Young's modulus 208 kN/mm², Poisson's ratio 0.3
Baseplate = Young's modulus 208 kN/mm², Poisson's ratio 0.3
Foundation = Shear modulus 0.9N/mm², Poisson's ratio 0.447

DESIRED RESULTS: Frequencies and mode descriptions in range 0-5000 Hz (concentrating primarily on the cantilever modes)

Appendix 7B

LLOYD'S REGISTER CORRELATION BENCHMARK (Ref: CIV/9334/jrm)

TEST RESULTS

Modal Description	Frequency in Hz			Frequency in Hz
	Company "A"	Company "B"	Company "C"	Average of 3
Rubber block	15→84	22→110	19→78	-
Cantilever NS1	321	306	312	313
Cantilever NS 2	1060	1061	1074	1065
Cantilever EW1	1200	1211	1219	1210
Cantilever Torsion 1	1340	1389	1388	1372
Cantilever NS3	3050	2997	3009	3019
Cantilever EW2	3610	3496	3498	3535
Cantilever Torsion 2	4330	4218	4203	4250

Notes

1. Only most significant/clearest test results given.
2. The number of rubber block modes measured clearly were as follows: "A" = 6, "B" = 8, "C" = 6.
3. Other modes measured were as follows: "A" = 1912 Hz, 1940 Hz, 3052 Hz, 4297 Hz, 4500 Hz; "B" = 1882 Hz, 2591 Hz, 3194 Hz, 4257 Hz, 4403 Hz, 4651 Hz; "C" = no other clear modes.
4. The above model descriptions are simplified for ease of description.